UNIVERSITY OF NAPLES FEDERICO II

Polytechnic and Basic Sciences School

PHD IN CHEMICAL SCIENCES

XXXI CYCLE

2015-2018

SELECTIVITY OF BIOMOLECULAR RECOGNITION PROCESSES: SYNTHESIS AND PHARMACOLOGICAL ACTIVITY OF NOVEL BIOMIMETIC AGENTS

MARIA DE FENZA

ADVISOR: DR. ANNALISA GUARAGNA
SUPERVISOR: PROF. ALFONSO IADONISI

UNIVERSITA' DI NAPOLI FEDERICO II

Scuola Politecnica e delle Scienze di Base

DOTTORATO DI RICERCA IN SCIENZE CHIMICHE

XXXI CICLO

2015-2018

SELETTIVITÀ DEI PROCESSI DI RICONOSCIMENTO BIOMOLECOLARE: SINTESI ED ATTIVITÀ FARMACOLOGICA DI NUOVI AGENTI BIOMIMETICI

MARIA DE FENZA

TUTORE: DOTT. ANNALISA GUARAGNA
RELATORE: PROF. ALFONSO IADONISI

UNIVERSITÀ DEGLI STUDI DI NAPOLI FEDERICO II
POLYTECHNIC AND BASIC SCIENCES SCHOOL

PHD IN CHEMICAL SCIENCES – XXXI CYCLE

SELECTIVITY OF BIOMOLECULAR RECOGNITION PROCESSES: SYNTHESIS AND

Advisor: Dr Annalisa Guaragna

PhD Student: Maria De Fenza

Supervisor: Prof. Alfonso Iadonisi

PHARMACOLOGICAL ACTIVITY OF NOVEL BIOMIMETIC AGENTS

Biomimetic agents are synthetic compounds devised to resemble structures and properties of natural biomolecules with the aim to solve complex human problems. Glycomimetics, nucleoside analogues (NAs) and modified oligonucleotides (MOs) represent biomimetic agents that have found various pharmacological applications and constitute the topic of the three main sections in which this PhD thesis has been organized. The design, the synthesis and then the biological evaluation of such molecules have been undertaken in these years; in all cases the aim was the development of new agents with targeted pharmacological activity or improved biological selectivity in several medicinal chemistry contexts (**FIGURE 1**).

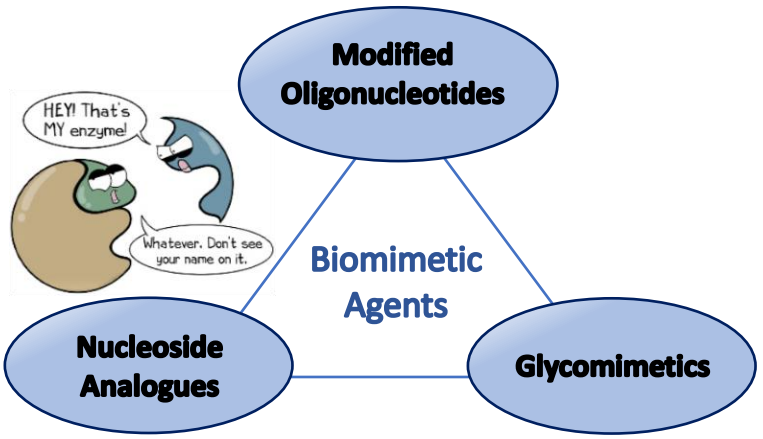

FIGURE 1. Biomimetic agents and enzymatic selectivity.

GLYCOMIMETICS

The term glycomimetics refers to molecules that mimic the structure and the activity of natural carbohydrates improving their biological, pharmacological or drug-like properties. Among a variety of glycomimetics of synthetic or natural origin an important

position is occupied by iminosugars.[1] Iminosugars ("nitrogen in the ring"- containing carbohydrate analogues), also called erroneously azasugars, represent the most important class of glycomimetics discovered so far and have received great attention[2] in the last four decades as therapeutic agents against many diseases due their great ability to act as inhibitors[3] or enhancers (e.g. pharamacological chaperones)[4] of glycosidases and glycosyltransferases. Their pharmacological application is however significantly hampered by their limited *in vivo* selectivity. Thus, they can be used for a plethora of therapeutic purposes, but they are always accompanied by a wide variety of side effects due to their activities against other cellular enzymes. On the other hand, L-iminosugars[5] (unnatural enantiomers) have displayed in several contexts more efficient pharmacological properties than their D-antipodes and, especially, improved enzymatic selectivity.[6] In this context, inspired by these observations, we have first tuned up a synthetic strategy to prepare by a *de novo* stereocontrolled method (starting by the synthetically available enol thioether **2** and the Garner aldehyde, **3**) enantiomerically pure L-DNJ *ent*-**1**,[7] e.g. L-deoxynojirimycin (to the best of our knowledge never reported before) (**FIGURE 2**). Then, since lipophilicity has been postulated to enhance the selectivity of iminosugars, we have developed an alternative route to the existing methods for *N*-alkylation of iminosugars and alkyl chain assembly. Particularly, the strategy relies on the combined use of polymer-bound triphenylphosphine (PS-DPP)/iodine[8] as a "clean" and potentially recyclable iodination reagent by an iterative procedure not requiring extractive work-up and chromatographic purification steps (**FIGURE 2**).

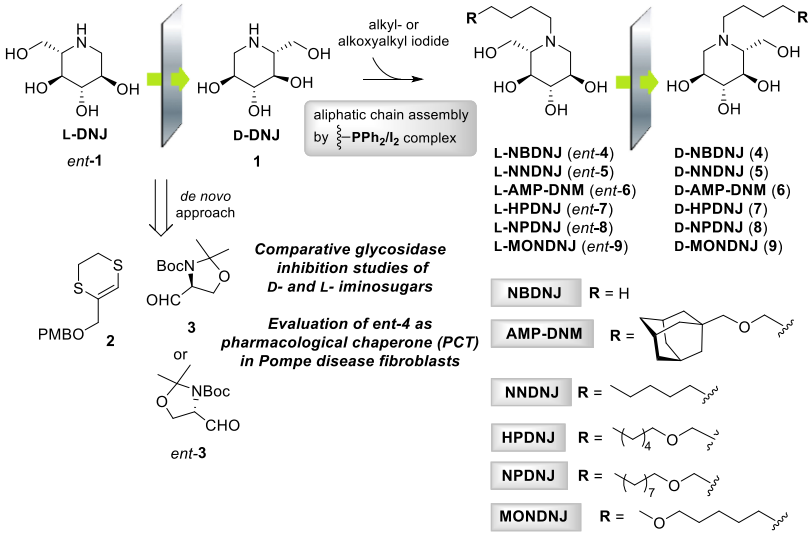

FIGURE 2. Synthesis and pharmacological applications of L-iminosugars.

With the target compounds **4-9** and *ent*-**4-9** in hand, the analysis of their glycosidase inhibition properties was extensively explored, in collaboration with Dr Massimo Aureli, Prof. Marco Moracci first and then, during a period spent abroad at Department of Pharmacology of Oxford University supervised by Dr David Priestman and Prof. Frances Platt. Finally, the chaperoning potential of *ent*-**4** in the context of PCT applied to Pompe Disease was preliminarily explored (in collaboration with Prof. Giancarlo Parenti).

NUCLEOSIDE ANALOGUES

Nucleoside analogues (hereafter NAs) are synthetic, chemically modified compounds developed to mimic the physiological counterparts to exert their cellular functions.[9] They have become cornerstones of treatment of viral infections and today many efforts are still made to discover more potent, selective and less toxic antiviral NAs.
In this context three classes of NAs have been herein explored.
β-L-2'-Fluoro-3'-thiacytidine (F-3TC) stereoisomers*:* for a long period, it was assumed that only D-configured nucleoside analogues (NAs) in analogy with the natural ones, could be recognized by suitable enzymes to exhibit their biological activity. After the discovery of an unusual nucleoside, 2',3'-dideoxy-3'-thiacytidine ((+)-BCH-189, **10**) (**FIGURE 3**) and of its more potent and less toxic β-L-isomer (Lamivudine, (-)-3TC, **11**) this paradigm has been challenged. Since then, many L-configured NAs[10] have been synthetized and the molecular basis for their therapeutic activation, as antiviral or anticancer agents, have been elucidated. In efforts to improve 3TC pharmacological properties, a great deal of modifications has been explored over the past decades. However, no synthetic endeavours have been devoted to the preparation of 3TC derivatives having a fluorine atom in the "sugar" backbone at the C2′-position. Thus, considered that the selective introduction of fluorine atom into a bioactive nucleoside has become an important strategy in the design and discovery of novel drug candidates, we explored the synthesis of 2'-fluorinated 3TC derivatives having either (1'*S*,2'*S*,4'*R*) or (1'*S*,2'*R*,4'*R*) configuration [i.e. (2'*S*)-F-3TC (**12**) and (2'*R*)-F-3TC (**13**)] (**FIGURE 3**).[11] As depicted in the retrosynthetic pathway, the asymmetric sulfoxidation of 3TC afforded **14** and its Pummerer rearrangement allowed us to obtain **15**, suitable substrate to stereoselectively introduce the fluorine atom in the desired position.

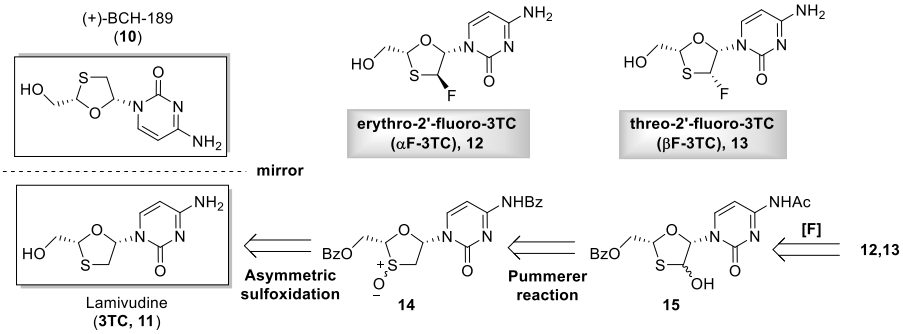

FIGURE 3. Synthesis and antiviral activity of β-L-2′-Fluoro-3′-thiacytidine (F-3TC) stereoisomers.

The nucleoside **13** has been evaluated *in vitro* as antiviral agent against Hepatitis C Virus (HCV), Respiratory Sinctial Virus (RSV) and HIV. The experiments have been performed at Gilead Sciences.

Piperidinyl Nucleosides: in recent times, the fusion of two principal concepts behind the research areas of glycomimetics and biomimetic agents has resulted in the development of a new class of molecules, defined as iminosugar-based nucleosides.[12] On one hand, the structural mimicking of carbohydrates (the sugar oxygen atom is replaced by an amino function), achieved by iminosugars, has enabled to identify highly efficient modulators of the activity of carbohydrate processing enzymes. On the other hand, the conformational mimicking of natural nucleosides, achieved with sugar modified nucleoside analogues, revealed as a winning strategy for the treatment of viral infections (e.g. DNA viruses). Accordingly, iminosugar-based nucleosides have been conceived to exploit the efficiency of enzyme inhibition of the iminosugar core for the modulation of the activity of nucleoside processing enzymes. In this context, with the aim to expand the repertoire of such compounds, we have herein explored the synthesis of piperidinyl nucleosides **16** and **17** (**FIGURE 4**). Learning from the lesson of anti-HHV hexitol nucleosides,[13] compounds **16** and **17** are conceived to act as conformational preorganized nucleosides, exploiting the rigidity of the piperidinyl core with the aim to further improve inhibition potency and selectivity and to act as mutagenic antiviral agents.

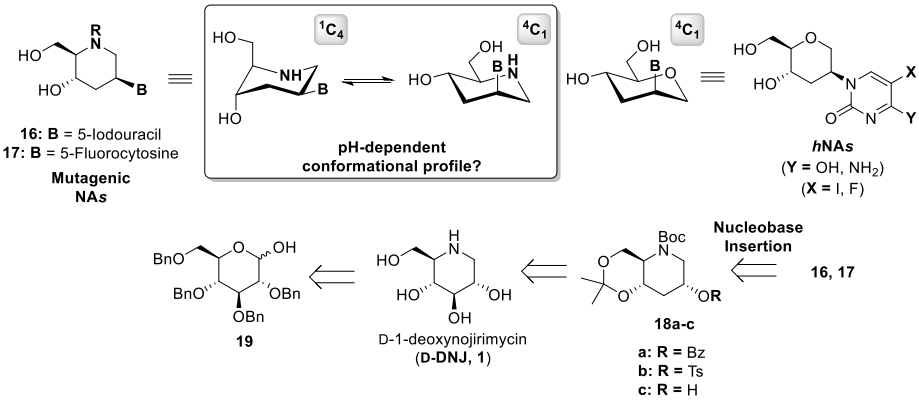

FIGURE 4. Novel piperidinyl iminosugar-based nucleosides as selective pharmacological tools.

As depicted in the retrosynthetic analysis, our synthetic approach starts from the well-known glucosidase inhibitor 1-deoxynojirimycin (**D-DNJ, 1**) prepared on large scale from **19**. Through studied protection and functionalization reactions, C-3 deoxygenated key intermediates **18a-c** are readily synthetized and the nucleobase insertion is then performed by nucleophilic displacement of a good leaving group (from **18b**) or by Mitsunobu procedure (from **18c**, obtained by **18a**), leading to the target piperidinyl NAs **16** and **17**. A conformational analysis devoted to study of preferred chair conformation (e.g. $^4C_1 \rightarrow {}^1C_4$ inversion owing to occurring 1,3-diaxial interactions) of **16** has been undertaken. Finally, preliminary biological *in vitro* assays of **16** against a variety of DNA viruses (HSV-1 and 2, VZV, HCMV, Vaccinia Virus and Adenovirus) has been performed at Rega Institute for Medical Research (KU Leuven, Belgium).

D- and L-Cyclohexenyl Nucleosides: as highlighted above, replacement of the (deoxy)ribose core of natural nucleosides with conformationally restricted bioisosteric moieties has demonstrated to greatly improve the thermodynamic stability of enzyme-substrate recognition processes, while providing molecules able to be selectively recognized by viral enzymes over their natural counterparts. In this area, nucleosides bearing cyclohexenyl scaffolds have deserved considerable attention over the last years.[14] Indeed, the peculiar nature of the cyclohexenyl ring (fluctuating between low energy $^2H_3$ and $^3H_2$ conformations, see **FIGURE 5**) allows the corresponding nucleosides (remarkably, in both enantiomeric series) to closely resemble the bioactive conformations adopted by natural deoxynucleosides while interacting with host/viral kinases and polymerases.

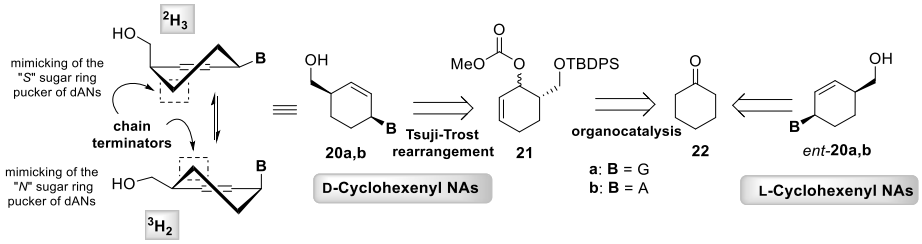

FIGURE 5. Asymmetric synthesis of D- and L-cyclohexenyl nucleosides.

With the aim to expand the repertoire of bioactive cyclohexenyl nucleosides, we have herein explored the synthesis and the antiviral potential of novel cyclohexenyl nucleosides **20a,b** and *ent*-**20a,b**, lacking the OH group at C5' position and therefore being conceived as chain terminators (**FIGURE 5**). The synthetic path involves an enantioselective organocatalytic aldol addition of cyclohexanone **22**, to set the chirality of target nucleosides, and a stereoconvergent Tsuji-Trost rearrangement of carbonates **21**, to set the relative *cis* configuration of the substituents. Nucleosides **20a,b** and *ent*-**20a,b** are currently undergoing extensive *in vitro* assays aimed at determining their potential against a variety of DNA viruses and retroviruses.

MODIFIED OLIGONUCLEOTIDES

The challenge of chemists in this field is the construction of modified oligonucleotides (MOs) with deep structural changes compared to natural oligonucleotides (ODNs), able to keep their potential for selective cross communication but, on the other hand, able to enhance nuclease stability, target binding affinity, enzyme interaction, hybridization properties, cellular uptake and pharmacokinetic/pharmacodynamic properties.[15] Among MOs, those having aptameric properties (ability to bind a molecular target with high affinity and specificity) represent the new frontier of their medicinal use.[16] Looking for the preparation of novel selective aptamers, the attention has been focused on NU172[17] (**FIGURE 6**), a 26-mer whose structure has been hypothesised and, on the basis of the sequence (5'-CGCCTAGGTTGGGTAGGGTGGTGGCG-3'), seems to belong to the class of bimodular oligonucleotides that adopt a so called duplex/quadruplex conformation. Particularly, NU172 is able to bind the thrombin (a trypsin-like serine protease involved in the coagulation cascade) at very low concentration (K_d = 100 pM) and it is currently in Phase II of clinical trials as anticoagulant agent. The project arises in the frame of a scientific collaboration with Prof. P. Herdewijn (Rega Institute for Medical Research, KU Leuven) and has concerned the replacement of several residues of NU172 sequence with *h*NA (1',5'-anhydro-D-arabino-hexitol nucleotides) in order to study the influence of hexitol nucleosides **23** and **24** in the ability of resulting MOs (**NU172A-E0618**) to bind the thrombin acting as its aptamers and as anticoagulant agents (**FIGURE 6**).

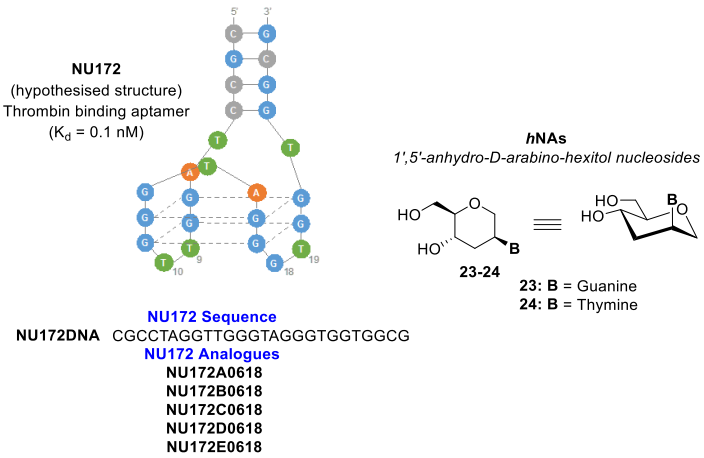

FIGURE 6. Synthesis of modified thrombin aptamers as potential anticoagulant agents.

REFERENCES

[1] Harit, V.K.; Ramesh, N. *RSC Adv*. **2016**, *6*, 109528.

[2] Compain, P.; Martin, O. R. *Iminosugars – From Synthesis to Therapeutic Applications*, John Wiley & Sons Ltd: West Sussex, England **2007.**

[3] Ghisaidoobe, A.; Bikker, P.; de Bruijn, A. C. J.; Godschalk, F.D.; Rogaar, E.; Guijt, M. C.; Hagens, P.; Halma, J.M.; van't Hart, S.M.; Luitjens, S.B.; van Rixel, V.H.S., Wijzenbroek, M.; Zweegers, T.; Donker-Koopman, W.E.; Strijland, A.; Boot, R.; van der Marel, G.; Overkleeft, H.S.; Aerts, J.M.F.G.; van der Berg, R.J.B.H.N. *ACS Med. Chem. Lett.* **2011**, *2*, 119.

[4] Parenti, G.; Andria, G.; Valenzano, K. J. *Mol. Ther*. **2015**, *23*, 1138.

[5] D'Alonzo, D.; Guaragna, A.; Palumbo, G. *Curr. Med. Chem.* **2009**, *16*, 473.

[6] Wennekes, T.; Meijer, A.J.; Groen, A.K.; Boot, R.G.; Groener, J.E.; van Eijk, M.; Ottenhoff, R.; Bijl, N.; Ghauharali, K.; Song, H.; O'Shea, T.J.; Liu, H.; Yew, N.; Copeland, D.; van den Berg, R.J.; van der Marel, G.A.; Overkleeft, H.S.; Aerts, J.M. *J. Med. Chem.* **2010**, *53*, 689.

[7] (1) Guaragna, A.; D'Errico, S.; D'Alonzo, D.; Pedatella, S.; Palumbo, G. *Org. Lett.* **2007**, *9*, 3473; (2) Guaragna, A.; D'Alonzo, D.; Paolella, C.; Palumbo, G. *Tetrahedron Lett.* **2009**, *50*, 2045; (3) D'Alonzo, D.; De Fenza, M.; Porto, C.; Iacono, R.; Huebecker, M.; Cobucci-Ponzano, B.; Priestman, D.A.; Platt, F.; Parenti, G.; Moracci, M.; Palumbo, G.; Guaragna, A. *J. Med. Chem.* **2017**, *60*, 9462.

[8] Pedatella, S.; Guaragna, A.; D'Alonzo, D.; De Nisco, M.; Palumbo G. *Synlett* **2006**, *2*, 305.

[9] Pedro, M. *Chemical Synthesis of Nucleoside Analogues* **2013**, John Wiley & Sons Inc. Publication.

[10] Mathé, C.; Gosselin, G. *Antiviral Res.* **2006**, *71*, 276.

[11] D'Alonzo, D.; De Fenza, M.; Palumbo, G.; Romanucci, V.; Di Fabio, G.; Guaragna, G. *Synthesis* **2017**, *49*, 998.

[12] Evans, G.B.; Tyler, P.C.; Schramm, V.L. *ACS Infect. Dis.* **2018**, *4*,107.

[13] Ostrowski, T.; Wroblowski, B.; Busson, R.; Rozenski, J.; De Clercq, E.; Bennett, M. S.; Champness, J. N.; Summers, W. C.; Sanderson, M. R.; Herdewijn, P. *J. Med. Chem.* **1998**, *41*, 4343.

[14] Paolella, C.; D'Alonzo, D.; Schepers, G.; Van Aerschot, A.; Di Fabio, G.; Palumbo, G.; Herdewijn, P.; Guaragna, A. *Org. Biomol. Chem.* **2015**, *13*, 10041.
[15] Ichikawa, E.; Kato, K. *Curr. Med. Chem.* **2001**, *8*, 385.
[16] Zhou, J.; Rossi, J. *Nat. Rev. Drug Discovery* **2017**, *16*, 181.
[17] (1) Zavyalova, E.; Golovin, A.; Pavlova, G.; Kopylov, A. *Curr. Med. Chem.* **2013**, *20*, 4836. (2) Russo Krauss, I.; Napolitano, V.; Petraccone, L.; Troisi, R.; Spiridinova, V.; Mattia, C.A.; Sica, F. *Int. J. Biol. Macromol.* **2018**, *107*, 1697.

LIST OF ABBREVIATIONS

A	Adenine
Ac	Acetyl group
Ac_2O	Acetic anhydride
AcOH	Acetic acid
ACV	Acyclovir
Ag_2O	Silver oxide
AIBN	Azobisisobutyronitrile
AIDS	Acquired Immune Deficiency Syndrome
AMP DNM	*N*-(5-adamantane-1-yl-methoxypentyl)-DNJ
Ar	Aryl group
BCH-189	2'-deoxy-3'-thiacytidine
Boc	*t*-Butoxycarbonyl group
Bn	Benzyl group
BnBr	Benzyl bromide
BSA	*N*,*N*-*bis*-dimethylsilylacetamide
BuLi	butyllithium
t-BuOH	*tert*-butanol
BVDU	Brivudin
Bz	Benzoyl
BzCl	Benzoyl chloride
C	Cytosine
CD	Circular Dichroism
CeNA	Cyclohexenyl Nucleic Acid
Cer	Ceramide
CerGlcT	Ceramide GlucosylTransferase
CF_3COCH_3	Trifluoroacetone
CF	Cystic Fibrosis
CFTR	Cystic Fibrosis Transmembrane Conductance Regulator

CH_2Cl_2	Dichloromethane
$CHCl_3$	Chloroform
CH_3CN	Acetonitrile
CH_3OH	Methanol
CMV	Citomegalovirus
m-CPBA	*m*-chloroperbenzoic acid
DBTO	Dibutyltin oxide
DBU	1,8-diazobicyclo[5.4.0]undec-7-ene
dC	Deoxycytidine
DCE	Dichloroethane
dCK	dCK deoxycytidine kinase
dCTP	2'-deoxycytidine 5'-triphosphate
DCM	Dichloromethane
ddC	2',3'-dideoxycytidine
DDQ	2,3-dichloro-5,6-dicyano-1,4-benzoquinone
DEAD	diethyl azodicarboxylate
dG	Deoxyguanosine
DGJ	Deoxygalactonojirimicyn
dGTP	Deoxyguanosine Triphosphate
DIPEA	Diisopropylethylamine
DM	Diabetes Mellitus
DMAP	Dimethylaminopyridine
DMDP	((*2R,3R,4R,5R*)-2,5-dihydroxymethyl-3,4-dihydroxypyrrolidine)
DMF	*N*,*N*- Dimethylformamide
DMJ	Deoxymannonojirimicin
DMP	Dimethoxypropane
DMSO	Dimethyl Sulfoxide
DMT	Dimethoxytrityl group
DNA	Deoxyribonucleic Acid

dNTP	2´-deoxynucleoside 5´-triphosphate
DNJ	1-deoxy-nojirimicin
dr	diastereomeric ratio
ds	double stranded
EC_{50}	half maximal effective concentration
ee	enantiomeric eccess
ER	Endoplasmatic Reticulum
ERT	Enzyme Replacement Therapy
Et_2O	Diethyl ether
EtOAc	Ethyl acetate
EtOH	Ethanol
Et_3SiH	Triethylsilane
FAG	Fagomine
FDA	Food and Drug Administration
FTC	5-fluoro-β-L-thiocytidine
G	Guanina
GAA	acid α-glucosidase
GBA1	acid β-Glucosidase 1
GBA2	acid β-Glucosidase 2
GL-3	glotriaosylceramide
GCS	Ceramide glucosyltransferase
GCV	Ganciclovir
GlcCer	Glucosyl Ceramide
GSL	Glycosphingolipid
HBV	Hepatitis B Virus
HCl	hydrogen chloride
$HClO_4$	perchloric acid
HCV	Hepatitis C Virus
HHV	Human Herpes Viruses
HIV	Human Immunodeficiency Virus

HMBC	Heteronuclear Multiple Bond Correlation experiment
HNA	Hexitol Nucleic Acid
*h*HNAs	1',5'-Anhydro-D-*arabino*-Hexitol Nucleoside Analogues
HNJ	Homonojirimycin
HPDNJ	*N*-[5-(Hexoxy)pentyl]-deoxynojirimycin
HPMPA	Cidofovir
H_2SO_4	sulphuric acid
HSV-1	Herpes Simplex Virus - Type 1
HSV-2	Herpes Simplex Virus -Type 2
I_2	Iodine
IC_{50}	Half maximal inhibitory concentration
IL-8	Interleukin-8
J	Coupling constant
K_2CO_3	Potassium carbonate
LSD	Lysosomal Storage Disorder
Me	Methyl
MeOH	Methanol
MeONa	Sodium Methoxide
MOMCl	Methoxy methyl chloride
MON DNJ	*N*-[9-(Methoxyl)nonyl]-deoxynojirimycin
MOs	Modified Oligonucleotides
4-MU	4-methylumbelliferyl-D-glycopyranoside
*m*RNA	messenger ribonucleic acid
NaH	Sodium hydride
NaOH	Sodium hydroxide
NAs	Nucleoside Analogues
NH_4Cl	Ammonium chloride
Ni/Ra	Raney Nickel
NJ	Nojirimicin
NMR	Nuclear Magnetic Resonance Spectroscopy

NBDNJ	*N*-butyl-deoxynojirimycin
NPDNJ	*N*-[5-(Nonyloxy)pentyl]deoxynojirimycin
NNDNJ	*N*-nonyl-deoxynojirimycin
ODNs	Oligonucleotides
PCT	Pharmacological Chaperone Therapy
PD	Pompe Disease
PNP	Purine Nucleoside Phosphorylase
PPh_3	Triphenylphosphine
ppm	parts per million
PTSA	*p*-Toluensulfonic Acid
PS-DPP	Polystyryl diphenylphosphine
Py	Pyridine
RCM	Ring Close Metathesis
rhGAA	recombinant human GAA
RNA	Ribose Nucleic Acid
RSV	Respiratory Sinctial Virus
RT	Reverse Transcriptase
SAR	Structure-Activity Relationship
SRT	Substrate Reduction Therapy
T	Thymine
TBAF	tetrabutylammonium fluoride
TBDPS	*t*-butyldiphenylsilyl group
3TC	β-L-thiocytidine
TEA	Triethylamine
THF	Tetrahydrofuran
tK	Thymidine Kinase
TLC	Thin Layer Chromatography
T_m	melting temperature
TMS	Tetramethylsilane
TPP	triphenylphosphine

TS	Transition state
Ts	Tosyl
TsCl	*p*-toluenesulfonyl chloride
VZV	Varicella Zoster Virus

TABLE OF CONTENTS

PREFACE

BIOMIMETICS AND BIOLOGICAL SELECTIVITY

Organic synthesis, medicinal chemistry and drug discovery represent today the main direction toward which the modern organic chemistry is reorienting. Drug discovery needs indeed basic study into the medicinal and chemical nature of the diseases to treat and, with this aim, the synthesis of newer organic molecules with more favourable therapeutic properties or their conversion into derivatives which show optimum medicinal activity, is necessary. The role of organic synthesis, and particularly of asymmetric synthesis, results central in this context considering that a minor change in the molecule chemical structure (i.e. change in stereochemistry, geometry, functional group, removal of groups, chelate formation, salt formation) may strongly modify its medicinal activity. The drug discovery usually progresses through several standard stages; these include: the selection of the biological target; identification of the starting building block and/or leads; compound design and synthesis; SAR studies; computers and computational chemistry; screening of the synthesised compound in biological in vitro assay and finally, pharmacokinetic and in vivo studies. Several of the above described stages have been the principal phases of the research projects undertaken in the last three years and fully described in the present PhD thesis; they were aimed to the study of the selectivity associated to biomolecular recognition processes in which novel synthetized biomimetic agents with potential pharmacological applications have been involved. The term "biomimetics" refers to human-made (unnatural) systems that imitate the natural ones. In the context of drug discovery, nucleoside analogues (NAs), glycomimetics and modified oligonucleotides (MOs) are examples of biomimetic agents that found over the years pharmacological application and represent the three sections of the following PhD thesis. On the basis of the scientific concept introduced by Paul Ehrlich (Physiology Nobel Prize in 1908) about the development of substances that would seek out specific disease-causing agents, called "magic bullets", the attention has been focused, as mentioned above, on the development of such biomimetic agents with targeted pharmacological activity or improved biological selectivity in several medicinal chemistry contexts. To this aim, the role of conformation and configuration of such molecules has been deeply investigated.

GLYCOMIMETICS

1

GLYCOMIMETICS

The term "glycomimetics" refers to natural or synthetic molecules that mimic the structure and the activity of natural carbohydrates. The need to synthesize glycomimetics derives from the fact that the carbohydrates themselves are often degraded too rapidly in vivo and because they weakly bind the proteins. Therefore, a research line is focused on the design of carbohydrate analogues with shapes and polarities resembling natural sugars and able to mimic, alter or replace native carbohydrate moieties, for improving their biological, pharmacological or drug-like properties. Glycomimetics are indeed able to inhibit the activity of carbohydrate-processing enzymes, especially glycosidases and glycosyltransferases; these are ubiquitous enzymes involved, respectively, in the breakdown of oligo- and polysaccharides and in their biosynthesis from smaller oligosaccharide sequences or even starting from single monosaccharides. These processes are of key importance, inter alia, for the synthesis of glycoproteins, which play a role in cell communication processes. In most cases, the inhibition capacity of glycomimetics against glycosidases and glycosyltransferases is due to their aptitude to mimic the transition state of the process of cleavage or formation of a glycosidic bond. Glycomimetic research has thus so far progressed in numerous fields of investigation, developing structures alternative to native carbohydrate buildings for the treatment of a broad range of inflammatory and infectious diseases. In ***Figure 1*** *are reported several prominent examples of glycomimetic-based drugs.*

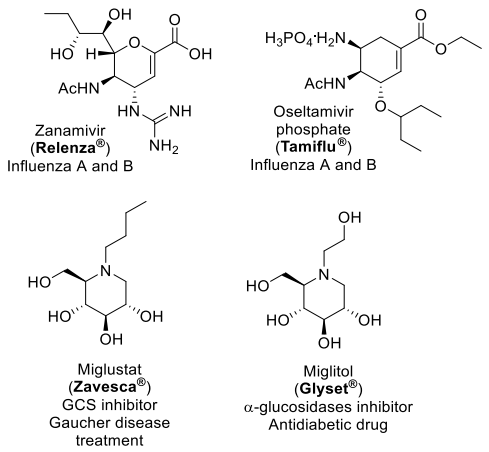

Figure 1. *Examples of glycomimetic-based drugs on the market.*

Among the most effective and studied glycomimetics (as seen in ***Figure 1****), an important position is occupied by iminosugars. Iminosugars ("nitrogen in the ring"- containing carbohydrate analogues), also called erroneously azasugars, represent the most important class of glycomimetics discovered so far and have received considerable*

attention over the last four decades as therapeutic agents against many diseases. Their pharmacological application is however significantly hampered by their limited selectivity in vivo. Thus, they can be used for a plethora of therapeutic purposes, but they are always accompanied by a wide variety of side effects due to their activities against other cellular enzymes.

During this PhD research project that is aimed at exploring the stereoselectivity of biomolecular recognition processes, great attention has been focused on the stereoselective synthesis of the unnatural enantiomer of the well-known glycosidase inhibitor DNJ and of its N-alkylated congeners. The aim was to study those configurational and structural features of iminosugars (chirality and lipophilicity) useful to reach an improvement of their selectivity toward glycosidases, either in the inhibition of their biological activity or in the enhancement of their catalytic function, with specific applications in medicinal chemistry.

1.1 Synthesis and Pharmacological Applications of L-Iminosugars

1.1.1 INTRODUCTION

1.1.1.1 IMINOSUGARS: CHEMICAL STRUCTURE AND NATURAL OCCURRENCE

Iminosugars are naturally occurring or synthetic small organic compounds that mimic carbohydrates but contain a nitrogen atom instead of oxygen in the ring system template.[1] The iminosugar motif is present in several classes of monocyclic and bicyclic compounds, leading to a large and structurally diverse class of molecules (**FIGURES 1-4**). However, the wide diversity of natural occurring iminosugars suggests, undoubtedly, that further structures can be identified in the next future.

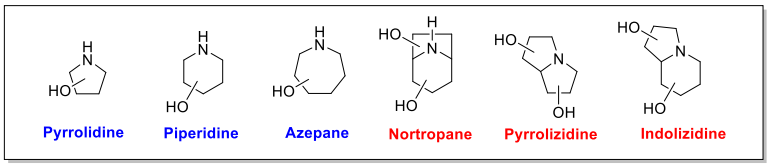

FIGURE 1. Main structural (monocyclic and bicyclic) motifs of iminosugars commonly available by synthetic methods or from natural sources.

The template is typically substituted with hydroxyls, but many other functional groups are found in nature and easily introduced by synthetic approaches. Among iminosugar pyrrolidine analogues, DMDP ((*2R,3R,4R,5R*)-2,5-dihydroxymethyl-3,4-dihydroxypyrrolidine) is a naturally occurring glycomimetic[2] and it is one of the most widespread of secondary metabolite sugar mimics. DMDP can be viewed as a nitrogen-containing β-fructose mimic and it is related to another natural product D-AB-1 by the removal of one of the two hydroxymethyl groups (**FIGURE 2**).[3]

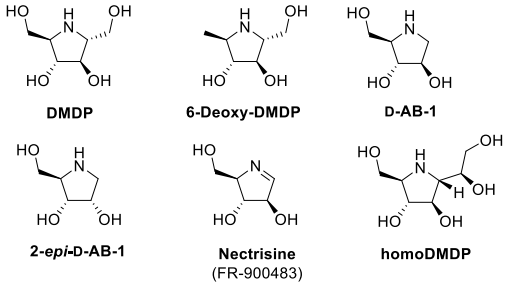

FIGURE 2. Some pyrrolidine iminosugars.

In 1966 NJ (Nojirimycin) was discovered as a first natural glucose mimic isolated from a *Streptomyces roseochromogenes* filtrate; *manno*-NJ (Nojirimycin B) and *galacto*-NJ (Galactostatin) were isolated soon after (**FIGURE 3**).[4] Despite their remarkable biological activity, they are fairly unstable due to the lability of hemiaminal function that rapidly gives the corresponding dehydration by-product. Therefore, they are stored as bisulfite

adducts or reduced as 1-deoxy-derivatives. DNJ (**1**; 1-deoxynojirimycin) was for the first time prepared by NJ reduction[5] and then isolated from the roots of mulberry trees as well as from *Streptomyces* cultures. FAG (Fagomine) is the 1,2-dideoxy analogue of DNJ and was isolated from the seeds of Japanese buckwheat and then in the leaves and roots of *Xanthocercis zambesiaca*.[6] α-HNJ (α-homonojirimycin) was the first discovered, naturally occurring C1-branched DNJ derivative;[7] however, before its isolation, its β-D-glucoside has been designed as a potential drug for the treatment of diabetes mellitus and only subsequently it was isolated from natural sources (**FIGURE 3**).

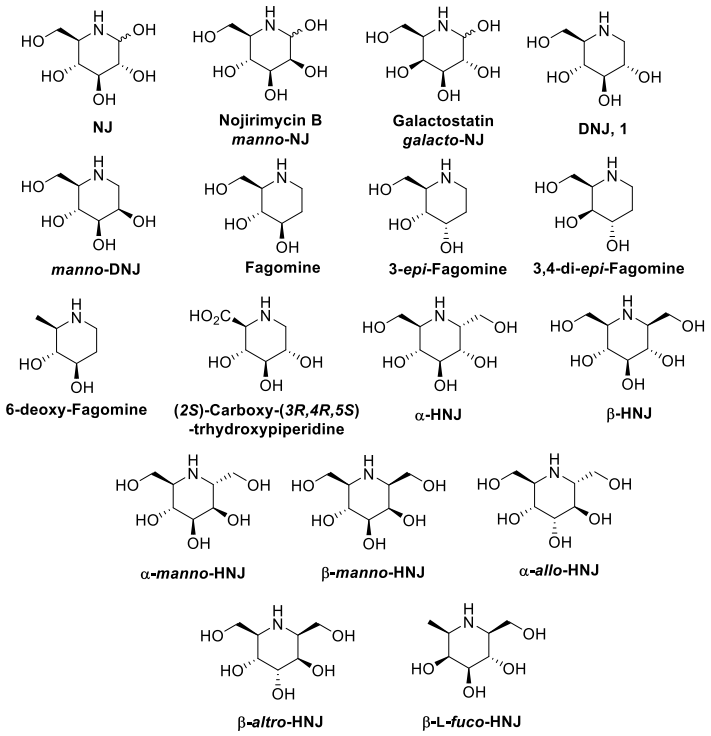

FIGURE 3. Some piperidine iminosugars.

As highlighted in **FIGURE 1**, there are three groups of bicyclic polyhydroxy-heterocyclic compounds, in which two five-membered rings (pyrrolizidines) or one five-membered ring and one six-membered ring (indolizidines and nortropanes) are fused together. These molecules have less obvious structural similarity toward monosaccharides but in each case the hydroxyl substituent configurations can be correlated to those of sugars. Castanospermine can be viewed as a bicyclic derivative of DNJ, with an ethylene bridge between the hydroxymethyl group and the ring nitrogen (**FIGURE 4**).

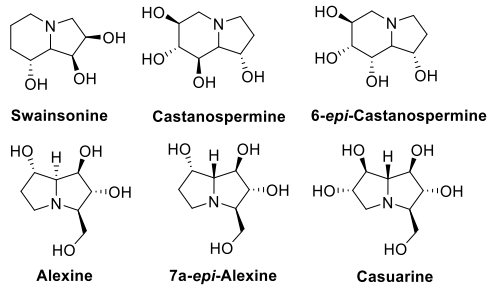

FIGURE 4. Some bicyclic iminosugars.

1.1.1.2 NITROGEN IN THE RING: STRUCTURAL BASIS TO EXPLAIN THE VERSATILE IMINOSUGAR BIOLOGICAL POTENTIAL

An attractive approach devoted to developing novel compounds able to selectively and potently interact with target enzymes relies on the design of mimics of their reaction (enzyme catalysed) transition state. The Transition State Theory is the rationale behind this method; it states that the reaction point in which the reactants have equal probability of going forward to products or reverting to reactants, is called transition state (TS) and the binding constant (K_d) with which the enzyme interacts with the TS is proposed to be 10^{10}-10^{15} fold more high then to the reactants. Therefore, ideally, chemically stable analogues of TS are expected to be efficient enzymatic competitive inhibitors. Iminosugars are sometimes defined "powerful glycomimetics" because of their great ability to interact as transition state analogues of carbohydrates processing enzymes, glycosidases and glycosyltransferases (**FIGURE 5**). In both cases, the TS is supposed to be quite close to a cation/oxocarbenium ion with a sp^2 character at the anomeric carbon (as deduced by isotope effects measurements) and spatially oriented in a half-chair conformation.[8] Therefore, it is easy to understand why the protonated forms of iminosugars, resembling in terms of charge such oxocarbenium TS, are able to efficiently interact with such enzymes, resulting their inhibitors[9] or enhancers. The resulting ammonium ion indeed would be expected to mimic the partial positive charge developing on the endocyclic oxygen and bind to the enzymatic anionic residues.[10] It must be noted that piperidinyl iminosugar such as NJ or DNJ typically adopt a chair-like conformation and, therefore, they cannot be expected to be perfect TS analogues (**FIGURE 5**). This assumption may be true, but as these derivatives bind 10^3-10^4 times more strongly to such enzymes than glucose, the protonated nitrogen must play an important role in the binding process.[11]

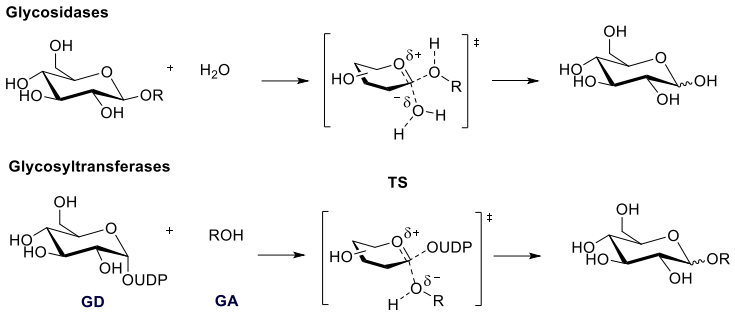

FIGURE 5. Reaction mechanism involving catalysis of glycosidases and glycosyltransferases. **GD** = Glycosyl Donor; **GA** = Glycosyl Acceptor; **TS** = Transition State.

Since glycosidases and glycosyltransferases are involved in a wide range of anabolic and catabolic processes (i.e. GSLs biosynthesis, lysosomal catabolism of glycoconjugates, glycoprotein biosynthesis, ER quality control and ER-associated degradation of glycoproteins) their *in vivo* modification or block by use of inhibitors or enhancers is of a great interest from a therapeutic point of view.

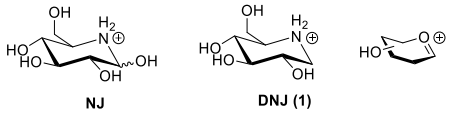

FIGURE 6. Conformational preferences of piperidinyl iminosugars and TS.

1.1.1.3 PHARMACOLOGICAL APPLICATIONS

The initial pharmaceutical interest in these compounds was related to their inhibitory activity toward a wide range of carbohydrate processing enzymes (as underlined in the above paragraph); thus, extensive efforts devoted to their isolation from natural sources or their synthetic preparation were made. However, over the last ten years, it has become clear that they can exploit biological function not only as enzyme inhibitors but also as their active-site chaperones and/or allosteric modulators. The difficult aim of the present section is to describe the main emerging and promising pharmacological applications[12] of this class of molecules, giving attention to those in which the iminosugars have displayed great efficacy and specificity.

1.1.1.3.1 IMINOSUGARS AS GLYCOSIDASE INHIBITORS

1.1.1.3.1.1 GAUCHER DISEASE: GCS INHIBITION

Lysosomal Storage Diseases (LSDs) are a collection of genetic disorders that typically occur in infancy or early childhood.[13] Over 40 different LDSs have been identified and are characterized by the accumulation of storage molecules in late

endosomes/lysosomes. Most of these disorders results from mutations in the genes that encode the catabolic enzymes of lysosome[14] leading to lysosomal storage of GSLs (glycosphingolipids);[15] Gaucher disease belongs to this specific subgroup. It is caused by the deficiency of β-glucocerebrosidase (acid β-glucosidase GBA1 or GCase; EC 3.2.1.45) and leads to accumulation of GlcCer[a] (GlucosylCeramide; see **FIGURES 7** and **9**).

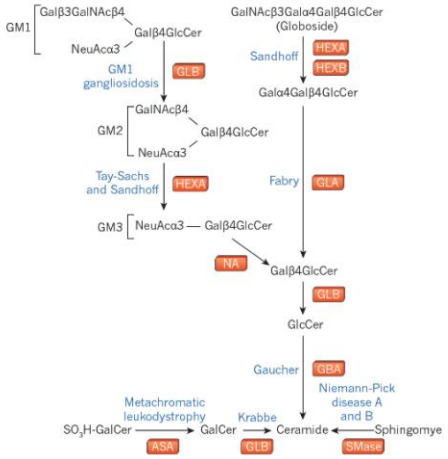

FIGURE 7. Glycosphingolipid catabolism and associated LSDs (adapted from ref. 15).

The ERT (Enzyme Replacement Therapy)[16] is one of the two approved clinical treatment for Gaucher disease; it consists in frequent intravenous infusions of the recombinant forms of wild-type enzymes (Cerezyme®). However, despite the remarkable efficacy of ERT in treating patients with Gaucher disease, lysosomal enzymes do not cross the blood-brain barrier; moreover, the high costs of ERT limit its global access. The only alternative approved therapy for LSDs is an oral, small-molecule approach termed Substrate Reduction Therapy (SRT) and it was applied for the first time in the treatment of Gaucher disease type 1. *N*-butyl-D-deoxynojirimycin (**2**, NBDNJ, Miglustat, Zavesca®; Actelion Pharmaceuticals Ltd) is the small molecule (see **FIGURE 8**) able to inhibit the first step in GSL biosynthesis – the conversion of Ceramide to GlcCer, catalysed by GlcCer Synthase, GCS (Ceramide glucosyltransferase, GlcCerT; EC 2.4.1.80). NBDNJ, because its structural homology with ceramide may in part explain its competitive inhibitory activity toward GCS (**TABLE 1**).[17] During their studies, Overkleeft *et al.* developed selective and potent inhibitors of GBA1, GBA2 and GCS, finding that *N*-[5-(adamantan-1-yl-methoxy)-pentyl]-1-deoxynojirimicyn (AMPDNM, **8**) was a 100-fold more potent GCS inhibitor than NBDNJ. However, **8** also strongly inhibited GBA1, GBA2 as well as intestinal lactase, sucrase and isomaltase resulting in

[a] GlcCer is substrate either of GBA1 and of GBA2 (as specified in the next paragraph).

a not selective compound; moreover, replacement of the adamantanemethyl group with linear alkyl substituents (butyl up to nonyl) led to comparable strong inhibition but not to selectivity (**FIGURE 8** and **TABLE 1**).[18]

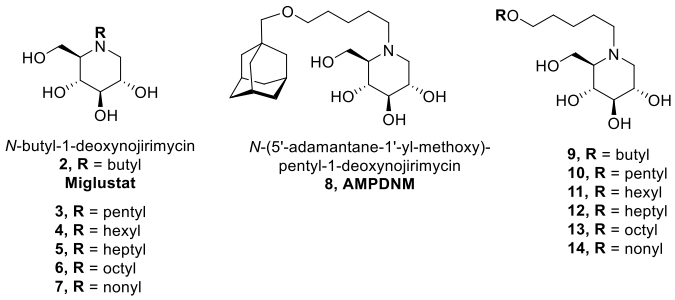

FIGURE 8. *N*-alkyl-D-iminosugars.

TABLE 1. IC_{50} (μM) of *N*-alkyl-D-iminosugars toward various enzymes.

Compound	*GCS*	*GBA1*	*GBA2*	*Sucrase*	*Lactase*	*Maltase*
2	50	400	0.23	0.6	750	9
3	>20	500	0.4	2	>1000	10
4	>20	80	0.11	1	700	10
5	40	18.5	0.045	0.5	500	10
6	4	4	0.020	0.75	300	8
7	4	1.5	0.007	0.4	200	8
8	0.2	0.2	0.001	2.5	35	4
9	4	30	0.06	2	300	8
10	2	705	0.04	1.2	300	4
11	1	205	0.008	2	200	5
12	0.3	1.75	0.015	0.8	250	7
13	0.2	0.5	0.010	1	200	10
14	0.1	0.5	0.040	1	350	25

1.1.1.3.1.2 CYSTIC FIBROSIS: GBA2 INHIBITION

Cystic Fibrosis (also referred as CF) is a genetic (inherited) disease caused by mutations in the gene which encodes for the Cystic Fibrosis Transmembrane Conductance Regulator (CFTR) protein.[19] The main CF severe symptoms and complications, due to

the chronic lung inflammation, are treated with antibiotics, non-steroidal anti-inflammatory drugs or glucocorticoids.[20]

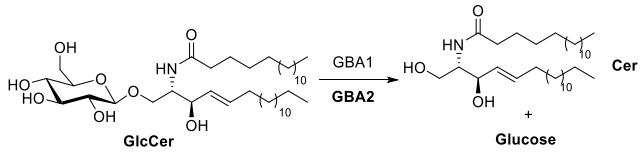

FIGURE 9. GlcCer metabolism.

Ceramide[b]-enriched membrane platforms have been identified as central to the host's cellular and tissue responses to *P. aeruginosa* infection in CF patients. These findings have suggested the possibility to correct the infection by modulating (reducing) ceramide levels to their physiological range opening the possibility of targeting Cer metabolism as new therapeutic strategy for CF lung disease.[21] Similarly to GBA1, also the neutral GBA2,[22] a non-lysosomal glucosylceramidase (β-glucosidase) residing in the cytoplasm, is able to degrade glucosylceramide (GlcCer) into Cer and glucose (**FIGURE 9**). *N*-alkylated iminosugars employed in several medicinal chemistry studies (e.g. SRT, Substrate Reduction Therapy) also inhibit GBA2 (**TABLE 1**). Particularly, D-NBDNJ (**2**, Miglustat, see **FIGURE 8**) inhibits GBA2 with IC_{50} values in the nanomolar range, whereas it inhibits GlcCerT and GBA1 at μM concentrations.[23] These values indicate that Miglustat holds a higher affinity to GBA2, compared with GlcCerT and GBA1. DeChecchi *et al.* have recently demonstrated that Miglustat reduces the *P. aeuriginosa*-dependent transcription of IL-8 in human bronchial epithelial cells *in vitro* and downmodulates neutrophil chemotaxis in murine lungs *in vivo*, providing clinical evidence to support the use of Miglustat in treating CF lung inflammation.[24,25]

1.1.1.3.2 IMINOSUGAR CHAPERONING ACTIVITY

As above mentioned for Gaucher Disease, most of the LSDs originate from the arrest of GSLs metabolism (the critical step at which it blocks depends by the specific disease), thus reactivation of the substrate hydrolysis with pharmacological chaperones could represent a valid strategy to rescue the precise defected glycosidase without interfering with any other enzymatic process.[26] This is the concept behind the Pharmacological Chaperone Therapy (PCT) applied for the first time in the treatment of Pompe disease (see **PARAGRAPH 1.1.1.3.2.1**) and then, successfully, for other LDSs (see for example **PARAGRAPH 1.1.1.3.2.2**). The main advantage in its formulation relies on the possibility to choose the glycomimetic chaperone tuning its configurational properties depending

[b] The cell membrane contains domains enriched with sphingolipids (SLs) and glycosphingolipids (GSLs); ceramide (Cer) (**FIGURE 9**) represents the SL metabolism cornerstone.

by its glycosidase discrimination capabilities (enzymes acting on *gluco* or *galacto*, α- or β-pyranosyl substrates). Pompe and Fabry diseases are perfect examples to well explain the latter concept.

1.1.1.3.2.1 POMPE DISEASE: GAA REACTIVATION

Acid α-glucosidase (GAA; EC 3.2.1.20) is a lysosomal enzyme enabling the degradation of glycogen to glucose (glycosyl hydrolase family, GH31).[27] A deficiency in GAA activity leads to intralysosomal glycogen storage, causing extensive and progressive damages to cardiac and skeletal muscles.[28] The genetic disorder due to mutations-induced functional defects of GAA is known as Pompe disease (PD; glycogen storage disease type II) and represents one of the most common lysosomal storage disorders (LSDs).[29] To date, the only clinically approved strategy for the treatment of the disease is the enzyme replacement therapy (ERT) based on intravenous administration of recombinant human GAA (rhGAA, Myozyme).[30] Even though ERT has shown to stabilize the disease course, use of rhGAA has some major limitations, regarding, *inter alia*, its adequate delivery to lysosomes and the stability to nonacidic conditions. Looking for alternative approaches, the identification of small molecule chaperones able to restore functions and properties of the mutated enzyme (the core of the so-called Pharmacological Chaperone Therapy, PCT) is representing an emerging strategy and a formidable challenge of the modern biomedical research.[31] According to PCT, the use of suitable GAA ligands enables stabilization of protein conformation, inhibits premature misfolding and facilitates enzyme translocation into the lysosome, thereby preventing ER-associated degradation processes. Among pharmacological chaperones,[32] the iminosugar drug[33] *N*-butyl-D-deoxynojirimycin (D-NBDNJ, **2**) currently represents one of the most promising candidates under development for the treatment of Pompe Disease. In early studies, Miglustat has been found to improve residual activity and lysosomal trafficking of mutated GAA in cultured fibroblasts from Pompe patients.[34] Even more remarkably, the chaperone has subsequently demonstrated to enhance the physical stability and therapeutic efficacy of rhGAA itself.[35] This finding has represented the first documented example of a synergistic effect deriving from the combined use of PCT and ERT, which has opened the way to the so-called "combination therapy" for the treatment of various LSDs. Higher lysosomal GAA levels in blood as resulting from co-administration of rhGAA and Miglustat have been recently found in animal models and in PD patients.[36]

1.1.1.3.2.2 FABRY DISEASE: α-Gal A REACTIVATION

Fabry Disease is a LSD caused by mutations in the GLA gene that encodes for lysosomal α-galactosidase A (α-Gal A; EC 3.2.1.22); α-Gal A cleaves α-linked galactopyranosyl

moieties of neutral GSLs, mainly GL-3 (glotriaosylceramide, **FIGURE 10**). Deficiency in α-Gal A activity results in the accumulation of GL-3, which gives rise to a variety of clinical manifestations such as cardiomyopathy, renal disfunction, stroke and neurological symptoms.[37] ERT using recombinant human α-Gal A has been available since 2001; two preparations are marketed: Replagal® (produced by Shire Human Genetic Therpies, Cambridge, MA) approved in the European countries and Fabrazyme® (produced by Genzyme Corporation, Cambrdige, MA) approved in the United States. Adverse effects of ERT include fever, rigors and chills; moreover, during ERT, disease progression may occur due to low physical stability of recombinant enzyme, a short circulating half-life and variable uptake in different tissues. Thus, novel therapeutic strategies are needed to treat patients with Fabry disease.

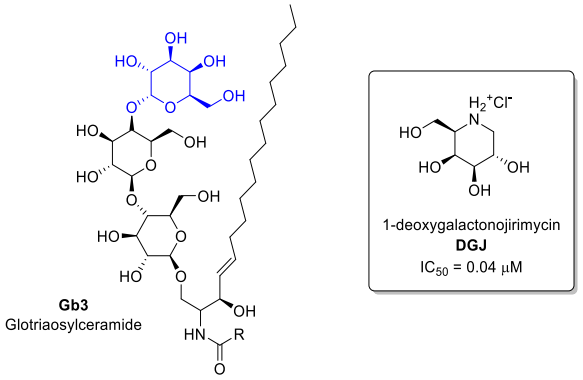

FIGURE 10. Gb3 and Migalastat.

Recently, 1-deoxygalactonojirimycin (DGJ, Migalastat, Galafold®) has been designed as orphan drug by FDA (2004) and then it has been approved by European Commission as drug for the treatment of Fabry disease (2016). The molecule is able to inhibit α-Gal A (it mimics the terminal galactose of Gb3, see **FIGURE 10**), but at sub-inihibitory concentration it is able to act as pharmacologic chaperone of the defected enzyme restoring its biological functions.[38] Furthermore, co-administration improves the pharmacological properties of recombinant human α-Gal A preventing its denaturation and activity loss.[39]

1.1.1.4 PHARMACEUTICAL ADVANTAGES AND DISADVANTAGES IN THE CLINICAL USE OF IMINOSUGARS

- *Advantageous properties:* iminosugars have several intrinsic positive properties useful to their candidature as potential drugs. Many potent small molecules have only marginal solubility and enormous resources and efforts are be made to address this issue both in medicinal chemistry and formulation. The iminosugars,

because of their polar nature, have instead adequate water solubility. The entry of iminosugars into cells appears to work by passive, non-facilitated diffusion, or by flip-flop across the membrane.[40] The rate of entry seems be independent of *N*-alkyl chain length but increasing lipophilicity results in more protein and membrane binding.[c] *In vivo* studies have also revealed a correlation between increasing *N*-alkyl-iminosugar hydrophobicity and tissue access and sequestration; for example a greater liver and brain penetration was observed for NNDNJ (**7**) (containing a 9-carbon chain) than for NBDNJ (**2**) (containing 4-carbon chain).[41] These factors, if extrapolated to humans, offer considerable potential benefit for treating the neuronopathic disorders where ERT is of marginal efficacy due to lack of blood–brain barrier access. Iminosugars are chemically and metabolically stable molecules; they are typically excreted unchanged in urine.[42] Such properties and others distinguish iminosugars from other small polar molecules and increase the attraction of using them as drug molecules.

- *Disadvantageous properties:* despite their enormous potential as therapeutics, to date very few iminosugars have reached the pharmaceutical market. In fact, their pharmacological applications are significantly hampered by the limited selectivity *in vivo*. Thus, they can be used for a plethora of therapeutic purposes, as seen above, but they are always accompanied by a wide variety of side effects due to their activities against other cellular enzymes. Adverse effects are: abdominal bloating, flatulence, diarrhoea (due to the inhibition of intestinal glucosidases), transient tremor, weight loss, axonal and peripheral neuropathy.[43] In order to overcome these problems, the effect of either the lipophilicity or the configuration of iminosugars has been explored over the last years.

1.1.1.5 Strategies Developed to Improve Iminosugar Enzymatic Selectivity

1.1.1.5.1 The Role of The Alkyl Chain

Lipophilicity has been postulated to enhance the selectivity of an iminosugar since lipophilic moieties can only be hosted by enzymes having lipophilic character. Studies have been conducted to determine some of the molecular features of *N*-alkylated iminosugars that contribute to enhance their selective recognition by GCS in comparison with ER α-glucosidase I.[44] The presence of an alkyl chain is obligatory for the transferase inhibition and, moreover, there is a direct correlation between inhibition potency and

[c] The effect of the alkyl chain lenght on the binding and inhibition potency exhibited by *N*-alkyl iminosugars toward glycosidases will be discussed in detail in the next paragharphs.

chain length, probably due to the greater ceramide mimicry (**FIGURE 11a**). On the other hand, the α-glucosidase inhibition is independent of the *N*-alkyl chain and changes in chain length; the inhibition seems mediated in this case by the close resemblance to the charged character of the oxocarbenium TS (**FIGURE 11b**). These studies offer the possibility to develop inhibitors able to selectively interact with one or the other enzyme leading to compounds for the potential treatment of LSDs and viral infections, respectively.[45]

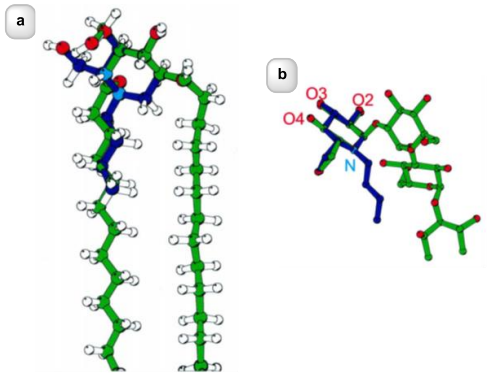

FIGURE 11. a) Overlay between NBDNJ (**2**) and Ceramide; b) Superposition of NBDNJ (**2**) and the terminal glucose residue of $Glc_3Man_9GlcNAc_2$ which is removed by α-glucosidase I (figure adapted from ref. 44).

As another example explaining the role of the alkyl chain, Sussman *et al.* solved the crystal structures of the complexes of both NBDNJ (**2**) and NNDNJ (**7**) bound to GBA1 (**FIGURE 12**).[46] NNDNJ clearly shows a stronger and more stable interaction with the enzyme than NBDNJ, due to the additional interactions with the hydrophobic residues in the active site of the enzyme. NNDNJ has in fact demonstrated to keep inhibitory properties only toward specific glycosidases (see **TABLE 1**). Therefore, this approach represents an interesting opportunity to increase the selectivity in glycosidase inhibition.

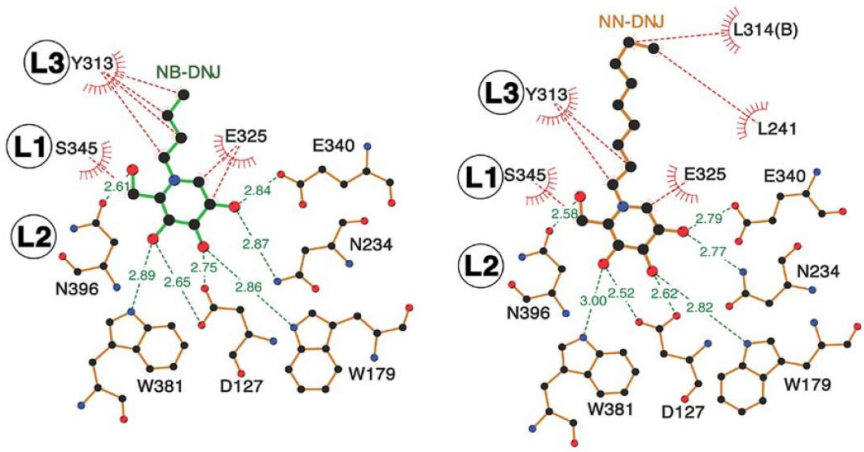

FIGURE 12. NBDNJ and NNDNJ in complex with GBA1 (taken from ref. 46).

1.1.1.6 LOOKING-GLASS GLYCOMIMETICS: L-IMINOSUGARS

As widely reported, the pharmacological interest around iminosugars is principally devoted to those belonging to D-series but, in recent times, their unnatural mirror images, i.e. L-iminosugars, have been completely re-evaluated.[47] Asano *et al*. reported[48] the first comparative inhibition study of D- and L-deoxyiminosugars toward various glycosidases revealing that L-DNJ (*ent*-**1**) and L-DGJ (**FIGURE 13**) are, surprisingly, inhibitors of α-glucosidases and of α-galactosidase respectively (L-DNJ: IC_{50} = 4.3 μM; L-DGJ: IC_{50} = 13 μM), even if with less potency showed by the corresponding natural enantiomers. L-*allo*-DNJ is an inhibitor of α-mannosidases (IC_{50} = 30 μM) despite D-*allo*-DNJ and, more interestingly, it is able to inhibit the same enzymes better then D-*manno*-DNJ (D-DNM: IC_{50} = 840 μM).

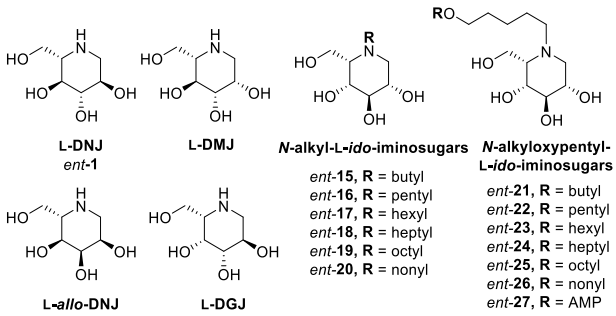

FIGURE 13. L-iminosugars.

L-DGJ is a less potent inhibitor of α-galactosidases but is strong inhibitor of α-L-fucosidase (IC_{50} = 0.63 μM) (**FIGURE 13**). In more recent times, Overkleeft *et al.* identified[49] in various C-5 *gluco* epimers (L-*ido* congeners) potent, but especially,

strongly selective GCS inhibitors; they observed, moreover, that the ether oxygen atom positioned at C5' leads to much more potent GCS inhibitors when compared to the *N*-alkyl series[50] (**TABLE 2**). From this extensive study, *ent*-**27** has resulted the most potent and selective iminosugar-based GCS inhibitor and might be considered in the treatment of Gaucher disease in the frame of SRT. It is difficult to soon understand why L-iminosugars are able to act as inhibitors and in some cases able to mimic the transition state of glycosidase and glycosyltransferase catalysed reactions, but some exceptions may occur.

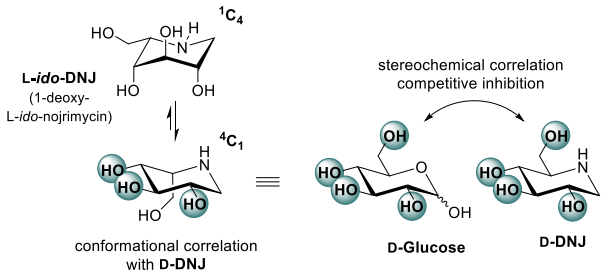

FIGURE 14. Stereochemical correlation between L-*ido* congeners and D-glucose.

As an example, **FIGURE 14** shows the structure of the iminosugars with L-*ido* configuration, whose conformation fluctuates between the $^{1}C_{4}$ and $^{4}C_{1}$ forms. In the latter conformation, L-*ido*-DNJ partially resembles the structure of natural D-glucose; this stereochemical correlation could explain the inhibitory potency showed by L-*ido*-congeners. On the other hand, when no stereochemical correlation can be found, the inhibitory character can be related to a non-competitive mechanism, additionally only toward specific, non-enantioselective glycosidases. Because of these collected data and considerations, it is easy to understand the reasons why the synthesis of *N*-alkyl-L-iminosugars currently represents a challenging task in this field. Some selected and innovative procedures devoted to this aim are briefly reported in the next paragraph.

TABLE 2. IC_{50} (μM) of *N*-Alkyl-L-*ido*-iminosugars toward various enzymes.

Compound	*GCS*	*GBA1*	*GBA2*	*Sucrase*	*Lactase*	*Maltase*
*ent-**15***	20	>1000	1	>1000	>1000	>1000
*ent-**16***	15	>1000	0.25	>1000	>1000	>1000
*ent-**17***	40	>1000	0.14	600	700	10
*ent-**18***	40	18.5	0.045	0.5	500	>1000
*ent-**19***	4	25	0.02	60	100	600
*ent-**20***	2	50	0.01	>1000	>1000	>1000
*ent-**21***	2	>1000	0.09	>1000	400	>1000
*ent-**22***	0.15	100	0.015	>1000	200	>1000
*ent-**23***	0.1	95	0.025	>1000	200	>1000
*ent-**24***	0.05	40	0.015	>1000	250	>1000
*ent-**25***	0.05	15	0.015	>1000	300	>1000
*ent-**26***	<0.05	012	0.045	>1000	350	>1000
*ent-**27***	0.1	2	0.03	>1000	>1000	>1000

1.1.1.7 SYNTHETIC APPROACHES TO *N*-ALKYL-L-IMINOSUGARS

The access to L-iminosugars is clearly hampered by their poor availability from natural sources. Accordingly, a variety of innovative strategies, including those aiming at obtaining the whole series of compounds, has been devised over the past few years. In one of these approaches, Kato *et al.*[48] prepared DNJ epimers with L-*altro*, L-*ido*, L-*galacto* and L-*gulo* configurations as single compounds under highly stereoselective conditions; on the other hand, L-*gluco*-DNJ, L-*allo*-DNJ and L-*manno*-DNJ were prepared as diastereoisomeric mixtures. The procedure involved the use of dioxanylpiperidine **30** as starting material; the latter was obtained (as depicted in retrosynthetic path, **SCHEME 1a**) from L-Garner aldehyde. The crucial step is the conversion of the diolefin product **29** to give **30** through a ring closing methatesis (RCM) in presence of Grubbs' catalyst.[51,52]

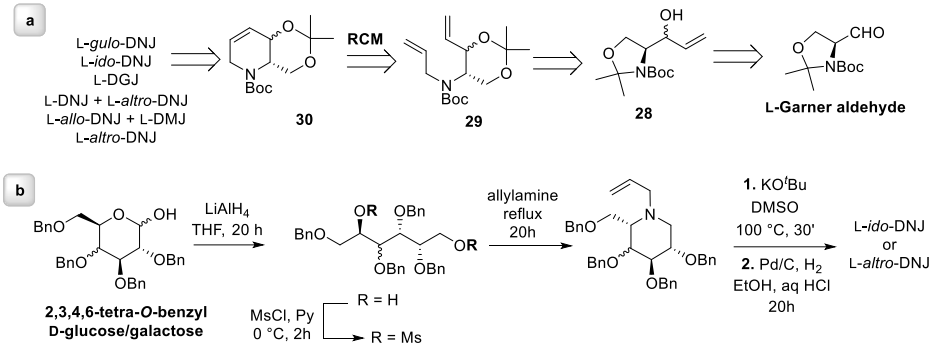

SCHEME 1. a) *De novo* strategy to prepare L-iminosugars; b) carbohydrate-based route to prepare L-iminosugars.

The procedures proposed by Overkleeft *et al.* to prepare the L-*ido* and L-*altro* congeners,[53] differently from the previous strategy, are carbohydrate-based routes. Particularly, L-*ido* and L-*altro* congeners were synthetized starting from 2,3,4,6-tetra-*O*-benzyl-D-glucitol or from 2,3,4,6-tetra-*O*-benzyl-D-galactitol respectively (**SCHEME 1b**).

More recently, Guaragna *et al.* finely tuned a highly stereocontrolled *de novo* strategy[54] to obtain enantiomerically pure D- and L-iminosugars (**SCHEME 2**). The synthesis involves the use of an heterocyclic synthon, the 5,6-dihydro-1,4-dithiin-2-yl- [(4-methoxybenzyl)oxy]methane[55] **31**, a reagent capable of three-carbon homologation of electrophiles, such as the Garner aldehyde **32**. As depicted in the retrosynthetic scheme, the two synthons (the reaction conditions were tuned in order to "pre-establish" the C4 chirality) were useful to afford the bicyclic compound **33**, from which, by dithioethylene bridge removal, the key olefin **34** could be obtained. Then, *syn* or *anti* dihydroxylations of **34** allowed us to obtain six of the eight possible L-epimers (**SCHEME 2**).[54,56]

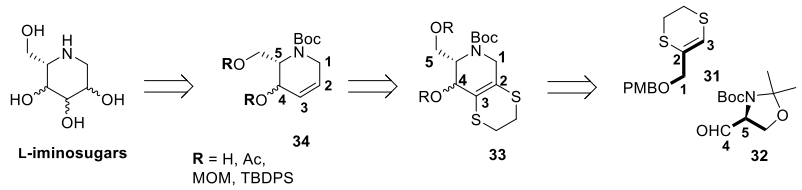

SCHEME 2. *De novo* stereocontrolled method to prepare L-iminosugars.

The introduction of the alkyl chain is generally performed by typical reductive amination conditions ($CH_3(CH_2)_nCHO/NaBH_3CN/AcOH$ in MeOH). Overkleeft *et al*. developed a simple strategy to this aim which involves the use of alkylbromides as electrophiles in the coupling reaction with the iminosugar core. The same procedure can be easily applied also to prepare alkoxypentyl iminosugars (**SCHEME 3**).

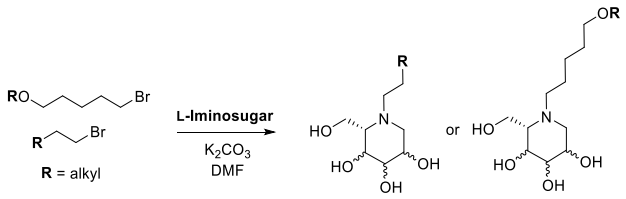

SCHEME 3. Synthetic strategy to prepare *N*-alkyl and *N*-alkoxypentyl-L-iminosugars.

L-AMP-congeners were prepared by condensation (via reductive amination) of the iminosacaridic core with 5-(adamantan-1-yl-methoxy)-pentanal **39**. In this regard, Overkleeft *et al*. developed a pilot-scale procedure[57] to prepare **39** in five steps starting by 1,5-pentandiol (**35**) with a 47% of overall yield (**SCHEME 4a**).

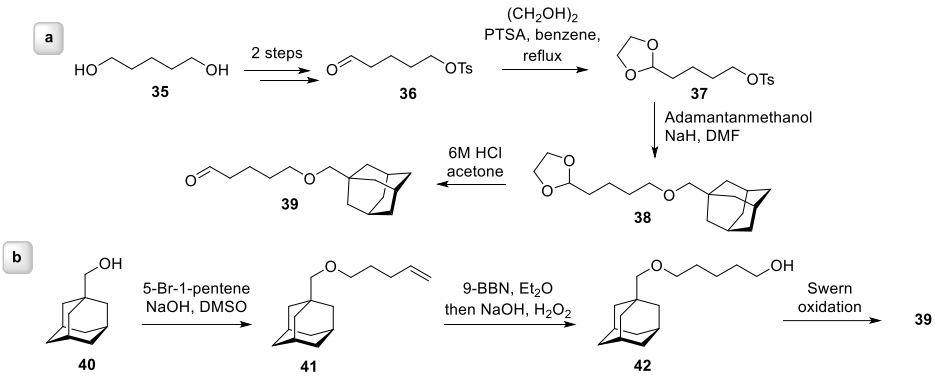

SCHEME 4. Synthetic strategies to obtain **39**.

Since this procedure was affected by difficult purification procedures, a more expeditious method to afford **39** with higher yield (55% o.y.) was later conceived by Cooper *et al.* (**SCHEME 4b**).[58]

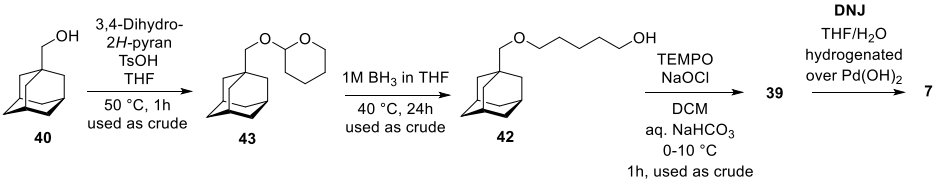

SCHEME 5. Industrial synthetic procedure to prepare **8**.

However, this method also required optimization before large scale applications. In the same paper[58] the authors reported the direct production of AMPDNM (**8**) by an economic and scalable method that involves the three-step synthesis of **39** with high yield and purity by selective cleavage of an endocyclic C-O bond of a THP ether using borane/THF as the key step. The subsequent coupling of **39** with DNJ gave **8** in 50% o.y. (**SCHEME 5**).

1.1.2 RESULTS AND DISCUSSION

On the basis of the data discussed in the previous section, one of the main topic of this PhD research program was focused on the study of the role of chirality on the activity and selectivity of *N*-alkyl iminosugars in various research areas with therapeutic relevance. Particularly, a highly stereocontrolled *de novo* synthesis of L-DNJ (*ent*-**1**) was efficiently accomplished (**FIGURE 15**).[56] Synthetic efforts were also aimed to the assembly of a variety of alkyl chains, leading to the target *N*-alkyl iminosugars (**FIGURE 15**).

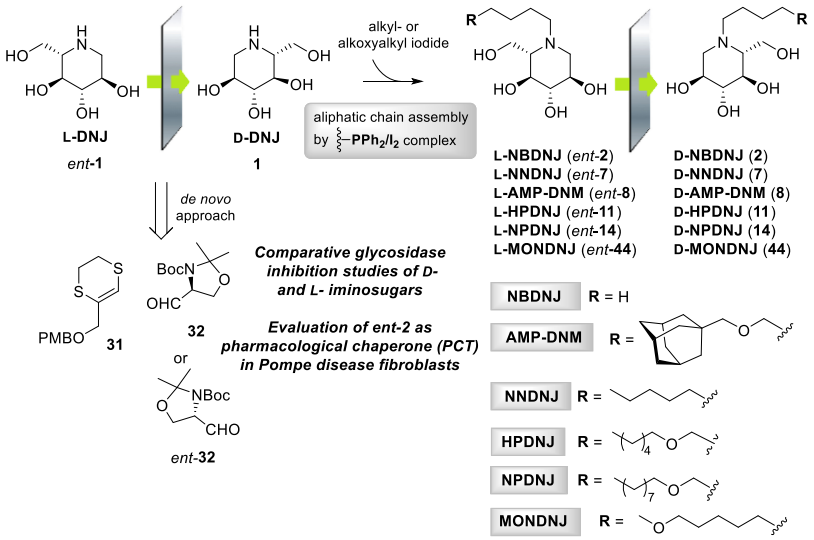

FIGURE 15. Synthetic approaches developed to prepare enantiopure *N*-alkyl-D- and L-iminosugars.

With D- and L- *N*-alkyl-iminosugars in hand, the analysis of their glycosidase inhibition properties was extensively performed; furthermore, the chaperoning potential of *ent*-**2** in the context of PCT applied to Pompe Disease was preliminarily explored.

1.1.2.1 *DE NOVO* SYNTHESIS OF L-DNJ

To the best of our knowledge, the synthesis of *ent*-**1** has never been reported before.[59] More generally, as mentioned above, the access to L-iminosugars is often problematic due to the limited commercial availability of almost all L-hexoses, which hampers their use as starting materials. Alternatively, in an extension of a long studied[60] *de novo* methodology, already devised to obtain unnatural carbohydrates and biomimetic agents[61] including iminosugars[52] and their precursors,[62] the synthesis of *ent*-**1** was explored from the synthetically available alcohol **45** (**SCHEME 6**).

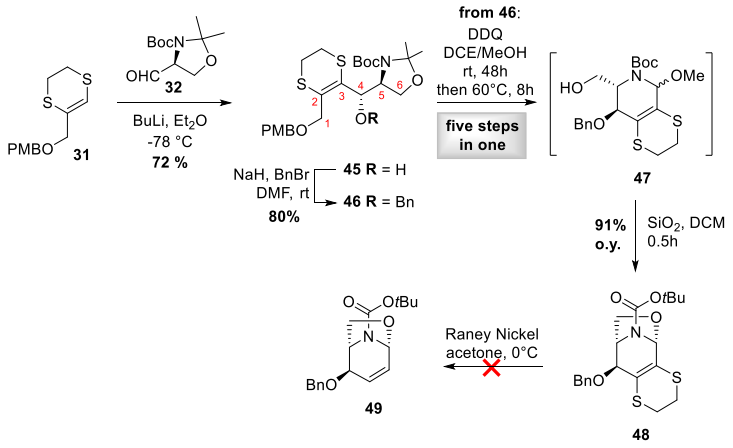

SCHEME 6. *sec*-Alcohol **45** elaboration.

In early attempts, inspired by previous results on L-glucose synthesis,[63] the preparation and stereoselective functionalization of 1,6- anhydro-iminosugar was considered (**SCHEME 6**). *sec*-Alcohol **45** was first benzylated under common conditions (NaH, BnBr). The resulting benzyl ether **46** was then treated with a DCE/ MeOH solution of 2,3-dichloro-5,6-dicyano-1,4-benzoquinone (DDQ), directly providing, after 48h at rt and then 8 h at 60 °C, the bicyclic compound **47**. Spontaneous cyclization of **47** into 1,6-anhydro-iminosugar precursor **48** was even observed during chromatographic purification procedures. In spite of the synthetic utility of the reaction, **48** could not be further functionalized, as the subsequent double-bond unmasking step (Ra−Ni) did not provide the expected olefin **49** (**SCHEME 6**).

Looking for alternative strategies, we then investigated the reactivity of oxirane **53**, obtained from alcohol **45** as previously described[54a] (**SCHEME 7**).

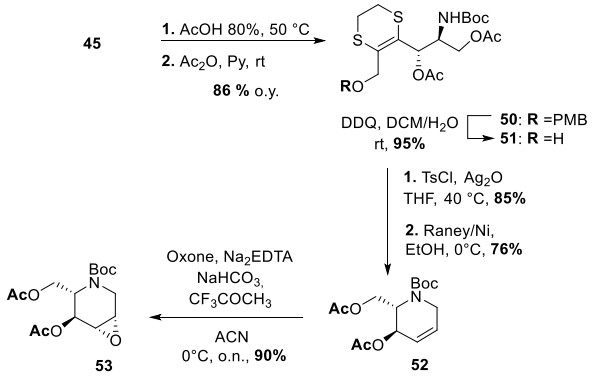

SCHEME 7. Synthetic route to oxirane **53** (ref 54a).

Particularly, the synthetic problem at this stage was the introduction of the two remaining stereocenters at C2 and C3 positions, having a *trans*-diequatorial orientation of the substituents. Indeed, as depicted in **SCHEME 8**, the *trans*-diaxial opening of oxirane would allow us to obtain, depending on the adopted conformation $^{4}C_{1}$ or $^{1}C_{4}$, two different stereoisomers, the desired L-*gluco* epimer and the undesired L-*altro* epimer, respectively.

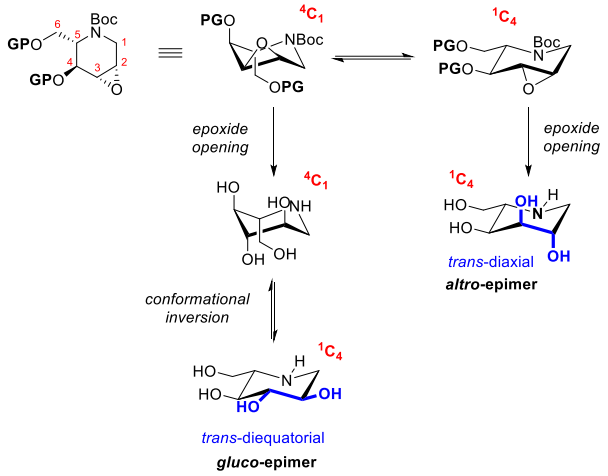

SCHEME 8. Synthetic problem to stereoselectively obtain *ent*-**1**.

Treatment of **53** with refluxing NaOH directly produced the unprotected iminosugar with L-*altro* configuration *ent*-**54** (*altro*:*gluco* > 20:1; **SCHEME 9**). Conversely, treatment of *bis*-MOM acetal **56** (from **53**: MeONa, then MOMCl/DIPEA) under the same conditions gave, after the subsequent HCl addition to the crude mixture, the desired *gluco* epimer *ent*-**1** as the only detected stereoisomer (dr > 99:1).

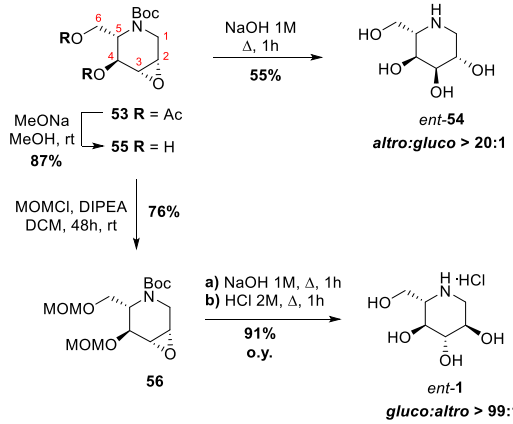

SCHEME 9. Stereocontrolled *de novo* synthesis of *ent*-**1**.

The stereodivergent outcome of the reactions was assumed to rely on the conformational preferences of epoxides **53** and **56** depending by the nature of C4 and C6 substituents. We observed[54a] that diacetate **53** adopts a $^{3}S_{1}$ sugar conformation having both C4 and C6 substituents in pseudodiaxial orientations (**SCHEME 10**).

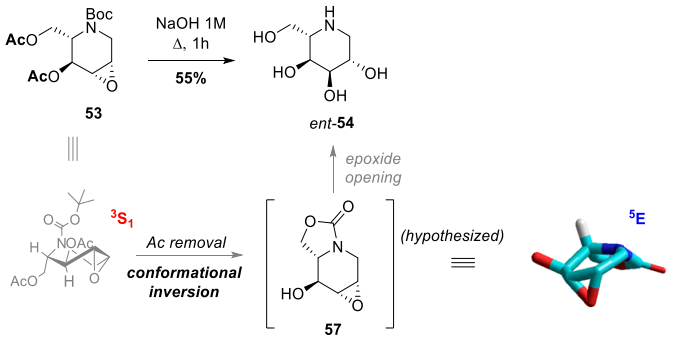

SCHEME 10. Basic treatment of **53** to afford L-*altro*-DNJ.

In line with previous findings, this behaviour was judged to be a consequence of the steric clash occurring between the *N*-Boc and the pseudoequatorially oriented C6 acetate group. Accordingly, the formation of *altro*-DNJ from **53** was hypothesized to take place via the base-labile cyclic carbamate[64] intermediate **57** (**SCHEME 10**). In agreement with literature data,[65] an energy-minimized structure of **57** suggested that it was firmly locked in a quasi-planar conformation close to a ^{5}E form with a pseudo-equatorially oriented methyleneoxy moiety (**SCHEME 10**). The conformational inversion from epoxide **53** to **57** justified the formation of *altro*-DNJ after *trans*-diaxial epoxide ring opening of **57**. Conversely, when the Ac group was replaced by the base-stable MOM group, the oxirane ring cleavage of *bis*-acetal **56** only provided the *gluco*-configured diol **58** (**SCHEME 11**). Even though the broadness of most NMR signals of epoxide **56** hampered the identification of its preferred conformation, NMR analysis of diol **58** (obtained by NaOH treatment of **56**) indicated a conformation with all substituents in near axial orientations ($J_{1,2}$ = 2.5 Hz; $J_{3,4}$ = 1.8 Hz; $J_{4,5}$ = 2.6 Hz). Close agreement between these calculated *J* values and those obtained from an energy-minimized structure[66] (**SCHEME 11**) suggested that a $^{4}C_{1}$ chair was adopted in this case. Eventually, the "all-equatorial" L-DNJ·HCl *ent*-**1** was obtained by the concurrent removal of *N*-Boc and MOM groups, enabling as expected a conformational inversion from $^{4}C_{1}$ to $^{1}C_{4}$ chair.

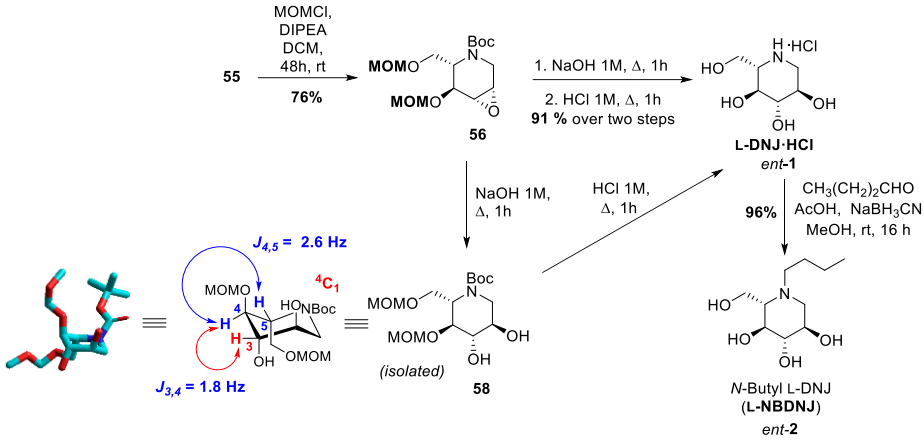

SCHEME 11. Stereoselective synthesis of L-DNJ.

1.1.2.2 SYNTHESIS OF *N*-ALKYL-L-DEOXYIMINOSUGARS

With L-DNJ in hand, the access to the corresponding *ent*-**2** (L-NBDNJ) was achieved under standard *N*-alkylation conditions (**SCHEME 11**). The synthesis of other *N*-alkyl-L-deoxyiminosugars *ent*-**7**, *ent*-**8**, *ent*-**11**, *ent*-**14** and *ent*-**44** was instead accomplished exploring alternative routes, aimed first to the assembly of the alkyl chains and then to their insertion into L-DNJ by *N*-alkylation. Particularly, we studied expeditious procedures to obtain alkyl or alkoxypentyl iodides (to be used as electrophiles in the subsequent alkylation reaction with L-DNJ) using the established method[67] of triarylphosphine and iodine (**SCHEMES 12-14**). In early studies, we devised a procedure to convert alcohols **59a-c** into alkoxypentyl iodides **62a-c** by iodination of **59a-c**, subsequent coupling reaction of **60a-c** with 1,5-pentandiol (**35**) and eventual iodination of alcohols **61a-c**. While the synthetic protocol was tuned at first using TPP/I_2 (TPP: triphenylphosphine) as the iodination reagent (**SCHEME 12,** Method A), TPP was later replaced by the recyclable polystyryl diphenylphosphine (PS-DPP, Method B). Indeed, given the efficiency of the reactions, the synthetic conditions were optimized to obtain a sequence of steps not requiring extractive work-up and chromatographic purifications. As a result, NMR analysis of the crude mixtures of **62a-c** demonstrated that high-yielding conversions (70-88% o.y.) could be obtained in all cases, with virtually no side products attributable to the limiting reagents (**SCHEME 12**).

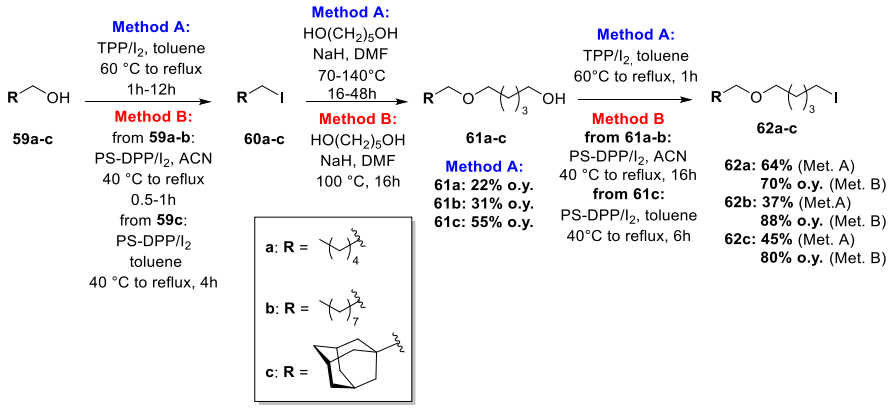

SCHEME 12. Iterative iodination reactions to prepare alkyl and alkoxypentyl iodides **62a-c**.

The strategies reported in **SCHEME 12** represent faster alternatives to most procedures devised for the preparation of alkyl and alkoxypentyl chains. In search for an even more expeditious protocol, in subsequent studies an alternative synthetic route was conceived, involving a double iodination of 1,5-pentandiol (**35**), to provide 1,5-diiodopentane (**63**, see **TABLE 3**), followed by coupling reactions with alcohols **59a-c** (**SCHEME 13**). In this case, the use of PS-DPP was only examined.

TABLE 3. Reaction conditions for the double iodination of 1,5-pentandiol (**35**).

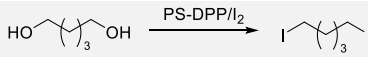

Entry	Solvent	T (°C)	t (h)	Yield (%)
1	1,4-Dioxane	reflux	12	46
2	1,4-Dioxane	50	3	52
3	ACN	25	12	86
4	DCM	25	1	95

The efficiency of the double iodination reaction to obtain **63** was markedly influenced by the reaction conditions: over a variety of solvents tested (**TABLE 3**), the most convenient conversion (95%) involved the use of DCM for 1h at rt (entry 4). The subsequent coupling reaction of **63** with alcohols **59a-c** proceeded smoothly with hexanol (**59a**) and nonanol (**59b**), providing, after 48h at rt, the corresponding alkoxyalkyl iodides **62a,b** in 65 and 64% yields, respectively (**SCHEME 13**). On the other hand, the reaction with adamantane-methanol (**59c**) was slower, and the corresponding iodide **62c** was obtained with a 62% yield after 72h at rt (**SCHEME 13**).

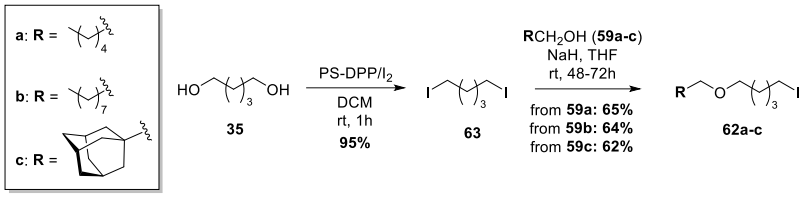

SCHEME 13. A more expeditious route to prepare iodides **62a-c.**

With **62a-c** in hand, their eventual reaction with L-DNJ was carried out under standard conditions. Treatment of L-DNJ (*ent*-**1**) with nonyl iodide **60b** (K_2CO_3) smoothly provided *ent*-**7** in 80% yield. Under the same conditions, the reaction of *ent*-**1** with iodides **62a-c** gave the corresponding *N*-alkyl L-DNJ derivatives *ent*-**8**, *ent*-**11** and *ent*-**14** in satisfactory 75-80% yields (**SCHEME 14**). The same *N*-alkylation reactions using D-DNJ as the nucleophile afforded the corresponding natural enantiomers **7**, **8**, **11** and **14**.

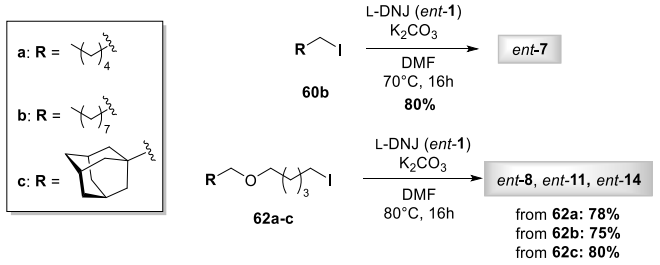

SCHEME 14. Coupling reactions to afford to *ent*-**7**, *ent*-**8**, *ent*-**11** and *ent*-**14.**

Compounds **44** and *ent*-**44** were instead prepared as depicted in **SCHEME 15**. The reaction of iodomethane with monoalcoholate of 1,9-nonandiol (**64**) afforded alcohol **65** (90%), whose subsequent iodination reaction to provide **66** (TPP/I_2) was unfortunately unsuccessful.[68] Other studies are currently ongoing to explore more efficient strategies to this aim. Alternatively, **65** was treated under typical Swern conditions to give aldehyde **67**; the subsequent condensation reaction with D- or L-DNJ eventually provided **44** and *ent*-**44**, respectively.

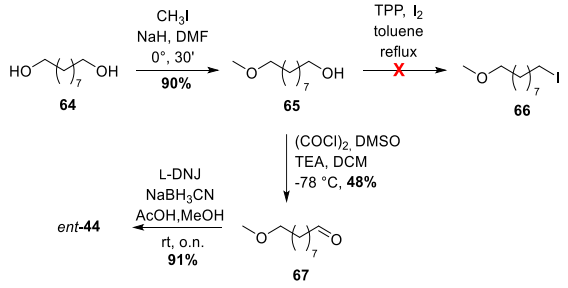

SCHEME 15. Synthetic route to **44** and *ent*-**44.**

1.1.3 BIOLOGICAL ASSAYS

The biological studies of this project were at first focused on the comparative analysis of the inhibition potential of **1, 2, 7, 8, 11, 14, 44** and *ent*-**1**, *ent*-**2,** *ent*-**7,** *ent*-**8,** *ent*-**11,** *ent*-**14,** *ent*-**44** as well as of the corresponding racemic mixtures against a variety of glycosidases, including the pharmacologically relevant rhGBA1 (Cerezyme®, β-glucosidase) and GAA (acid α-glucosidase). The experiments were performed under the supervision of Dr David Priestman and Prof. Frances Platt at Department of Pharmacology (University of Oxford) and by the research group of Prof. Marco Moracci at the National Council of Research (CNR) of Naples. In subsequent studies (in collaboration with Prof. G. Parenti), a preliminary evaluation of the potential of L-iminosugars, especially of *ent*-**2**, as enhancer of GAA activity was performed, with concrete applications in the treatment of Pompe disease.

1.1.3.1 GLYCOSIDASE INHIBITION STUDIES

In preliminary assays, the comparative analysis of the inhibition properties of D- and L-iminosugars were tested using D- and L-NBDNJ (**2** and *ent*-**2**) as model inhibitors, while selected glycosidases were chosen as representative examples of various GH families (**TABLE 4**). The enzymatic assays rely on the use of 4-methylumbelliferyl-D-glycopyranoside as substrate (**SCHEME 16**), exploiting the fluorescent properties of 4-MU to evaluate the residual activity of the glycosidases.

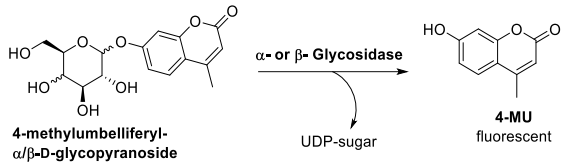

SCHEME 16. Fluorescence assay of 4-MU.

No inhibitory effect up to 1 mM was found for *ent*-**2** in most cases, except for the very weak inhibition of intestinal sucrase/isomaltase (38% inhibition, IC_{50} 2 mM, entry 2), lactase (30% inhibition, IC_{50} > 5 mM, entry 4) and α-fucosidase (19%, entry 13). Instead, rhGAA (Myozyme) and β-glucosidases from *Pyrococcus furiosus* and *Sulfolobus solfataricus* P2 even showed a 20−25% activation even though no significant enhancement in the melting temperature (T_m) of rhGAA by *ent*-**2** was indicated by differential scanning fluorimetry experiments (**FIGURE 16**).

TABLE 4. Residual activities (%) of various glycosidases after treatment with either **2** or *ent*-**2**.

Entry	*Enzyme*	*GH family*	*2*	*ent-2*
1	Rice α-glucosidase	GH31	17	98
2	Intestinal sucrase/isomaltase	GH31	3	62
3	rh-GAA (Myozyme™)	GH1	19	125
4	Intestinal lactase	GH1	62	70
5	β-glucosidase (*P. furiosus*)	GH1	81	120
6	β-glucosidase (*S. solfataricus P2*)	GH1	94	124
7	rh-GBA1 (Cerezyme)	GH30	35	97
8	Human β-hexosaminidase	GH20	98	98
9	α-galactosidase (*T. maritima*)	GH36	82	100
10	rh-Gal A	GH27	100	104
11	β-galactosidase (*A. acidocaldarius*)	GH42	98	102
12	Human β-galactosidase	GH35	87	98
13	α-fucosidase (*S. solfataricus*)	GH29	83	81

Addition of 0.1 or 1 mM D-NBDNJ **2** to a phosphate buffer (pH 7.4) containing Myozyme significantly enhanced the melting temperature (T_m) of the latter (0.1 mM: ΔT_m = +12°C; 1 mM: ΔT_m = +14.8°C).

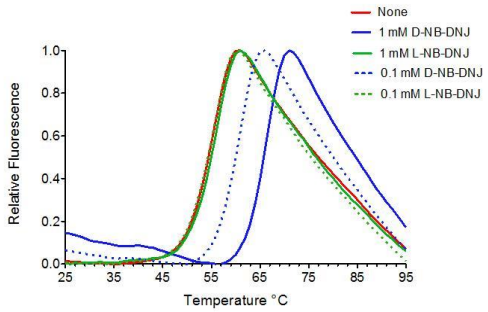

FIGURE 16. Stabilization of rhGAA (Myozyme™) by D-NBDNJ and L-NBDNJ as suggested by differential scanning fluorimetry.

Conversely, no significant stabilizing effect was observed with L-NBDNJ *ent*-**2** under the same conditions (0.1 mM: ΔT_m= +0.3°C; 1 mM: ΔT_m = +1.4°C). Conversely, **2** displayed inhibition of rice α-glucosidase (IC_{50} = 275 μM, entry 1), sucrase/isomaltase (IC_{50}= 1.5 μM, entry 2) and recombinant human β-glucocerebrosidase (rhGBA1 or

Cerezyme: IC_{50}=0.3 mM, entry 7). Inhibition of rhGAA was also observed (IC_{50}=158 μM, entry 3). In subsequent studies, the comparative analysis of glycosidation inhibition was extended to a number of *N*-alkyl-D- and L-iminosugars and focused on the inhibition of some pharmacologically relevant glycosidases, including lysosomal glucocerebrosidase 1 (GBA1) and acid α-glucosidase (GAA). These enzymes are involved in the onset of specific lysosomal storage disorders, including Gaucher's disease (GBA1) and the Pompe disease (GAA). The compounds were tested individually first and then as racemic mixtures in the search for potential synergistic effects. Their inhibitory activities toward the easily accessible recombinant form of GBA1, rhGBA1 (Cerezyme®) are reported in **FIGURE 17** and **TABLE 5**. As expected, **FIGURE 17** highlights a stronger inhibition by D-enantiomers than the corresponding L-enantiomers. Particularly, even though D- and L-DNJ had broadly same low activity (D-DNJ: IC_{50} = 0.74 mM; L-DNJ: IC_{50} = 0.83 mM), the effect of alkyl chain was much more markedly beneficial for D-iminosugars: as an example, activity was increasingly higher from D-MONDNJ (**44**) (IC_{50} = 18 μM, entry 19) to D-AMPDNM (**8**) (IC_{50} = 1 μM, entry 10); on the other hand, L-AMPDNM (*ent*-**8**) was a moderate inhibitor of rhGBA1 (IC_{50} = 50 μM, entry 11).

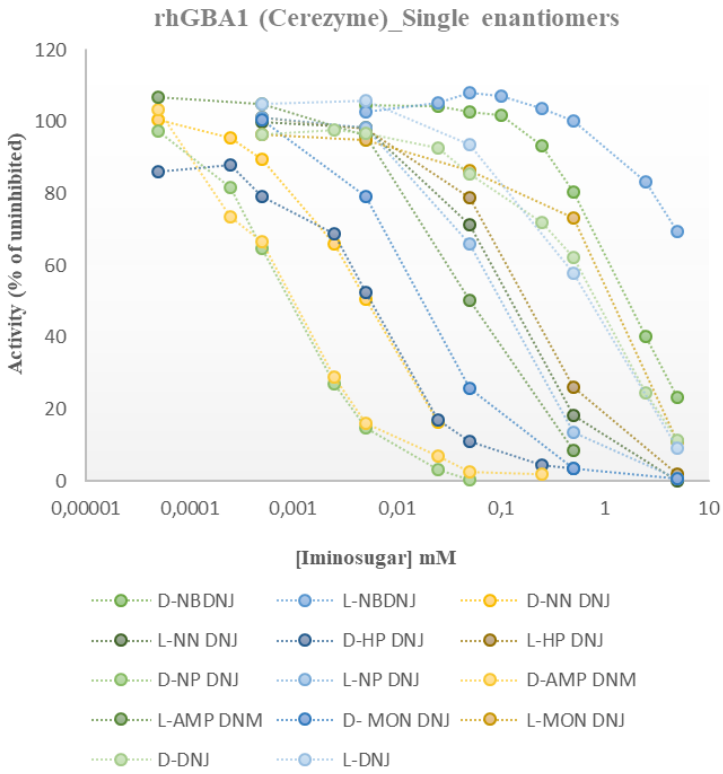

FIGURE 17. rhGBA1 inhibition curves.

Noteworthy, L-NBDNJ showed, analogously to previous results (**TABLE 4**), an enhancing effect when co-incubated at concentrations in the range of 5-50 μM (see **FIGURE 17**).

TABLE 5. IC_{50} (μM) of D- and L-iminosugars and of the corresponding racemates toward rhGBA1.

Entry	Sample	IC_{50} (μM)
1	D-DNJ **(1)**	830
2	L-DNJ **(*ent*-1)**	740
3	D-DNJ + L-DNJ **(*rac*-1)**	870
4	D-NBDNJ **(2)**	>1000
5	L-NBDNJ **(*ent*-2)**	/
6	D-NBDNJ + L-NBDNJ **(*rac*-2)**	>1000
7	D-NNDNJ **(7)**	5
8	L-NNDNJ **(*ent*-7)**	125
9	D-NNDNJ + L-NNDNJ **(*rac*-7)**	4
10	D-AMPDNM **(8)**	1
11	L-AMPDNM **(*ent*-8)**	50
12	D-AMPDNM+ L-AMPDNM **(*rac*-8)**	7
13	D-HPDNJ **(11)**	5.5
14	L-HPDNJ **(*ent*-11)**	180
15	D-HPDNJ + L-HPDNJ **(*rac*-11)**	9
16	D-NPDNJ **(14)**	1
17	L-NPDNJ **(*ent*-14)**	100
18	D-NPDNJ + L-NPDNJ **(*rac*-14)**	3.6
19	D-MON DNJ **(44)**	18
20	L-MON DNJ **(*ent*-44)**	>1000
21	D-MON DNJ + L-MON DNJ **(*rac*-44)**	26

The same assays were performed using equimolar mixtures of enantiomeric iminosugars. The enzymatic residual activities and the IC_{50} values are summarized in **FIGURE 18** and **TABLE 5**. In any case, the combination of the two enantiomers did not lead to an increase of the inhibitory activity showed by the single enantiomers. As the only exception, the combined use of D- and L-NNDNJ (*rac*-**7**) led to a slight enhancement of the inhibitory activity (IC_{50} = 4 μM, entry 9), approaching that of the D-enantiomer (**7**: IC_{50} = 5 μM, entry 7), while it was far higher than that of *ent*-**7** (IC_{50} = 125 μM, entry 8).

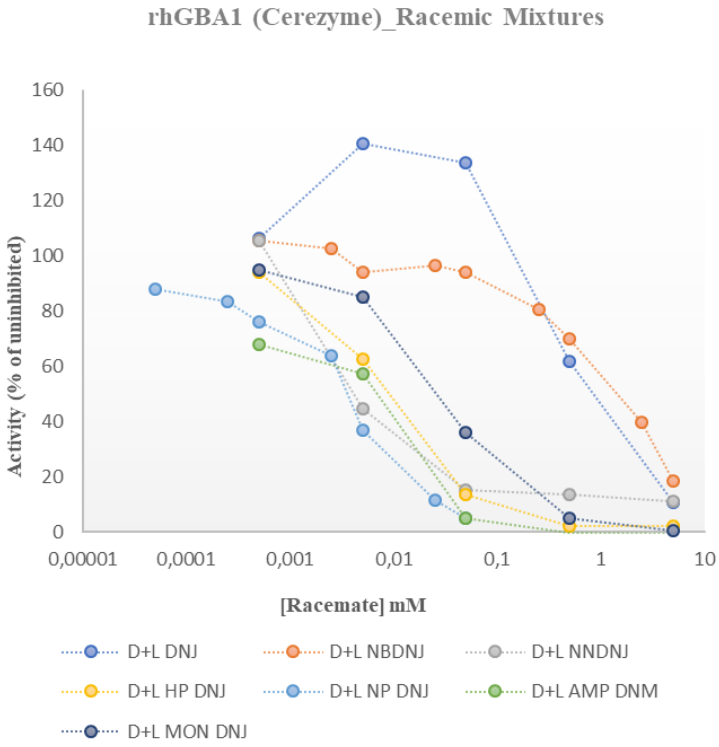

FIGURE 18. rhGBA1 inhibition curves in the presence of racemates.

The most interesting result is the strong enhancement of rhGBA1 residual activity in the presence of DNJ racemate, which is totally absent when the enzyme is co-incubated with the single enantiomers. The observed phenomenon could be explained in terms of positive cooperativity between the two enantiomers, allowing an extra stabilization of the enzyme. In **FIGURE 19** and **TABLE 6** the inhibitory activities of the same compounds against GAA are summarized. The curves obtained (**FIGURE 19**) show that the inhibition was exerted by the only D-enantiomers, while L-iminosugars were substantially inactive. Furthermore, in this case the inhibition potency seems independent from the alkyl chain (length and structure), since D-DNJ was endowed with the strongest potency (IC_{50} = 4 μM; entry 1, **TABLE 6**).

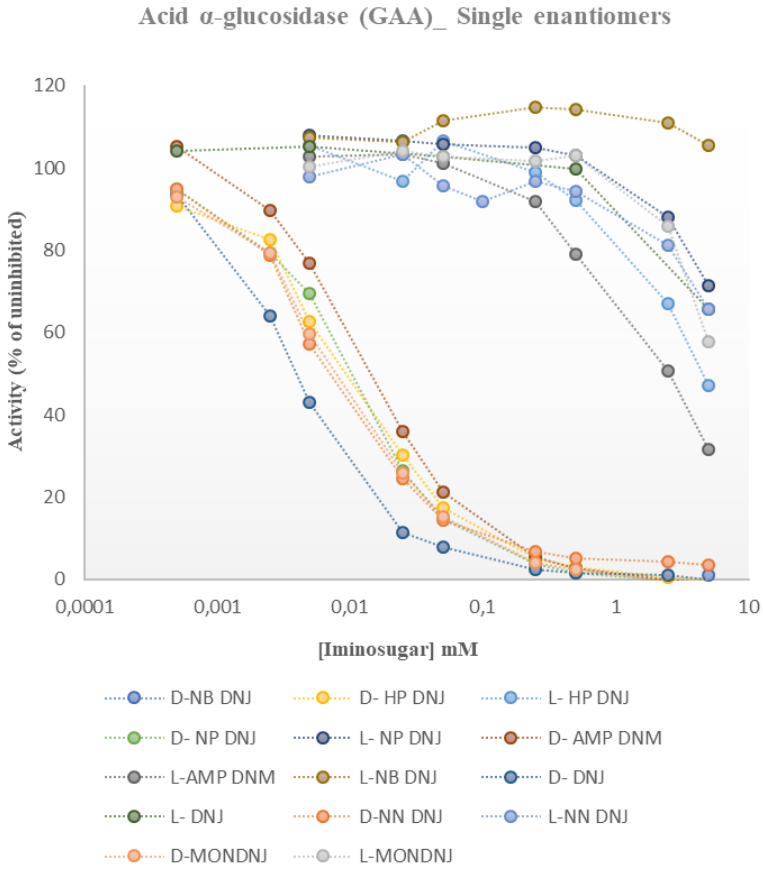

FIGURE 19. Inhibition curves of D- and L-iminosugars toward GAA.

TABLE 6. IC_{50} (μM) of D- and L-iminosugars and of the corresponding racemates toward GAA.

ENTRY	SAMPLE	IC_{50} (μM)
1	D-DNJ **(1)**	4
2	L-DNJ **(*ent*-1)**	/
3	D-DNJ + L-DNJ **(*rac*-1)**	10
4	D-NBDNJ **(2)**	24
5	L-NBDNJ **(*ent*-2)**	/
6	D-NBDNJ + L-NBDNJ **(*rac*-2)**	37
7	D-NNDNJ **(7)**	7.3
8	L-NNDNJ **(*ent*-7)**	/
9	D-NNDNJ + L-NNDNJ **(*rac*-7)**	10
10	D-AMPDNM **(8)**	14
11	L-AMPDNM **(*ent*-8)**	>1000
12	D-AMPDNM+ L-AMPDNM **(*rac*-8)**	39
13	D-HPDNJ **(11)**	9
14	L-HPDNJ **(*ent*-11)**	>1000
15	D-HPDNJ + L-HPDNJ **(*rac*-11)**	28
16	D-NPDNJ **(14)**	10
17	L-NPDNJ **(*ent*-14)**	/
18	D-NPDNJ + L-NPDNJ **(*rac*-14)**	25
19	D-MON DNJ **(44)**	8
20	L-MON DNJ **(*ent*-44)**	/
21	D-MON DNJ + L-MON DNJ **(*rac*-44)**	14

As for GBA1, the analysis of the racemates tested against GAA suggested that no synergistic effect deriving by the combination of the two enantiomers occurred (**TABLE 6**).

1.1.3.2 L-NBDNJ AS ALLOSTERIC ENHANCER OF α-GLUCOSIDASE ACTIVITY FOR THE TREATMENT OF POMPE DISEASE

The results reported so far underline a weak propensity of *N*-alkyl-L-iminosugars to act as glycosidase inhibitors; conversely, in a number of examples the increase in the enzymatic activity of α- and β-glucosidases suggests a potential role of these compounds as enhancers (e.g. pharmacological chaperones) of carbohydrate processing enzymes, with a perspective application in the treatment of LSDs. As an early evaluation of the chaperoning potential of *N*-alkyl-L-iminosugars, the role of iminosugar chirality was explored evaluating the increase of the levels of lysosomal glucosidase

(GAA) deriving from patients with Pompe disease (PD), using D- and L-NBDNJ as model chaperones. As mentioned above, the corresponding D-enantiomer was an established pharmacological chaperone for this enzyme, which is currently undergoing clinical evaluation. In a first set of experiments, PD fibroblasts from a patient carrying the mutation p.L552P/p.L552P (homozygous mutation) were incubated in the absence or in the presence of 20 μM *ent*-**2** or its D-enantiomer[69] (**FIGURE 20**). The administration of *ent*-**2** actually increased the residual activity of mutated GAA (**FIGURE 20**). The activating effect (1.5-fold increase) was slightly higher than that observed for **2** under the same experimental conditions (1.3-fold increase).

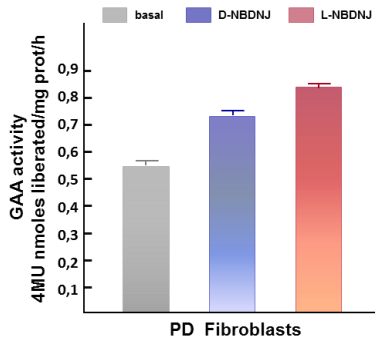

FIGURE 20. Effect of D- and L-NBDNJ (20 μM) on residual activity of mutated GAA in fibroblasts from a PD patient carrying the p.L552P/p.L552P mutation.

Potential synergistic effects deriving from co-administration of *ent*-**2** and rhGAA in PD fibroblasts were also considered. PD fibroblasts from three patients carrying various mutations (**FIGURE 21**) were incubated with rhGAA and *ent*-**2** or its D enantiomer (20 μM).

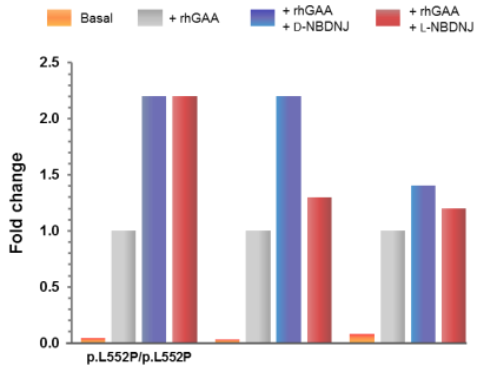

FIGURE 21. Synergy between rhGAA and D- or L-NBDNJ in PD fibroblasts.

In all cases, co-incubation of *ent*-**2** and rhGAA provided a higher increase in GAA levels than those provided by rhGAA when incubated singularly. Especially when PD

fibroblasts carrying the mutation p.L552P/p.L552P were evaluated, a 2-fold increase of GAA activity was found; this value was the same observed by treatment of the cells with **2**/rhGAA. In the remaining cases, the enhancing effect was less marked (and lower than that found for **2**/rhGAA) (**FIGURE 21**). Western blot analysis was eventually performed in *ent*-**2** treated and untreated fibroblasts carrying the mutation p.L552P/p.L552P (**FIGURE 22**) to provide first clues on the mechanisms enabling the observed enhancement of GAA activity.

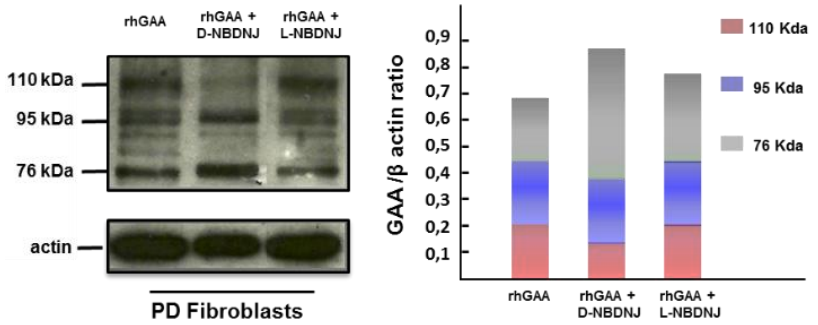

FIGURE 22. Western blot analysis of rhGAA processing in Pompe fibroblasts carrying the p.L552P/p.L552P mutation incubated with rhGAA alone, rhGAA + D-NBDNJ, or rhGAA + L-NBDNJ.

In this case, density scans of rhGAA bands indicated that the mature 76 kDa isoform was more represented in the presence of both enantiomers, even though the increase with rhGAA/*ent*-**2** was less marked with respect to that observed in cells treated with rhGAA/**2.**

1.1.4 CONCLUDING REMARKS AND FUTURE PERSPECTIVES

One of the main topics of this PhD project is focused on the study the role of chirality of *N*-alkyl iminosugars in glycosidase inhibition/activation. From a synthetic standpoint, we were able to gain access to *ent*-**1**, the unnatural enantiomer of D-DNJ, accomplished by a highly stereocontrolled *de novo* strategy, exploiting the different reactivity and conformational preferences of epoxide intermediates **53** and **56**. Then, with the aim to prepare the corresponding *N*-alkylated derivatives, we explored expeditious approaches enabling the assembly of the bioactive alkyl or alkoxyalkyl chains onto the iminosugar core. All the explored methods rely on the combined use of triphenylphosphine (either solvent-soluble or polymer bound phosphine: PS-DPP) and iodine as the iodination system of alkyl or alkoxyalkyl alcohols **59a-c** and **61a-c**. With target compounds in hand, an exhaustive comparative analysis of the inhibition properties of D- and L-iminosugars was performed using D- and L-NBDNJ (**2** and *ent*-**2**) as model substrates. In addition, the remaining D- and L-iminosugars were evaluated in the potential inhibition of pharmacologically relevant GBA1 and GAA. In all cases, differently from the D-enantiomers, L-iminosugars were not found to act as glycosidase inhibitors. On the other hand, either as single enantiomers (e.g. L-NBDNJ) or as racemic mixtures (D- and L-DNJ), L-iminosugars were able to enhance the activity of both β- and α-glucosidases. This has suggested a potential role of L-iminosugars as pharmacological chaperones. Indeed, when tested in cell lines deriving from Pompe disease, *ent*-**2** was found to enhance the activity of lysosomal α-glucosidase. In addition, when co-incubated with rhGAA, we found a synergistic enhancing effect, which was comparable to that observed for rhGAA/**2**. It's worthy to underline that the chaperoning activity of an L-piperidine iminosugar has been reported only seldom before; in addition, to the best of our knowledge, the higher enhancing effect of an L-piperidine iminosugar compared to that of the corresponding natural enantiomer is even unprecedented. The lack of inhibition of the deficient enzyme and of the other glycosidases further augments the activating potential of *ent*-**2**, especially if compared with its enantiomer. It's also worth noting that, unexpectedly, *ent*-**2** seems not to affect the stability of the enzyme, while enhancing the activity of the latter in cells. Thus, although the molecule cannot be considered a conventional pharmacological chaperone of GAA, it represents a promising new candidate for the combination therapy of Pompe disease. Further studies aimed at elucidating the nature of the enhancing effect of *ent*-**2** are currently ongoing.

1.1.5 EXPERIMENTAL SECTION

L-DNJ SYNTHESIS

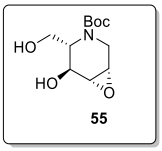

55

Diol 55. Zemplén deacetylation was accomplished by treatment of a solution of **53** (0.24 g, 0.76 mmol) in MeOH (5 mL) with MeONa (41 mg, 0.76 mmol) for 4 h at room temperature. The mixture was neutralized with few drops of acetic acid and then the volatiles were removed under reduced pressure. The crude residue was dissolved in $CHCl_3$ and filtered through a short pad of silica gel. The resulting filtrate was eventually concentrated to dryness, giving **55**, which was used in the following step without further purification; oily. ^{1}H NMR (400 MHz, DMSO-d^6), δ: 1.39 (*s*, 9H), 3.14 (*bs*, 1H), 3.35 (*bs*, 1H), 3.41−3.57 (*m*, 1H), 3.87 (*bt*, J = 7.2 Hz, 1H), 3.91−3.98 (*m*, 1H), 4.02−4.13 (*m*, 1H), 4.14−4.23 (*m*, 1H), 4.62 (*bt*, J = 4.9 Hz, 1H). ^{1}H NMR (400 MHz, 55 °C, DMSO-d^6), δ: 1.40 (*s*, 9H), 3.11−3.20 (*m*, 2H), 3.32−3.41 (*m*, 2H), 3.46−3.55 (*m*, 1H), 3.84−3.96 (*m*, 2H), 4.13 (*bs*, 1H), 4.47 (*t*, J = 5.7 Hz, 1H), 5.19 (*d*, J = 5.2 Hz, 1H). ^{13}C NMR (100 MHz), δ: 28.4, 43.1, 50.2, 53.6, 60.0, 61.1, 63.1, 81.2, 156.9. Anal. Calcd for $C_{11}H_{19}NO_5$: C, 53.87; H, 7.81; N, 5.71. Found: C, 53.94; H, 7.79; N, 5.73. HRMS: m/z $[M + Na]^+$ calcd 268.1155, found 268.1144.

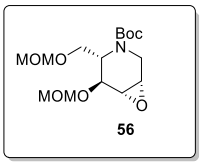

56

Bis-Acetal 56. To a stirring solution of the crude diol **55** (26 mg, 0.1 mmol) in DCM (2 mL), DIPEA (35 μL, 0.2 mmol) and MOMCl (15 μL, 0.2 mmol) were sequentially added at room temperature. The resulting mixture was stirred at the same temperature for 48 h and then the reaction was quenched by the addition of H_2O (1 mL). The mixture was diluted with DCM and washed with brine (pH 7). The organic phases were dried (Na_2SO_4), filtered, and concentrated under reduced pressure. Chromatography of the crude residue gave bis-acetal **56** (25 mg, 76% yield) as a colourless oil. ^{1}H NMR (400 MHz, $CDCl_3$), δ: 1.45 (*s*, 9H), 3.31 (*bs*, 1H), 3.45 (*s*, 3H), 3.37−3.46 (*m*, 4H), 3.56−3.70 (*m*, 4H), 4.18 (*bs*, 1H), 4.30 (*bd*, J = 13.3 Hz, 1H), 4.54−4.68 (*m*, 2H), 4,71 (*d*, J = 6.7 Hz, 1H), 4.79 (*d*, J = 6.7 Hz, 1H). ^{1}H NMR (400 MHz, $CDCl_3$, 45 °C), δ: 1.53 (*s*, 9H), 3.31−3.35 (*m*, 2H), 3.38 (*t*, 3H), 3.45 (*t*, 3H), 3.47−3.53 (*m*, 1H), 3.60−3.64 (*m*, 1H),

3.68 (*t*, J = 7.9 Hz, 2H), 4.20−4.45 (*m*, 2H), 4.61 (*d*, J = 6.6 Hz, 1H), 4.63 (*d*, J = 6.7 Hz, 1H), 4.73 (*d*, J = 6.6 Hz, 1H), 4.82 (*d*, J = 6.8 Hz, 1H). ^{13}C NMR (100 MHz, $CDCl_3$), δ: 28.3, 50.4, 51.1, 53.8, 55.2, 55.7, 65.1, 69.7, 72.8, 80.2, 96.0, 155.5. Anal. Calcd for $C_{15}H_{27}NO_7$: C, 54.04; H, 8.16; N, 4.20. Found: C, C, 54.20; H, 8.14; N, 4.19.

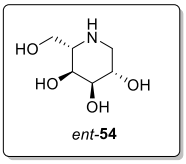

ent-**54**

L-*altro*-Deoxynojirimycin (*ent*-**54**). Acetate **53** (33 mg, 0.1 mmol) was suspended in a 1 M NaOH solution (3 mL). The suspension was warmed to reflux and stirred at the same temperature for 1 h. Temperature was then cooled to rt and the mixture was eluted through a short pad containing a Dowex 50WX8 (H^+ form) resin. The resulting filtrate was concentrated, and chromatography of the crude residue provided *ent*-**54** (9.0 mg, 55% yield) as an oil. NMR data of *ent*-**54** were consistent with those reported elsewhere. HRMS: m/z $[M + H]^+$ calcd 164.085, found 164.0902.

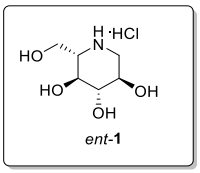

ent-**1**

L-Deoxynojirimycin hydrochloride (*ent*-1). Oxirane **56** (25 mg, 75 μmol) was suspended in a NaOH 1 M solution (2 mL). The reaction mixture was warmed to reflux for 1 h and then temperature was cooled to rt. The mixture was eluted through a short pad containing a Dowex 50WX8 (H^+ form) resin. The resulting filtrate was concentrated, acidified with HCl 2 M (3 mL), and refluxed for 1 h. Removal of the volatiles under reduced pressure yielded *ent*-**1** (15 mg, 91% over two steps) as a white solid. ^{1}H NMR (400 MHz, D_2O), δ: 3.03 (*dd*, J = 11.6, 12.6 Hz, 1H), 3.26 (*ddd*, J = 3.2, 5.2, 10.5 Hz, 1H), 3.56 (*dd*, J = 5.4, 12.6 Hz, 1H), 3.65 (*dd*, J = 9.3, 10.5 Hz, 1H), 3.77−3.87 (*m*, 2H), 3.93 (*dd*, J = 5.2, 12.8 Hz, 1H), 4.00 (*dd*, J = 3.2, 12.8 Hz, 1H). ^{13}C NMR (100 MHz, D_2O), δ: 41.5, 53.6, 55.8, 62.8, 63.7, 72.2. Anal. Calcd for $C_6H_{14}ClNO_4$: C, 36.10; H, 7.07; N, 7.02. Found: C, 36.22; H, 7.05; N, 7.00. HRMS: m/z $[M + H]^+$ calcd 164.0917, found 164.0910.

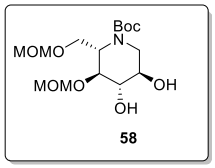

Diol 58. A small amount of the crude residue deriving from oxirane ring cleavage of **56** was purified by column chromatography (hexane:EtOAc, from 100:0 to 70:30), to provide the pure **58** as a pale-yellow oil. ^{1}H NMR (400 MHz, $CDCl_3$), δ: 1.47 (*s*, 9H), 3.36 (*s*, 3H), 3.39 (*bd*, J = 14.3 Hz, 1H), 3.43 (*s*, 3H), 3.71 (*bd*, J = 2.5 Hz, 1H), 3.77 (*dd*, J = 4.8, 10.3 Hz, 1H), 3.85 (*dd*, J = 5.5, 10.3 Hz, 1H), 3.88 (*bt*, J = 1.8 Hz, 1H), 3.91 (*bt*, J = 2.6 Hz, 1H), 4.07 (*dd*, J = 2.5, 14.3 Hz, 1H), 4.47 (*bt*, J = 5.1 Hz, 1H), 4.62 (*d*, J = 6.6 Hz, 1H), 4.65 (*d*, J = 6.6 Hz, 1H), 4.71 (*d*, J = 7.0 Hz, 1H), 4.74 (*d*, J = 7.0 Hz, 1H). ^{13}C NMR (100 MHz, acetone-d^6), δ: 27.8, 51.6, 51.8, 54.3, 55.0, 64.8, 69.3, 69.6, 74.3, 78.7, 95.4. 95.9, 155.3. Anal. Calcd for $C_{15}H_{29}NO_8$: C, 51.27; H, 8.32; N, 3.99. Found: C, 51.40; H, 8.30; N, 3.98. HRMS: m/ z $[M + Na]^+$ calcd 374.1785, found 374.1769.

N-ALKYL-L-DNJ SYNTHESIS

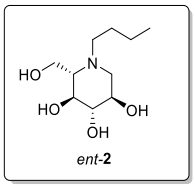

***N*-Butyl-L-deoxynojirimycin** (*ent*-**2**). Butanal (16.4 μL, 0.18 mmol) was added to a stirring solution of L-DNJ·HCl (11, 28 mg, 0.14 mmol) in an acetic acid/methanol (2 mL, 1:200 v/v) solution. After a few minutes, $NaBH_3CN$ (8.8 mg, 0.14 mmol) was added. The resulting mixture was stirred at the same temperature for 16 h and then the volatiles were removed under reduced pressure. Flash chromatography of the crude residue (DCM:MeOH:NH_4OH = 70:28:2) and subsequent filtration though a short pad containing a Dowex 1X8 (chloride form) resin yielded the pure *ent*-**2** (30 mg, 96% yield) as a colourless oil; $[\alpha]_D$ +17.0, c 0.27, H_2O (**2**: −15.9, c 0.77, H_2O).[70] 1H NMR (400 MHz, D_2O), δ: 0.92 (*t*, J = 7.3 Hz, 3H), 1.31 (*sext*, J = 7.3 Hz, 2H), 1.47−1.59 (*m*, 2H), 2.40−2.55 (*m*, 2H), 2.68−2.80 (*m*, 1H), 2.82−2.95 (*m*, 1H), 3.10−3.21 (*m*, 1H), 3.32 (*t*, J = 9.3 Hz, 1H), 3.45 (*t*, J = 9.5 Hz, 1H), 3.61 (*ddd*, J = 10.7, 9.3, 4.9 Hz, 1H), 3.89 (*dd*, J = 12.9, 2.5 Hz, 1H), 3.94 (*dd*, J = 12.9, 2.5 Hz, 1H). ^{13}C NMR (100 MHz, CD_3OD), δ: 14.2, 21.4, 27.0, 53.7, 56.5, 57.7, 67.4, 69.6, 70.8, 79.6. Anal. Calcd for C10H21NO4: C, 54.77; H, 9.65; N, 6.39. Found: C, 54.88; H, 9.62; N, 6.37. HRMS: m/z $[M + H]^+$ calcd 220.1471, found 220.1533.

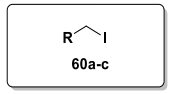

TPP/I_2 as the iodination reagent. Iodination of alcohols 59a-c: general procedure. Alcohol **59** (1.0 equiv.) was dissolved in anhydrous toluene (35 mL); then triphenylphosphine (**59a** and **59b**: 1.5 equiv; **59c**: 2.0 equiv.) was added. The mixture was warmed to 60°C and iodine (**59a** and **59b**: 1.5 equiv; **59c**: 2.0 equiv.) was quickly added. The reaction was then stirred at reflux temperature for the appropriate time (**59a**: 0.5 h; **59b**: 1h and **59c**: 12h). Toluene was removed under diminished pressure; the crude was dissolved in DCM, washed with saturated aq$Na_2S_2O_3$ and brine. DCM was removed under reduced pressure and the compound was used in the subsequent step without further purification. **1-Iodohexane** (**60a**) and **1-iodononane** (**60b**): ^{1}H and ^{13}C NMR spectra were fully in line with those reported in the literature.[71] **Adamantanemethyl iodide** (**60c**). ^{1}H NMR (500 MHz, $CDCl_3$), δ: 1.51 (*d*, J = 2.5 Hz, 6H), 1.64-1.67 (*m*, 3H), 1.72-1.75 (*m*, 3H), 1.99 (*s*, 3H), 3.20 (*s*, 2H). ^{13}C NMR (125 MHz, $CDCl_3$), δ: 27.1, 28.8, 36.7, 42.2.

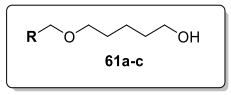

Reaction of iodides 60a-c with 1,5-pentanediol: general procedure. 1,5-pentanediol (5.0 equiv.) was dissolved in anhydrous DMF (35 mL) and NaH (60% dispersion in mineral oil; 5.0 equiv.) was added. The mixture was stirred for 30 min at room temperature. Then a solution of the crude iodide **60** (1.0 equiv.) in DMF (15 mL) was added. The reaction was warmed to the appropriate temperature (**60a**: 70°C; **60b** and **60c**: 140°C) and stirred at the same temperature for an appropriate time (**60a** and **60b**: 16h; **60c**: 48h). The mixture was then dissolved in DCM, washed with sat NH_4Cl and brine. DCM was eventually removed under reduced pressure; column chromatography of the crude (petroleum ether/EtOAc) gave the pure alcohol **61**. **5-Hexyloxyl-1-pentanol** (**61a**): 22% o.y. from **60a**. ^{1}H NMR (400 MHz, $CDCl_3$), δ: 0.88 (*t*, J = 6.4 Hz, 3H), 1.25-1.35 (*m*, 6H), 1.41-1.47 (*m*, 2H), 1.52-1.64 (*m*, 6H), 3.40 (*q*, J = 6.7 Hz, 4H), 3.65 (*t*, J = 6.5 Hz, 2H). ^{13}C NMR (100 MHz, $CDCl_3$), δ: 14.20, 22.69, 22.78, 26.01, 29.59, 29.87, 31.86, 32.67, 63.04, 70.89, 71.22. **5-Nonyloxyl-1-pentanol** (**61b**): 31% o.y. from **60b**. ^{1}H NMR (400 MHz, $CDCl_3$), δ: 0.87 (*t*, J = 6.6, 3H), 1.21–1.36 (*m*, 12H), 1.38–1.46 (*m*, 2H), 1.51–1.65 (*m*, 6H), 3.39 (*q*, J = 6.6, 4H), 3.65 (*t*, J = 6.5 Hz, 2H). ^{13}C NMR (125 MHz, $CDCl_3$), δ: 14.2, 22.5, 22.7, 26.3, 29.3, 29.5, 29.6, 29.6, 29.8, 32.0, 32.6, 63.0, 70.8, 71.1. **5-Adamantanemethoxypentanol** (**61c**): 55% o.y. from **60c**. ^{1}H NMR (500 MHz, $CDCl_3$), δ: 1.39-1.45 (*m*, 2H), 1.52-1.53 (*m*, 6H), 1.56-1.61 (*m*, 4H), 1.63-1.72 (*m*,

6H), 1.95 (*bs*, 3H), 2.96 (*s*, 2H), 3.39 (*t*, J = 6.5 Hz, 2H), 3.66 (*t*, J = 6.6 Hz, 2H). ^{13}C NMR (125 MHz, $CDCl_3$), δ: 22.6, 28.5, 29.4, 32.7, 34.3, 37.4, 39.9, 63.1, 71.7, 82.1.

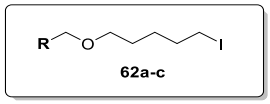

62a-c

Iodination of alcohols 61a-c: general procedure. Alcohol **61** (1.0 equiv.) was dissolved in anhydrous toluene (10 mL), then triphenylphosphine (1.5 equiv.) was added. The mixture was warmed to 60°C and iodine (1.5 equiv.) was added. The reaction was stirred to reflux for 1h. The mixture was then dissolved in DCM, washed with saturated $Na_2S_2O_3$ and $NaHCO_3$ solutions and with brine. DCM was removed under reduced pressure; column chromatography of the crude residue (petroleum ether/EtOAc) gave the pure iodide **62**. **1-Iodo-5-hexyloxyl-pentane** (**62a**): 64% yield. ^{1}H NMR (400 MHz, $CDCl_3$), δ: 0.89 (*t*, J = 6.7 Hz, 3H), 1.25-1.37 (*m*, 5H), 1.42-1.50 (*m*, 2H), 1.52-1.63 (*m*, 5H), 1.82-1.89 (*m*, 2H), 3.19 (*t*, J = 7.0 Hz, 2H), 3.39 (*t*, J = 5.0 Hz, 2H), 3.41 (*t*, J = 4.4 Hz, 2H). ^{13}C NMR (100 MHz, $CDCl_3$), δ: 7.1, 14.2, 22.7, 26.0, 27.4, 28.8, 29.9, 31.9, 33.5, 70.6, 71.2. **1-Iodo-5-nonyloxyl-pentane** (**62b**): 37% yield. ^{1}H NMR (500 MHz, $CDCl_3$), δ: 0.88 (*t*, 3H, J = 6.8 Hz),1.25-1.34 (*m*, 12H), 1.43-1.49 (*m*, 2H), 1.53-.63 (*m*, 4H),1.82-1.88 (*m*, 2H, J = 7.1 Hz), 3.19 (*t*, 2H, J = 7.0 Hz), 3.4 (*q*, J = 6.4 Hz, 4H). ^{13}C NMR (125 MHz, $CDCl_3$), δ: 7.3, 14.5, 23.1, 26.6, 27.7, 29.1, 29.7, 29.9, 30.0, 30.2, 32.3, 33.8, 70.9, 71.5. **1-Iodo-5-adamantanemethoxyl-pentane** (**62c**): 45% yield. ^{1}H NMR (500 MHz, $CDCl_3$), δ: 1.41-1.50 (*m*, 2H), 1.50-1.54 (*m*, 6H), 1.54-1.60 (*m*, 2H), 1.60-1.74 (*m*, 6H), 1.80-1.89 (*m*, 2H), 1.92-1.99 (*m*, 3H), 2.94 (*s*, 2H), 3.19 (*t*, J = 7.1 Hz, 2H), 3.37 (*t*, J = 6.3 Hz, 2H). ^{13}C NMR (125 MHz, $CDCl_3$), δ: 7.2, 27.4, 28.4, 28.5, 28.6, 28.7, 29.8, 31.4, 32.2, 33.5, 34.2, 37.4, 37.5, 39.9, 71.4, 82.1.

PS-DPP/I_2 as the iodination reagent: general procedure for the conversion of alcohols 59a-c into 1-iodo-5-alkyloxyl-pentanes 62a-c. *Step 1*: alcohol **59** (1.0 mmol) was dissolved in the appropriate anhydrous solvent (**59a** and **59b**: ACN; **59c**: toluene), then polystyryldiphenylphosphine (PS-DPP; 100-200 mesh, extent of labelling: ~3 mmol/g triphenylphosphine loading) (3.5 equiv.) was added. The mixture was warmed to 40 °C and was added I_2 (2.0 equiv.). After warming the reaction to reflux and leaving the suspension for the appropriate time (**59a**: 0.5h; **59b**: 1h; **59c**: 4h), the mixture was filtered, and the solvent was removed at rt under reduced pressure, affording iodide **60**. *Step 2*: an appropriate amount of 1,5-pentandiol (**60a** and **60b**: 1.0 equiv.; **60c**: 5 equiv.) was dissolved in dry DMF (**60a** and **60b**: 1.0 mL; **60c**: 5.0 mL) and NaH (60% dispersion in mineral oil; **60a** and **60b**: 1.2 equiv.; **60c**: 5 equiv.) was added. The mixture was stirred for 30 min at room temperature. Then a solution of the crude iodide **60** in dry DMF (0.5 mL) was added dropwise. After 16h at 100 °C, the mixture was concentrated under reduced pressure to furnish **61**. In the case of **61c**, the reaction was washed with hexane

repeatedly in order to remove the excess of 1,5-pentandiol. *Step 3*: alcohol **61** was dissolved in the appropriate anhydrous solvent (**61a** and **61b**: ACN, 2.5 mL; **61c**: toluene, 5 mL), then PS-DPP (2.0 equiv.) was added. The mixture was warmed to 40 °C and I_2 was added (2.0 equiv.). After warming the reaction to reflux and leaving the suspension under stirring at the same temperature for the appropriate time (**61a** and **61b**: 16h; **61c**: 6h), the mixture was filtered, and the filtrate was evaporated under reduced pressure giving the pure iodide **62** (**62a**: 70 % o.y.; **62b**: 88% o.y.; **62c**: 80% o.y.– deduced by NMR analysis of the crudes).

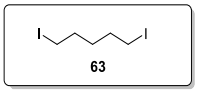

63

1,5-Diiodopentane (**63**). To a solution of PS-DPP (100-200 mesh, extent of labeling: ~3 mmol/g triphenylphosphine loading) (4.0 equiv.) and iodine (4.0 equiv.) in anhydrous DCM, 1,5-pentandiol (1.0 equiv.) was added dropwise. The reaction was stirred at room temperature for 1h; the mixture was then filtered, and the filtrate was evaporated under reduced pressure. The resulting crude was dissolved in DCM, washed with saturated aq $Na_2S_2O_3$ and brine. DCM was removed under diminished pressure. Column chromatography of the crude residue (petroleum ether) gave the pure 1,5-diiodopentane (**63**) as a pale-yellow oil (95% yield). ^{1}H NMR (500 MHz, $CDCl_3$), δ: 1.49-1.55 (*m*, 2H), 1.82-1.88 (*m*, 4H), 3.19 (*t*, J = 7.0 Hz, 4H). ^{13}C NMR (100 MHz, $CDCl_3$), δ: 6.3, 31.1, 32.5.

General procedure for the preparation of iodides 62 from 63. NaH (60% dispersion in mineral oil; 1.0 equiv.) was added to a stirring solution of alcohol **59a-c** (1.5 equiv.) in dry THF (1.5 mL) at 0°C. The reaction mixture was stirred at the same temperature for 2h. *Bis*-iodide **63** (0.70 mmol) was then added and the mixture was warmed to rt. After the appropriate time (**59a** and **59b**: 48h; **59c**: 72h) the mixture was diluted with DCM and washed with aq NH_4Cl and brine. The organic layer was dried with Na_2SO_4 and the solvent evaporated under reduced pressure. Chromatography of the crude residue over silica gel provided the pure iodide **62** (**62a**: 65% yield; **62b**: 64% yield; **62c**: 62% yield).

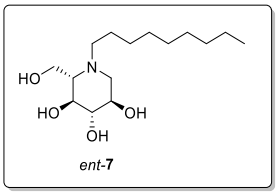

ent-**7**

L-*N*-nonyl DNJ (*ent*-**7**). Iodide **60b** (0.21 g, 0.83 mmol) was dissolved in anhydrous DMF (2 mL) and added dropwise to a solution of L-DNJ (*ent*-**1**; 0.10 g, 0.613 mmol) and K_2CO_3 (0.25 g, 1.84 mmol) in DMF (2 mL). The reaction was warmed to 70 °C and stirred at the same temperature for 16h. Afterwards, the solvent was removed under diminished pressure. Chromatography of the crude residue over silica gel (acetone/MeOH = 80:20) afforded *ent*-**7** as an oil; the compound, dissolved in water, was further purified with Dowex® 1X8, 50-100 mesh, ion-exchange resin (0.14 g, 80% yield). ^{1}H NMR (400 MHz, MeOD), δ: 0.90 (*t*, 3H, *J* = 7.0 Hz), 1.22-1.38 (*m*, 12H), 1.45-1.57 (*m*, 2H), 2.18-2.20 (*m*, 1H), 2.24 (*t*, J = 10.9 Hz, 1H), 2.60-2.66 (*m*, 1H), 2.81-2.87 (*m*, 1H), 3.02 (*dd*, J = 4.8, 11.3 Hz, 1H), 3.15 (*t*, J = 9.1 Hz, 1H), 3.37 (*t*, J = 9.3 Hz, 1H), 3.49 (*dt*, 1H, *J*= 4.9, 5.3 Hz), 3.86 (*bs*, 2H). ^{13}C NMR (100 MHz, $CDCl_3$), δ: 14.4, 23.7, 24.5, 27.9, 30.3, 30.4, 30.6, 33.0, 54.1, 55.5, 56.4, 67.4, 68.6, 69.7, 78.7. LC-TOF MS: *m/z* $[M + H]^+$, calcd: 290.23; found: 290.23.

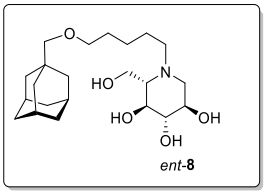

ent-**8**

L-*N*-Adamantanemethoxypentyl-DNJ (**L-AMP-DNM**) (*ent*-**8**). Iodide **62c** (0.30 g, 0.83 mmol) was dissolved in anhydrous DMF (2 mL) and added dropwise to a solution of *ent*-**1** (0.10 g, 0.61 mmol) and K_2CO_3 (0.25 g, 1.83 mmol) in DMF (2 mL). The reaction was warmed to 80 °C and stirred at the same temperature for 16h. Afterwards, the solvent was removed under reduced pressure. Chromatography of the crude residue over silica gel (acetone/MeOH = 80:20) afforded *ent*-**8** as an oil; the compound, dissolved in water, was further purified with Dowex® 1X8, 50-100 mesh, ion-exchange resin (0.19 g, 80% yield). ^{1}H NMR (MeOD, 500 MHz): δ 1.31-1.40 (*m*, 2H), 1.50-1.64 (*m*, 10H), 1.69 (*bd*, J = 11.9 Hz, 3H), 1.76 (*bd*, J = 12.0 Hz, 3H), 1.95 (*bs*, 3H), 2.09-2.15 (*m*, 1H), 2.16-2.22 (*m*, 1H), 2.55-2.63 (*m*, 1H), 2.77-2.83 (*m*, 1H), 2.97 (*s*, 2H), 2.99 (*dd*, J = 4.8, 11.3 Hz, 1H), 3.13 (*t*, J = 9.1 Hz, 1H), 3.35 (*t*, J = 8.9 Hz, 1H), 3.39 (*t*, J = 6.2 Hz, 2H), 3.45-3.50 (*m*, 1H), 3.84 (*dd*, J = 1.7, 12.0 Hz, 1H), 3.87 (*dd*, J = 2.3, 12.2 Hz, 1H). ^{13}C NMR (100 MHz, $CDCl_3$), δ: 24.2, 24.7, 29.7, 30.2, 33.4, 38.3, 40.8, 55.1, 55.7, 67.4, 68.1, 69.2, 72.2, 72.6, 78.4, 831. LC-TOF MS: *m/z* $[M + H]^+$, calcd: 398.29; found: 398.29.

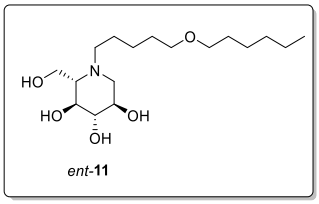

ent-**11**

L-*N*-[5-(Hexoxy)pentyl]-DNJ (*ent*-**11**). Iodide **62a** (0.25 g, 0.83 mmol) was dissolved in anhydrous DMF (2 mL) and added dropwise to a solution of *ent*-**1** (0.1 g, 0.61 mmol) and K_2CO_3 (0.25 g, 1.84 mmol) in DMF (2 mL). The reaction was warmed to 70 °C and stirred at the same temperature for 16h. Afterwards, the solvent was removed under reduced pressure. Chromatography of the crude residue over silica gel (acetone/MeOH = 80:20) afforded *ent*-**11** as an oil; the compound, dissolved in water, was further purified with Dowex® 1X8, 50-100 mesh, ion-exchange resin (0.16 g, 78% yield). ^{1}H NMR (500 MHz, MeOD), δ: 0.93 *(t*, J = 6.7 Hz, 3H), 1.31-1.39 (*m*, 8H), 1.52-1.65 (*m*, 6H), 2.15-2.24 (*m*, 2H), 2.59-2.65 (*m*, 1H), 2.81-2.87 (*m*, 1H), 3.02 (*dd*, J = 4.9, 11.2 Hz, 1H), 3.15 *(t*, J = 9.1 Hz, 1H), 3.37 (*dd*, J = 9.4, 12.0 Hz, 1H), 3.45 (*q*, J = 6.2 Hz, 4H), 3.49 (*dt*, J = 4.9, 10.3 Hz, 1H), 3.86 (*dd*, J = 2.7, 12.0 Hz, 1H), 3.89 (*dd*, J =2.6, 12.0 Hz, 1H). 13 C NMR (500 MHz, MeOD), δ: 14.4, 23.7, 23.9, 24.5, 26.9, 30.1, 30.7, 32.8, 54.3, 54.9, 54.9, 67.4, 67.8, 68.8, 71.4, 72.1, 78.1. LC-TOF MS: *m/z* $[M + H]^+$, calcd: 334.26; found: 334.25.

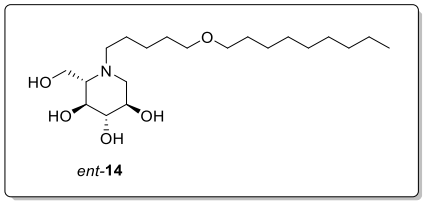

ent-**14**

L-*N*-[5-(Nonyloxy)pentyl]DNJ (*ent*-**14**). Iodide **62b** (0.28 g, 0.83 mmol) was dissolved in anhydrous DMF (2 mL) and added dropwise to a solution of *ent*-**1** (0.100 g, 0.61 mmol) and K_2CO_3 (0.25 g, 1.84 mmol) in DMF (2 mL). The reaction was warmed to 70 °C and stirred at the same temperature for 16h. Afterwards, the solvent was removed under reduced pressure. Chromatography of the crude residue over silica gel (acetone/MeOH = 90:10) afforded *ent*-**14** as an oil; the compound, dissolved in water, was further purified with Dowex® 1X8, 50-100 mesh, ion-exchange resin (0.17 g, 75% yield). ^{1}H NMR (500 MHz, MeOD), δ: 0.92 (*t*, *J* = 6.6 Hz, 3H), 1.29-1.41 (*m*, 14H), 1.51-1.64 (*m*, 6H), 2.13 (*bd*, J = 9.5 Hz, 1H), 2.19 (*dd*, J = 6.7, 10.8 Hz, 1H), 2.57-2.63 (*m*, 1H), 2.79-2.85 (*m*, 1H), 3.01 (*dd*, J = 4.9, 11.2 Hz, 1H), 3.14 (*t*, J = 9.1 Hz, 1H), 3.37 (*t*, J = 9.0 Hz, 1H), 3.44 (*q*, J = 6.3 Hz, 4H), 3.49 (*dt*, J = 4.8, Hz, 1H), 3.85 (*dd*, J = 2.2, 11.9 Hz, 1H), 3.89 (*dd*, J = 1.9, 11.9 Hz, 1H). ^{13}C NMR (100 MHz, MeOD), δ: 14.4.

23.7, 24.0, 24.5, 27.3, 30.2, 30.4, 30.6, 30.7, 30.8, 33.0, 54.3, 54.8, 54.9, 67.4, 67.8, 68.8, 71.4, 72.1, 78.2. LC-TOF MS: *m/z* $[M + H]^+$, calcd: 376.31; found: 376.30.

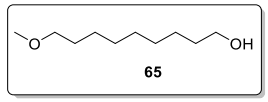

65

Mehoxyl 1-nonanol (65). To a solution of 1,9-nonandiol (0.57 g, 3.53 mmol) in dry DMF (5.0 mL), NaH (0.09 g, 3.53 mmol) was added at 0 °C. The mixture was stirred at the same temperature for 15 minutes and CH_3I (0.1 g, 0.71 mmol) was then added dropwise. After 30 minutes the reaction was quenched with a saturated solution of NH_4Cl. The mixture was then extracted with EtOAc and brine, the organic layers dried over Na_2SO_4 and concentrated under reduced pressure. Purification over silica gel of the crude (hexane:Acetone=80:20) afforded the pure **65** (0.11 g, 90% reaction yield) as colourless oil. ^{1}H NMR (400 MHz, $CDCl_3$), δ: 1.29 (*bs*, 10H), 1.52-1.58 (*m*, 4H), 3.32 (*s*, 3H), 3.35 (*t*, J= 6.6 Hz, 2H), 3.62 (*t*, J= 6.6 Hz, 2H). ^{13}C NMR (100 MHz, $CDCl_3$), δ: 25.8, 26.2, 29.5, 29.6, 29.7, 29.8, 33.0, 58.7, 63.1, 73.0.

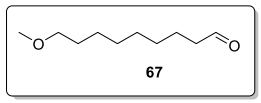

67

Mehoxyl 1-nonanal (67). The reaction flask contains oxalyl chloride (0.08 g, 0.63 mmol) dissolved in dry DCM (1.7 mL), cooled to -78 °C. Once added DMSO (0.1 g, 1.26 mmol) to dry DCM (0.6 mL) in another flask, its content was added to the reaction flask. After stirred the mixture for 30 minutes at the same temperature, **65** (0.1 g, 0.57 mmol), dissolved in dry DCM (1.0 mL) was dropwise added. After 2h at -78 °C, triethylamine (0.29 g, 2.87 mmol) was added and the mixture was warmed to 0 °C. After 2h the mixture was extracted with DCM and brine, the organic layers dried over Na_2SO_4 and concentrated under reduced pressure. The crude was purified over silica gel (hexane:Acetone=95:5) affording the pure **67** (0.05 g, 48 % reaction yield) as white solid. ^{1}H NMR (500 MHz, $CDCl_3$), δ: 1.31 (*bs*, 8H), 1.53-1.63 (*m*, 4H), 2.41 (*t*, J= 7.3 Hz, 2H), 3.33 (*s*, 3H), 3.36 (*t*, J =6.5 Hz, 2H), 9.76 (*s*, 1H). ^{13}C NMR (125 MHz, $CDCl_3$), δ: 25.8, 26.3, 29.3, 29.4, 29.5, 29.6, 36.1, 58.5, 73.9, 198.5.

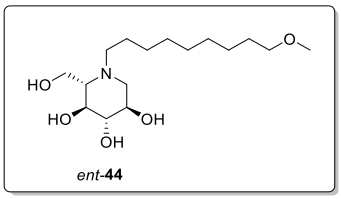

ent-**44**

L-*N*-[9-(Methoxyl)nonyl]DNJ (*ent*-**44**). L-DNJ *ent*-**1** (0.035 g, 0.22 mmol) was dissolved in an acetic acid/methanol (1:200 v/v) solution (18 μL AcOH in 3.48 mL of dry MeOH), then the aldehyde **67** (0.044 g, 0.26 mmol) and $NaBH_3CN$ (0.014 g, 0.22 mol) were added at room temperature. The mixture was stirred at the same temperature until TLC showed disappearance of the starting material (12h). The reaction mixture was concentrated under reduced pressure and the crude purified over silica gel (hexane:Acetone=80:20) affording the pure *ent*-**44** (0.063 g, 91 % reaction yield) as white solid. ^{1}H NMR (400 MHz, MeOD), δ: 1.33 (*bs*, 10H), 1.47-1.60 (*m*, 4H), 2.15-2.32 (*m*, 2H), 2.64-2.70 (*m*, 1H), 2.84-2.91 (*m*, 1H), 3.05 (*dd*, J =4.8, 11.3 Hz, 1H), 3.16 (*t*, J= 9.0 Hz, 1H), 3.34 (*s*, 3H), 3.38 (*t*, J= 6.5 Hz, 2H), 3.50 (*dt*, J= 4.8 Hz, 1H), 3.87 (*bs*, 2H). ^{13}C NMR (100 MHz, MeOD), δ: 25.1, 27.1, 28.5, 30.4, 30.5, 30.6, 30.7, 53.8, 57.4, 58.7, 59.0, 67.4, 70.5, 71.8, 73.9, 80.3.

GLYCOSIDASES INHIBITION STUDY

Cerezyme assay: Cerezyme (Genzyme. Cambridge, MA) has been provided by courtesy of Department of Medicine, University of Cambridge, UK. The assay buffer was 50 mM citric acid, 176 Mm K_2HPO_4, pH 5.9, 0.01% Tween-20 and 10 mM sodium taurocholate. Cerezyme (40U/Ml) was diluted in the assay buffer in presence of 1% BSA (Bovine Serum Albumin) to reach the final concentration of 1:50000. The artificial substrate, 4-methylumbelliferyl-β-D-glucopyranoside, was dissolved in the assay buffer (4.5 mM). The blank mixture (in triplicate) contains 10 μL of assay buffer, 10 μL of enzyme solution and 40 μL of substrate. Each incubation mixture (at different inhibitor concentrations, in triplicate) contains 10 μL of enzyme, 10 μL of inhibitor and 40 μL of substrate. The tubes containing the mixtures were incubated at 37° for 30 minutes; then the assay was stopped by the addition, in each tube, of a stop solution (0.4 mL, 0.5 M Na_2CO_3). The mixtures were transferred in a plate and the fluorescence was measured with a BMG Labtech CLARIOSTAR plate-reader (excitation λ= 365 nm; emission λ= 450 nm).

GAA assay: the enzyme source (0.020 g, liver extract) of acid α-glucosidase (GAA) has been suspended and homogenised in 2.0 mL of cold water. The assay buffer was 0.1 mM citric acid, 0.1 M phosphate, pH 4.0, 0.1% Triton X-100. The artificial substrate, 4-methylumbelliferyl-α-D-glucopyranoside, was dissolved in the assay buffer (1.47 mM). The blank mixture (in triplicate) contains 10 μL of assay buffer, 10 μL of tissue extract and 60 μL of substrate. Each incubation mixture (at different inhibitor concentrations, in triplicate) contains 10 μL of enzyme, 10 μL of inhibitor and 60 μL of substrate. The tubes containing the mixtures were incubated at 37° for 30 minutes; then the assay was stopped by the addition, in each tube, of a stop solution (0.4 mL, 0.5 M Na_2CO_3). The

mixtures were transferred in a plate and the fluorescence was measured with a BMG Labtech CLARIOSTAR plate-reader (excitation λ= 365 nm; emission λ= 450 nm).

1.1.6 REFERENCES

[1] (1) Stütz, A., Ed. *Iminosugars as Glycosidase Inhibitors*; *Nojirimycin and Beyond*; Wiley-VCH: Weinheim, Germany, **1999;** (2) Horne, G.; Wilson, F.X.; Tinsley, J.; Williams, D.H.; Storer, R. *Drug Discovery Today* **2011**, *16*, 107; (3) Asano, N.; Hashimoto, H. Azaglycomimetics: synthesis and chemical biology, in *Glycoscience*, B. O. Fraser-Reid, K. Tatsuta, J. Thiem, Eds. (Springer, Berlin, **2001**), Chapter 10.2, 2542; (4) Compain, P.; Martin, O. R. *Iminosugars – From Synthesis to Therapeutic Applications*, John Wiley & Sons Ltd: West Sussex, England **2007**.

[2] Asano, N.; Nishida, M.; Miyauchi, M.; Ikeda, K.; Yamamoto, M.; Kizua, H.; Kamedaa, Y.; Watsonb, A.A.; Nash, R.J.; Fleet, G.W.J. *Phytochemistry* **2000**, *53*, 379.

[3] Yu, C.; Asano, N.; Ikeda, K.; Wang, M.; Butters, T.D.; Wormald, M.R.; Dwek, R.A.; Winters, A.L.; Nashe, R.J.; Fleet, G.W.J. *Chem. Commun.* **2004**, 1936.

[4] (1) Inouye, S.; Tsuruoka, T.; Niida, T. *J. Antibiot.* **1966**, *19*, 288; (2) Miyake, Y.; Ebata, M. *Agric. Biol. Chem.* **1988**, *52*, 661.

[5] Inouye, S.; Tsuruoka, T.; Ito, T.; Niida, T. *Tetrahedron* **1968**, *24*, 2125.

[6] Koyama, M.; Sakumara, S. *Agric. Biol. Chem.* **1974**, *38*, 1111.

[7] Kite, G.C.; Fellows, L.E.; Fleet, G.W.J.; Liu, P.S.; Scofield, A.M.; Smith, N.G.; *Tetrahedron Lett.* **1988**, *29*, 6483.

[8] Mooser, G. Glycosidases and Glycosyl Transferases in *The Enzymes*, Vol. XX, Sigman, D.S. (Academic Press Inc., **1992)**; chapter 5, 187.

[9] Winchester, B.; Fleet, G.W.J. *Glycobiology* **1992**, *2*, 199.

[10] Vasella, A.; Davies, G. J.; Böhm, M. *Curr. Opin. Chem. Biol.* **2002**, *6*, 619.

[11] Bols, M. *Acc. Chem. Res.* **1998**, *31*, 1.

[12] Nash, R.J.; Kato, A.; Yu, C.; Fleet, G.W.J. *Future Med. Chem*. **2011**, *3*, 1513.

[13] Platt, F.M.; Boland, B.; van der Spoel, A.C. *Am. J. Cell. Biol.* **2012**, *199*, 723.

[14] Platt, F.M.; Jeyakumar, M. *Acta Paediatr.* **2008**, *97*, 88.

[15] Platt, F.M. *Nature* **2014**, *510*, 68.

[16] Brady, R. O. *Annu. Rev. Med.* **2006**, *57*, 283.

[17] Wennekes, T.; Lang, B.; Leeman, M.; van der Marel, G.A.; Smits, E.; Weber, M.; van Wiltenburg, J.; Wolberg, M.; Aerts, J.M.F.G.; Overkleeft, H.S. *Org. Process Res, Dev.* **2008**, *12*, 414.

[18] Ghisaidoobe, A.; Bikker, P.; de Bruijn, A. C. J.; Godschalk, F.D.; Rogaar, E.; Guijt, M. C.; Hagens, P.; Halma, J.M.; van't Hart, S.M.; Luitjens, S.B.; van Rixel, V.H.S., Wijzenbroek, M.; Zweegers, T.; Donker-Koopman, W.E.; Strijland, A.; Boot, R.; van der Marel, G.; Overkleeft, H.S.; Aerts, J.M.F.G.; van der Berg, R.J.B.H.N. *ACS Med. Chem. Lett.* **2011**, *2*, 119.

[19] Bonnie, W.R; Banks-Schlegel, S.; Accurso, F.J.; Boucher, R.C.; Cutting, G.R.; Engelhardt, J.F.; Guggino, W.B.; Karp, C.L; Knowles, M.R.; Kolls, J.K.; LiPuma, J.J.; Lynch, S.; McCray, P.B. Jr.; Rubenstein, R.C.; Singh, P.K..; Sorscher, E.; Welsh, M. *Am. J. Respir. Crit. Care Med.* **2012**, *185*, 887.

[20] Hoffman, L.R.; Ramsey, B.W. *Chest* **2013**, *143*, 207.

[21] Grassmé, H.; Jendrossek, V.M; Riehle1, A.; Von Kürthy, G.; Berger, J.; Schwarz, H.; Weller, M.; Kolesnick, R.; Gulbins, E. *Nat. Med.* **2003**, *9*, 322.

[22] Boot R.G.; Verhoek M.; Donker-Koopman W.; Strijland A.; van Marle J.; Overkleeft H.S.; Wennekes T.; Aerts J. M. *J. Biol. Chem*. **2007**, *282*, 1305.

[23] Overkleeft H. S.; Renkema G. H.; Neele J.; Vianello P.; Hung I. O.; Strijland A.; van der Burg A. M.; Koomen G. J.; Pandit U. K.; Aerts J. M. *J. Biol. Chem.* **1998**, *273*, 26522.

[24] Dechecchi, M.C.; Nicolis, E.; Norez, C.; Bezzerri, V.; Borgatti, M.; Mancini, I.; Rizzotti, P.; Ribeiro, C.M.; Gambari, R.; Becq, F.; Cabrini, G. *J. Cyst. Fibros*. **2008**, *7*, 555.

[25] Dechecchi, M.C.; Nicolis, E.; Mazzi, P; Cioffi, F.; Bezzerri, V.; Lampronti, I.; Huang, S.; Wiszniewski, L.; Gambari, R.; Scupoli, M.T.; Berton, G.; Cabrini, G. *Am. J. Respir. Cell Mol. Biol.* **2011**, *45*, 825.
[26] Sánchez-Fernández, E. M.; GarcÍa Fernández, J. M.; Ortiz Mellet, C. *Chem. Commun.* **2016**, *52*, 5497.
[27] Okuyama, M. *Biosci., Biotechnol., Biochem.* **2011**, *75*, 2269.
[28] van der Ploeg, A. T.; Reuser, A. J. *Lancet* **2008**, *372*, 1342.
[29] (1) Platt, F. M. *Nature* **2014**, *510*, 68; (2) Parenti, G.; Andria, G.; Ballabio, A. *Annu. Rev. Med.* **2015**, *66*, 471.
[30] van den Hout, H.; Reuser, A. J.; Vulto, A. G.; Loonen, M. C. B.; Cromme-Dijkhuis, A.; Van der Ploeg, A. T. *Lancet* **2000**, *356*, 397.
[31] (1) Parenti, G.; Andria, G.; Valenzano, K. J. *Mol. Ther.* **2015**, *23*, 1138; (2) Boyd, R. E.; Lee, G.; Rybczynski, P.; Benjamin, E. R.; Khanna, R.; Wustman, B. A.; Valenzano, K. J. *J. Med. Chem.* **2013**, *5*6, 2705.
[32] Convertino, M.; Das, J.; Dokholyan, N. V. *ACS Chem. Biol.* **2016**, *11*, 1471.
[33] Butters, T. D.; Dwek, R. A.; Platt, F. M. *Chem. Rev.* **2000**, *100*, 4683.
[34] Parenti, G.; Zuppaldi, A.; Pittis, M. G.; Tuzzi, M. R.; Annunziata, I.; Meroni, G.; Porto, C.; Donaudy, F.; Rossi, B.; Rossi, M.; Filocamo, M.; Donati, A.; Bembi, B.; Ballabio, A.; Andria, G. *Mol. Ther.* **2007**, *15*, 508.
[35] Porto, C.; Cardone, M.; Fontana, F.; Rossi, B.; Tuzzi, M. R.; Tarallo, A.; Barone, M. V.; Andria, G.; Parenti, G. *Mol. Ther.* **2009**, *17*, 964.
[36] Parenti, G.; Fecarotta, S.; la Marca, G.; Rossi, B.; Ascione, S.; Donati, M. A.; Morandi, L. O.; Ravaglia, S.; Pichiecchio, A.; Ombrone, D.; Sacchini, M.; Pasanisi, M. B.; De Filippi, P.; Danesino, C.; Della Casa, R.; Romano, A.; Mollica, C.; Rosa, M.; Agovino, T.; Nusco, E.; Porto, C.; Andria, G. *Mol. Ther.* **2014**, *22*, 2004.
[37] Svensson1, C.K.; Feldt-Rasmussen, U.; Backer, V. *Eur. Respir. J.* **2015**, *2*: 26721.
[38] Asano, N.; Ishii, S.; Kizu, H.; Ikeda, K.; Yasuda, K.; Kato, A.; Martin, O.R.; Fan, J. *Eur. J. Biochem.* **2000**, *267*, 4179.
[39] Sunder-Plassman, G.; Fodinger, M.; Kain, R. Fabry Disease, Section 7- Hereditary Kidney Disorders; Chapter 44, 381.
[40] (1) Mellor, H.R.; Neville, D.C.A.; Harvey, D.J.; Platt, F.M.; Dwek, R.A.; Butters, T.D. *Biochem. J.* **2004**, *381*, 861; (2) Mellor, H.R.; Neville, D.C.A.; Harvey, D.J.; Platt, F.M.; Dwek, R.A.; Butters, T.D. *Biochem. J.* **2004**, *381*, 867.
[41] Mellor, H.R.; Nolan, J.; Pickering, L.; Wormald, M.R.; Platt, F.M.; Dwek, R.A.; Fleet, G.W.J.; Butters, T.D *Biochem. J.* **2002**, *366*, 225.
[42] Horne, G.; Wilson, F.X. *Progress in Medicinal Chemistry* **2011**, *50*, 135.
[43] Cox, T.M.; Platt, F.M.; Aerts, J.M.F.G. "Medicinal use of iminosugars" in Compain, P.; Martin, O. R. *Iminosugars – From Synthesis to Therapeutic Applications*, John Wiley & Sons Ltd: West Sussex, England **2007**.
[44] Butters, T.D.; van den Broek, L.A.G.M.; Fleet, G.W.J.; Krulle, T.M.; Wormald, M. R.; Dwek, R.A.; Platt, F.M. *Tetrahedron: Asymmetry* **2000**, *11*, 113.
[45] Butter, T.D.; Dwek, R.A.; Platt, F.M. *Chem. Rev.* **2000**, *100*, 4683.
[46] Brumshtein, B.; Greenblatt, H.M.; Butter, T.D.; Shaaltiel, Y.; Aviezer, D.M. Silman, I.; Futerman, A.H.; Sussman, J.L. *J. Biol. Chem.* **2007**, *39*, 29052.
[47] D'Alonzo, D.; Guaragna, A.; Palumbo, G. *Curr. Med. Chem.* **2009**, *16*, 473.
[48] Kato, A.; Kato, N.; Kano, E.; Adachi, I.; Ikeda, K.; Yu, L.; Okamoto, T.; Banba, Y.; Ouchi, H.; Takahata, H.; Asano, N. *J. Med. Chem.* **2005**, *48*, 2036.
[49] Wennekes, T.; Meijer, A.J.; Groen, A.K.; Boot, R.G.; Groener, J.E.; van Eijk, M.; Ottenhoff, R.; Bijl, N.; Ghauharali, K.; Song, H.; O'Shea, T.J.; Liu, H.; Yew, N.; Copeland, D.; van den Berg, R.J.; van der Marel, G.A.; Overkleeft, H.S.; Aerts, J.M. *J. Med. Chem.* **2010**, *53*, 689.

[50] It must be noted that this trend has been observed also for the corresponding *N*-alkyl *gluco* congeners (see **TABLE 1**).
[51] Takahata, H.; Banba, Y.; Ouchi, H.; Nemoto, H. *Org. Lett.* **2003**, *5*, 2527.
[52] Grubbs, R.H.; Chang, S. *Tetrahedron* **1998**, *54*, 4413.
[53] Wennekes, T.; van den Berg, R.J.; Donker, W.; van der Marel, G.A.; Strijland, A.; Aerts, J.M.; Overkleeft, H.S. *J. Org. Chem.* **2007**, *72*, 1088.
[54] (1) Guaragna, A.; D'Errico, S.; D'Alonzo, D.; Pedatella, S.; Palumbo,G. *Org. Lett.* **2007**, *9*, 3473; (2) Guaragna, A.; D'Alonzo, D.; Paolella, C.; Palumbo, G. *Tetrahedron Lett.* **2009**, *50*, 2045
[55] Caputo, R.; Guaragna, A.; Palumbo, G.; Pedatella, S. *J. Org. Chem.* **1997,** *62*, 9369.
[56] D'Alonzo, D.; De Fenza, M.; Porto, C.; Iacono, R.; Huebecker, M.; Cobucci-Ponzano, B.; Priestman, D.A.; Platt, F.; Parenti, G.; Moracci, M.; Palumbo, G.; Guaragna, A. *J. Med. Chem.* **2017**, *60*, 9462.
[57] Wennekes, T.; Lang, B.; Leeman, M.; van der Marel, G.A.; Smits, E.; Weber, M.; van Wiltenburg, J.; Wolberg, M.; Aerts, J.M.; Overkleeft, H.S. *Org. Process Res. Dev.* **2008**, *12*, 414.
[58] Cooper, C. G.F.; Lee, E.R.; Silva, R.A.; Bourque, A.J.; Clark, S.; Katti, S.; Nivorozhkin, V. *Org. Process Res. Dev.* **2012**, *16*, 1090.
[59] It must be observed that a few synthetic routes to L-DNJ have been reported, see for example: (a) Chida, N.; Furuno, Y.; Ikemoto, H.; Ogawa, S. *Carbohydr. Res.* **1992**, *237*, 185. (b) Best, D.; Wang, C.; Weymouth-Wilson, A. C.; Clarkson, R. A.; Wilson, F. X.; Nash, R. J.; Miyauchi, S.; Kato, A.; Fleet, G. W. J. *Tetrahedron: Asymmetry* **2010**, *21*, 311.
[60] D'Alonzo, D.; Palumbo, G.; Guaragna, A. "Multistep transformations of bis-thioenol ether-containing chiral building blocks: new avenues in glycochemistry" in *Domino and Intramolecular Rearrangement Reactions as Advanced Synthetic Methods in Glycoscience*, 1st ed.; Witczak, Z. J., Bielski, R., Eds.; John Wiley & Sons Ltd.: Hoboken, NJ, **2016**; pp 97−113.
[61] (1) Guaragna, A.; D'Alonzo, D.; Paolella, C.; Napolitano, C.; Palumbo, G. *J. Org. Chem.* **2010**, *75*, 3558; (2) D'Alonzo, D.; Van Aerschot, A.; Guaragna, A.; Palumbo, G.; Schepers, G.; Capone, S.; Rozenski, J.; Herdewijn, P. *Chem. - Eur. J.* **2009**, *15*, 10121; (3) Paolella, C.; D'Alonzo, D.; Palumbo, G.; Guaragna, A. *Org. Biomol. Chem*. **2013**, *11*, 7825.
[62] Guaragna, A.; Dell'Isola, A.; D'Errico, S.; Palumbo, G.; D'Alonzo, D. *Tetrahedron Lett.* **2014**, *55*, 7007.
[63] D'Alonzo, D.; Guaragna, A.; Napolitano, C.; Palumbo, G. *J. Org. Chem.* **2008**, *73*, 5636.
[64] The formation of **57** allows explaining the NaOH-mediated cleavage of the *N*-Boc group, despite the recognized stability of the latter to alkaline conditions, see: Agami, C.; Couty, F. *Tetrahedron* **2002**, *58*, 2701.
[65] Singh, A.; Kim, B.; Lee, W. K.; Ha, H.-J. *Org. Biomol. Chem.* **2011**, *9*, 1372.
[66] Theoretical J values were obtained by applying the Haasnoot− de Leeuw−Altona equation: Navarro-Vázquez, A.; Cobas, J. C.; Sardina, F. J.; Casanueva, J.; Díez, E. *J. Chem. Inf. Comput. Sci.* **2004**, *44*, 1680.
[67] Pedatella, S.; Guaragna, A.; D'Alonzo, D.; De Nisco, M.; Palumbo G. *Synlett* **2006**, *2*, 305.
[68] NMR analysis of the reaction crude showed the conversion of **65** in 1,9-diiodononane; the concurrent ether cleavage by HI is probably the cause.
[69] For a comparative analysis of the biological activity of the two enantiomers, experiments using 20 μM solutions of *ent*-**2**, the optimal concentration value found for **2** (ref 34), were conducted in this study.
[70] Asano, N.; Kizu, H.; Oseki, K.; Tomioka, E.; Matsui, K.; Okamoto, M.; Baba, M. *J. Med. Chem.* **1995**, *38*, 2349.
[71] Montoro, R.; Wirth, T. *Synthesis* **2005**, *9*, 1473.

NUCLEOSIDE ANALOGUES

2

NUCLEOSIDE ANALOGUES

*Nucleosides are endogenous compounds involved in several cellular processes such as nucleic acids synthesis, cell signalling, enzyme regulation and metabolism. Nucleoside analogues (NAs) are synthetic, chemically modified compounds developed to mimic the physiological counterparts in order to exert their cellular functions. They have become cornerstones of treatment of viral infections and today many efforts are still made to discover in the next future more potent, selective and less toxic antiviral NAs. The metabolic pathway of NAs is the same of that exploited by endogenous ones; inside the cells, NAs are subsequently phosphorylated until triphosphate substrates (active form) are accumulated in virus-infected cells. This mechanism results easy for those NAs conceived to be inhibitors of DNA viruses (such as HHVs) that possess their own kinases characterized by obvious broader substrate specificity than mammalian counterparts; it is more difficult instead to develop new anti-HIV NAs because of the obligate recognition by cellular kinases to make them active. At this point, they can act as intracellular enzymes inhibitors, as well as they can be incorporated into newly synthetized DNA and RNA inducing termination of chain elongation, accumulation of mutations in viral progeny (lethal mutagenesis) or inducing cell apoptosis. The wide chemical diversity of NAs relies on the possibility to insert chemical modifications at different levels of their basic structure (**Figure 1**), that are the sugar moiety, the nucleobase or the phosphate groups (nucleotide analogues). The antiviral nucleosides currently on the market were discovered through the intuitive thinking of chemists as to which structural analogues of natural substrates might confound the viruses, or on the basis of already existing antiviral compounds. However, a nucleoside is more than the sum of carbohydrate plus nucleobase; there is still so much we do not understand about nucleosides and about their antiviral pathways or biological targets. This research field is thus still open and continuously in evolution.*

*In the above described context, during this PhD research program, the attention has been focused on the synthesis and biological evaluation of three different class of NAs: 2'-fluorinated oxathiolanyl nucleosides (**2.1**), piperidinyl nucleosides (**2.2**) and cyclohexenyl nucleosides (**2.3**). In the first case, the aim was to enhance (through the stereoselective introduction of a fluorine atom) the already well-known anti-HIV activity of (-)-3TC (L-NA) as terminator chain. In the other two cases (examples of NAs with a six-membered sugar core), the nucleoside conformational preferences have been considered and exploited with the aim to mimic the bioactive ones and at the same time to pre-organize the NAs in order to improve the selectivity associated to the host-guest recognition processes crucial for the viral replication.*

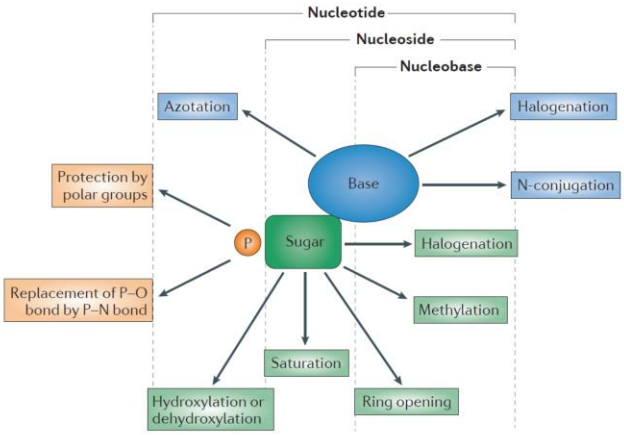

Figure 1 *(taken by* Jordheim, L.P. *et al. Nat. Rev. Drug Discovery* **2013**, *12*, 447*): structural and chemical modifications of NAs.*

2.1 Synthesis and Antiviral Activity of β-L-2'-Fluoro-3'-Thiacytidine (F-3TC) Stereoisomers

2.1.1 INTRODUCTION

2.1.1.1 ANTIVIRALS AT MIRROR: L-NUCLEOSIDE ANALOGUES

Louis Pasteur, some years after discovery that not only objects but also molecules and chemical reactions exhibit chirality, in his speech at French Academy of Sciences, said "l'Univers est dissymétrique".[1] The chirality in its biological meaning explains the reason why proteins are built up only with L-amino acids and nucleic acids with nucleotides whose sugar moiety is only in D-configuration (ensuring the formation of right-handed helices). The enantioselectivity characterizing the enzyme-substrate recognition processes (namely the property of enzymes to recognize and metabolize only one of the two enantiomers of chiral molecules), is dictates by the intrinsic chiral structure of the enzymes (due to three-dimensional folding of the polypeptide backbone and to amino-acids side chain orientation).[2] In this context, L-nucleosides however represent a surprising exception to the mentioned rule (**FIGURE 1**). For a long period, indeed, it was assumed that nucleoside analogues (NAs) having only a natural D-configuration, by analogy with the natural ones, could be recognized by enzymes to exhibit their biological activity.

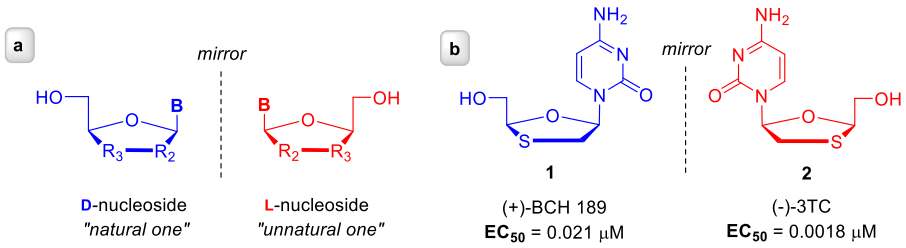

FIGURE 1. a) Mirror relationship between D- and L-nucleosides; b) (+)-BCH189 and (-)-3TC (Lamivudine).

As a matter of fact, at the beginning of the 1990s, this paradigm has been challenged and unnatural L-nucleosides emerged as new class of therapeutic agents.[3] Indeed, Schinazi *et al*.[4] reported the synthesis and anti-HIV-1 activity of all possible stereoisomers of an unusual nucleoside, 2',3'-dideoxy-3'-thiacytidine ((+)-**BCH-189, 1**) (**FIGURE 1**), and surprisingly the β-L-isomer (Lamivudine, (-)-**3TC**, **2**) resulted as the most potent and less toxic nucleoside. Since then, many L-NAs have been synthetized (**FIGURE 2**) and the molecular basis for their therapeutic activation as antiviral or anticancer agents have been elucidated.

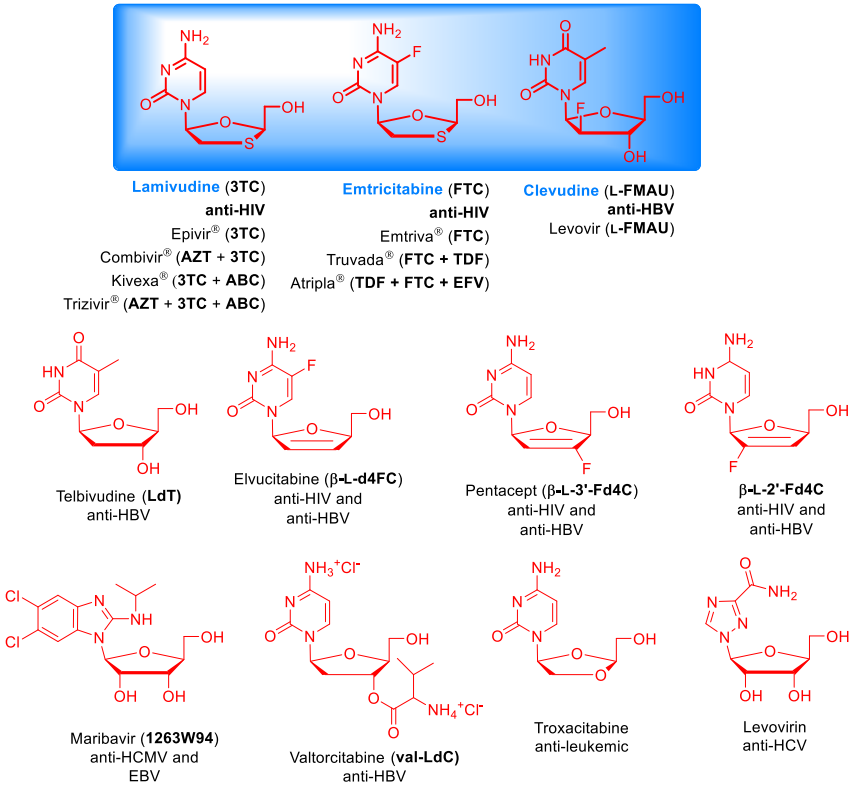

FIGURE 2. L-NAs endowed with biological activity (approved drugs in the blue panel).

2.1.1.2 LACK OF ENANTIOSELECTIVITY OF VIRAL AND HUMAN ENZYMES: MOLECULAR BASIS TO DEVELOP SELECTIVE ANTIVIRAL AGENTS

In order to gain pharmacological activity, both D- and L-NAs require serial phosphorylation (**SCHEME 1**), via the mono- and diphosphate intermediates to the triphosphorylated form (NA-TP). This implies that, gives their inverted configuration, the pharmacological activity of L-nucleoside analogues is dependent on the capacity of all the enzymes of the activation pathway to phosphorylate enantiomers of opposite chirality, plus the ability of the L-NA-TP to successfully compete with physiological nucleoside triphosphates (NTPs) and to distinctively inhibit the viral target DNA (or RNA) polymerase.[5]

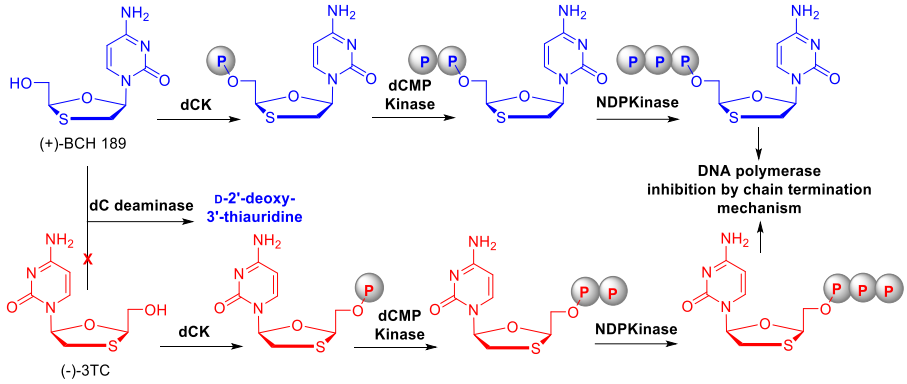

SCHEME 1. Metabolism of (+)-BCH 189 and (-)-3TC.

The virus encoded enzymes often show properties similar to those exhibited by their cellular equivalents; for this reason, the design of selective antiviral agents able to not interfere with the host cells metabolism (harming the whole organism), is a difficult task to reach. HSV-TK (*Herpes Simplex Virus Thymidine Kinase*) represents a lucky case in which the viral enzyme, despite its similar functionality to the cellular counterpart (the human TK), possess unique catalytic properties being not enantioselective.[2] Indeed, beside to its great ability to accept a wide range of modified NAs (e.g. acyclovir, idoxuridine, brivudine [BVdU] and ganciclovir [DHPG]),[6,7] it is able to phosphorylate with similar efficiency both D- and L-enantiomers of idoxuridine and BVdU. Similar results were obtained for HSV-2 TK and Varicella Zoster TK, suggesting that the lack of stereospecificity could be a common feature shared by TKs encoded by HHVs (*Herpes Human Viruses*).[6]

On the other hand, for those viruses, such as HIV (*Human Immunodeficiency Virus*) or HBV (*Hepatitis B Virus*), which do not possess their own kinases, the crucial phosphorylation step must be accomplished by host kinases such as thymidine kinase 1 (TK1), deoxycytidine kinase (dCK), thymidine kinase 2 (TK2) and deoxyguanosine kinase (dGK). While TK1 is highly specific for thymidine (dT), dCK, TK2 and dGK are able to accept several substrates.[8] As an example, 3TC and FTC (**FIGURES 1** and **2**) are both substrates of dCK, being converted to the corresponding MP-NAs (for 3TC, see **SCHEME 1**) more efficiently than the corresponding D-forms. Further phosphorylation leading to di- and triphosphate forms is then accomplished by UMP/CMP kinase and 3-phosphoglycerate kinase, respectively. L-NA-TPs act as dCTP analogues, competitively inhibiting HIV Reverse Transcriptase (RT) and HBV DNA polymerase, by incorporation into viral DNA behaving as chain terminator.[9] In order to understand the "relaxed" enantioselectivity showed by dCK-like enzymes,[10] Sabini *et al.* solved the dCK three-dimensional structure in complex with D- or L-NAs. They concluded that the interaction between dCK and NAs is mediated by the overlay of "fingerprint" groups:

the nucleobase moiety (whose binding requires obligate changes of the sugar moiety) and the 5'OH group (**FIGURE 3**).

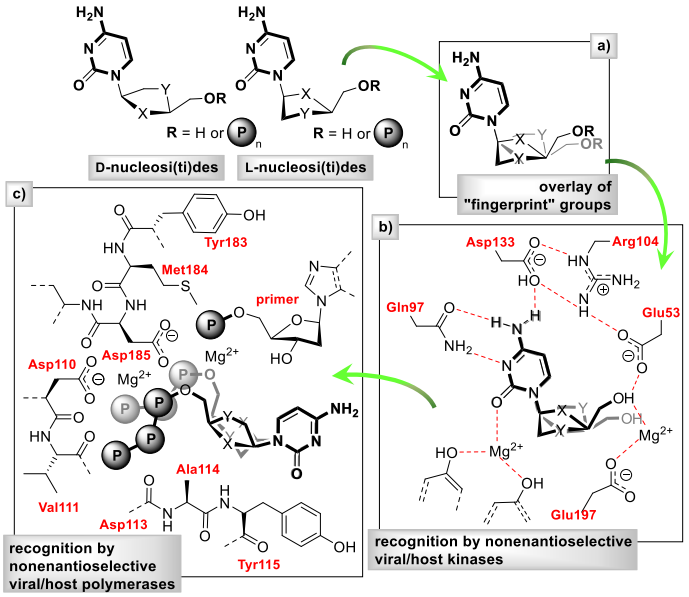

FIGURE 3 (adapted from *Chemical Synthesis of Nucleoside Analogues*).[3] *Schematic representation of the structural features determining the biological activity of* D- *and* L-NAs *(cytidine analogues; X, Y = O, S, C). a) "Fingerprint" groups overlay. b) Phosphorylation of* D- *or* L-NA *by non-enantioselective viral/host kinases. c) Recognition of* D- *or* L-NA *by viral/host polymerases.*

Precisely, once established the interactions between polar atoms of the base and side chains of the enzyme active site, the structure of the L-nucleoside needs only of a small tilt of the base and a change in the glycosidic bond torsion angle to fit the plastic dCK active site. The **FIGURE 3a** clearly shows how the 5'-OH group positioning in the dCK active site is independent of chirality and how the mirror relationship still allows a nearly perfect overlay of the critical O5' atoms.[11] Therefore, if internal symmetry and intrinsic conformational flexibility of L-NAs are suitable to satisfy these structural changes, dCK will exert catalytic activity giving the corresponding MP-NA.

It is worth noting that, despite the described enzymatic plasticity exerted by some examples of host/viral enzymes, other strictly enantioselective hydrolytic enzymes (e.g. deoxycytidine deaminase, see **SCHEME 1**) are not able to recognize unnatural L-NAs, resulting in their low displayed cellular/mitochondrial toxicity.[12]

2.1.1.3 SYNTHESIS OF L-NUCLEOSIDES

As a consequence of displayed dCK (and of other related kinases) peculiar enantioselectivity, the field of L-nucleosides holds promise for the identification of

efficient and selective drugs, whose increasing clinical request (especially as antiviral agents) justifies the development of a wide variety of synthetic approaches devoted to their preparation. Numerous are the sugar-modified L-NAs classes: ribose and 2'-deoxyribose, 2',3'-deoxyribose, carbocyclic, pyrrolidinyl, dioxolanyl and others. However, driven by the great antiretroviral activity displayed by 3TC and FTC,[13] the L-nucleosides having a 1,3-oxathiolane sugar moiety as bioisoster of the 2',3'-deoxyribose unit, represent the most prominent examples among all existing nucleoside analogues equipped with a heterocycle sugar ring. Their preparation can be approached by either *de novo* strategies (involving small starting materials such as 1,4-dithiane-2,5-diol) or by *chiron* strategies (using enantiomerically pure and commercially available starting materials such as carbohydrates) (**SCHEME 2**). All the methods share the synthesis of the 1,3-oxathiolanyl intermediate **3** that, in the following Vorbruggen *N*-glycosidation reaction, leads to the target L-nucleosides (**SCHEME 2a**).[14]
Among the possible oxathiolane nucleoside precursors **3**, the acetate **4** has been widely used as electrophilic "sugar" in the stereoselective methods developed for the synthesis of both 3TC and FTC.[15] In this context, recently, Guaragna *et al*. reported a novel highly stereoselective *N*-glycosidation procedure consisting in the combined use of I_2 and silanes (TMS or PMHS) as substrate activators and glycosydation promoters (**SCHEME 2b**).[16]

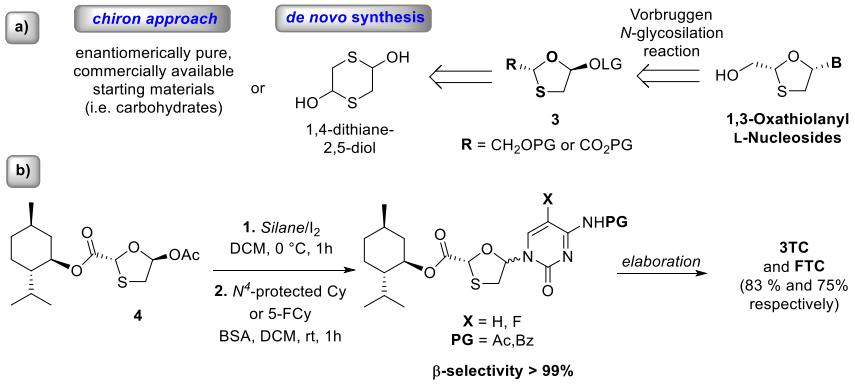

SCHEME 2. a) Simplified scheme of the synthetic approaches used to prepare 1,3-oxathiolanyl-L-nucleosides. b) Highly stereoselective synthesis of 3TC and FTC by a novel *N*-glycosylation procedure (ref. 16).

2.1.1.4 THE ROLE OF FLUORINE IN THE DESIGN OF BIOACTIVE NAS

Fluorinated NAs (namely nucleosides containing fluorine atom(s) or fluorine-containing groups in their sugar or base moiety) have drawn increasing attention in the last 30 years;[17] as a consequence, a wide number of important fluorinated pharmaceuticals have been discovered and developed by modifying the skeleton of biologically active

nucleosides (**FIGURE 4**).[18] The advantages deriving from incorporation of fluorine atom(s) into biologically active molecules are based on its unique characteristics: (1) fluorine is the second smallest atom and closely mimics hydrogen without much distortion of the geometry;[19] (2) fluorine is the most electronegative element and can act as an isopolar and isosteric mimic of a hydroxyl group (the C–F bond length, 1.35 Å, is close to the C–O bond length, 1.43 Å), as well as fluorine is a hydrogen-bond acceptor;[20] (3) the strength of C–F bond exceeds that of C–H bond resulting often in increased biological/chemical stability, improved lipophilicity and better pharmacokinetic and pharmacodynamic properties of the corresponding compounds.[21] Therefore, the selective introduction of fluorine atom(s) into a bioactive nucleoside has become an important strategy in the design and discovery of novel drug candidates.[22]

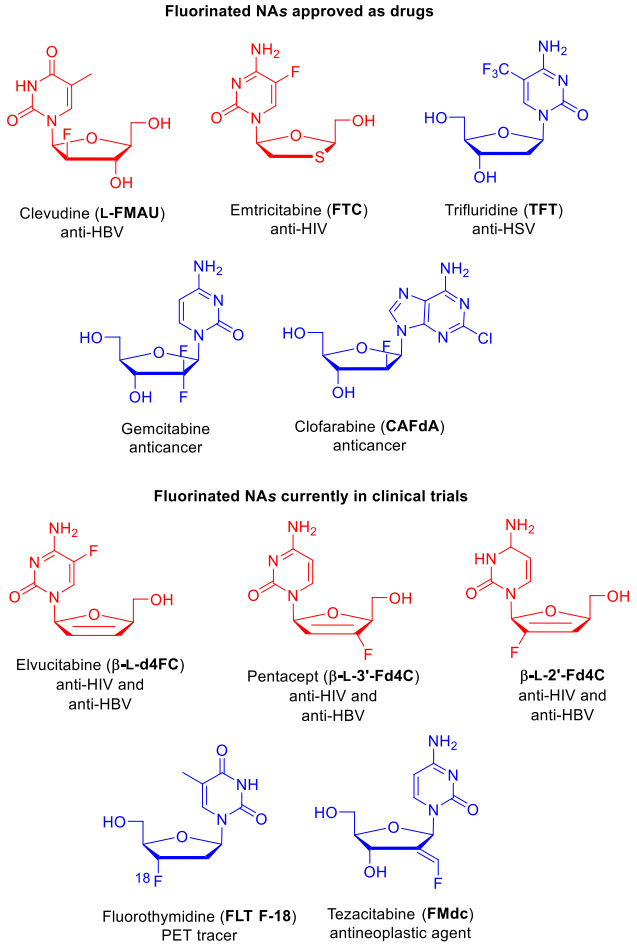

FIGURE 4. Examples of D- (in blue) and L- (in red) fluorinated NAs approved as drugs or in clinical trials.

2.1.1.4.1 FLUORINATION SYNTHETIC METHODOLOGIES

Therefore, the synthesis of fluorinated NAs has required the development of novel fluorination methodologies and fluorinating reagents to allow the stereoselective introduction of one or more fluorine atoms. The fluorination reactions are mainly classified dependently by the chemical nature, electrophilic or nucleophilic, of the fluorine source reagent.

a) Nucleophilic fluorinating reagents

Depending on the reaction environment, the fluoride ion (F^-) can act either as a poor nucleophile (in a protic solvent) or as a good nucleophile (in polar aprotic solvents, especially in presence of large lipophilic countercations). Activation of alcohols with good leaving groups, such as mesylate, tosylate or triflate, followed by a S_N2 substitution by a fluoride ion has become a standard method to replace OH with F. Commonly used nucleophilic fluorinating reagents are the Olah's reagents (Py·nHF and $^{i}Pr_2NH \cdot 3HF$) and DAST ([(diethylamino)sulfur trifluoride], Et_2NSF_3) (**FIGURE 5**). The latter is a really versatile fluorinating agent; it is able to give the classical S_N2 reaction (in presence of a suitably introduced good leaving group) but also: a) one-step exchange of a hydroxyl group (primary, secondary, tertiary and allylic OH) by fluorine in excellent yields, mainly with a complete inversion of configuration; b) conversion of most aldehydes and ketones to the corresponding *gem*-difluorides; c) sulphoxide conversion in the corresponding α-fluoro-thioether by a modified Pummerer reaction.[23]

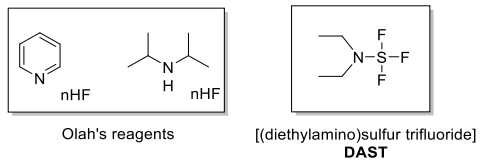

FIGURE 5. Commonly used nucleophilic fluorinating reagents.

b) *Electrophilic fluorinating reagents*

When a fluorine atom binds to an electronegative nitrogen (F–X) it acts as a 'real' F^+ source in reactions with electron-rich double bonds or in the replacement of a proton on aromatic systems. NFSI (*N*-fluorobenzenesulfonimide) and Selectfluor® (1-chloromethyl-4-fluoro-1,4-diazoniabicyclo [2.2.2] octanebis(tetrafluoroborate) are the most used and efficient electrophilic fluorinating agents (**FIGURE 6**). The latter is a stable, easily handled and solid electrophilic fluorinating agent, soluble in polar solvents, such as MeCN, DMF and H_2O. Selecfluor® is an equivalent of F_2, but much more effective and selective. Asymmetric fluorinations are also achieved with Selectfluor® in the presence of various chiral catalysts.[24]

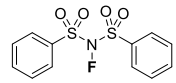

N-fluorobenzensulfonimide
NFSI

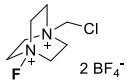

(1-Chloromethyl-4-fluoro-1,4-diazoniabicyclo
[2.2.2] octanebis(tetrafluoroborate)
Selectfluor®

FIGURE 6. Commonly used electrophilic fluorinating reagents.

2.1.2 RESULTS AND DISCUSSION

2.1.2.1 SYNTHESIS OF β-L-2′-FLUORO-3′-THIACYTIDINE (F-3TC) STEREOISOMERS

In an effort to improve the pharmacological properties of 3TC (**2**), a great deal of modifications has been explored over the past decades.[25] The most effective change in this area has been the formal replacement of a hydrogen by a fluorine atom at C5 position of cytosine, leading to Emtricitabine [(–)-2',3'-dideoxy-3'-thia-5-fluorocytidine or FTC] and Racivir [(±)-FTC or RCV] (**FIGURE 7**). Conversely, no synthetic endeavours have been so far devoted to the preparation of 3TC derivatives having a fluorine atom in the "sugar" backbone. If on the one hand, fluorine introduction at the C2′ β-position is reported to increase the stability of the corresponding *N*-glycosidic bond[26] (keeping the antiviral potential), on the other hand the occurrence of up to three labile stereocentres in such a small molecule could potentially affect the stability of the molecule.

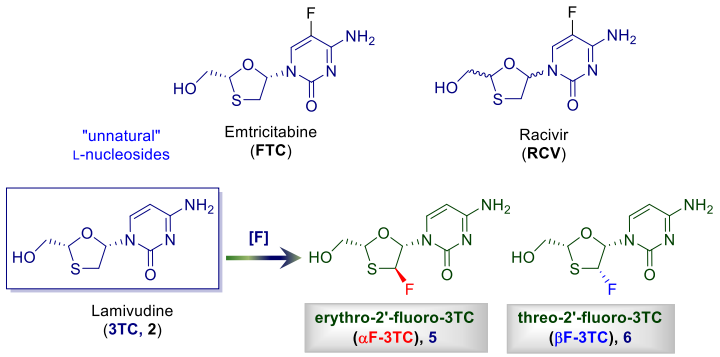

FIGURE 7. Oxathiolane nucleosides 3TC (**2**), FTC, RCV and 2'-fluorinated 3TC congeners (2'*S*)-F-3TC (**5**) and (2'*R*)-F-3TC (**6**).

Intrigued by these observations, the aim of the project herein reported has been the synthesis of 2'-fluorinated 3TC derivatives having either (1'*S*,2'*S*,4'*R*) or (1'*S*,2'*R*,4'*R*) configuration [i.e. (2'*S*)-F-3TC (**5**) and (2'*R*)-F-3TC (**6**)] (**FIGURE 7**).[27] Furthermore, the nucleoside **6** has been evaluated *in vitro* as antiviral agent against Hepatitis C Virus (HCV), Respiratory Sinctial Virus (RSV) and HIV. The experiments have been performed at Gilead Sciences.

2.1.2.2 PRELIMINARY ORGANOCATALYTIC ELECTROPHILIC FLUORINATION REACTIONS

In initial attempts, fluorine atom introduction was conceived at an early stage of the synthesis by an asymmetric, organocatalytic electrophilic fluorination of oxathiolanones **10a,b** (**SCHEME 3** and **TABLE 1**). These last were prepared starting from ethylene glycol **7** and glycerol **8** via aldehydes **9a,b** respectively, as previously reported (**SCHEME 3**).[28,29,30,31]

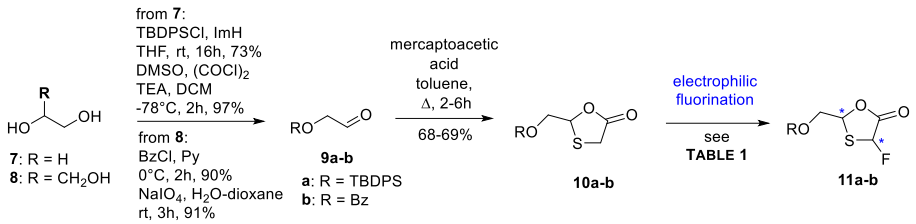

SCHEME 3. Synthesis of fluorinated oxathiolanes **11a-b** starting from **7-8**.

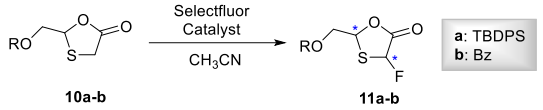

TABLE 1. Organocatalytic asymmetric fluorination of oxathiolanones **10a,b**.

All reactions were carried out at room temperature unless otherwise specified. [a] *i-PrOH used as co-solvent (CH_3CN:i-PrOH = 10:1 v/v).* [b] *Minor amounts (10-12%) of mercaptolactones* ***12a-b*** *(**FIGURE 8**) were also detected.* [c] *The reaction was carried out at 0°C.* [d] *The enantiomeric excess was determined by ^{1}H NMR analysis of the major trans isomer using Eu(hfc)$_3$ as shift reagent.* [e] *ND: not detected (owing to broadness of NMR signals following Eu(hfc)$_3$ addition).* [f] *The (–)-enantiomer was obtained as deduced by polarimetric analysis.*

entry	compound	time (h)	yield (%)	*trans*:*cis*	*ee* (%)[d]
1	**10a**	16	50	>20:1	<5
2	**10b**	16	55	>20:1	<5
3	**10a**[a,b]	1	50	4:1	ND[e]
4	**10b**[a,b]	1	47	4:1	52[f]
5	**10a**[a,c]	10	65	4:1	ND[e]
6	**10b**[a,c]	12	85	4:1	60[f]

The fluorination reaction (**TABLE 1**) was studied using L-proline as chiral organocatalyst; Selectfluor® was chosen as the fluorine source in place of the more effective *N*-fluorobenzenesulfonimide (NFSI), since use of the latter rapidly altered the starting oxathiolanones **10a,b** (releasing the parent aldehydes **9a,b**). Treatment of mercaptolactones **10a,b** with Selectfluor and proline in CH_3CN[32] smoothly provided (16h) the corresponding fluorination products **11a-b** (50-55% yields; **TABLE 1**, entries 1-2). In both cases, the reaction exhibited a high degree of diastereoselectivity (*trans*:*cis* >20:1). Considering that starting compounds **10a-b** were racemic mixtures, this last result was invariably associated to an exceedingly poor enantioselectivity (<5% *ee*), as confirmed by ^{1}H NMR analysis of the *trans* isomer of **11a-b** following treatment with

$Eu(hfc)_3$. In line with previous reports,[33] in subsequent attempts, use of *i*-PrOH as co-solvent (CH_3CN:*i*-PrOH = 10:1 v/v) led to a significant improvement in the enantioselectivity of the reaction [e.g., **11b**: *trans*:*cis* = 4:1; 52% *ee* (*trans* isomer)]. A preference for the (–)-enantiomer was found, as suggested by polarimetric analysis (entry 4). Furthermore, the reaction was much faster in this case (1h). The formation of minor amounts of byproducts **12a-b** (10-12%) was also detected[34,35] (**FIGURE 8**). When the same reaction was performed at 0°C, only traces of the last ones were found; in addition, a further improvement in the enantioselectivity (**11b**: 60% *ee*) and in the reaction yields (65-85%) was observed (entries 5-6).

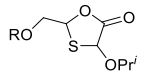

12a-b
a: R = TBDPS
b: R = Bz

FIGURE 8. Byproducts **12a-b** of the organocatalytic fluorination reactions.

Despite the synthetic relevance of these first promising results, a more comprehensive study of oxathiolanone fluorination involving the use of other chiral organocatalysts[36] and methodologies[37] was not performed. Indeed, α-fluorinated compounds **11a-b** did not show any stability to the typical reduction conditions of the lactone group (DIBAL-H, DIBAL-H/Ac_2O, DIBAL-H/MeI, Red-Al/Ac_2O, $NaBH_4$/Ac_2O, BH_3-THF, PTSA/Ac_2O), required for the subsequent nucleobase insertion step.
On the basis of described unsuccessful results, the synthetic strategy to obtain **5** and **6** was then changed and alternative routes were explored trying to accomplish the fluorination step at the late stage of the synthesis, namely once performed the preparation of 3TC.

2.1.2.3 *EN ROUTE* TO 2'-FLUORO-OXATHIOLANYL NUCLEOSIDES

In an early approach aimed to prepare the nucleoside **16** (**SCHEME 4**), ketone group reduction of **10a** and subsequent acetylation of the resulting hemiacetal function gave oxathiolanyl acetate **13** (71% o.y.; **SCHEME 4**), which was used as an achiral model substrate. Thioether oxidation of the latter (MCPBA) led to a 2:1 mixture of sulfoxides **14** (66%), which were subjected to a Pummerer rearrangement (Ac_2O, AcONa). Acetyl ester **15** was formed with slight stereoselectivity; a concurrent acetoxy group anomerization (α/β = 1/1) was also found under these conditions (69% o.y.).

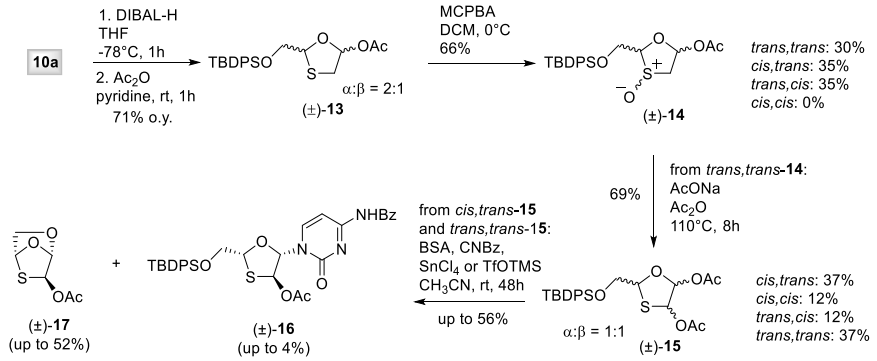

SCHEME 4. Oxathiolanone **10a** elaboration.

The newly installed acetoxy ester function in **15** was conceived both as a stereodirecting moiety in the subsequent *N*-glycosidation step and as a leaving group for the nucleophilic fluorination reaction. However, **15** displayed limited synthetic utility: when treated under typical *N*-glycosidation conditions (Cy^{NBz}/BSA/$SnCl_4$ or TfOTMS), it was converted into the desired nucleoside **16** only in traces (up to 4%); anhydrosugar **17** was instead recovered as the major reaction product (up to 52%), despite the known compatibility of the reagents with the TBDPS group (**SCHEME 4**).

A further alternative route was then considered and unprotected Lamivudine (3TC, **2**) was first of all prepared exploiting a highly stereoselective Et_3SiH/I_2-mediated *N*-glycosidation method of menthyl oxathiolane **4**, briefly described before (see **PARAGRAPH 2.1.1.3**).[16] 3TC was next converted into the *bis*-benzoylated derivative **18** by treatment with BzCl in pyridine (95%). When **18** was subjected to common sulfoxidation conditions (MCPBA), a 7:3 mixture of (*1'S,3'R,4'R*) and (1'*S*,3'*S*,4'*R*) configured nucleosides **19** was attained (80%). Conversely, treatment of **18** under Kagan's conditions[38] [Ti-(*O*-*i*-Pr)$_4$, L-DET, H_2O, CuOOH] yielded protected 3TC sulfoxide **19** (64%) with a remarkably higher stereoselectivity [(3'*R*)-**19**:(3'*S*)-**19** > 20:1]. Unexpectedly, the nucleophilic fluorination of **19**, devised by treatment of the latter with diethylaminosulfur trifluoride (DAST) and ZnI_2, restored the starting sulfide[39] **18** in place of the desired fluorinated nucleoside (**SCHEME 5**).

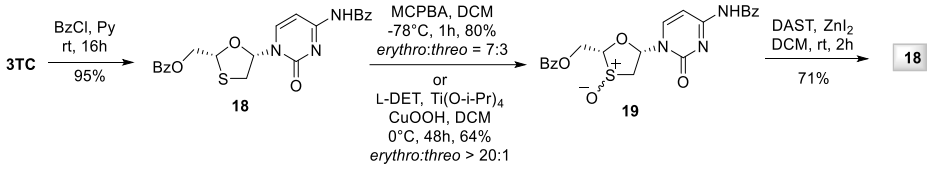

SCHEME 5. Asymmetric sulfoxidation reactions to obtain **19**.

On the other hand, Pummerer rearrangement of **19** led to the corresponding 2'-*O*-acetyl ester **20** (**SCHEME 6**). When typical conditions were used (Ac_2O, AcONa, 110°C, 8h),

no stereoselectivity was found (*d.r.* = 1:1) starting from an equimolar mixture of (3'*R*)-**19** and (3'*S*)-**19**; the displacement of the *N*-benzoyl group into a *N*-acetyl derivative **20a** was also concurrently observed (73%). Interestingly, if a catalytic amount (0.2 equiv.) of Ti(O-*i*-Pr)$_4$ was added to the reaction mixture, the rearrangement of (3'*R*)-**19** proceeded without formation of any side product and with very high stereoselectivity, obtaining nucleoside (2'*S*)-**20b** as the only detected reaction product (73%). When a 1:1 mixture of diastereomeric sulfoxides (3'*R*)-**19** and (3'*S*)-**19** was engaged in the reaction, we even found that the only (3'*R*) isomer was converted, while the (3'*S*) congener was recovered unreacted (**SCHEME 6**). Direct fluorination of **20a** with HF-pyridine[40] did not give the desired fluorinated nucleoside, even after prolonged reaction times; the de-*N*-acetylated nucleoside **21** was instead recovered (71%).

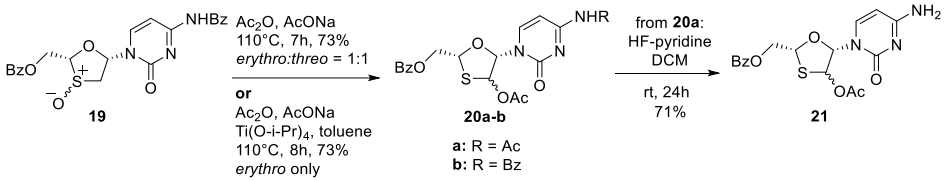

SCHEME 6. En route to 2'F-oxathiolanyl nucleosides via Pummerer rearrangement.

On the other hand, treatment of **20a-b** with lithium trifluoroethoxide (CF_3CH_2OLi, obtained *in situ* by reaction of CF_3CH_2OH with BuLi)[41] in CF_3CH_2OH led to a C2'-selective de-*O*-acylation, providing hemithioacetals **22a-b** in satisfying 60-63% yields (**SCHEME 7**). The reaction of **22a-b** with DAST eventually enabled OH→F displacement by nucleophilic fluorination to give, already after 0.5h at 0°C, 2'-fluoronucleosides **23** and **24** (**23a**-**24a**, R = Ac, 66% o.y.; **23b**-**24b**, R = Bz, 72% o.y.). Relative configuration assignment was based on the observation of a NOE contact between H2' and H4' nuclei in **23a**, which was therefore identified as the (2'*R*)-isomer. It should be however noted that a not negligible NOE signal between the same nuclei was also found in the corresponding (2'*S*) epimer **24a**. Noteworthy, a strong interaction between distant F2' and H4' nuclei (^4J = 7.2 Hz) was observed in **23b**, while it was not detected in **24b**. In line with literature data,[42] the long-range hydrogen-fluorine coupling (LRHFC)[41a] was thought to be correlated with HOMO-LUMO interactions involving fluorine atom orbitals and those on C4'. The reaction proceeded with a slight stereoselectivity for the (2'*S*) isomer (d.r. = 3:1). Any attempt to improve or reverse the stereochemical outcome of the reaction was unsuccessful: as an example, replacement of DCM with THF gave a 2.4:1 ratio of (2'*S*):(2'*R*); in addition, the use of DMF (6 equiv.) as stereodirecting agent[43] increased the amount of (2'*R*) isomer only up to (2'*S*):(2'*R*) = 1.5:1. When the reaction was performed starting from the single isomer (2'*S*)-**22b**, an even equimolar amount of the two fluorinated nucleosides was obtained.

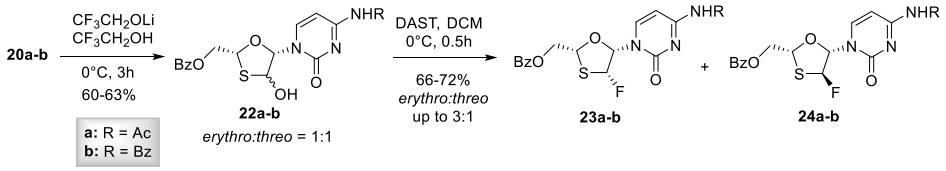

SCHEME 7. Nucleophilic fluorination reactions to nucleosides **23-24a,b.**

Protective groups removal of **24a** (NH_3/MeOH) eventually provided (92%) the first 2'-fluorinated 3TC derivative **5** [(2'*S*)-F-3TC; **SCHEME 8**]. However, over time (2-4h) the latter underwent to a spontaneous cyclization, leading to the undesired cyclonucleoside **25** (99%). The same compound was formed even faster when the crude was treated with Et_2O/MeOH during recrystallization attempts. It's worth noting that treatment of **25** with Ac_2O/AcONa along with a catalytic amount of Ti(*O*-*i*-Pr)$_4$ provided back triacetate **26** in a high stereoselective manner [(2'*S*)(2'*R*) >20:1] (**SCHEME 8**). The fluorinated 3TC **6** [(2'*R*)-F-3TC] was similarly obtained by ammonolysis of **23b** (90%). In this case, we were glad to observe that **6** was stable throughout the deprotection process as well as during the subsequent purification procedures.

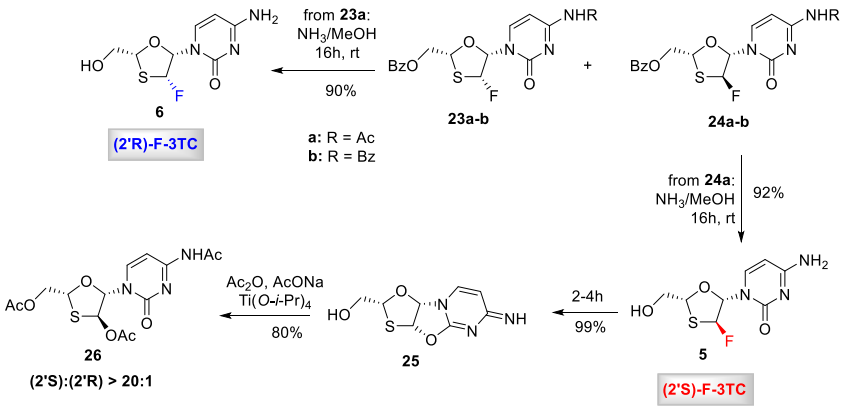

SCHEME 8. Deprotected fluorinated 3TC congeners **5-6**.

With the aim to unambiguously determine the relative configuration of the fluorination products, our efforts were eventually devoted to the determination of their structure by X-ray analysis. Since crystals of either **23a-b**, **24a-b** or **6** were unsuitable to this end, the latter was protected as *bis*-4-bromobenzoyl derivative **27** (*p*-BrBzCl/DMAP, 69%). X-ray analysis of the latter confirmed the *cis* orientation of the nucleobase, the fluorine atom and the hydroxymethylene group: indeed, the absolute configuration of the three stereogenic centres, established by X-ray anomalous dispersion effects, resulted to be (1'*S*,2'*R*,4'*R*) (**SCHEME 9**).

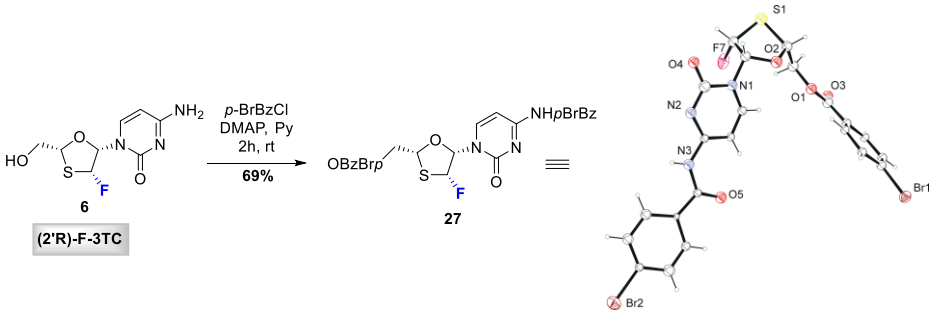

SCHEME 9. X-Ray analysis of **27** to confirm its stereocenters configuration.

2.1.3 BIOLOGICAL DATA

In order to study the antiviral potential of 2'-fluorinated 3TC derivatives, nucleoside **6** was evaluated for its *in vitro* antiviral activity. The experiments were performed under the supervision of Dr. Richard Mackman (Gilead Sciences). Particularly, compound **6** was evaluated for its inhibitory effect on the cytopathicity of Respiratory Syncytial Virus, RSV (strain A2) in Hep2 cells using Ribavirin as reference compound (**TABLE 2**). Nucleoside **6** was also evaluated for its ability to inhibit the replication of HIV-1 (3b) in MT4 cells (**TABLE 2**), using AZT as reference control. Finally, **6** was tested for wild-type replicon potency and selectivity against HCV in 1b R-luc cells (harboring a genotype 1b replicon), in 1a R-luc cells (harboring a genotype 1a replicon) and in 2aLucNeo-25 cells (harboring a genotype 2a JFH-1 replicon) (**TABLE 2**). In this case, 2'C-methyl-adenosine (2'CMeA) was used as control compound. Unfortunately, **6** did not show measurable antiviral activities in all cases. In order to explain the lack of expected antiviral activity of **6**, minimized energy structures of **6** and the parent anti-HIV drug 3TC were preliminary obtained (HyperChem Software 8.0), with the aim to search conformational differences between the two compounds. We found that in both cases the C3'-*endo* (or North) conformation resulted the only adopted conformation as shown in **FIGURE 9**. This result is in line with previous crystallographic data[5,11] and highlights the peculiarity of 3TC, which adopts a pseudo-sugar ring pucker opposite to the C3'-*exo* (or South) conformation adopted, *inter alia*, by both D- and L-dC when in complex with dCK (**FIGURE 10**). The conformational profile of 3TC represents thus an exception to the general rule about the conformational requirements of NAs for enzymatic (kinases and polymerases) recognition.[44]

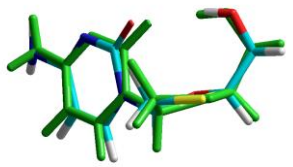

FIGURE 9. Overlay of the C3'-*endo* conformers of **2** and **6** (in green).

Accordingly, data suggest that the occurrence of the fluorine atom at C2' position does not affect the conformational preferences of the oxathiolane sugar moiety. However, even though the recognition between **6** and dCK is expected by conformational reasons, we can speculate that just the presence of a highly electronegative atom may make difficult this process. Indeed, considering that the fluorine atom is reported to also act as a OH mimic because of the similar electronic densities, the presence of fluorine in such

an unusual conformation could make **6** a poor substrate for dCK, as it could be regarded as a 2-OH (*arabino*) nucleoside.

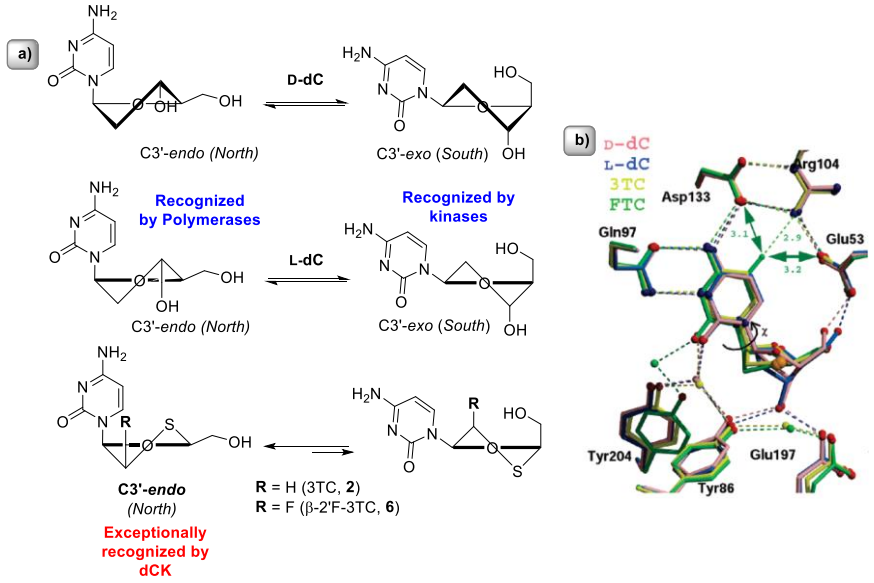

FIGURE 10. a) D-dC, L-dC, 3TC and β-2F'-3TC conformations recognized by kinases and polymerases; b) comparison of the binding of D-dC, L-dC, 3TC and FTC in the active site od dCK (*adapted from ref. 5*).

TABLE 2. Antiviral evaluation of **6** (EC_{50}, μM).

	6	**Ribavirin**	**AZT**	**2'CMeA**
RSV	>100	16.0	ND	ND
CC_{50}	>100	88.7	ND	ND
HIV-1	>53	ND	0.047	ND
CC_{50}	>53	ND	27.5	ND
GT 1b	>44.4	ND	ND	0.78
CC_{50}	>44.4	ND	ND	>44.4
GT 1a	>44.4	ND	ND	0.67
CC_{50}	>44.4	ND	ND	>44.4
GT 2a	>44.4	ND	ND	0.67
CC_{50}	>44.4	ND	ND	>44.4

2.1.4 CONCLUSIONS

This topic has concerned the development of a stereoselective synthetic methodology devoted to the preparation of novel class of 3TC derivatives, 2'-fluorinated having either (1'*S*,2'*S*,4'*R* or α–F3TC, **5**) or (1'*S*,2'*R*,4'*R* or β–F3TC, **6**) configuration. The insertion of fluorine atom has been conceived on the basis of other reported examples of 2'-fluorinated D-NAs resulted antiviral agents (e.g. α and β-FddA)[45] and with the aim to enhance the pharmacological properties already observed for 3TC, **2**. Despite several encountered synthetic difficulties because of the presence of three labile centres in the same molecule, the target nucleosides have been efficiently synthetized; unfortunately, **5** showed remarkable instability affording the intramolecular cyclization byproduct **25**. On the other side, **6**, once confirmed the stereocenters chirality by X-ray diffraction of its derivative **27**, has been tested as antiviral agent (anti-HCV, anti-HIV and anti-RSV) but did not show any interesting antiviral activity. A preliminary computational approach in order to explain the lack of expected activity has been conducted, and allowed us to detect for **6** and **2** the same unconventional conformational behaviour. In both cases a C3'-*endo* conformation (typically recognized by viral polymerases) is indeed adopted. This preliminary study led us to assume that the fluorine atom in C2', due its electronic mimicking of a hydroxyl group, could give to **6** *arabino* nucleoside resemblance explaining thus its poor recognition by dCK.

2.1.5 EXPERIMENTAL SECTION

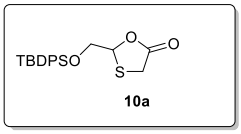

10a

2-[(tert-Butyldiphenylsilyloxy)methyl]-1,3-oxathiolan-5-one (10a). Mercaptoacetic acid (0.61 mL, 8.72 mmol) was added to a stirred solution of aldehyde **9a** (2.60 g, 8.72 mmol) in toluene (18 mL) at rt. The mixture was warmed to reflux and stirred for 2 h, the H_2O formed was removed by means of a Dean–Stark apparatus. The reaction was then concentrated under reduced pressure. Flash chromatography of the crude residue (hexane:Et_2O=95:5) gave the pure oxathiolactone **10a** (2.20 g, 68% reaction yield) as a pale yellow oil. ^{1}H NMR (200 MHz, $CDCl_3$), δ: 1.06 (*s*, 9 H), 3.59 (*d*, J = 16.4 Hz, 1 H), 3.82 (*dd*, J = 16.4, 0.8 Hz, 1 H), 3.82 (*dd*, J = 11.2, 3.4 Hz, 1 H), 3.95 (*dd*, J = 11.2, 3.4 Hz, 1 H), 5.82 (*dt*, J = 3.4, 0.8 Hz, 1 H), 7.37–7.52 (*m*, 6 H), 7.62–7.78 (*m*, 4 H). ^{13}C NMR (50 MHz, $CDCl_3$), δ: 19.1, 26.6, 31.2, 67.4, 81.2, 128.0, 130.0, 132.4, 135.6, 173.1. Anal. Calcd for $C_{20}H_{24}O_3SSi$: C, 64.48; H, 6.49; S, 8.61. Found: C, 64.35; H, 6.52; S, 8.60.

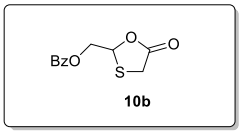

10b

2-[(Benzoyloxy)methyl]-1,3-oxathiolan-5-one (10b). Following the procedure for **10a** using aldehyde **9b** (2.36 g, 14.4 mmol) gave **10b** (2.36 g, 69% reaction yield) as a pale-yellow oil. ^{1}H NMR (500 MHz, $CDCl_3$), δ: 3.68 (*d*, J = 16.4 Hz, 1 H), 3.76 (*d*, J = 16.4 Hz, 1 H), 4.59 (*dd*, J = 12.3, 4.1 Hz, 1 H), 4.61 (*dd*, J = 12.3, 4.9 Hz, 1 H), 5.79 (*dd*, J = 4.9, 4.1 Hz, 1 H), 7.47 (*t*, J = 7.3 Hz, 2 H), 7.61 (*t*, J = 7.5 Hz, 1 H), 8.05 (*d*, J = 7.5 Hz, 2 H). ^{13}C NMR (50 MHz, $CDCl_3$), δ: 30.8, 66.5, 78.4, 128.6, 129.0, 129.8, 133.5, 165.8, 172.3. Anal. Calcd for $C_{11}H_{10}O_4S$: C, 55.45; H, 4.23; S, 13.46. Found: C, 55.30; H, 4.20; S, 13.53.

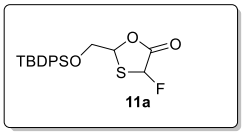

11a

2-[(*tert*-Butyldiphenylsilyloxy)methyl]-4-fluoro-1,3-oxathiolan-5-one (11a). L-Proline (10 mg, 86 μmol) and Selectfluor (0.61 g, 1.72 mmol) were sequentially added to a cooled (0 °C) and stirred mixture of lactone **10a** (0.32 g, 0.86 mmol) in MeCN/*i*-PrOH (10:1, 2.16 mL). The mixture was stirred at this temperature for 10 h; then it was diluted with EtOAc and washed with sat. $NaHCO_3$ until neutral. The organic layer was dried (Na_2SO_4) and the solvent evaporated under reduced pressure. Flash chromatography of the crude residue (hexane:EtOAc= 90:10) provided **11a** (0.22 g, 65% reaction yield) as an oil; mixture of stereoisomers *cis*/*trans*, 1:4.

***trans*-11a:** ^{1}H NMR (200 MHz, $CDCl_3$), δ: 1.06 (*s*, 9 H), 3.87 (*dd*, J = 10.7, 5.1 Hz, 1 H), 3.98 (*dd*, J = 10.7, 4.7 Hz, 1 H), 5.78 (*q*, J = 4.8 Hz, 1 H), 6.20 (*d*, J = 56.6 Hz, 1 H), 7.27–7.52 (*m*, 6 H), 7.54–7.78 (*m*, 4 H). ^{13}C NMR (50 MHz, $CDCl_3$), δ: 19.2, 26.6, 65.3, 81.4, 92.2 (*d*, J = 225.8 Hz), 127.8, 130.1, 132.2, 135.5, 167.6. MS (MALDI): *m*/*z* [M + Na]$^+$ calcd: 413.11; found: 413.12. Anal. Calcd for $C_{20}H_{23}FO_3SSi$: C, 61.51; H, 5.94; S, 8.21. Found: C, 61.60; H, 5.96; S, 8.24.

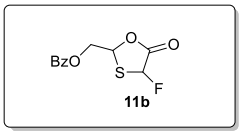

11b

2-[(Benzoyloxy)methyl]-4-fluoro-1,3-oxathiolan-5-one (11b). Following the procedure for **11a** using mercaptolactone **10b** (0.24 g, 1.0 mmol) gave **11b** (0.22 g, 85% reaction yield) as an oil; mixture of stereoisomers *cis*/*trans*, 1:4.

***trans*-11b:** 60% ee (NMR analysis, Eu(hfc)$_3$ used as shift reagent). ^{1}H NMR (500 MHz, $CDCl_3$), δ: 4.63 (*dd*, J = 12.6, 5.2 Hz, 1 H), 4.66 (*dd*, J = 12.6, 4.2 Hz, 1 H), 6.02 (*q*, J = 5.2 Hz, 1 H), 6.25 (*d*, J = 56.2 Hz, 1 H), 7.46 (*t*, J = 7.3 Hz, 2 H), 7.61 (*t*, J = 7.8 Hz, 1 H), 8.04 (*d*, J = 7.6 Hz, 2 H). ^{13}C NMR (125 MHz, $CDCl_3$), δ: 64.3, 78.8, 92.1 (*d*, J = 232.0 Hz), 128.6, 129.7, 133.6, 165.5, 166.7 (*d*, J = 25.2 Hz). MS (MALDI): *m*/*z* [M + Na]$^+$ calcd: 279.02; found: 279.11. Anal. Calcd for $C_{11}H_9FO_4S$: C, 51.56; H, 3.54; S, 12.51. Found: C, 51.45; H, 3.56; S, 12.48.

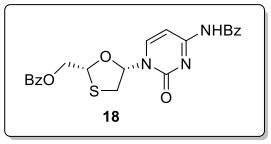

18

(1′*S*,4′*R*)-*N*^{4}-Benzoyl-5′-*O*-benzoyl-2′,3′-dideoxy-3′-thiacytidine (18). Benzoyl chloride (1.27 mL, 11 mmol) was added to a cooled (0 °C) solution of lamivudine **2** (1.00 g, 4.37 mmol) in anhydrous pyridine (3.0 mL). The resulting solution was warmed to rt and stirred for 16 h. The mixture was then concentrated under reduced pressure; the solid was partitioned between CH_2Cl_2 and brine. The organic layer was dried (Na_2SO_4)

and concentrated under reduced pressure. Chromatography of the crude residue (silica gel, CH_2Cl_2:MeOH=95:5) provided **18** (1.8 g, 95% reaction yield) as a white solid. FT-IR (KBr): 3056, 1718, 1694, 1671, 1670, 1262, 785 cm^{-1}. ^1H NMR (500 MHz, $CDCl_3$), δ: 3.34 (*dd*, J = 12.8, 2.6 Hz, 1 H), 3.70 (*dd*, J = 12.8, 5.4 Hz, 1 H), 4.79 (*dd*, J = 12.6, 2.7 Hz, 1 H), 4.90 (*dd*, J = 12.6, 4.3 Hz, 1 H), 5.55 (*dd*, J = 4.3, 2.7 Hz, 1 H), 6.41 (*dd*, J = 5.4, 2.6 Hz, 1 H), 7.46 (*t*, J = 7.3 Hz, 4 H), 7.60 (*t*, J = 7.3 Hz, 2 H), 8.12 (*d*, J = 7.4 Hz, 4 H), 8.33 (*d*, J = 7.6 Hz, 1 H), 11.61 (*br s*, 1 H). ^{13}C NMR (125 MHz, $CDCl_3$), δ: 39.3, 63.3, 85.5, 87.7, 96.7, 127.5, 128.5, 128.6, 128.7, 129.1, 132.6, 133.2, 133.7, 144.7, 154.3, 162.4, 165.8. Anal. Calcd for $C_{22}H_{19}N_3O_5S$: C, 60.40; H, 4.38; N, 9.61; S, 7.33. Found: C, 60.48; H, 4.40; N, 9.58; S, 7.31.

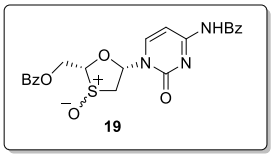

19

(1′*S*,3′*R*/*S*,4′*R*)-*N*^{4}-Benzoyl-5′-*O*-benzoyl-2′,3′-dideoxy-3′ thiacytidine *S*-Oxide (19). *Method A*: a solution of MCPBA (0.23 g, 1.29 mmol) in anhydrous CH_2Cl_2 (3.0 mL) was added dropwise to a stirred and cold (–78 °C) solution of thioether **18** (0.43 g, 0.99 mmol) in anhyd CH_2Cl_2 (10 mL). The resulting mixture was stirred at this temperature for 1 h; then it was warmed to rt, diluted with further CH_2Cl_2 and washed with sat. $NaHCO_3$ solution and with brine. The organic layer was dried (Na_2SO_4) and concentrated under reduced pressure. Chromatography of the crude residue (silica gel, CH_2Cl_2:MeOH=98:2) provided **19** (0.36 g, 80% reaction yield) as a white solid; mixture of diastereomers dr (1′*S*,3′*R*,4′*R*)/(1′*S*,3′*S*,4′*R*) ~ 7:3). *Method B*: Ti(*O*-*i*-Pr)$_4$ (0.29 mL, 0.99 mmol) was added dropwise to a stirred solution of (+)-L-DET (0.33 mL, 1.98 mmol) in anhyd CH_2Cl_2 (7.0 mL) at rt. After 20 min, H_2O (18.0 μL, 0.99 mmol) was added. After 10 min, temperature was cooled to –20 °C and a solution of nucleoside **18** (0.43 g, 0.99 mmol) in anhydrous CH_2Cl_2 (13 mL) was added within 5 min. Cumyl hydroperoxide (0.29 mL, 1.98 mmol) was then added dropwise. The resulting solution was eventually warmed to 0 °C and stirred at this temperature for 48 h. Afterwards, H_2O (10 mL) was added to the mixture. After 10 min, the resulting emulsion was filtered over a Celite pad, the solid was rinsed with further CH_2Cl_2 (2 × 60 mL). The collected filtrate was treated with 10% $Na_2S_2O_5$ solution (30 mL), then with 5% NaOH solution (30 mL) until neutrality and finally with brine. The organic layer was dried (Na_2SO_4) and concentrated under reduced pressure. Chromatography of the crude residue (silica gel, CH_2Cl_2:MeOH=98:2) provided (3′*R*)-**19** (0.29 g, 64% reaction yield) as a white solid; one main isomer dr (1′*S*,3′*R*,4′*R*)/(1′*S*,3′*S*,4′*R*) >20:1.

(3′*R*)-19: FT-IR (KBr): 3020, 2924, 1734, 1714, 1636, 1252, 1068, 795 cm^{-1}. ^1H NMR (400 MHz, DMSO-d^6), δ: 3.53 (*dd*, J = 13.9, 8.6 Hz, 1 H), 3.64 (*dd*, J = 13.9, 5.0 Hz, 1

H), 4.82 (*dd*, J = 12.3, 5.1 Hz, 1 H), 4.88 (*dd*, J = 12.3, 5.0 Hz, 1 H), 5.12 (*t*, J = 5.0 Hz, 1 H), 6.73 (*dd*, J = 8.5, 5.0 Hz, 1 H), 7.37 (*d*, J = 7.5 Hz, 1 H), 7.53 (*t*, J = 7.5 Hz, 2 H), 7.56 (*t*, J = 7.6 Hz, 2 H), 7.64 (*br t*, J = 7.4 Hz, 1 H), 7.70 (*br t*, J = 7.5 Hz, 1 H), 7.98 (*br d*, J = 7.8 Hz, 4 H), 8.19 (*br d*, J = 7.5 Hz, 1 H). ^{13}C NMR (100 MHz, DMSO-d^6), δ: 54.9, 62.3, 88.9, 97.6, 102.9, 128.9, 129.0, 129.4, 129.7, 129.8, 133.3, 134.2, 146.0, 154.3, 164.2, 165.7, 168.0. Anal. Calcd for $C_{22}H_{19}N_3O_6S$: C, 58.27; H, 4.22; N, 9.27; S, 7.07. Found: C, 58.39; H, 4.20; N, 9.24; S, 7.04.

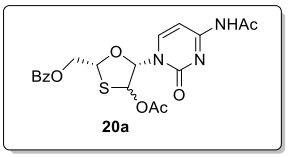

20a

(1′*S*,2′*R*/*S*,4′*R*)-*N*^{4}-Acetyl-2′-*O*-acetyl-5′-*O*-benzoyl-3′-deoxy-3′-thiacytidine (20a). AcONa (0.20 g, 2.5 mmol) was added to a stirred solution of sulfoxides (3′*R*)- and (3′*S*)-**19** (0.11 g, 0.25 mmol) in Ac_2O (10 mL) at rt. After 5 min, the suspension was warmed to 110 °C and stirred at this temperature for 7 h. The resulting solution was then cooled to rt, washed with sat. $NaHCO_3$ until neutral and extracted with EtOAc. The organic layer was dried (Na_2SO_4) and concentrated under reduced pressure. Chromatography of the crude residue (silica gel, hexane:EtOAc=1:1) gave **20a** (79 mg, 73% reaction yield) as a pale yellow oil; mixture of stereoisomers dr 1:1. FT-IR (KBr): 3076, 2919, 1737, 1721, 1664, 1613, 1215, 792 cm^{-1}. ^{1}H NMR (500 MHz, $CDCl_3$), δ: 1.85 (*s*, 1.5 H), 2.17 (*s*, 1.5 H), 2.23 (*s*, 1.5 H), 2.26 (*s*, 1.5 H), 4.65 (*dd*, J = 12.2, 3.3 Hz, 0.5 H), 4.69 (*dd*, J = 12.2, 6.0 Hz, 0.5 H), 4.87 (*dd*, J = 12.5, 3.5 Hz, 0.5 H), 4.91 (*dd*, J = 12.5, 3.4 Hz, 0.5 H), 5.59 (*dd*, J = 6.0, 3.3 Hz, 0.5 H), 5.84 (*t*, J = 3.1 Hz, 0.5 H), 6.24 (*s*, 0.5 H), 6.27 (*d*, J = 2.8 Hz, 0.5 H), 6.34 (*d*, J = 2.8 Hz, 0.5 H), 6.48 (*s*, 0.5 H), 7.47 (*t*, J = 7.7 Hz, 1 H), 7.54 (*t*, J = 7.6 Hz, 1 H), 7.60 (*t*, J = 7.5 Hz, 0.5 H), 7.67 (*t*, J = 7.5 Hz, 0.5 H), 8.06 (*d*, J = 7.6 Hz, 1 H), 8.08 (*d*, J = 7.2 Hz, 2 H), 8.18 (*d*, J = 7.6 Hz, 1 H), 8.99 (*br s*, 1 H). ^{13}C NMR (125 MHz, $CDCl_3$), δ: 20.5, 24.8, 29.5, 62.4, 65.5, 79.2, 85.3, 86.4, 89.0, 91.9, 96.3, 128.0, 128.5, 128.7, 129.7, 129.9, 133.5, 133.9, 144.0, 145.2, 163.0, 165.8, 168.7, 170.9.

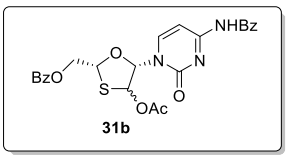

31b

(1′*S*,2′*S*,4′*R*)-2′-*O*-Acetyl-*N*^{4}-benzoyl-5′-*O*-benzoyl-3′-deoxy-3′-thiacytidine (20b). Ac_2O (0.27 mL, 2.9 mmol), AcONa (0.24 g, 2.9 mmol), and Ti(*O*-*i*-Pr)$_4$ (17.0 μL, 0.06 mmol) were sequentially added to a stirred solution of (3′*R*)-**19** (0.13 g, 0.29 mmol) in

anhydrous toluene (9.0 mL) at rt. The resulting mixture was warmed to 110 °C and stirred at this temperature for 8 h. The solution was then cooled to rt, washed with sat. $NaHCO_3$ until neutral and extracted with EtOAc. The organic layer was dried (Na_2SO_4) and concentrated under reduced pressure. Chromatography of the crude residue (silica gel, hexane:EtOAc=1:1) gave **20b** (0.10 g, 73% reaction yield) as a white solid as the single (2′*S*)-isomer. FT-IR (KBr): 3062, 2924, 1733, 1704, 1698, 1622, 1221, 790 cm^{-1}. ^1H NMR (500 MHz, $CDCl_3$), δ: 2.19 (*s*, 3 H), 4.87 (*dd*, J = 12.7, 2.5 Hz, 1 H), 4.92 (*dd*, J = 12.7, 3.5 Hz, 1 H), 5.86 (*t*, J = 3.3 Hz, 1 H), 6.27 (*s*, 1 H), 6.54 (*s*, 1 H), 7.53 (*t*, J = 7.7 Hz, 2 H), 7.56 (*t*, J = 7.5 Hz, 2 H), 7.63 (*t*, J = 7.5 Hz, 1 H), 7.68 (*t*, J = 7.6 Hz, 1 H), 7.88 (*br d*, J = 7.7 Hz, 3 H), 8.10 (*d*, J = 7.8 Hz, 2 H), 8.23 (*d*, J = 7.7 Hz, 1 H), 8.67 (*br s*, 1 H). ^{13}C NMR (125 MHz, $CDCl_3$), δ: 20.9, 62.7, 85.4, 86.4, 96.8, 127.3, 128.7, 128.8, 129.1, 129.6, 133.2, 133.9, 145.4, 154.0, 162.8, 166.0, 168.8. Anal. Calcd for $C_{24}H_{21}N_3O_7S$: C, 58.17; H, 4.27; N, 8.48; O, 22.60; S, 6.47. Found: C, 58.05; H, 4.28; N, 8.51; S, 6.45.

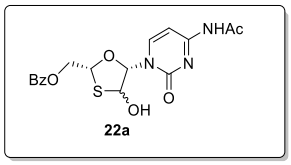

22a

(1′*S*,2′*S*/*R*,4′*R*)-N^4-Acetyl-5′-*O*-benzoyl-3′-deoxy-2′-hydroxy-3′-thiacytidine (22a). A solution of acetyl esters (2′*S*)- and (2′*R*)-**20a** (0.10 g, 0.23 mmol) in CF_3CH_2OH (0.58 mL) was added dropwise to a cold (0 °C) solution of 1.6 M BuLi in *n*-hexane (0.29 mL, 0.47 mmol) in CF_3CH_2OH (1.2 mL). The mixture was stirred at this temperature for 3 h; then it was transferred to a separatory funnel, washed with a 10% NH_4Cl solution until neutral and extracted with EtOAc. The organic layer was dried (Na_2SO_4) and concentrated under reduced pressure. Chromatography of the crude residue (silica gel, CH_2Cl_2:MeOH=98:2) gave **22a** (57 mg, 63% reaction yield) as an oil; approx. equimolar mixture of (2′*S*) and (2′*R*) diastereomers. FT-IR (KBr): 3615, 3083, 2901, 1715, 1640, 1621, 1233, 794 cm^{-1}. ^1H NMR (500 MHz, $CDCl_3$), δ: 2.22 (*s*, 1.5 H), 2.25 (*s*, 1.5 H), 4.59 (*dd*, J = 11.9, 3.2 Hz, 0.5 H), 4.80 (*dd*, J = 11.9, 7.4 Hz, 0.5 H), 4.86 (*dd*, J = 12.9, 1.9 Hz, 0.5 H), 4.93 (*dd*, J = 12.9, 3.6 Hz, 0.5 H), 5.55 (*br d*, J = 7.3, 3.1 Hz, 0.5 H), 5.76 (*s*, 0.5 H), 5.89 (*br d*, J = 2.3 Hz, 0.5 H), 5.99 (*br t*, J = 3.4 Hz, 0.5 H), 6.13 (*br s*, 0.5 H), 6.27 (*s*, 0.5 H), 7.29 (*d*, J = 7.5 Hz, 0.5 H), 7.42–7.68 (*m*, 3.5 H), 8.07 (*br d*, J = 7.8 Hz, 2 H), 8.15 (*d*, J = 7.5 Hz, 0.5 H), 8.24 (*d*, J = 7.4 Hz, 0.5 H), 9.13–9.50 (*m*, 1 H). ^{13}C NMR (125 MHz, $CDCl_3$), δ: 24.8, 62.8, 67.1, 76.5, 79.3, 86.6, 86.9, 91.6, 94.6, 96.3, 96.8, 128.4, 128.7, 129.0, 129.4, 129.6, 129.7, 133.4, 133.8, 144.6, 146.7, 155.6, 155.7, 162.6, 162.7, 166.0, 166.1, 170.5, 170.8. Anal. Calcd for $C_{17}H_{17}N_3O_6S$: C, 52.17; H, 4.38; N, 10.74; S, 8.19. Found: C, 52.30: H, 4.36; N, 10.70; S, 8.22.

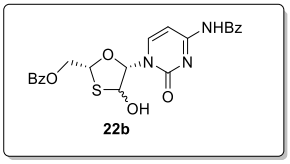

22b

(1′*S*,2′*S*,4′*R*)-*N*^{4}-Benzoyl-5′-*O*-benzoyl-3′-deoxy-2′-hydroxy-3′-thiacytidine (22b). A solution of acetyl ester (2′*S*)-**20b** (50 mg, 0.10 mmol) in CF_3CH_2OH (0.29 mL) was added dropwise to a cold (0 °C) solution of 1.6 M BuLi in *n*-hexane (0.14 mL, 0.23 mmol) in CF_3CH_2OH (0.6 mL). The mixture was stirred at this temperature for 3 h; then it was transferred into a separatory funnel, washed with a 10% NH_4Cl solution until neutral, and extracted with EtOAc. The organic layer was dried (Na_2SO_4) and concentrated under reduced pressure. Chromatography of the crude residue (silica gel, CH_2Cl_2:MeOH=98:2) provided **22b** (30 mg, 65% reaction yield) as a mixture of stereoisomers (dr 1:1), recrystallization of the mixture gave (2′*S*)-**22b** (27.5 mg, 60% reaction yield) as the main stereoisomer; dr >20:1. FT-IR (KBr): 3607, 3068, 2909, 1702, 1647, 1617, 1245, 789 cm^{-1}. ^{1}H NMR (400 MHz, $CDCl_3$), δ: 4.85 (*dd*, J = 12.8, 2.7 Hz, 1 H), 4.92 (*dd*, J = 12.9, 3.6 Hz, 1 H), 5.74 (*s*, 1 H), 6.00 (*app t*, J = 3.4, 2.9 Hz, 1 H), 6.29 (*s*, 1 H), 7.42–7.56 (*m*, 5 H), 7.59 (*t*, J = 7.5 Hz, 1 H), 7.65 (*t*, J = 7.5 Hz, 1 H), 7.98 (*d*, J = 7.5 Hz, 2 H), 8.07 (*d*, J = 7.5 Hz, 2 H), 8.33 (*d*, J = 7.6 Hz, 1 H). ^{13}C NMR (100 MHz, $CDCl_3$), δ: 62.7, 77.1, 86.4, 86.7, 94.6, 96.5, 128.0, 128.7, 128.8, 129.0, 129.6, 129.7, 132.3, 133.4, 133.8, 145.5, 153.5, 162.2, 165.9, 166.7. Anal. Calcd for $C_{22}H_{19}N_3O_6S$: C, 58.27; H, 4.22; N, 9.27; S, 7.07. Found: C, 58.40; H, 4.20; N, 9.30; S, 7.05.

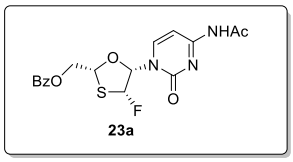

23a

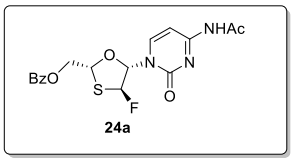

24a

(1′*S*,2′*R*,4′*R*)-*N*^{4}-Acetyl-5′-*O*-benzoyl-3′-deoxy-2′- fluoro-3′-thiacytidine (23a) and (1′*S*,2′*S*,4′*R*)-*N*^{4}-Acetyl-5′-*O*-benzoyl-3′-deoxy-2′-fluoro-3′-thiacytidine (24a). DAST (0.04 mL, 0.32 mmol) was carefully added to a stirred solution of hemithioacetals (2′*S*)- and (2′*R*)-**22a** (0.09 g, 0.24 mmol) in anhyd CH_2Cl_2 (9 mL) at 0 °C. The mixture was stirred at this temperature for 30 min, then sat. $NaHCO_3$ (1 mL) was added in one portion. The resulting emulsion was washed with further $NaHCO_3$ solution until neutral and extracted with CH_2Cl_2. The organic layer was dried (Na_2SO_4) and concentrated under reduced pressure. Flash chromatography of the crude residue (EtOAc) gave the two separated diastereomers (2′*R*)-**23a** (15 mg; white solid) and (2′*S*)-**24a** (45 mg; white solid) (66% total reaction yield).

23a: FT-IR (KBr): 2980, 2921, 1734, 675, 1679, 1647, 1316, 1279, 829 cm^{-1}. ^{1}H NMR (500 MHz, $CDCl_3$), δ: 2.13 (*s*, 3 H), 4.68–4.76 (*m*, 2 H), 5.60–5.66 (*m*, 1 H), 6.26 (*d*, J = 15.1 Hz, 1 H), 6.38 (*d*, J = 60.0 Hz, 1 H), 7.26 (*d*, J = 7.8 Hz, 1 H), 7.48 (*t*, J = 7.8 Hz, 2 H), 7.60 (*t*, J = 7.8 Hz, 1 H), 7.98 (*d*, J = 7.8 Hz, 1 H), 8.10 (*d*, J = 7.8 Hz, 2 H), 9.15 (*br s*, 1 H). ^{13}C NMR (125 MHz, $CDCl_3$), δ: 25.0, 65.6, 79.4, 90.6 (*d*, J = 18.0 Hz), 95.4 (*d*, J = 231.7 Hz), 96.8, 129.7, 129.8, 130.9, 135.6, 145.2, 154.7, 163.1, 166.0, 170.5. Anal. Calcd for $C_{17}H_{16}FN_3O_5S$: C, 51.90; H, 4.10; F, 4.83; N, 10.68; S, 8.15. Found: C, 51.79; H, 4.12; N, 10.72; S, 8.12.

24a: FT-IR (KBr): 2970, 2925, 1724, 689, 1673, 1634, 1315, 1276, 819 cm^{-1}. ^{1}H NMR (500 MHz, $CDCl_3$), δ: 2.25 (*s*, 3 H), 4.90 (*dd*, J = 13.0, 2.4 Hz, 1 H), 4.98 (*dd*, J = 13.0, 3.2 Hz, 1 H), 5.94 (*br s*, 1 H), 6.26 (*d*, J = 52.0 Hz, 1 H), 6.55 (*d*, J = 11.6 Hz, 1 H), 7.27 (*d*, J = 7.0 Hz, 1 H), 7.54 (*t*, J = 7.7 Hz, 2 H), 7.67 (*t*, J = 7.5 Hz, 1 H), 8.07 (*d*, J = 7.3 Hz, 2 H), 8.15 (*d*, J = 7.5 Hz, 1 H), 9.42 (*br s*, 1 H). ^{13}C NMR (125 MHz, $CDCl_3$), δ: 25.0, 62.1, 87.4, 93.2 (*d*, J = 47.9 Hz), 96.5, 103.6 (*d*, J = 233.2 Hz), 124.9, 128.6, 129.6, 133.9, 143.7, 154.5, 162.7, 165.7, 170.1. Anal. Calcd for $C_{17}H_{16}FN_3O_5S$: C, 51.90; H, 4.10; N, 10.68; S, 8.15. Found: C, 51.76; H, 4.11; N, 10.72; S, 8.18.

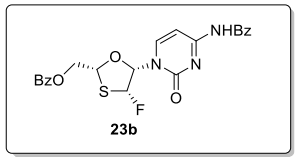

23b

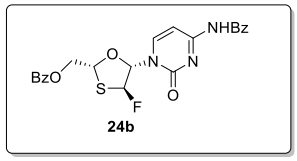

24b

(1′*S*,2′*R*,4′*R*)-*N*^{4}-Benzoyl-5′-*O*-benzoyl-3′-deoxy-2′-fluoro-3′-thiacytidine (23b) and (1′*S*,2′*S*,4′*R*)-*N*^{4}-Benzoyl-5′-*O*-benzoyl-3′-deoxy-2′-fluoro-3′-thiacytidine (24b). Following the procedure for **23a** and **24a** using (2′*S*)- and (2′*R*)-**22b** (50.0 mg, 0.11 mmol) gave fluoronucleosides **23b** (9 mg; white solid) and **24b** (27.1 mg; white solid) (72% total reaction yield).

23b: FT-IR (KBr): 2955, 2923, 1735, 715, 1659, 1627, 1331, 1267, 814 cm^{-1}. ^{1}H NMR (400 MHz, $CDCl^3$), δ: 4.72 (*d*, J = 4.6 Hz, 2 H), 5.64 (*dt*, J = 7.2, 4.5 Hz, 1 H), 6.33 (*dd*, J = 13.7, 1.9 Hz, 1 H), 6.39 (*dd*, J = 58.7, 2.3 Hz, 1 H), 7.48 (*t*, J = 7.7 Hz, 2 H), 7.54 (*t*, J = 7.5 Hz, 2 H), 7.58–7.67 (*m*, 3 H), 7.91 (*d*, J = 7.2 Hz, 2 H), 8.07 (*d*, J = 7.2 Hz, 1 H), 8.09 (*d*, J = 7.9 Hz, 2 H), 8.03 (*br s*, 1 H). ^{13}C NMR (100 MHz, $CDCl_3$), δ: 65.6, 79.9, 90.5 (*d*, J = 19.2 Hz), 95.4 (*d*, J = 235.8 Hz), 96.8, 127.6, 128.5, 128.9, 129.1, 129.7, 132.8, 133.2, 133.4, 145.2, 154.3, 162.9, 165.9, 168.7. ^{19}F {^{1}H dec} NMR (376 MHz, $CDCl_3$), δ: –158.1. Anal. Calcd for $C_{22}H_{18}FN_3O_5S$: C, 58.02; H, 3.98; F, 4.17; N, 9.23; O, 17.56; S, 7.04. Found: C, 58.19; H, 3.98; N, 9.23; S, 7.04.

24b: FT-IR (KBr): 2951, 2919, 1733, 699, 1652, 1617, 1319, 1265, 805 cm^{-1}. ^{1}H NMR (400 MHz, $CDCl_3$), δ: 4.92 (*dd*, J = 13.0, 2.2 Hz, 1 H), 5.01 (*dd*, J = 13.0, 3.3 Hz, 1 H), 5.97 (*br t*, J = 2.5 Hz, 1 H), 6.30 (*d*, J = 52.0 Hz, 1 H), 6.60 (*d*, J = 11.7 Hz, 1 H), 7.44

(*br d*, J = 7.3 Hz, 1 H), 7.53 (*t*, J = 7.5 Hz, 2 H), 7.57 (*t*, J = 7.5 Hz, 2 H), 7.63 (*t*, J = 7.5 Hz, 1 H), 7.70 (*t*, J = 7.5 Hz, 1 H), 7.90 (*d*, J = 7.4 Hz, 2 H), 8.10 (*d*, J = 7.6 Hz, 2 H), 8.22 (*d*, J = 7.3 Hz, 1 H), 8.93 (*br s*, 1 H). ^{13}C NMR (100 MHz, $CDCl_3$), δ: 62.2, 87.5, 93.2 (*d*, J = 42.4 Hz), 103.0 (*d*, J = 242.9 Hz), 127.7, 128.8, 128.9, 129.1, 129.7, 133.5, 134.1, 144.3, 155.0, 161.9, 166.0, 170.0**.** ^{19}F {^{1}H dec} NMR (376 MHz, $CDCl_3$), δ: –158.2. Anal. Calcd for $C_{22}H_{18}FN_3O_5S$: C, 58.02; H, 3.98; N, 9.23; S, 7.04. Found: C, 58.20; H, 3.99; N, 9.20; S, 7.01.

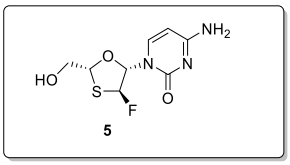

5

(1′*S*,2′*S*,4′*R*)-2′,3′-Dideoxy-2′-fluoro-3′-thiacytidine [(2′*S*)-F-3TC, 5]. Nucleoside **24a** (40 mg, 0.10 mmol) was treated with 7 M NH_3/MeOH solution (2.7 mL) at 0 °C. The resulting suspension was stirred at this temperature for 16 h. The volatiles were then removed under reduced pressure. Chromatography of the crude residue (silica gel, CH_2Cl_2:MeOH=90:10) provided (2′*S*)-F-3TC **5** (23 mg, 92% reaction yield) as a white solid. ^{1}H NMR (400 MHz, CD_3OD), δ: 3.96 (*dd*, J = 13.0, 3.0 Hz, 1 H), 4.12 (*dd*, J = 13.0, 3.1 Hz, 2 H), 5.63 (*br t*, J = 3.0 Hz, 1 H), 5.87 (*d*, J = 7.5 Hz, 1 H), 6.31 (*d*, J = 53.8 Hz, 1 H), 6.51 (*d*, J = 13.1 Hz, 1 H), 8.07 (*d*, J = 7.5 Hz, 1 H).

As discussed in the previous section, an extensive characterization of **5** was hampered by the spontaneous, undesired cyclization of the latter, leading to cyclonucleoside **25** as a white solid (99% reaction yield).

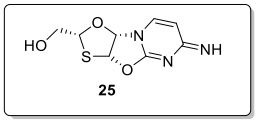

25

Cyclonucleoside 25: ^{1}H NMR (400 MHz, CD_3OD), δ: 3.44 (*dd*, J = 12.7, 2.6 Hz, 1 H), 3.65 (*dd*, J = 12.7, 1.5 Hz, 1 H), 5.86 (*t*, J = 2.4 Hz, 1 H), 6.53 (*d*, J = 7.3 Hz, 1 H), 6.78 (*d*, J = 5.8 Hz, 1 H), 7.00 (*d*, J = 5.8 Hz, 1 H), 8.15 (*d*, J = 7.4 Hz, 1 H). ^{13}C NMR (100 MHz, CD_3OD), δ: 65.0, 93.5, 95.4, 96.5, 103.2, 141.1. Anal. Calcd for $C_8H_9N_3O_3S$: C, 42.28; H, 3.99; N, 18.49; S, 14.11. Found: C, 42.39; H, 3.98; N, 18.42; S, 14.05.

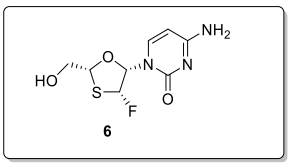

6

(1′*S*,2′*R*,4′*R*)-2′,3′-Dideoxy-2′-fluoro-3′-thiacytidine [(2′*R*)-F-3TC, 6]. Following the procedure for **5** using nucleoside **23a** (26 mg) gave (2′*R*)-F-3TC **6** (14 mg, 90% reaction yield) as a white solid. FT-IR (KBr): 3378, 3364, 2923, 1726, 1253 cm^{-1}. ^{1}H NMR (400 MHz, CD_3OD), δ: 3.83 (*dd*, J = 12.3, 4.2 Hz, 1 H), 3.87 (*dd*, J = 12.3, 5.4 Hz, 1 H), 5.35 (*dt*, J = 7.7, 4.9 Hz, 1 H), 5.91 (*d*, J = 7.6 Hz, 1 H), 6.16 (*dd*, J= 15.9, 2.0 Hz, 1 H), 6.32 (*dd*, J = 59.8, 2.0 Hz, 1 H), 7.80 (*dd*, J = 7.6, 2.1 Hz, 1 H). ^{13}C NMR (100 MHz, CD_3OD), δ: 66.5, 84.5, 92.2 (*d*, J = 19.0 Hz), 96.5, 98.3 (*d*, J = 231.0 Hz), 143.8, 158.5, 168.7. ^{19}F {^{1}H dec} NMR (376 MHz, CD_3OD), δ: –160.1. Anal. Calcd for $C_8H_{10}FN_3O_3S$: C, 38.86; H, 4.08; N, 17.00; S, 12.97. Found: C, 38.72; H, 4.09; N, 17.06; S, 13.00.

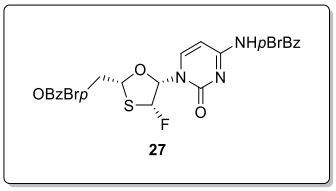

27

(1′*S*,2′*R*,4′*R*)-*N*^{4}-(4-Bromobenzoyl)-5′-*O*-(4-bromobenzoyl)-3′-deoxy-2′-fluoro-3′-thiacytidine (27). 4-Bromobenzoyl chloride (0.18 g, 0.82 mmol) and a catalytic amount of DMAP (5 mg, 0.04 mmol) were added to a cooled (0 °C) solution of nucleoside **6** (82 mg, 0.33 mmol) in anhyd pyridine (3 mL). The resulting mixture was then warmed to rt and stirred at this temperature for 2 h. The mixture was then diluted with H_2O, extracted with EtOAc and washed with brine. The organic layer was dried (Na_2SO_4), filtered and the solvent removed under reduced pressure. Chromatography of the crude residue (CH_2Cl_2:MeOH=90:10) provided pure **27** (0.14 g, 0.22 mmol, 69% reaction yield) as white crystals; mp 227.6–227.8 °C (Et_2O/MeOH). FT-IR (KBr): 3053, 2920, 2847, 1720, 1684, 1661, 1591, 1253, 1107, 784 cm^{-1}. ^{1}H NMR (200 MHz, DMSO-d^6), δ: 4.87–4.99 (*m*, 2 H), 5.73–5.80 (*m*, 1 H), 6.25 (*d*, J = 16.0 Hz, 1 H), 6.60 (*d*, J = 58.9 Hz, 1 H), 7.36 (*d*, J = 7.7 Hz, 1 H), 7.71 (*d*, J = 8.7 Hz, 4 H), 7.91 (*d*, J = 8.7 Hz, 4 H), 8.11 (*d*, J = 6.7 Hz, 1 H), 11.47 (*br s*, 1 H). ^{13}C NMR (50 MHz, DMSO-d^6), δ: 65.8, 79.8 (*d*, J = 22 Hz), 90.1 (*d*, J = 18 Hz), 96.5 (*d*, J = 229 Hz), 96.9, 127.3, 128.2, 128.8, 131.1, 131.7, 131.9, 132.4, 145.8, 154.1, 164.1, 165.2, 167.0. Anal. Calcd for $C_{22}H_{16}Br_2FN_3O_5S$: C, 43.09; H, 2.63; N, 6.85; S, 5.23. Found: C, 43.22; H, 2.62; N, 6.82; S, 5.21.

X-ray Crystallography of 27.

Single crystals of **27** suitable for X-ray diffraction were obtained by slow evaporation of a Et_2O/MeOH solution at rt. One crystal (colorless 0.50 × 0.06 × 0.01 mm) was selected and mounted at 173 K under N_2 flow on a Bruker-Nonius KappaCCD diffractometer equipped with a graphite monochromated MoK_α radiation (λ = 0.71073 Å, CCD rotation images, thick slices, ϕ and ω scans to fill asymmetric unit). Unit cell parameters were

determined by least squares refinement of the θ angles of 134 reflections in the range $3.509° < \theta < 18.771°$. SADABS program was used for scaling and multiscan absorption corrections. The structure was solved by direct methods (SIR97 program) and anisotropically refined (SHELXL-97 program) by the full matrix least-squares method on F^2 against all independent measured reflections in WinGX45 suite programs. Hydrogen atoms were introduced in calculated positions and refined according to a riding model. Absolute configuration *R*/*R*/*S* at C9/C10/C11 was established by anomalous dispersion effects due to the presence of strong scattered atoms.

Crystal data for **27**: empirical formula: $C_{22}H_{16}Br_2FN_3O_5S$; formula weight: 613.26; crystal system: monoclinic; space group: $P2_1$; a = 10.234(3) Å; b = 6.692(2) Å; c = 16.433(3) Å; β = 100.989(15)°; V = 1104.8(5) Å^3; Z = 2; calculated density = 1.843 g/cm^3; abs. coeff. = 3.814 mm^{-1}; θ range 3.30–25.10°; reflections/unique: 6828/3533 (R_{int} = 0.1948); data/restraints/parameters: 3553/163/307; goodness of fit on F^2: 1.029; R_1/wR_2 [$I > 2\sigma(I)$]: 0.0934/0.1469; R_1/wR_2 (all data): 0.2247/0.1932; abs. struc. param.: 0.03(3); Largest diff. peak and hole 0.792, –1.071 e/Å^3.

2.1.6 REFERENCES

[1] Spadari, S.; Maga, G.; Verri, A.; Focher, F. *Expert Opin. Invest. Drugs* **1998**, *7*, 1285.
[2] Focher, F.; Spadari, S.; Maga, G. *Infect. Disord.: Drug Targets* **2003**, *3*, 41.
[3] Pedro, M. *Chemical Synthesis of Nucleoside Analogues* **2013**, John Wiley & Sons Inc. Publication.
[4] Schinazi, R.F.; Chu, C.K.; Peck, A.; Mcmillan, A.; Mathis, R.; Cannon, D.; Jeong, L-S.; Beach, J.W.; Choi, W-B.; Yeola, S.; Liotta, D.L. *Antimicrob. Agents Chemother.* **1992**, 36, 672.
[5] Sabini, E.; Hazra, S.; Konrad, M.; Lavie, A. *J. Med. Chem*. **2007**, *50*, 3004.
[6] Spadari, S.; Ciarrocchi, G.; Focher, F.; Verri, A.; Maga, G.; Arcamone, F.; Iafrate, E.; Manzini, S.; Garbesi, A.; Tondelli, L. *Mol. Pharmacol.* **1995**, *47*, 1231
[7] Balzarini, J.; De Clercq, E.; Baumgartner, H.; Bodenteich, M.; Griengl, H. *Mol. Pharmacol.* **1990**, *37*, 395.
[8] dCK activates deoxycytidine (dC), deoxyadenosine (dA) and deoxyguanosine (dG). See for example: Eriksson, S.; Munch-Petersen, B.; Johansson, K.; Eklund, H. *Cell. Mol. Life Sci.* **2002**, *59*, 1327.
[9] Maga, G.; Amacker, M.; Hubscher, U.; Gosselin, G.; Imbach, J.L.; Mathé, C.; Faraj, A.; Sommadossi, J.; Spadari, S. *Nucleic Acids Res*. **1999**, *27*, 972.
[10] It must note that dCK, dGK, TK2 and HSV-1 TK share high sequence similarity (dCK-dGK, 47% identity over 263 residues; dCK-TK2, 40% identity over 198 residues) and, structurally, these four enzymes belong to the same nucleoside kinase family, while TK1 makes a family of its own.
[11] Sabini, E.; Hazra, S.; Konrad, M.; Burley, S.; Lavie, A. *Nucleic Acids Res*. **2007**, *35*, 186.
[12] Maury, G. Antivir. *Chem. Chemother.* **2000**, *11*, 165.
[13] (a) Wang, P.; Hong, J. H.; Cooperwood, J. S.; Chu, C. K. *Antiviral Res.* **1998**, *40*, 19. (b) Gumina, G.; Song, G.-Y.; Chu, C. K. *FEMS Microbiol. Lett.* **2001**, *202*, 9. (c) Gumina, G.; Chong, Y.; Choo, H.; Song, G.-Y.; Chu, C. K. *Curr. Top. Med. Chem.* **2002**, *2*, 1065.
[14] (a) Belleau, B.; Dixit, D.; Nguyen-Bu, N.; Kraus, J.-L. International Conference on AIDS. Montreal, Canada, June 4–9, paper T.C.O.1, **1989**; (b) Choi, W.-B.; Yeola, S.; Liotta, D. C.; Schinazi, R. F.; Painter, G. R.; Davis, M.; St. Clair, M.; Furman, P. A. *Bioorg. Med. Chem. Lett.* **1993**, *3*, 693.
[15] (a) Mansour, T.; Jin, H.; Tse, A. H. L.; Siddiqui, M. A. PCT Int. Appl. WO 92/20669, **1992**. (b) Jin, H.; Siddiqui, A.; Evans, C. A.; Tse, A.; Mansour, T. S.; Goodyear, M. D.; Ravenscroft, P.; Beels, C. D. *J. Org. Chem*. **1995**, *60*, 2621. (c) Goodyear, M. D.; Hill, M. L.; West, J. P.; Whitehead, A. J. *Tetrahedron Lett.* **2005**, *46*, 8535.
[16] Caso, M.F.; D'Alonzo, D.; D'Errico, S.; Palumbo, G.; Guaragna, A. *Org. Lett.* **2015**, *17*, 2626.
[17] (a) Purser, S.; Moore, P.R.; Swallow, S.; Gouverneur, V. *Chem. Soc. Rev.* **2008**, *37*, 320. (b) Qiu, X.; Xu, X.; Qing, F. *Tetrahedron* **2010**, *66*, 789.
[18] Pankiewicz, K. W. *Carbohydr. Res.* **2000**, *327*, 87.
[19] Hagmann, W. K. *J. Med. Chem.* **2008**, *51*, 4359.
[20] O'Hagan, D. *Chem. Soc. Rev.* **2008**, *37*, 308.
[21] Park, B. K.; Kitteringham, N. R.; O'Neill, P. M. *Annu. Rev. Pharmacol. Toxicol.* **2001**, *41*, 443.
[22] Liu, P.; Sharon, A.; Chu, C. K. *J. Fluor. Chem.* **2008**, *129*, 743.
[23] McCarthy, J. R.; Matthews, D. P.; Paolini, J. P. *Org. Synth.* **1998**, *9*, 446.
[24] (a) Prakash, G. K. S.; Beier, P. *Angew. Chem., Int. Ed.* **2006**, *45*, 2172. (b) Pihko, P. M. *Angew. Chem., Int. Ed.* **2006**, *45*, 544.

[25] (a) Romeo, G.; Chiacchio, U.; Corsaro, A.; Merino, P. *Chem. Rev.* **2010**, *110*, 3337; (b) Li, Q.; Du, Y. Z.; Yuan, H.; Zhang, X. G.; Miao, J.; Cui, F. D.; Hu, F. Q. *Eur. J. Pharm. Sci.* **2010**, *41*, 498; (c) Aquaro, S.; Wedgwood, O.; Yarnold, C.; Cahard, D.; Pathinara, R.; Mcguigan, C.; Caliò, R.; De Clercq, E.; Balzarini, J.; Perno, C. F. *Antimicrob. Agents Chemother.* **2000**, *44*, 173; (d) Ravetti, S.; Gualdesi, M. S.; Trinchero-Hernández, J. S.; Turk, G.; Briñón, M. C. *Bioorg. Med. Chem.* **2009**, *17*, 6407; (e) Anastasi, C.; Hantz, O.; De Clercq, E.; Pannecouque, C.; Clayette, P.; Dereuddre-Bosquet, N.; Dormont, D.; Gondois-Rey, F.; Hirsch, I.; Kraus, J.-L. *J. Med. Chem.* **2004**, *47*, 1183.

[26] (a) Marquez, V. E.; Tseng, C. K.-H.; Mitsuya, H.; Aoki, S.; Kelley, J. A.; Ford Jr, H.; Roth, J. S.; Broder, S.; Johns, D. G., Driscoll, J. S. *J. Med. Chem.* **1990**, *33*, 978; (b) Mu, L.; Sarafianos, S. G.; Nicklaus, M. C.; Russ, P.; Siddiqui, M. A.; Ford Jr., H.; Mitsuya, H.; Le, R.; Kodama, E.; Meier, C.; Knispel, T.; Anderson, L.; Barchi Jr., J. J.; Marquez, V. E. *Biochemistry* **2000**, *39*, 11205.

[27] D'Alonzo, D.; De Fenza, M.; Palumbo, G.; Romanucci, V.; Di Fabio, G.; Guaragna, G. *Synthesis* **2017**, *49*, 998.

[28] Ayala, L.; Lucero, C. G.; Romero, J. A. C.; Tabacco, S. A.; Woerpel, K. A. *J. Am. Chem. Soc.* **2003**, *125*, 15521.

[29] Choi, W.-B.; Wilson, L. J.; Yeola, S.; Liotta, D. C.; Schinazi, R. F. *J. Am. Chem. Soc.* **1991**, *113*, 9377.

[30] Caputo, R.; Guaragna, A.; Palumbo, G.; Pedatella, S. *Eur. J. Org. Chem.* **1999**, 1455.

[31] Steiner, D. D.; Mase, N.; Barbas, C. F. III *Angew. Chem., Int. Ed.* **2005**, *44*, 3706.

[32] Fluorination attempts were also conducted in DMF, obtaining however a complex mixture of reaction products.

[33] Beeson, T. D.; MacMillan, D. W. C. *J. Am. Chem. Soc.* **2005**, *127*, 8826.

[34] We do not currently have sufficient information to establish whether the enhancement in the reaction efficiency by *i*-PrOH may deal with a catalyst's activation or with a direct participation of the *sec*-alcohol in the catalytic cycle. Studies aimed to elucidate this uncommon behaviour are, however, underway.

[35] A S_N1-type fluorine displacement from compounds **11a-b** (via thionium ion) was hypothesized to explain formation of **12**:

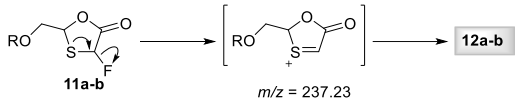

In support of this conjecture, the thionium ion was detected (*m*/*z* = 237.23) during MS analysis of **11a-b.**

[36] Kwiatkowski, P.; Beeson, T. D.; Conrad, J. C.; MacMillan, D. W. C. *J. Am. Chem. Soc.* **2011**, *133*, 1738.

[37] (a) Ma, J.-A.; Cahard, D. *Chem. Rev.* **2008**, *108*, PR1; (b) Cahard, D.; Xu, X.; Couve-Bonnaire, S.; Pannecoucke, X. *Chem. Soc. Rev.* **2010**, *39*, 558.

[38] Brunel, J.-M.; Diter, P.; Duetsch, M.; Kagan, H. B. *J. Org. Chem.* **1995**, *60*, 8086.

[39] As witnessed by the colour change of the reaction mixture (from colourless to purple), the reaction mechanism is expected to involve formation of molecular iodine according to following scheme.

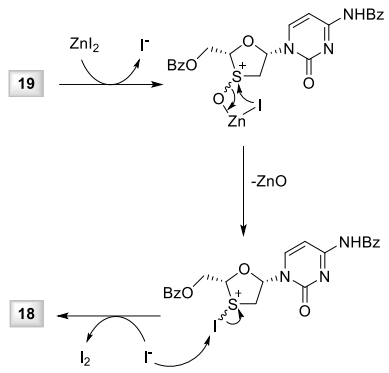

[40] Hayashi, M.; Hashimoto, S.; Noyori, R. *Chem. Lett.* **1984**, 1747.
[41] Nowak, I.; Jones, C. T.; Robins, M. J. *J. Org. Chem.* **2006**, *71*, 3077.
[42] (a) Wasylishen, R. E.; Barfield, M. *J. Am. Chem. Soc.* **1975**, *97*, 4545; (b) Trempe, J.-C.; Wilds, C. J.; Denisov, A. Y.; Pon, R. T.; Damha, M. J.; Gehring, K. *J. Am. Chem. Soc.* **2001**, *123*, 4896.
[43] Lu, S.-R.; Lai, Y.-H.; Chen, J.-H.; Liu, C.-Y. Mong, K.-K. T. *Angew. Chem., Int. Ed.* **2011**, *123*, 7453.
[44] Marquez, V.E.; Ben-Kasus, T.; Barchi, J.J.; Green, K.M.; Nicklaus, M.C.; Agbaria, R. *J. Am. Chem. Soc.* **2004**, *126*, 543.
[45] (1) Thibaudeau, C.; Acharya, P.; Chattopadhyaya, J. *Stereoelectronic Effects in Nucleosides and Nucleotides and their Structural Implications,* Uppsala University Press, **1999**. (2) Marquez, V. E.; Tseng, C.; Kelley, K.-H.; Mitsuya, J. A.; Broder, H.; Roth, S.; Driscoll, J. S. *Biochem. Pharmacol.* **1987**, *36*, 2719. (3) Roth, J. S.; McCully, C. M.; Balis, F. M.; Poplack, D. G.; Kelley, J. A. *Drug Metab. Dispos.* **1999**, *27*, 1128.

2.2 Novel Piperidinyl Iminosugar-Based Nucleosides as Selective Pharmacological Tools

2.2.1 INTRODUCTION

As described in the last chapter, viral diseases are the primary cause of death among human infectious diseases worldwide.[1] Vaccination and antiviral chemotherapies are typically used to prevent or treat viral infections.[2] While the vaccination is not available for viruses such as HIV or HCV (in the case of HHVs, an effective vaccine is today available only for Varicella Zoster Virus, VZV),[3] the antiviral chemotherapy proven to be a successful choice in many cases. However, given the increasing emergence of drug-resistant clinical isolates due to the viruses' high mutation rate, the search of new antiviral therapies remains critical. The field of nucleoside analogues (NAs) represents, as already mentioned, a valid alternative to this aim. In this chapter, two novel concepts will be introduced: the possibility to conformationally preorganize the nucleoside in order to enhance the selectivity associated to the host-guest recognition process and then, the possibility to design mutagenic nucleosides that, together with the chain termination, constitutes one of the most used antiviral strategies in this context. Both concepts have been merged to synthetize a novel class of mutagenic piperidinyl nucleosides, subject of the following chapter.

2.2.1.1 PREORGANIZED HOST-GUEST CHEMISTRY

"The first step in enzymatic catalysis is the formation of highly *selective* molecular complexes that orient the reactants and catalysts. […] In host-guest chemistry, the host molecule is the larger and the guest molecule is the smaller of the two. The host molecule must *recognize* by complexing best those guest molecules that contain the *array* of binding sites and steric features that *complement* those of the host."[4] In this paper Donald Cram introduced for the first time the "preorganization" concept analysing several examples of small organic guest-host complexes.[4] The formation of these kind of complexes is thermodynamically unlikely for two main reasons: first, three degrees of translational and rotational entropy are lost while forming a complex from two separate molecules, and second, if each molecule has free internal bond rotations (necessarily locked in the complex), several degrees of freedom for each bond will be lost and the "freezing out" of all such rotations will be entropically unfavourable. If the first effect results totally unavoidable, the second one could be easily addressed by chemists designing guest molecules "frozen" in the binding conformation before the recognition processes; then any entropy cost, due to fixing bond rotations, will not be necessary in binding.[5] In few and easier words, reduction of all possible conformational states of a guest molecule to those fitting with the geometric and stereochemical requirements of a host molecule may lead to an entropic benefit of complex formation, and thus to enhanced complex stability. The concept of preorganization has been widely used to design nucleoside analogues (NAs) (and particularly, modified oligonucleotides, MOs;

this aspect will be extensively discussed in the **Chapter 3.1**) endowed with modifications able to restrict the number of conformations and to increase the desired complementarity between the parties. The main result is the strong improvement of the host-guest selectivity because of the drastic reduction of the possible mismatched host-guest processes.[6]

2.2.1.2 THE CENTRAL ROLE OF SUGAR CONFORMATION IN THE ANTIVIRAL ACTIVITY OF NUCLEOSIDE ANALOGUES

The complete definition of the nucleoside conformation usually involves the determination of three groups of structural parameters: (a) the deviation from planarity of the sugar ring, measured by the phase angle of pseudorotation (*P)*, (b) the orientation of the glycosylic bond (χ) and (c) the orientation of the hydroxymethyl group (γ).

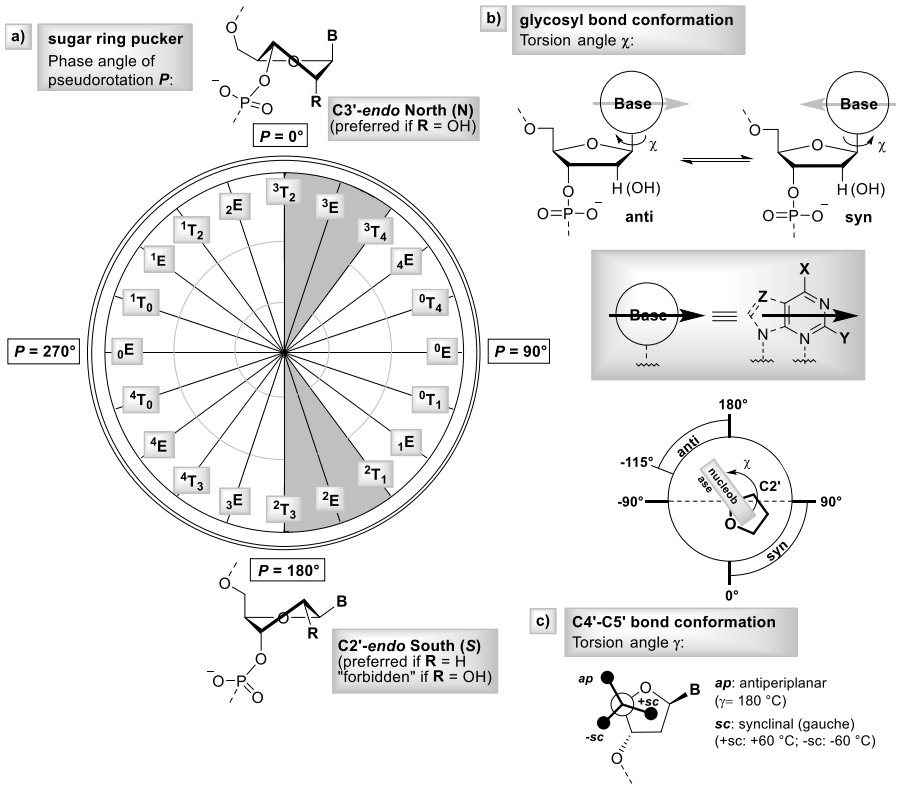

FIGURE 1 ***(taken from ref. 8).*** Structural parameters defining the conformation of a (deoxy)ribonucleoside. a) Phase angle of pseudorotation ***P*** (0°→360°): the nucleoside furanose ring fluctuates between the **C3'-endo** (approx., 0°< *P* <+40°) and the **C2'-endo** (approx., +140°< *P* <+180°) sugar ring conformations. b) Torsion angle **χ** (0°→±180°): the value ranges between two principal low energy domains, **anti** (-115°> χ > -180°), and **syn** (0< χ <90°). c) Orientation of the hydroxymethyl group (**γ**): γ typically ranges between antiperiplanar (**ap**, γ ~ 180°) and synclinal (**sc**, γ = ± 60°) conformations.

The first parameter has been introduced to describe the continuous interconversions among a (virtually) infinite number of puckered forms related to the furanose ring of natural (deoxy)ribonucleosi(ti)des. Thus, the nucleoside conformation can be conveniently described (summarized) by the *P* value (°) as showed in the conformational cycle (**FIGURE 1**).[7,8] Conventionally, *P* = 0° describes a *C*-3'-*endo* puckering, while *P* = 180° the *C*-2'-*endo* antipode; they are also generically defined as *N* (North) and *S* (South) conformations respectively (**FIGURE 1**). The *N* and *S* regions are nearly equally populated for ribonucleosides whereas for 2'-deoxyribonucleosides there is a clear preference for *S* type geometries (≈ 3:1 for the ratio of *S* versus *N* pseudorotamer populations). NMR studies have shown that the puckered geometries of the furanose moiety in nucleos(t)ides interconvert rapidly in solution (in the NMR timescale); this means that the activation energy barrier between the interconverting pseudorotamers in solution is significantly low ($\Delta G \sim 20$ kJ mol^{-1}). However, when the sugar rings of natural (deoxy)ribonucleotides are involved in polymeric structures (i.e. RNA and DNA), the energy differences between A- and B- right handed helical structures are magnified and the A-form prefers the *N* pseudorotamer while the B- form the *S* one (**FIGURE 2**).[9]

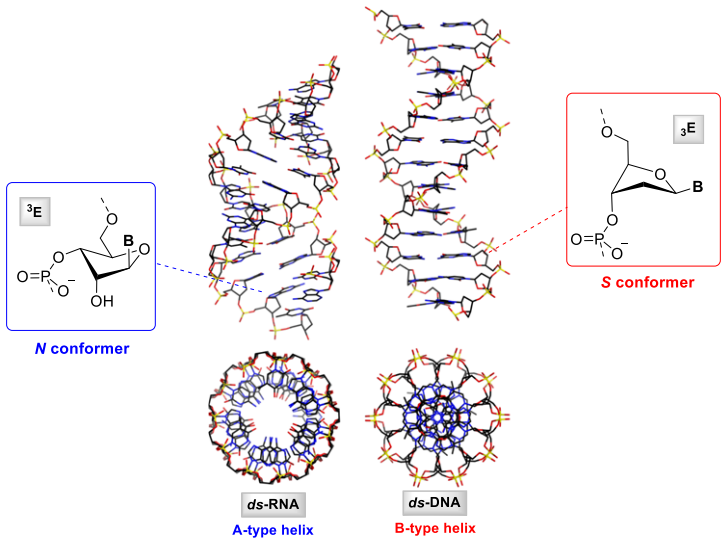

FIGURE 2. Side and top view of A- and B-type duplexes.

The preference for one or for another conformation seems to derive from the nature of the *C*-2' group. In the presence of a withdrawing group (e.g. OH), the *C*-3'-*endo* (*N*) pucker is the only conformation observed (such as in *ds*RNA, A-type helix), whereas in its absence the *C*-2'-*endo* (*S*) pucker is preferred (such as in *ds*DNA, B-type helix) (**FIGURE 2**).

What happen when a single nueoside(-tide) binds to an organized macromolecule (i.e. an enzyme)? It is expected that the architecture of the binding pocket will impose a specific conformational demand on the sugar ring (*N* or *S*) for an optimal fit.[10] This means that even though a NA may show comparable populations of *N* and *S* conformers under equilibrium conditions, during the binding process, in order to exert biological activity, one conformer preferentially will interact with the enzyme itself.

In the biochemical path leading to NA incorporation into a nucleic acid chain, two specific enzymatic systems are involved. On one hand, kinases convert nucleosides to their corresponding triphosphate forms. As widely described in the last chapter, some viruses (e.g. *Herpes Simplex Viruses*, HSV-1 and -2) use their own viral kinases (e.g. HSV-tk) to enable serial phosphorylation,[11] otherwise, other viruses (e.g. *Human Immunodeficiency Viruses* HIV-1 and HIV-2) exploit cellular enzymes to this end (e.g. dCK and dGK).[12] On the other hand, RNA or DNA polymerases [e.g., viral HSV-DNApol for HHV[13] and HIV-RT (reverse transcriptase) for HIV[14] viruses] are responsible for the incorporation of the nucleotides into the growing RNA or DNA chain. Studies have been conducted in order to establish if these activating enzymes, select their substrates on the basis of conformational preferences of the individual nucleosides. To unambiguously address this question, locked NAs built on a rigid template, i.e. the bicyclo[3.1.0]-hexane scaffold (*North* and *South* methano-carbathymidine, *N*-MCT and *S*-MCT), were designed and biologically evaluated (**FIGURE 3**).[15]

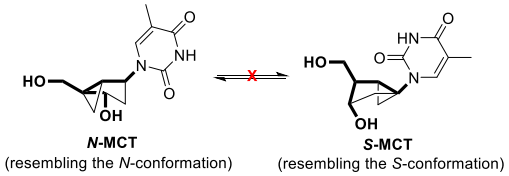

***N*-MCT**
(resembling the *N*-conformation)

***S*-MCT**
(resembling the *S*-conformation)

FIGURE 3. Bicyclo[3.1.0]hexane nucleosides locked in two non-equilibrating *North* and *South* conformations.

In this novel structure, the cyclopentane ring mimics the deoxyfuranose and the fused cyclopropane ring locks the conformation of the cyclopentane in the North hemisphere of pseudorotational cycle or in the antipodean South area. These two isomers displayed opposite affinities for HSV-tk and DNA polymerases.[15] With regards to the phosphorylation steps, *S*-MCT was the preferred substrate of the kinases. However, despite the high levels of *S*-MCT-5'-triphosphate formed, only negligible amounts were incorporated into DNA by polymerases. On the other hand, even if *N*-MCT resulted a poorer substrate for these kinases, *N*-MCT is recognized by DNA polymerases and it is a potent anti-HSV drug (EC_{50}=0.02 μM) while *S*-MCT was totally ineffective.[15]

Thus, the conformational preferences by kinases and polymerases to recognize NAs as their natural counterparts have been unambiguously identified. Particularly, the overall

lesson learned from these studies was that while kinases recognize natural nucleosides and their analogues in a C2'-*endo* (*S*) pucker, polymerases require the C3'-*endo* (*N*) form of the corresponding nucleotide triphosphates for the subsequent incorporation process. Importantly, it was observed that while DNA polymerases (HSV-DNApol, HIV-RT) do not accept NAs-TP in the "wrong" *S* pucker, some viral kinases, such as HSV-tk, allow, although to a limited extent, phosphorylation of a nucleoside locked in an *N* pucker. The broad substrate specificity of some viral enzymes, which do not accurately discriminate on the basis of nucleoside structure and conformation owing to the need for a rapid virus replication, is one of the key elements for the development of novel NAs as antiviral agents.

2.2.1.3 CONFORMATIONALLY CONSTRAINED NUCLEOSIDE ANALOGUES

One of the most efficient approaches devised to probe the conformational requirements of NAs by cellular/viral enzymes for an effective interaction is to "freeze" the conformations of sugar backbone by synthetically creating conformationally restricted NAs, in which the sugar ring pucker is chemically locked in one of the two main conformations required for recognition. A leading example is represented by the replacement of the natural furanose ring with a six-membered sugar moiety in the nucleoside architecture[16] in which the conformational flexibility is significantly reduced, thanks to the considerable energy required for chair flip between two conformations ($^1C_4 \leftrightarrow {}^4C_1$). Therefore, the conformations will be restricted to those adopted on the basis of the energetic requirements of the substituents (**FIGURE 4**). One of the most important examples of constrained six-membered nucleosides has been represented by the 1',5'-anhydro-*arabino*-D-hexitol nucleosides (*h*NAs, **FIGURE 4**).[17] NMR studies first and X-ray crystallographic studies then, have demonstrated that *h*NA monomer conformation has the heterocyclic base placed in an axial position, while both the primary and secondary hydroxyl are in an equatorial position resembling a distorted $^4C_1$ conformation mimic of the ^{3}E conformation (North, *N*) exhibited by natural deoxynucleosides.

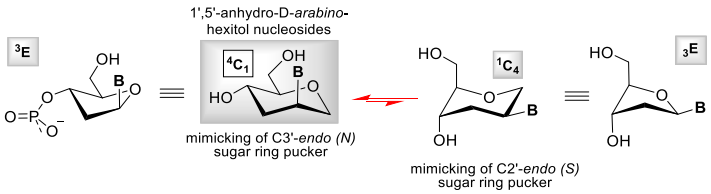

FIGURE 4. *h*NAs as mimics of natural nucleosides.

*h*NAs equipped with natural and/or modified nucleobases demonstrated to be selectively phosphorylated by viral kinases (e.g. HSV-tk), determining a remarkable activity[17] against most Human Herpes Viruses (HHV) such as HSV-1 (HHV-1), HSV-2 (HHV-2),

VZV (HHV-3), EBV (HHV-4) and HCMV (HHV-5), comparable *in vitro* to that of the currently marketed anti-HHV agent, acyclovir (ACV, Zovirax™). On the other hand, *h*NAs were not incorporated by human kinases: this, on one side, determined a high selectivity of *h*NAs toward viral enzymes, on the other side, was responsible for their lack of activity against HIV-1 and HIV-2 viruses.[18] The lesson learned from the study of *h*NAs was that the C3'-*endo* (*N*) conformation was that required for the enzymatic recognition processes leading to inhibition of HHV replication. In the further attempt to develop other bioactive NAs, cyclohexanyl nucleosides (*c*NAs, obtained by replacement of the endocyclic oxygen of *h*NAs with a methylene group) were later designed (**FIGURE 5**),[19] but, surprisingly, they displayed any antiviral activity. As revealed earlier by computational calculations and later by NMR and X-ray studies, *c*NAs, contrarily to *h*NAs, occurred in conformations with an equatorially-oriented nucleobase. This conformational preference was mainly ascribed to the unfavourable 1,3-diaxial interactions between the nucleobase and the hydrogen atoms (**FIGURE 5**), which did not occur in *h*NAs, owing to the presence of endocyclic oxygen.

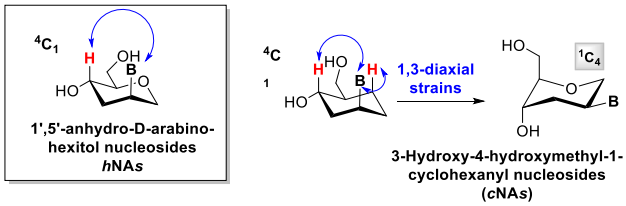

FIGURE 5. Conformational preferences of *h*NAs and *c*NAs.

2.2.1.4 ANTIVIRAL STRATEGY: LETHAL MUTAGENESIS

As already mentioned above, the lethal mutagenesis antiviral mechanism has been proposed as a novel chemotherapeutic strategy for drug resistance.[20] It is widely known that the viruses survive on the basis of quasispecies theory which states that there is a maximum error rate (defined also "error threshold") above which genetic information would not be effectively transmitted.[21] So the viral genetic information may be lost (if the virus quasispecies exceeds the above mentioned threshold) or it may results in a lethal accumulation of errors, defined lethal mutagenesis (**FIGURE 6**). Therefore, this strategy may be effective in reducing the viral infection but also in weakening the capacity of the virus to the drug resistance. The hypermutation can be induced by direct or indirect[22] mutagenesis; the direct approach, in which nucleoside analogues are incorporated in the growing viral DNA, represents the most efficient method to hamper its replication. It also results the most selective approach avoiding the inhibition of other biochemical pathways (as found for DNA alkylators or intercalators).[23]

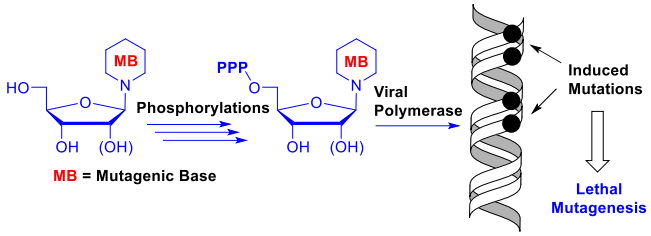

FIGURE 6. Mutagenic nucleosides activation.

Once accomplished the incorporation of mutagenic NA-TP in the viral transcript, the base mispairing can lead to increased mutation rate (**FIGURE 6**). The mentioned goal can be reached acting at nucleobase level on its (1) conformational flexibility, (2) chemical rearrangement, (3) existence as tautomeric forms, (4) *p*Ka leading to the presence of both protonate and deprotonated forms at physiological pH. Ribavirin **1**, is the best example to describe the first case, whose mutagenicity results from the rotation around the C^3-carbonyl bond to give the *s*-cis (able to give pair with uridine residues) and *s*-trans (able to give pair with cytidine residues) conformers (**FIGURE 7**).

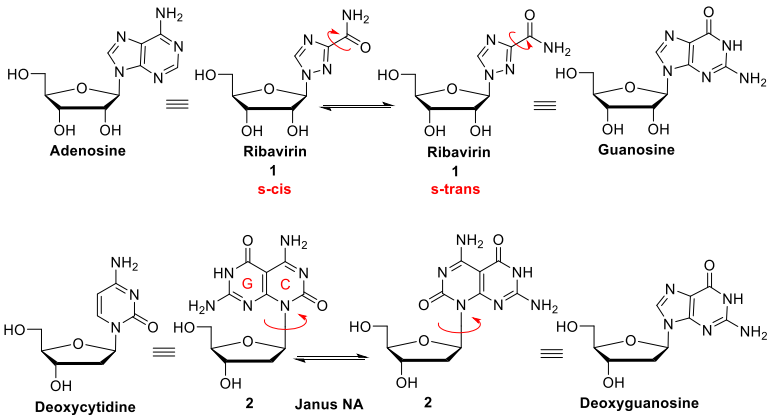

FIGURE 7. Examples of mutagenic NAs and their conformational flexibility inducing base mispairing.

The Janus nucleoside **2**, active against HBV,[24] is another example of NA able to give nonselective base-pairing by conformational flexibility. 5-Hydroxycytidine **3** (**FIGURE 8**) is suspected to be a mutagenic agent because of the presence of both the amino (**3a**) (resulting a cytidine analogue) and imino (**3b**) (resulting a thymidine analogue) tautomer.[25] Besides, the increasing of the imino form with pH and temperature, suggested a possible deprotonation of the 5-hydroxyl moiety in this observed equilibrium. Finally, 5-halouridine derivatives (with 5-bromouracil or 5-fluorouracil as nucleobase), represent a classical example of NAs in which the base ionization (due to

the presence of an electrowithdrawing group in C5 position) seems to be responsible of the observed mispairing (**FIGURE 8**).[26]

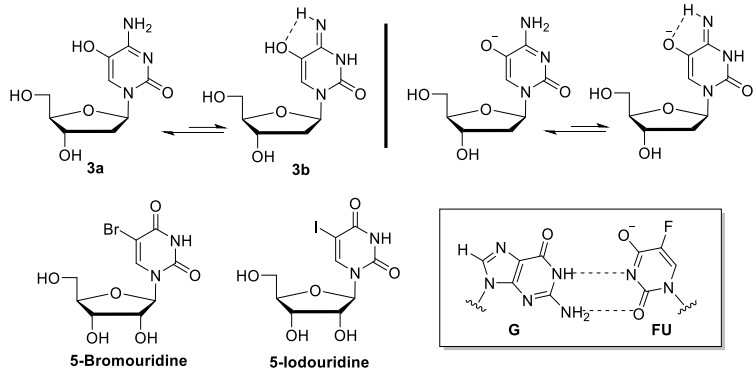

FIGURE 8. Tautomeric forms of 5-hydroxycytidine **3** and ionized base-pairing of 5-halouridines.

2.2.2 Results and Discussion

2.2.2.1 Synthesis and Antiviral Activity of Novel Piperidinyl Nucleoside Analogues

On the basis of the considerations made on the conformational requirements needed to ensure the efficacy and selectivity of NAs for the treatment of viral infections, this project has concerned the synthesis of novel iminosugar-based nucleosides as **4** and **5**[d] (**Scheme 1**).

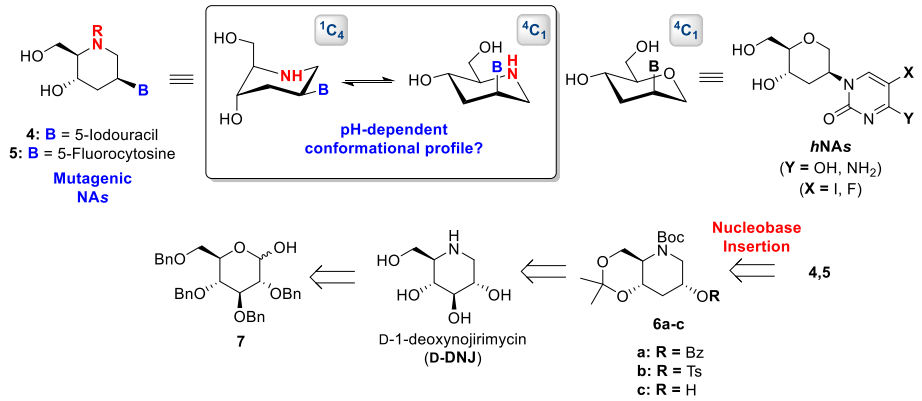

Scheme 1. Target mutagenic NAs **4**,**5** and retrosynthetic pathway to prepare them.

Piperidinyl nucleosides hold a very intriguing structure of the sugar moiety, enabling their potential use in a wide range of applications. Particularly, due to the close structural analogy with 1',5'-anhydro-D-*arabino*-hexitol nucleosides (they can be regarded as their aza-analogues, as the endocyclic oxygen of *h*NAs is formally replaced by an amino function, **Scheme 1**), they have been tested as potential anti-HHV agents. Moreover, on the basis of the previous discussion on NAs conformation in relation to biological activity, a conformational analysis devoted to study of the connection between pH (i.e. nitrogen protonation) and preferred chair conformation (i.e. $^4C_1 \rightarrow {}^1C_4$ inversion owing to occurring 1,3-diaxial interactions) has been undertaken. As depicted in the retrosynthetic analysis (**Scheme 1**), our synthetic approach starts from the well-known glucosidase inhibitor 1-deoxynojirimycin (**D-DNJ**) from which the *C*-3 deoxygenated key intermediates **6a-c** are readily synthetized. Nucleobase insertion is then performed

[d] In recent times, the fusion of the two concepts of glyco- and biomimetic, i.e. the structural mimicking (in terms of charge) of carbohydrate mimetics and the conformational mimicking of nucleoside mimetics, has resulted in the development of a new class of inhibitors, defined to as iminosugar-based nucleosides (see **Appendix A**).

by nucleophilic displacement of a good leaving group (from **7b**) or by Mitsunobu procedure (from **7c**, obtained by **7a**), leading to the target piperidinyl NAs **4** and **5**.

2.2.2.2 PIPERIDINYL SKELETON SYNTHESIS

A wide number of carbohydrate-based approaches are available in the literature for the synthesis of D-DNJ on large scale. To this aim, we used one of the most convenient procedures (also used for industrial preparations)[27] which involves the use of 2,3,4,6-tetra-*O*-benzyl-D-glucose (**7**) as starting material (**SCHEME 2**). The synthesis starts with $LiAlH_4$-mediated reduction of **7** that led to the corresponding glucitol **8**, consequently oxidized under classical Swern conditions [DMSO/$(CO)_2Cl_2$, then TEA] to yield the unstable ketoaldehyde **9** (**SCHEME 2**). The last is directly engaged in the next reductive amination step [$NaBH_3CN$/$AcONH_4$] to provide the 2,3,4,6-tetra-*O*-benzyl-D-1-deoxynojirimycin (**10**) in a good overall yield (75%).

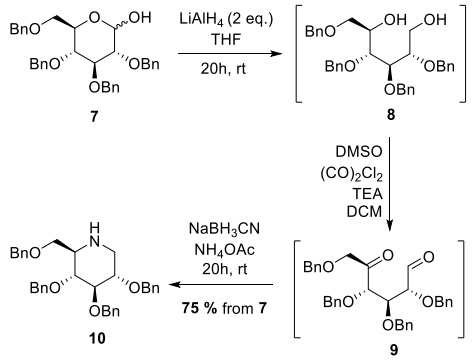

SCHEME 2. Synthesis on large scale of 2,3,4,6-tetra-*O*-benzyl D-1-deoxynojirimycin (**10**).

While standard hydrogenation with Pd/C under acidic conditions was unexpectedly unsuccessful,[28] benzyl groups removal was efficiently accomplished by treatment of **10** with boron trichloride (1M BCl_3 in DCM, 3.5 eq) affording the corresponding unprotected D-DNJ·HCl with an excellent yield (92%) (**SCHEME 3**).

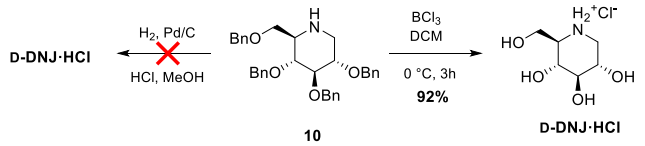

SCHEME 3. Efficient deprotection of **10** to afford D-DNJ hydrochloride.

To prepare the target mutagenic nucleosides **4** and **5**, DNJ·HCl was thus subjected to a series of carefully studied synthetic manipulations conceived to insert the nucleobase in

the desired C2 position and the correct axial orientation. First of all, the endocyclic amino group was protected with di-*tert*-butyl dicarbonate [$(Boc)_2O$, pH~9-10], affording *tert*-butylcarbamate **11** (87% yield). Then, through a regioselective isopropylidenation reaction, *N*-Boc-DNJ (**11**) was treated with 2,2-dimethoxypropane, 2-methoxypropene and PTSA (pH~4.5) to protect the C6 primary and C4 secondary OH functions affording the corresponding 4,6-*O*-isopropylidene-*N*-Boc-DNJ (**12**) (76% yield) (**SCHEME 4**).

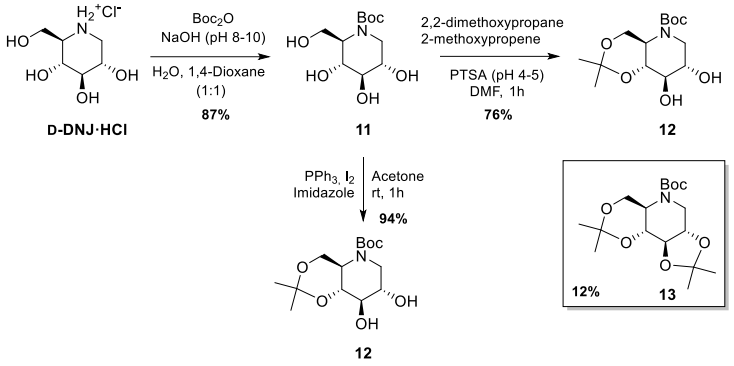

SCHEME 4. Protective group chemistry of D-DNJ·HCl.

However, an undesired double isopropylidenation byproduct **13** was also detected by NMR analysis of the crude mixture (~12%). Looking for more effective procedures, the long established isopropylidenation method,[29] exploiting triphenylphosphine (PPh_3) in combination with molecular iodine (I_2) and imidazole and using anhydrous acetone as acetonide source, was alternatively employed (**SCHEME 4**). Under these conditions, a high-yielding (94%) conversion of **11** into the diol **12** was observed, while no traces of the side product **13** were detected.

Subsequently, the development of a synthetic strategy leading to key *C*-3 deoxygenated intermediates **6a,b**, required a first regioselective protection reaction by the stannylene method.[30] To a solution of **12**, in refluxing MeOH, dibutyltin oxide (DBTO) was added and the resulting dibutyilstannylene acetal intermediate treated with BzCl/TsCl and TEA afforded quantitatively esters **14a,b**. Treatment with *O*-phenyl chlorothionoformate and DMAP gave xanthate intermediates **15a,b** (83-90%) that under Barton-McCombie deoxygenation condition (Bu_3SnH/AIBN)[31] led to **6a,b** with excellent yields (94-96%) (**SCHEME 5**).

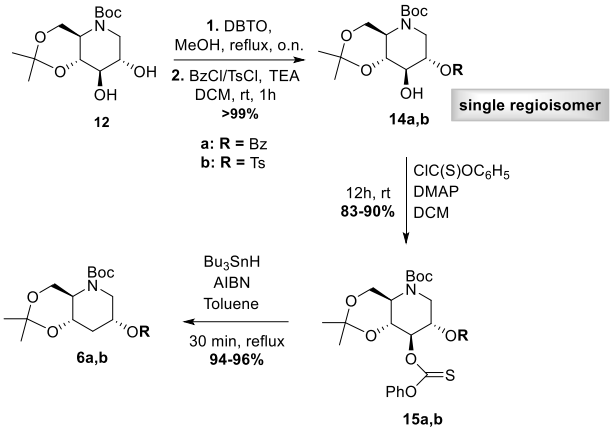

SCHEME 5. Synthetic route to obtain the *C*-3 deoxygenated intermediates **6a,b**.

2.2.2.3 SYNTHESIS OF MUTAGENIC NUCLEOSIDES

In order to obtain the mutagenic uracil nucleoside **4**, the *C*-3 deoxygenated intermediate **6b** was at first subjected to nucleophilic displacement of the leaving group under slightly milder activating conditions (DBU/Uracil/DMF/Δ, 38%) (**SCHEME 6**). Subsequent C-5 iodination (I_2, *m*CPBA) in anhydrous DMF then enabled conversion of **16** into 5-iodouridine analogue **17** (77 %). Alternatively, in order to favour the direct introduction of 5-iodouracil on the sugar moiety, Mitsunobu conditions were attempted and **6c**, (obtained by treatment of **6a** with MeONa in MeOH, 90%), was reacted with N^3-benzoylated-5-iodouracil. The resulting nucleoside, as crude, was then treated with 1M NH_3 in methanol to remove the Bz group leading to **17** but, unfortunately, with lower overall yields (43% yield over two steps). Final treatment of **17** with 1M HCl (60 °C) gave the desired free nucleoside **4** quantitatively (**SCHEME 6**).

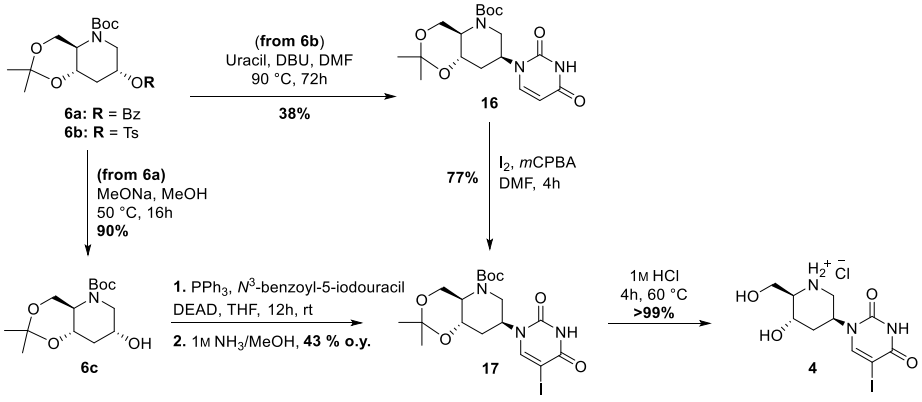

SCHEME 6. Synthesis of mutagenic nucleoside **4.**

Similarly, the synthesis of the 5-fluorouracil derivative **5** was carried out starting from **6c**, always under Mitsunobu conditions, using N^3-benzoyl-5-fluorouracil as nucleobase (**SCHEME 7**). Nucleoside **18,** obtained in 50% yield, was then treated with phosphorus oxychloride and triazole, followed by treatment with a solution of NH_4OH-1,4-dioxane (1:3) to allow the conversion of the uracil derivatives into the desired fluoro cytidine nucleoside **20** *via* the 4-triazolylpyrimidinone intermediate **19**[32] (**SCHEME 7**).

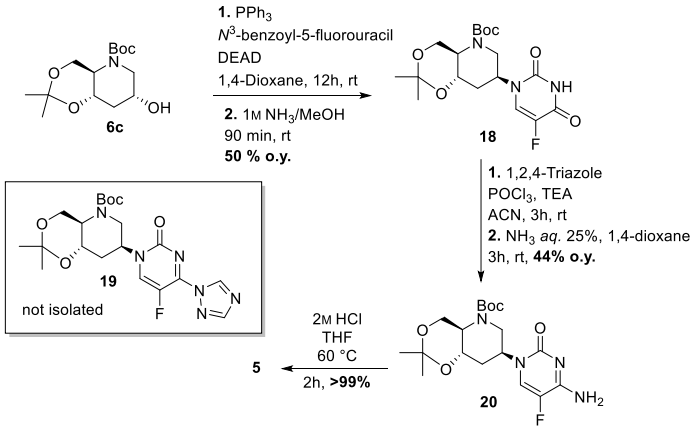

SCHEME 7. Synthesis of mutegenic nucleoside **5**.

Removal of protecting groups, under the same reaction conditions reported above (HCl) finally afforded the desired nucleoside **5**.

2.2.3 CONFORMATIONAL ANALYSIS OF PIPERIDINYL NUCLEOSIDES

NMR analysis has been performed to provide indications on the conformational profile of the synthetized nucleosides. NMR analysis of **4** (taken as model) was unfortunately hampered by the occurrence of a not so well resolved ^1H spectrum (**FIGURE 9**). However, the large coupling constants relative to H2' were indicative for a $^1C_4$ conformation, with an equatorially oriented nucleobase (**FIGURE 9**). This conformational trend is opposite to the $^4C_1$ conformation (axially oriented nucleobases) adopted by *h*NAs.

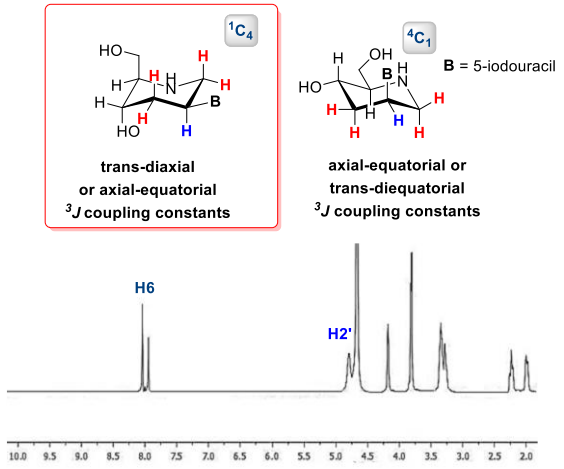

FIGURE 9. NMR conformational profile of **4** and its ^{1}H NMR spectra in D_2O.

It is to underline that ^{1}H NMR spectrum in D_2O of **4** shows two signals at 7.94 ppm (*s*) and 8.04 ppm (*s*) (**FIGURE 9**), which suggest the presence of two species; even, ^{1}H NMR spectra of **4** in DMSO-d_6 shows the presence of two singlets at 11.72 and 11.89 ppm (**FIGURE 10**). On the basis of literature data reported for 5-halo-substituted uridines,[33] these signals seemed to be ascribed to the existence of two tautomeric species such as those depicted in **FIGURE 10**. In support of this assumption, HMBC experiments were performed, highlighting dipolar correlations between the H nucleus bound to nitrogen atom (3-N*H*) and ketone carbon (*C*-4) in the A form, and between the H nucleus of the enol function (4-O*H*) and *C*-4 in the B form.

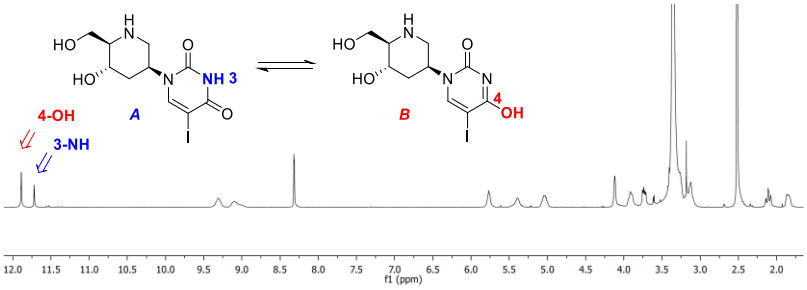

FIGURE 10. ^{1}H NMR spectrum of **4** in DMSO-d_6.

2.2.4 ANTIVIRAL EVALUATION

Piperidinyl nucleoside **4** was subjected to a preliminary antiviral screening at the Rega Institute for Medical Research (under the supervision of Prof. Graciela Andrei and Prof. Robert Snoeck), with the aim to study its capacity to interfere with the life cycles of

various *Human Herpes Viruses* (HHVs). Particularly, **4** was evaluated for its inhibitory effect on the cytopathicity of HSV-1 (strains KOS and KOS/ACV^r), HSV-2 (strain G), VZV (strains OKA and O7-1) and CMV (strains AD 169 and Davis). All experiments were performed using HEL cells; well-known anti-HHV drugs were used as reference compounds, including Cidofovir (CDV), Acyclovir (ACV) and (*E*)-5-(2-bromo-vinyl)-2'-deoxyuridine (BVDU) for HSV-1 and HSV-2 assays, CDV and GCV for VZV and ACV and BVDU for CMV assays. In all cases, the antiviral potential was measured calculating the concentration required to reduce the virus-induced cytophaticity (HSV) plaque formation (VZV, CMV) or cell growth by 50% (EC_{50}). As summarized in **TABLE 1**, only a weak activity of **4** as anti-HHV agent was found. Indeed, although **4** displayed activity in the micromolar range against all the examined viral infections, the observed EC_{50} values were always far higher than those reported by the reference drugs. These results are in agreement with the conformational analysis above discussed. As a matter of fact, nucleoside **4** adopts a sugar conformation (*south*-like) which makes it easily recognized by viral kinases, but not by viral polymerases, which typically recognize triphosphate nucleotides adopting *north*-like conformations. This makes **4** a poor substrate for these enzymes, and therefore not an efficient antiviral agent. One interesting observation from these assays is the activity of **4** against TK$^-$ strains. These mutated strains lack the viral kinases (e.g. HSV-TK) enabling nucleoside phosphorylation to the triphosphate form. While it is not clear why we observe activity in these cases, a conceivable hypothesis is that **4** is able to accurately mimic natural nucleosides frozen in the *South*-like conformation: accordingly, the nucleoside can be recognized by natural kinases despite their sophisticated control mechanisms. Although activity still needs to be improved, this observation suggests that this class of compounds may find useful application in the treatment of those viral infections not holding their own viral kinases, such as HIV.

TABLE 1. Antiviral evaluation of **4** against HHV infections (EC_{50}, µM).

	4	**BVDU**	**ACV**	**GCV**	**CDV**
HSV-1[a]	45	0,04	0,8	0,02	1,2
HSV-2[b]	45	96	0,4	0,02	1,0
HSV[c] (TK^-)	34	3,8	126	0,8	1,0
CMV[d]	76	ND	ND	8,27	0,38
CMV[e]	67	ND	ND	0,63	0,51
VZV[f] (TK^+)	50	0,042	0,7	ND	ND
VZV[g] (TK^-)	61	2,4	14,74	ND	ND
Vaccinia Virus	50	19	>250	>100	37
Adeno-Virus	50	ND	ND	ND	22

[a]KOS strains. [b]G strains. [c]KOS/ACVr strains. [d]AD-169 strains.
[e]Davis strains. [f] OKA strains. [g]O7-1 strains.

2.2.5 CONCLUDING REMARKS AND FUTURE PERSPECTIVES

As described in the introductive section, study of the conformational requirements of NAs to be recognized as the natural counterparts by the corresponding hosts (i.e. enzymes, nucleic acid partners) has enabled the development of a wide amount of biomimetic agents (i.e. NAs and modified oligonucleotides, MOs) based on the concept of structural preorganization that showed remarkable improvement of selectivity associated to their enzymatic recognition processes. In the same context, but looking for antiviral agents, the development of mutagenic nucleoside analogues may be effective in reducing the viral infection but also in weakening the capacity of the virus to the drug resistance. One of the main topic of this PhD project arises from the fusion of the two above mentioned concepts and at the same time has the aim to explore novel inhibition modes for the treatment of viral infections exploiting the endocyclic amino group that replaces the oxygen atom in the iminosugars (see **Chapter 1.1**). The designed mutagenic piperidinyl nucleosides **4** and **5** are thus novel examples of iminosugar-based nucleosides (see **APPENDIX A**). For this reason, the preparation of the target nucleosides proper starts from the well-known glucosidase inhibitor 1-deoxynojirimicin (DNJ) as chiral building block, efficiently synthetized in large scale. Thanks to appropriate functionalization and orthogonal protections of the hydroxyl functions of DNJ, it was possible to synthesize the desired nucleosides through the key intermediates **6a-c**, even if the final coupling reactions should be further studied in order to improve the low reaction yields. Conformational analysis of nucleoside **4** (taken as model molecule) underlined (despite the broadness of NMR spectra) the presence of an expected tautomeric equilibrium between two forms, already observed in 5-halouridine nucleosides.

A preliminary screening aimed to study the capacity of **4** to interfere with the life cycles of various Human Herpes Viruses (HHVs) has been carried out at the Rega Institute for Medical Research (under the supervision of Prof. Graciela Andrei and Prof. Robert Snoeck). The biological data shows a substrate poorly recognized by polymerases; this process could be reasonably improved attempting 6'OH triphosphorylation (e.g. Protide Approach)[34] in order to avoid this process *in vivo* and favour the nucleoside inversion toward the opposite $^4C_1$ conformation, mimic of the *North* one, typically recognized by viral polymerases.

2.2.6 EXPERIMENTAL SECTION

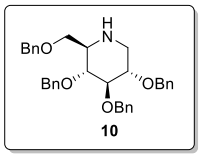

10

2,3,4,6-tetra-*O*-Benzyl-deoxynojirimycin (10). Reduction: To a solution of 2,3,4,6-tetra-*O*-benzyl-D-glucopyranose **7** (15.0 g, 27.7 mmol) in anhydrous THF (150.0 mL), cooled to 0 °C, $LiAlH_4$ (2.1 g, 55.5 mmol) was slowly added. The reaction mixture was kept to room temperature and magnetically stirred for 20h. $LiAlH_4$ excess was quenched with H_2O and EtOAc; the resulting suspension was extracted with EtOAc and brine. The organic layers were dried (Na_2SO_4) and concentrated under reduced pressure to obtain the corresponding glucitol **8** as a white oil. **Oxidation:** A solution of DMSO (9.0 mL, 126.7 mmol) in DCM (75.0 mL) was slowly added to a stirred solution of $(CO)_2Cl_2$ (9.0 mL, 104.8 mmol) in DCM (75.0 mL) at −78 °C. After 90 min., glucitol **8** (15.0 g, 30.8 mmol) solution in DCM (75.0 mL) was slowly added dropwise. After further 90 min., Et_3N (48.0 mL, 345.3 mmol) was added dropwise at −78 °C and the resulting mixture was stirred for 90 min. at 0 °C. **Reductive amination:** To a solution of NH_4OAc (24.0 g, 311.4 mmol) in MeOH (1.5 L), Na_2SO_4 (18.3 g, 128.8 mmol) and $NaBH_3CN$ (7.2 g, 114.6 mmol) were added. The resulting suspension was added to the mixture previously obtained and stirred for 20h at room temperature. NaOH was then added until pH~10 and the mixture extracted with DCM and brine. The organic layers were dried (Na_2SO_4), concentrated under reduced pressure and chromatographed over silica gel (hexane:EtOAc = 80:20) to give the pure **10** (10.9 g, 75% overall yield) as a white solid. $[\alpha]_D$ +27.7, $CHCl_3$. ^1H NMR (400 MHz, $CDCl_3$), δ: 1.95 (*bs*, 1H), 2.57 (*dd*, J= 12.3, 10.4 Hz, 1H), 2.79 (*ddd*, J= 2.5 Hz, 9.2 Hz, 1H), 3.31 (*dd*, J= 4.8 Hz, 12.3 Hz, 1H), 3.42 (*t*, J= 9.2 Hz, 1H), 3.51–3.67 (*m*, 2H), 3.73 (*dd*, J= 2.5 Hz, 1H), 4.49 (*d*, J= 11.7 Hz, 1H), 4.53 (*d*, J= 11.7 Hz, 1H), 4.56 (*d*, J= 10.9 Hz, 1H), 4.73 (*d*, J= 11.6 Hz, 1H), 4.77 (*d*, J= 11.6 Hz, 1H), 4.92 (*t*, J= 10.3 Hz, 2H), 5.05 (*d*, J= 10.9 Hz, 1H), 7.25 (*d*, J= 7.0 Hz, 2H), 7.28–7.46 (*m*, 18H). ^{13}C NMR (100 MHz, $CDCl_3$), δ: 46.7, 59.1, 68.3, 73.0, 73.3, 75.3, 75.6, 78.3, 78.7, 86.4, 127.5, 127.7, 127.8, 127.9, 128.3, 128.4, 137.4, 137.9, 138.0, 138.5.

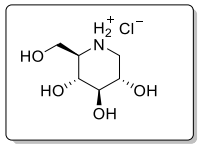

D-DNJ·HCl. To a solution of 2,3,4,6-tetra-*O*-benzyl-1-deoxynojirimicin **10** (6.8 g, 13.0 mmol) in DCM (350.0 mL), cooled at 0 °C, BCl_3 (1M, 45.5 mL, 45.5 mmol) was added. The mixture, stirred for 12h at 0 °C, was then quenched with MeOH (280.0 mL) at 0 °C and concentrated under reduced pressure. The crude was coevaporated with toluene and triturated with EtOAc to give pure **DNJ·HCl** (2.4 g, 92% reaction yield) as a white solid; $[\alpha]_D$ +34.7, MeOH. NMR analysis of **D-DNJ·HCl** is consistent with the NMR spectra reported for L-DNJ·HCl in the Chapter 1 of this thesis.

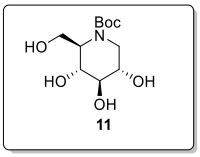

11

***N*-tert-Butoxycarbonyl-deoxynojirimycin (11).** To a solution of **DNJ·HCl** (2.3 g, 11.6 mmol) in a mixture of water (38.0 mL) and 1,4-dioxane (38.0 mL) at 0°C, $(Boc)_2O$ (5.0 g, 23.1 mmol) and NaOH (1N, until pH~9-10), were added. The reaction mixture stirred at room temperature for 16h, was then concentrated under reduced pressure and the crude purified by silica gel chromatography ($CHCl_3$:MeOH=95:5) to obtain the pure **11** (2.6 g, 87% reaction yield). $[\alpha]_D$ +24.3, MeOH. ^{1}H NMR (400 MHz, CD_3OD), δ: 1.47 (*s*, 9H), 3.38 (*dd*, J= 13.9 Hz, 1H), 3.59 – 3.66 (*m*, 2H), 3.67 – 3.74 (*m*, 1H), 3.77 (*dd*, J= 5.6, 11.4 Hz, 1H), 3.80 (*dd*, J= 9.3, 11.4 Hz, 1H), 3.90 (*d*, J= 13.9 Hz, 1H), 4.10 (*dd*, J= 5.6, 9.3 Hz, 1H). ^{13}C NMR (CD_3OD, 100 MHz), δ: 28.8, 44.3, 61.2, 61.3, 70.6, 71.5, 72.4, 81.4, 158.2.

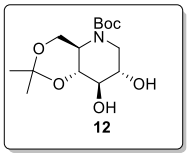

12

4,6-*O*-Isopropylidene-*N*-tert-butoxycarbonyl-deoxynojirimycin (12). Procedure A: to a solution of **11** (2.0 g, 7.6 mmol) in DMF (40.0 mL), 2,2-dimethoxypropane (1.9 mL, 15.2 mmol), 2-methoxypropene (1.5 mL, 15.2 mmol) and PTSA (to adjust the pH~4.5) were added. The reaction mixture was stirred at room temperature for 1h then aq. $NaHCO_3$ was added and stirred for further 30 min.; the mixture was extracted with DCM and brine and the organic layers dried (Na_2SO_4). Solvent was evaporated under reduced pressure and the crude purified by silica gel chromatography ($CHCl_3$:MeOH = 95:5) to provide **12** (1.8 g, 78% reaction yield). **Procedure B:** to a magnetically stirred solution of triphenyl phosphine (2.99 g, 11.4 mmol) in anhydrous acetone (50.0 mL) at rt, a solution of I_2 (2.9 g, 11.4 mmol) in the same solvent (20.0 mL) was added dropwise in

the dark and under Ar atmosphere. After 5 min solid imidazole was added (1.55 g, 22.8 mmol) and then **11** (2.0 g, 7.6 mmol) was added in one portion to the suspension. TLC monitoring ($CHCl_3$:MeOH = 9:1) showed that the starting sugar was completely consumed within 10 min. The reaction mixture was first treated with sodium tiosulphate then extracted with EtOAc and washed with brine. The organic layer was dried (Na_2SO_4) and evaporated under reduced pressure to give a crude product that after chromatography over silica gel column gave **10** (2.2 g, 94% reaction yield). $[\alpha]_D$ -28.9, $CHCl_3$. ^{1}H NMR ($CDCl_3$, 400 MHz), δ: 1.42 (*s*, 3H), 1.45 (*s*, 9H), 1.52 (*s*, 3H), 2.49 (*bs*, 1H), 2.64 (*dd*, J= 13.3 Hz, 1H), 2.70 (*bs*, 1H), 3.00 (*dt*, J= 5.0 Hz, 1H), 3.43 (*t*, J= 9.0 Hz, 1H), 3.56 (*t*, J= 9.0 Hz, 1H), 3.59□3.65 (*m*, 1H), 4.25 (*dd*, J=13.3 Hz, 1H), 4.33 (*dd*, J= 5.0, 11.8 Hz, 1H), 4.47 (*t*, J= 11.8 Hz, 1H). ^{13}C NMR (100 MHz, $CDCl_3$), δ: 21.1, 28.4, 28.6, 45.3, 46.5, 62.2, 65.5, 67.2, 68.3, 80.6, 98.8, 158.7.

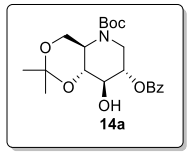

14a

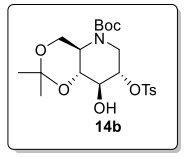

14b

2-*O*-Benzoyl-4,6-*O*-isopropylidene-*N*-tert-butoxycarbonyl-deoxynojirimycin (14a). To a solution of 4,6-*O*-isopropylidene-*N*-tert-butoxycarbonyl-1-deoxynojirimycin **12** (0.50 g, 1.6 mmol) in anhydrous MeOH (5.5 mL), Bu_2SnO (0.81 g, 3.3 mmol) was added under Ar atmosphere. Both **12** and Bu_2SnO were pre-dried under vacuum over KOH overnight. The reaction mixture was stirred at reflux temperature for 12h. The solvent was then removed by coevaporation with toluene. The residue was dissolved in anhydrous DCM (5.5 mL) and dry Et_3N (0.27 mL, 1.9 mmol), BzCl (0.19 mL, 1.6 mmol) were sequentially added. The resulting mixture was stirred for 1h at room temperature and aq. $NaHCO_3$ was then added. The suspension was extracted (EtOAc) and washed (brine) and the organic layers dried (Na_2SO_4). The solvent was removed under reduced pressure and the chromatography of the residue (Hexane:EtOAc = 85:15) gave the pure **14a** (0.67 g, >99% reaction yield). ^{1}H NMR (500 MHz, $CDCl_3$), δ: 1.48 (*bs*, 15H), 3.26 (*dt*, J= 4.8 Hz, 1H), 3.45 (*dd*, J= 7.0, 14.0 Hz, 1H), 3.79–3.90 (*m*, 2H), 3.98 (*dd*, J= 3.0, 14.0 Hz, 1H), 4.21 (*dd*, 1H), 4.39 (*dd*, J= 4.8 Hz, 1H), 5.02 (*ddd*, J= 3.0, 7.0 Hz, 1H), 7.44 (*t*, J= 7.7 Hz, 2H), 7.56 (*t*, J= 7.5 Hz, 1H), 8.00 (*d*, J= 7.2 Hz, 2H). ^{13}C NMR (125 MHz, $CDCl_3$), δ: 19.2, 28.3, 44.7, 53.2, 62.6, 72.7, 73.9, 74.5, 81.0, 99.3, 128.4, 129.8, 133.3, 155.0, 165.8. **2-*O*-*p*-toluensulfonyl-4,6-*O*-isopropylidene-*N*-tert-butoxycarbonyl-1-deoxynojirimycin (14b). 18b** has been prepared following the same procedure described above for **14a**, replacing BzCl with TsCl (1.0 eq.). Chromatographic purification of the residue (hexane:EtOAc = 70:30) gave the pure **14b** (>99% yield). $[\alpha]_D$ -14.2, $CHCl_3$. ^{1}H NMR (400 MHz, $CDCl_3$), δ: 1.39 (*s*, 3H), 1.44 (*s*,

9H), 1.48 (*s*, 3H), 2.44 (*s*, 3H), 2.94 (*dd*, J = 9.6, 14.0 Hz, 1H), 3.0 (*dt*, J = 4.9 Hz, 1H), 3.59 (*t*, J = 8.8 Hz, 1H), 3.64 (*dt*, J = 1.8, 8.7 Hz, 1H), 4.19 (*dd*, J = 4.9, 13.6 Hz, 1H), 4.26 (*dd*, J = 5.0, 11.7 Hz, 1H), 4.31-4.36 (*m*, 1H), 4.38 (*t*, J = 7.2 Hz, 1H), 7.34 (*d*, J = 8.0 Hz, 2H), 7.83 (*d*, J = 8.4 Hz, 2H). ^{13}C NMR (100 MHz, $CDCl_3$), δ: 19.3, 21.8, 28.4, 29.3, 47.6, 54.9, 62.1, 73.1, 74.7, 78.6, 81.5, 99.5, 128.1, 130.0, 133.6, 142.2, 154.2.

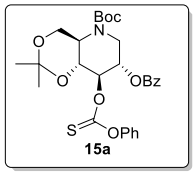

15a

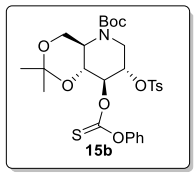

15b

2-*O*-Benzoyl-4,6-*O*-isopropylidene-3-*O*-phenylthionoformate-*N*-tertbutoxycarbonyl-deoxynojirimycin (15a). To a stirring solution of **14a** (0.44 g, 1.1 mmol) in DCM (7.0 mL), *O*-phenyl chlorothionoformate (0.18 mL, 1.3 mmol) and DMAP (0.27 g, 2.2 mmol) were sequentially added. After stirring for 12h, the mixture was quenched with NH_4Cl and extracted with DCM:Brine. The organic layer was dried (Na_2SO_4) and concentrated under reduced pressure. Chromatography of the residue (flash chromatography: DCM) gave **15a** as pure product (0.53 g, 90% reaction yield). ^{1}H NMR (500 MHz, C_6D_6), δ: 1.26 (*s*, 3H), 1.27 (*s*, 9H), 1.45 (*s*, 3H), 3.33 – 3.43 (*m*, 2H), 3.83 (*dd*, J= 2.9, 14.0 Hz, 1H), 4.14 (*dd*, J= 9.5, 11.0 Hz, 1H), 4.23 (*t*, J= 10.1 Hz, 1H), 4.57 (*dd*, J= 5.0, 11.5 Hz, 1H), 5.48 (*td*, J= 3.5, 7.2 Hz, 1H), 6.06 (*dd*, J= 5.5, 9.0 Hz, 1H), 6.70–6.75 (*m*, 2H), 6.76–6.81 (*m*, 1H), 6.87 (*t*, J= 7.8 Hz, 2H), 6.95–7.00 (*m*, 2H), 7.02–7.08 (*m*, 1H), 8.16 (*d*, J= 7.2 Hz, 2H). ^{13}C NMR (100 MHz, C_6D_6), δ: 18.68, 27.71, 29.00, 44.91, 53.47, 62.60, 70.62, 71.61, 80.36, 84.02, 99.36, 121.81, 126.07, 128.30, 129.20, 129.96, 133.01, 133.69, 153.70, 154.73, 164.82, 195.04. **2-*O*-*p*-toluensulfonyl-4,6-*O*-isopropylidene-3-*O*-phenylthionoformate-*N*-tertbutoxycarbonyl-deoxynojirimycin (15b). 15b** has been prepared following the same procedure described above for **15a.** Chromatographic purification of the residue (hexane:EtOAc = 85:15) gave the pure **15b** (83% reaction yield). $[\alpha]_D$ +8.06, $CHCl_3$. ^{1}H NMR (400 MHz, $CDCl_3$), δ: 1.38 (*s*, 3H), 1.47 (*s*, 6H), 1.48 (*s*, 3H), 1.51 (*s*, 3H), 2.41 (*s*, 3H), 3.14-3.24 (*m*, 1H), 3.52-3.63 (*m*, 1H), 3.92-4.05 (*m*, 2H), 4.24-4.43 (*m*, 2H), 4.57-4.64 (*m*, 1H), 5.58-5.62 (*m*, 1H), 7.04 (*d*, J = 8.4 Hz, 2H), 7.28-7.36 (*m*, 3H), 7.39-7.44 (*m*, 2H), 7.82 (*d*, J= 8.3 Hz, 2H). ^{13}C NMR (100 MHz, $CDCl_3$), δ: 21.9, 28.4, 31.2, 60.0, 61.6, 68.2, 75.3, 82.3, 121.9, 125.1, 127.0, 128.2, 129.8, 129.9, 130.3, 133.3, 145.5, 153.5, 155.6, 194.4, 207.2.

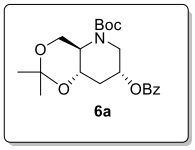

6a

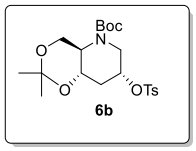

6b

2-*O*-Benzoyl-3-deoxy-4,6-*O*-isopropylidene-*N*-tertbutoxycarbonyl-1-deoxynojirimycin (6a). To a boiling solution of **15a** (0.50 g, 0.92 mmol) in anhydrous toluene (10.0 mL) a solution of Bu_3SnH (0.47 mL, 1.8 mmol) and AIBN (0.030 g, 0.18 mmol) in toluene (10.0 mL) was added dropwise. The resulting mixture was stirred, under Ar, for 30 minutes. The solvent was removed under reduced pressure and the crude was purified by silica gel chromatography (hexane:EtOAc = 90:10) to give **6a** as pure product (0.32 g, 96% reaction yield). ^{1}H NMR (400 MHz, C_6D_6), δ: 1.29 (*s*, 3H), 1.35 (*s*, 9H), 1.48 (*s*, 3H), 1.58–1.68 (*m*, 1H), 2.21–2.32 (*m*, 1H), 3.14 (*dd*, J= 7.4, 13.2 Hz, 1H), 3.18–3.24 (*m*, 1H), 3.62 (*td*, J= 5.1, 10.8 Hz, 1H), 3.79 (*dd*, J= 3.3, 13.4 Hz, 1H), 4.31 (*t*, J= 10.9 Hz, 1H), 4.61 (*dd*, J= 4.7, 11.4 Hz, 1H), 5.03 (*ddd*, J= 3.6, 7.7, 14.2 Hz, 1H), 6.99–7.05 (*m*, 2H), 7.13–7.08 (*m*, 1H), 8.05–8.09 (*m*, 2H). ^{13}C NMR (100 MHz, C_6D_6), δ: 14.90, 23.85, 25.33, 31.65, 43.10, 53.11, 58.91, 63.36, 63.67, 75.79, 94.52, 125.63, 128.65, 150.77, 160. 99.

2-*O*-*p*-toluensulfonyl-3-deoxy-4,6-*O*-isopropylidene-*N*-tertbutoxycarbonyl-1-deoxynojirimycin (6b). 6b has been prepared following the same procedure described above for **6a.** Chromatographic purification of the residue (hexane:EtOAc = 85:15) gave the pure **6b** (94 % reaction yield). $[\alpha]_D$ -1.26, $CHCl_3$. ^{1}H NMR (400 MHz, $CDCl_3$), δ: 1.35 (s, 3H), 1.40 (s, 9H), 1.45 (s, 3H), 2.21-2.28 (m, 1H), 2.44 (s, 3H), 2.82 (dd, J = 9.7, 13.2 Hz, 1H), 2.90 (dt, J = 4.9 Hz, 1H), 3.66 (dt, J = 4.6 Hz, 1H), 4.08-4.14 (m, 2H), 4.25 (dd, J = 4.9, 11.8 Hz, 1H), 4.35-4.46 (m, 2H), 7.34 (d, J = 8.0 Hz, 2H), 7.79 (d, J = 8.3 Hz, 2H). ^{13}C NMR (100 MHz, $CDCl_3$), δ: 19.3, 21.8, 28.4, 29.4, 37.4, 49.9, 58.0, 62.5, 67.9, 73.5, 81.2, 99.0, 127.9, 130.1, 134.0, 145.1, 154.2.

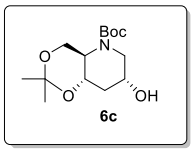

6c

3-deoxy-4,6-*O*-isopropylidene-*N*-tert-butoxycarbonyl-1-deoxynojirimycin (6c). To a solution of **6a** (0.32 g, 0.82 mmol) in anhydrous MeOH (10.0 mL), MeONa (0.044 g, 0.82 mmol) was added and the resulting suspension was heated to 50 °C. After stirring for 16h the mixture was extracted with DCM:Brine. The organic layer was dried (Na_2SO_4) and concentrated under reduced pressure. The resulting crude was chromatographed on silica gel (hexane:EtOAc = 70:30) to give **6c** as pure product (0.21

g, 90% reaction yield). ^{1}H NMR (400 MHz, C_6D_6), δ: 1.31 (*s*, 3H), 1.36 (*s*, 10H), 1.47 (*s*, 3H), 2.11–2.16 (*m*, 1H), 2.41 (*dd*, J= 9.6, 12.9 Hz, 1H), 2.90 (*dt*, J= 7.8, 9.8 Hz, 1H), 3.44 (*bs*, 1H), 3.49–3.58 (*m*, 1H), 4.07 (*ddd*, J= 1.6, 4.4,12.9 Hz, 1H), 4.55 (*d*, J= 7.5 Hz, 2H). ^{13}C NMR (100 MHz, C_6D_6), δ: 14.82, 23.96, 25.39, 36.28, 48.32, 54.11, 58.72, 60.74, 64.29, 75.61, 94.17, 150.32.

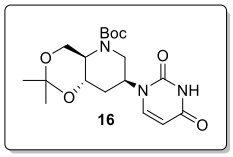

3'-deoxy-4',6'-*O*-isopropylidene-2'(uracil-1-yl)-*N*-tert-butoxycarbonyl deoxynojirimycin (16). Uracil (0.038 g, 0.329 mmol) and **6b** (0.063 g, 0.143 mmol) were suspensed in anhydrous DMF (3.0 mL) under N_2 for 15 min at room temperature. Then 1,8-diazobicyclo[5.4.0]undec-7-ene (DBU, 50.0 μL, 0.329 mmol) was added and the reaction mixture heated at 90 °C for 72h, after which the reaction was cooled to RT, quenched with NH_4Cl and concentrated. The residue was extracted with DCM and washed with brine. The organic layer was dried (Na_2SO_4) and the solvent evaporated under reduced pressure. Flash chromatography of the crude residue over silica gel (CH_3Cl/MeOH = 98:2) gave the corresponding pure **16** (0.047 g, 87% reaction yield). $[\alpha]_D$ -17.1, MeOH. ^{1}H NMR (500 MHz, $CDCl_3$), δ: 1.42 (*s*, 3H), 1.46 (*s*, 9H), 1.54 (*s*, 3H). 1.92 – 2.04 (*m*, 1H), 2.16–2.24 (*m*, 1H), 3.18 (*td*, J= 10.0, 4.4 Hz, 1H), 3.60 (*dd*, J= 14.1, 4.5 Hz, 1H), 3.98 (*dd*, J= 14.2, 6.5 Hz, 1H), 4.07 (*t*, J= 10.9 Hz, 1H), 4.21 (*td*, J= 11.0, 4.9 Hz, 1H), 4.40 (*dd*, J= 11.4, 4.3 Hz, 1H), 4.51 (*bs*, 1H), 5.73 (*d*, J= 7.6 Hz, 1H), 7.36 (*d*, J= 8.0 Hz, 1H). ^{13}C NMR (100 MHz, DMSO-d_6), δ: 20.03, 28.39, 29.67, 31.80, 50.55, 55.44, 62.92, 66.38, 80.31, 99.21, 101.95, 143.53, 151.21, 154.68, 163. 70.

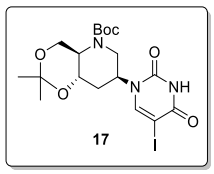

3'-deoxy-4',6'-*O*-isopropylidene-2'(5-iodouracil-1-yl)-*N*-tert-butoxycarbonyl deoxynojirimycin (17). *Uracil Iodination***:** to a solution of **16** (30 mg, 0.079 mmol) in DMF (1.0 mL), iodine (0.012 g, 0.047 mmol) and *m*CPBA (0.018 g, 0.104 mmol) were added at room temperature. After 4h the residue was extracted with AcOEt and washed with brine. The organic layer was dried (Na_2SO_4) and the solvent removed under reduced pressure. Flash chromatography (EtOAc) gave the pure **17** (0.031 mg, 77% reaction yield). *Mitsunobu Coupling*: to a suspension of **6c** (0.035 g, 0.13 mmol), N^3-benzoyl-5-

iodouracil (0.068 g, 0.20 mmol) and triphenylphosphine (0.052 g, 0.20 mmol) in 1,4-dioxane (3.0 mL), a solution of DEAD (0.031 mL, 0.20 mmol) in 1,4-dioxane (0.2 mL) was added via a dropping funnel over a period of 200 min. The reaction mixture was stirred overnight at room temperature. Then the solvent was removed under reduced pressure and the crude was treated with NH_3 in MeOH (1M, 1.5 mL). The mixture was stirred for 90 min at room temperature. The volatiles were removed, and the crude was coevaporated with toluene three times. Chromatography of the residue over silica gel (hexane:EtOA=50:50) gave the corresponding pure **17** (0.027 g, 43% overall yield). $[\alpha]_D$ -14.0, DMSO. ^{1}H NMR (500 MHz, acetone-d_6), δ: 1.33 (*s*, 3H), 1.49 (*s*, 3H), 1.52 (*s*, 9H), 2.01 (*dt*, J= 11.9, 10.7 Hz, 1H), 2.22–2.29 (*m*, 1H), 3.20–3.27 (*m*, 1H), 3.79–3.86 (*m*, 1H), 3. 78–3.98 (*m*, 2H), 4.32–4.38 (*m*, 1H), 4.51 (*td*, J= 10.2, 5.4 Hz, 1H), 4.65–4.72 (*m*, 1H), 8.12 (*s*, 1H). ^{13}C NMR (125 MHz, acetone-d_6), δ: 18.80, 27.62, 32.28, 42.68, 51.97, 55.55, 62.93 66.52, 67.33, 80.20, 98.67, 147.61, 150.49, 154.68, 159.96.

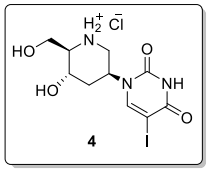

2'-(5-iodouracil-1-yl) deoxynojirimycin (4). To a solution of **17** (0.014 g, 0.023 mmol) in THF (0.9 mL), HCl (1M, 0.3 mL) was added and the reaction mixture was stirred to 60°C for 4h. Then the solvent was evaporated under reduced pressure and the crude residue was triturated with Et_2O to give the pure **4** as chlorohydrate salt (0.009 g, >99% yield). $[\alpha]_D$ +19.6, DMSO.^{1}H NMR (400 MHz, D_2O), δ: 2.07-2.15 (*m*, 2H), 2.32-2.40 (*m*, 2H), 3.40-3.56 (*m*, 6H), 3.91-3.95 (*m*, 4H), 4.30-4.33 (*m*, 2H), 4.88-4.98 (*m*, 2H), 8.04 (*s*, 1H), 8.14 (*s*, 1H). ^{1}H NMR (400 MHz, DMSO-d_6), δ: 1.80–1.90 (*m*, 2H), 2.05–2.17 (*m*, 2H), 3.08–3.44 (*m*, 6H), 3.73 (*dd*, J= 5.6, 11.8 Hz, 2H), 3.82–3.99 (*m*, 2H), 4.96–5.13 (*m*, 2H), 5.77 (*bs*, 2H), 8.32 (*s*, 2H), 9.10 (*bs*, 2H), 9.31 (*bs*, 2H), 11.72 (*s*, 1H), 11.89 (*s*, 1H). ^{13}C NMR (100 MHz, DMSO-d_6), δ: 27.16, 42.00, 52.64, 55.84, 56.53, 59.21, 66.03, 73.19, 147.09, 149.28, 156.91.

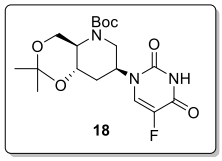

3'-deoxy-4',6'-*O*-isopropylidene-2'(5-fluorouracil-1-yl)-*N*-tert-butoxycarbonyl deoxynojirimycin (18). To a suspension of **6c** (0.070 g, 0.25 mmol), N^3-benzoyl-5-fluorouracil (0.086 g, 0.37 mmol) and triphenylphosphine (0.096 g, 0.37 mmol) in 1,4-

dioxane (3.0 mL), a solution of DEAD (0.058 mL, 0.37 mmol) in 1,4-dioxane (0.3 mL) was added via a dropping funnel over a period of 200 min. The reaction mixture was stirred overnight at room temperature. Then the solvent was evaporated under reduced pressure and the crude residue was treated with NH_3 in MeOH (1M, 1.5 mL). The mixture was stirred for 90 min at room temperature. The volatiles were removed and the crude coevaporated with toluene three times. Chromatography of the residue over silica gel (hexane:EtOAc = 50:50) gave the corresponding pure **18** (0.049 g, 50% overall yield). ^{1}H NMR (400 MHz, MeOD), δ: 1.32 (*s*, 9H), 1.36 (*s*, 3H), 1.55 (*s*, 3H), 1.78 (*ddd*, J= 3.2, 11.1, 14.2 Hz, 1H), 2.21–2.26 (*m*, 1H), 3.04 (*d*, J= 15.1 Hz, 1H), 3.10 (*dd*, J= 10.5, 4.8 Hz, 1H), 4.14–4.23 (*m*, 2H), 4.60 (*dt*, J= 14.7, 2.2 Hz, 1H), 4.74 (*t*, J= 11.3 Hz, 1H), 5.22 (*bs*, 1H), δ 7.79 (*d*, J = 3.2 Hz, 1H). ^{13}C NMR (100 MHz, MeOD), δ: 14.04, 23.07, 24.33, 31.06, 55.01, 57.73, 62.14, 68.67, 76.13, 94.61, 141.34, 143.88, 149.61, 150.51.

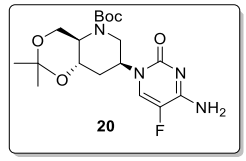

20

3'-deoxy-4',6'-*O*-isopropylidene-2'(5-fluorocytosine-1-yl)-*N*-tert-butoxycarbonyl deoxynojirimycin (20). To a suspension of 1,2,4-triazole (0.040 g, 0.59 mmol) in dry ACN (0.3 mL), $POCl_3$ (0.011 mL, 0.13 mmol) was added dropwise at 0 °C under Ar. After stirring for 5 min, TEA (0.081 mL, 0.59 mmol) was added dropwise and the mixture stirred for another 30 min at 0 °C. A solution of **18** (0.013 g, 0.033 mmol) in dry ACN (0.5 mL) was added slowly by cannula. The reaction mixture was stirred for 10 min at 0 °C and for 3 h at room temperature. The reaction mixture was extracted with EtOAc and brine. The combined organic phases were dried (Na_2SO_4) and the solvent was removed under reduced pressure. The crude was dissolved in dioxane (0.6 mL) and aq NH_3 (25%, 0.2 ml) was added. The mixture was stirred at room temperature for 3 h, then the solvent removed, and the residue purified by column chromatography (DCM:MeOH = 93:7) to yield cytidine derivates **20** as a white foam (0.005 g, 40% overall yield). $[\alpha]_D$ -2.8, MeOH. ^{1}H NMR (500 MHz, acetone d_6), δ: 1.33 (*s*, 3H), 1.46 (*s*, 9H), 1.52 (*s*, 3H), 1.96 (*dt*, J=10.6, 13.0 Hz, 1H), 2.20-2.24 (*m*, 1H,), 3.21 (*m*, 1H), 3.71 (*dd*, J= 3.7, 13.6 Hz, 1H), 3.90 (*dd*, J= 8.3, 13.4 Hz, 1H), 4.02 (*t*, J= 10.4 Hz, 1H), 4.32 (*dd*, J= 3.3, 11.1 Hz, 1H), 4.51 (*td*, J= 5.6, 10.8 Hz, 1H), 4.59–4.68 (*m*, 1H), 7.86 (*d*, J= 5.5 Hz, 1H), 8.24 (*bs*, 2H). ^{13}C NMR (100 MHz, acetone d_6), δ: 14.85, 23.51, 28.31, 39.27, 48.12, 51.86, 58.84, 58.84, 62.52, 75.92, 94.62, 124.12, 124.43, 149.77, 150.61, 153.44.

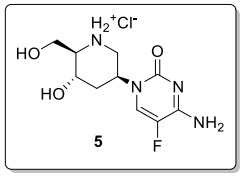

2'-(5-fluorocytosine-1-yl) deoxynojirimycin (5). To a solution of **20** (0.005 g, 0.013 mmol) in THF (0.6 mL), HCl (2M, 0.2 mL) was added and the reaction mixture was stirred to 60°C for 2h. Then the solvent was evaporated under reduced pressure and the crude residue was triturated with Et_2O to give the pure **5** as chlorohydrate salt (0.003 g, >99% yield). ^{1}H NMR (400 MHz, D_2O), δ: 2.14-2.19 (*m*, 1H), 2.32-2.40 (*m*, 1H), 3.51-5.53 (*m*, 2H), 3.57-3.61 (*m*, 1H), 3.94-4.00 (*m*, 2H), 4.36-4.38 (*m*, 1H), 4.92-5.00 (*m*, 1H), 8.12 (*d*, J = 6.4 Hz, 1H), 9.10 (*bs*, 1H).

APPENDIX A

IMINOSUGAR-BASED NUCLEOSIDES

Among nucleoside analogues bearing a modified sugar moiety, the azanucleosides (iminosugars-based nucleosides) deserve a pivotal role. This class of compounds exhibits a broad-spectrum therapeutic potential, with some of them involved in advanced clinical trials as antitumoral or for the treatment of immune diseases, such as viral infections. Modifications based on replacement of endocyclic oxygen of the natural ribose with a nitrogen atom and natural hypoxanthine or adenine with the corresponding 9-deazapurine have allowed to develop a new class of nucleoside analogues named the Immucillins (**FIGURE A1**).[35] Immucillin-H (Forodesine®) [Imm-H, (1*S*)-1-(9-deazahypoxantine-9-yl)-1,4-dideoxy-1,4-imino-D-ribitol] is an excellent inhibitor of bovine (K_i = 23 pM) and human (K_i = 56 pM) PNPs.[36]

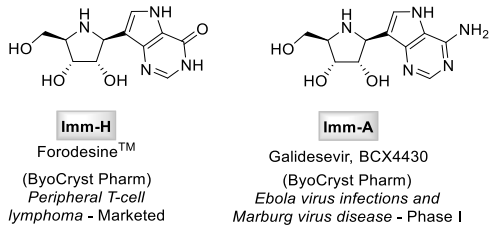

FIGURE A1. The Immucillins.

On the other hand, Immucillin-A (BCX4430) is another synthetic deazapurine iminosugar-C-nucleoside that has exhibited a broad-spectrum antiviral activity.[37]

2.2.7 REFERENCES

[1] Seley-Radtke, K.L.; Yates, M.K. *Antiviral Res.* **2018**, *154*, 66.
[2] Jiang, Y.C.; Feng, H.; Lin, Y.C.; Guo, X.R. *Int. J. Oral Sci.* **2016**, *8*, 1.
[3] Coen, D.M.; Schaffer, P.A. *Nat. Rev.* **2003**, *2*, 278.
[4] Cram, D.; Cram, M.J. *Science* **1974**, *183*, 803.
[5] Cram, D. *Chemtech* **1987**, *17*, 120.
[6] Kool, E. *Chem. Rev.* **1997**, *97*, 1473.
[7] Thibaudeau, C.; Acharya, P.; Chattopadhyaya, J. *Stereoelectronic Effects in Nucleosides and Nucleotides and their Structural Implications*, Uppsala University Press, **1999**.
[8] D'Alonzo, D.; Guaragna, A.; Palumbo, G. *Chem. Biodiversity* **2011**, *8*, 373.
[9] Lescrinier, E.; Froeyen, M.; Herdewijn, P. *Nucleic Acids Res.* **2003,** *31*, 2975.
[10] Marquez, V.E.; Ben-Kasus, T.; Barchi, J.; Green, K.M.; Nicklaus, M.; Agbaria, R. *J. Am. Chem. Soc.* **2004**, *126*, 543.
[11]Al-Madhound, A. S.; Tjarks, W.; Eriksson, S. *Curr. Med. Chem*. **2004**, *4*, 341.
[12] Eriksson, S.; Munch-Petersen, B.; Johansson, K.; Eklund, H. *Cell. Mol. Life Sci.* **2002**, *59*, 1327.
[13] Boehmer, P. E.; Lehman, I. R. *Annu. Rev. Biochem*. **1997**, *66*, 347.
[14] Sarafianos, S. G.; Marchand, B.; Das, K.; Himmel, D. M.; Parniak, M. A.; Hughes, S. H.; Arnold, E. *J. Mol. Biol.* **2009**, *385*, 693.
[15] Marquez, V. E.; Hughes S. H.; Sei S.; Agbaria R. *Antiviral Res.* **2006**, *71*, 268.
[16]See for example: Herdewijn, P. *Antiviral Res.* **2006**, *71*, 317.
[17] (a) Verheggen, I.; Van Aerschot, A.; Toppet, S.; Snoeck, R.; Janssen, G.; Balzarini, J.; De Clercq, E.; Herdewijn, P. *J. Med. Chem.* **1993**, *36*, 2033. (b) Verheggen, I.; Van Aerschot, A.; Meervelt, L.V.; Rozenski, J.; Wiebe, L.; Snoeck, R.; Andrei, G.; Balzarini, J.; Claes, P.; De Clercq, E.; Herdewijn, P. *J. Med. Chem.* **1995**, *38*, 826.
[18] Ostrowski, T.; Wroblowski, B.; Busson, R.; Rozenski, J.; De Clercq, E.; Bennett, M. S.; Champness, J. N.; Summers, W. C.; Sanderson, M. R.; Herdewijn, P. *J. Med. Chem.* **1998**, *41*, 4343.
[19] Maurinsh, Y.; Schraml, J.; De Winter, H.; Blaton, N.; Peeters, O.; Lescrinier, E.; Rozensky, J.; Van Aerschot, A.; De Clercq, E.; Busson, R.; Herdewijn, P. *J. Org. Chem*. **1997**, *62*, 2861.
[20] (a) Perales, C.; Martìn, V.; Domingo, E. *Curr. Opin. Virol.* **2011**, *1*, 419. (b) Bull, J.J.; Sanjua, R.; Wilke, C.O. *J. Virol.* **2007**, *81*, 2930.
[21] Domingo, E.; Sheldon, J. Perales, C. *Microbiol. Mol. Biol. Rev.* **2012**, *76*, 159.
[22] Bebenek, K.; Roberts, J. D.; Kunkel, T.A. *J. Biol. Chem.* **1992**, *267*, 3589.
[23] Ferguson, L.R.; Denny, W.A. *Mutat. Res.* **2007**, *623*, 14.
[24] Yang, H. Z.; Pan, M. Y.; Jiang, D. W.; He, Y. *Org. Biomol. Chem*. **2011**, *9*, 1516.
[25] Suen, W.; Spiro, T. G.; Sowers, L. C.; Fresco, J. R. *Proc. Natl. Acad. Sci. U.S.A.* **1999**, *96*, 4500.
[26] Yu, H.; Eritja, R.; Bloom, L. B.; Goodman, M. F. *J. Biol. Chem.* **1993**, *268*, 15935.

[27] Wennekes, T.; Lang, B.; Leeman, M.; van der Marel, G. A.; Smits, E.; Weber, M.; Jim van Wiltenburg, J.; Wolberg, M.; Aerts, J. M. F. G.; Overkleeft, H. S. *Org. Process Res. Dev.* **2008**, *12*, 414.

[28] This lack of reactivity could be ascribed just to the presence of endocyclic nitrogen, which could form a stable complex with Pd (catalyst poisoning).

[29] Pedatella, S.; Guaragna, A.; D'Alonzo, D.; De Nisco, M.; Palumbo, G. *Synthesis* **2006**, *2*, 305.

[30] Danieli, E.; Lalot, J.; Murphy, P. V. *Tetrahedron* **2007**, *63*, 6827.

[31] Crich, D.; Quintero, L. *Chem. Rev.* **1989**, *89*, 1413.

[32] Krug, A.; Schmidt, S.; Lekschars, J.; Lemke, K.; Cech, D. *J. Prakt. Chem.* **1989**, *331*, 835.

[33] 5-Halouridines are well known bioactive compounds able to induce lethal mutagenesis by inducing base mispairing in the growing nucleic acid chain through, *inter alia*, ionization or tautomerism: Bonnac, L. F.; Mansky, L. M.; Patterson, S. E. *J. Med. Chem.* **2013**, *56*, 9403–9414.

[34] Slusarczyk, M.; Serpi, M.; Pertusati, F. *Antiviral Chem. Chemother.* **2018**, *26*, 1.

[35] Schramm, V. L.; Tyler, P. C. "Transition state analogue inhibitors of *N*-.ribosyltransferases" in *Iminosugars: from synthesis to therapeutic applications*; Compain, P.; Martin, O. R.; John Wiley &Sons, Ltd.: West Sussex, **2007**.

[36] Kicska, G. A.; Long, L.; Hörig, H.; Fairchild, C.; Tyler, P. C.; Furneaux, R. H.; Schramm, V. L.; Kaufman, H. L. *Proc. Natl. Acad. Sci. U.S.A.* **2001**, *98*, 4593.

[37] Taylor, R.; Kotian, P.; Warren, T.; Panchal, R.; Bavari, S.; Julander, J.; Dobo, S.; Rose, A.; El-Kattan, Y.; Taubenheim, B.; Babu, Y.; Sheridan, W. P. *J. IPH* **2016**, *9*, 220.

2.3 Asymmetric Synthesis of D- and L-Cyclohexenyl Nucleosides (CeNAs)

2.3.1 INTRODUCTION

The concepts explained in the introductive section of the last two chapters regarding the critical role of the conformation and of the configuration in the research and design of selective antiviral agents, can be even applied to another class of nucleoside analogues bearing a cyclohexenyl sugar moiety, which attracted considerable attention over the last years. A brief overview about carbocyclic nucleosides, the synthetic methodologies devoted to their preparation, as well as their biological activity and selectivity is reported below.

2.3.1.1 CARBOCYCLIC ANALOGUES OF NUCLEOSIDES AND THEIR PHARMACOLOGICAL PROPERTIES

Carbocyclic nucleosides (also referred as carbanucleosides) born from the replacement of the oxygen atom of natural nucleosides with a methylene unit (**FIGURE 1**).[1]

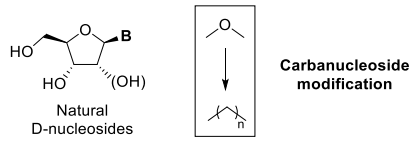

FIGURE 1. Formal replacement of the oxygen atom in the carbanucleosides.

Their cellular processing and mechanism of action are similar to those of natural nucleosides: progressive phosphorylation until their triphosphate forms and then interaction with viral polymerases leading, sometimes, to potent biological activity.[2,3] In 1966 it has been revealed the antibiotic and antitumor activity of two natural occurring carbocyclic nucleosides, Aristeomycin A and Neplanocin (**FIGURE 2**).[4] Since then the research on carbocyclic nucleosides with biological activity has been the subject of intense efforts. As widely explained in the last chapters, the design of NAs working as non-toxic and especially selective inhibitors of kinases and polymerases for the control of viral diseases and cancer, has been the main goal of this research area and the carbocyclic nucleosides seems to meet some of these challenging features. They are good substrates of enzymes that normally respond to standard nucleosides, but at the same time they are highly resistant to phosphorylases and hydrolases; as consequence showing extreme stability towards sugar-base cleavage.[5] For all the described reasons, their design and preparation represent an important topic in modern medicinal chemistry.

2.3.1.1.1 ANTIVIRAL CARBOCYCLIC NUCLEOSIDES

As above, after the discovery of the biological properties belonging to Aristeromycin A and Neplanocin A, other synthetic nucleosides with important therapeutic applications

were discovered.[6] The synthetic cytosine analogue of Aristeromycin A, the cyclopentenylcytosine (CPE-C) was developed as a potent antitumor and antiviral agent.[7] The displacement of the double bond to a different position relative to the neplanocins, has given rise to the potent and specific antiretroviral agent Carbovir (CBV)[8] and then its structurally related Abacavir (ABC)[9], approved drug to prevent and treat HIV/AIDS. Entecavir (ETV),[10] a guanosine analogue, was approved by FDA in 2005 for oral treatment of Hepatitis B infection (HBV); the homomethylene derivative of carbocyclic oxetanocin A ((-)-BCA) is a hybrid structure with excellent antiretroviral activity[11] and finally, another active carbanucleoside is the new transposed antiherpetic guanine isonucleoside BMS-181164[12]. All above mentioned carbanucleosides are only a fraction of some new and fascinating structures that have been synthesized in recent years.

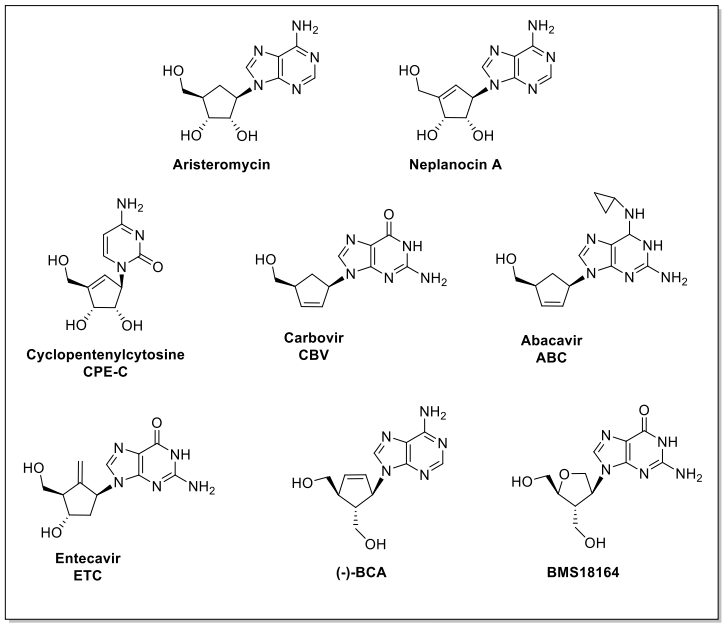

FIGURE 2. Chemical structures of some antiviral carbanucleosides.

2.3.1.2 BRIEF OVERVIEW ON THE MAIN ENANTIOSELECTIVE SYNTHETIC APPROACHES USED FOR THE CONSTRUCTION OF CARBOCYCLIC NUCLEOSIDES

The intense search for clinically useful carbocyclic nucleosides has resulted in the development of novel approaches for their synthesis, and especially, by enantioselective methodologies. The carbanucleosides can be prepared mainly by two approaches: 1) the convergent insertion of the nucleobase on a functionalized carbocyclic ring; 2) synthesis

of the carbocycle functionalized with an amino group from which the nucleobase is linearly constructed.

1) The *direct coupling* of the nucleobase with the carbocyclic pseudo sugar can be accomplished by several methods: from the S_N2 nucleophilic displacement of a halide ions or activated alcohols[13] to the epoxide ring opening,[14] or more interestingly, by a palladium catalysed displacement of allylic esters or carbonates (namely the Tsuji-Trost rearrangement)[15] (**SCHEME 1**). In the latter method the allylic substrate is typically treated with a bulky Pd(0) catalyst [such as tetrakis-triphenylphosphine palladium, $Pd(PPh_3)_4$] to generate an intermediate allyl palladium complex, that undergoing nucleophilic attack from the less hindered carbon atom, releases the corresponding nucleoside. Since the process involves a double substitution (palladium coordination takes place on the opposite side with respect to substituents and nucleophilic attack occurs on the opposite side with respect to palladium complex), the reaction overall proceeds with retention of configuration, providing the only *cis*-product.[16] Even if direct coupling of the nucleobase represents the most convergent approach, it suffers of some limitation due to the regioselectivity of base insertion. Indeed, with purines the attack can happen at the N9, N7 and N3 positions (**SCHEME 1**).

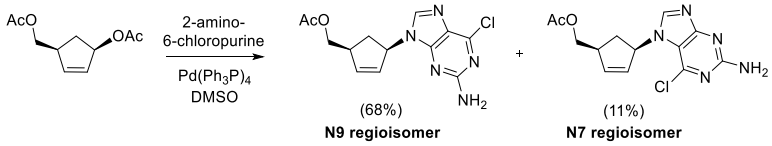

SCHEME 1. Tsuji-Trost Pd(0) allylic rearrangement.

2) The nucleobase can be literally constructed on the carbocyclic pseudo sugar moiety if the latter possess an exocyclic amino group, which becomes the N9 of a purine or the N1 of a pyrimidine (**SCHEME 2**).[17]

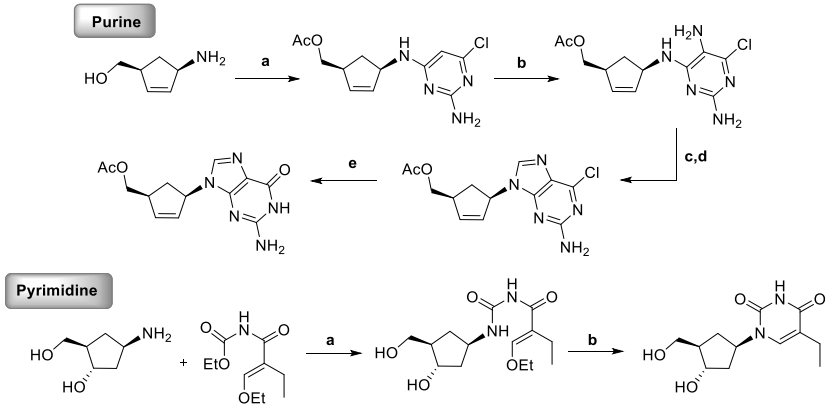

SCHEME 2. *Purine*: a) 2-amino-4,6-dichloropyrimidine, *i*-Pr_2NEt, BuOH, reflux, 80%; b) 4-$ClC_6H_4N_2^+Cl^-$, HOAc, NaOAc, H_2O, 69%; c) Zn, HOAc, EtOH, H_2O, 50%; d) $(EtO)_3CH$, HCl, H_2O; e) NaOH, H_2O, reflux, 74%. *Pyrimidine*: a) TEA, dioxane; b) 2% 2N HCl in dioxane. 80% o.y.

2.3.1.3 LOCKED CARBOCYCLIC NUCLEOSIDES

As widely highlighted in the **Chapter 2.2**[18] about the synthesis of *North* and *South* methano-carbathymidine, *N*-MCT and *S*-MCT, if the nucleoside sugar is structurally constrained into the optimal conformation required for the binding with the target enzyme, it could be endowed with high activity and, more interestingly, by a considerable selectivity.[19] This study has been extended by Herdewijn *et al.* and applied to the synthesis of carbanucleosides with a six-membered sugar moiety. Several mono-, di- and tri-substituted cyclohexane nucleoside analogues (**FIGURE 3**) have been prepared and tested as antiviral agents,[20] but none of them showed biological activity. Poor anabolism (phosphorylation) inside the cells could account for this lack of activity.

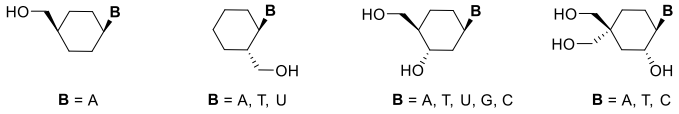

FIGURE 3. Cyclohexanyl nucleosides.

2.3.1.3.1 CYCLOHEXENYL NUCLEOSIDES

Among bioactive nucleosides bearing six-membered sugar moiety, those obtained replacing the furanose ring with a cyclohexene unit holds a privileged position. A cyclohexene ring mainly exists in two half-chair forms ($^3H_2$ and $^2H_3$), which interconvert via the symmetrical boat conformation (**FIGURE 4**). Differently from the furonase ring, for which all the possible forms are given by two-dimensional pseudorotational cycle,[21] the cylohexenyl moiety has a conformational behaviour described by a three-dimensional conformational globe (**FIGURE 4**).[22] The chair forms are located at the poles of the globe; the planar form is the highest energy form and it is located at the centre of the globe. The ellipsis represents the most stable conformers of cyclohexene, the half-boat (E) and the half-chair (H) forms with the corresponding inverted forms, located at antipodes of the globe.

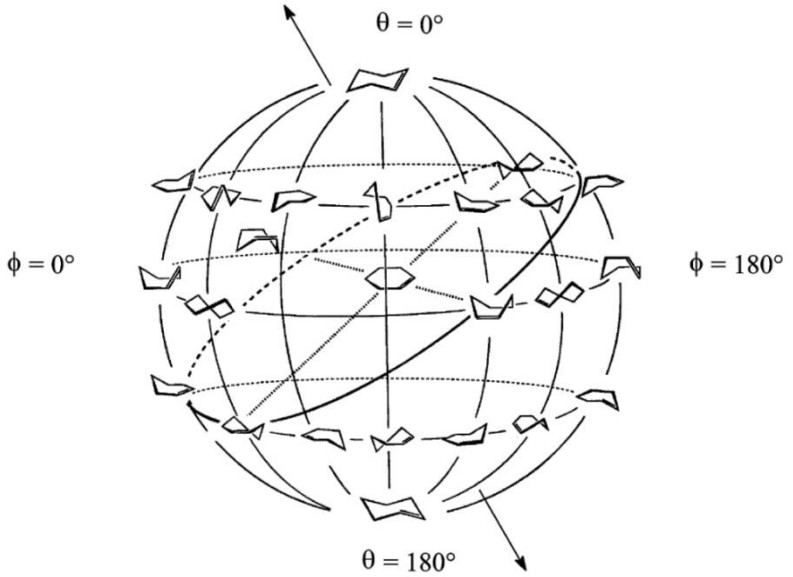

FIGURE 4 ***(taken from ref. 22).*** Conformational globe of cyclohexene.

In **FIGURE 5** is easy to identify the relationship between the pseudorotational cycle of furanose ring and the cyclohexene one; the $^{3}T_{2}$ (North) and $^{2}T_{3}$ (South) conformations of furanose find their structural equivalent in the $^{3}H_{2}$ (North) and $^{2}H_{3}$ (South) conformations of the cyclohexene ring. Therefore, the conformational profile of a cyclohexenyl ring is similar to that of a saturated five-member ring and this interesting finding explains why the cyclohexene ring demonstrated to be an efficient bioisostere of the natural furanose unit. Moreover, the energy gap required for the conformational change $^{3}H_{2} \rightleftharpoons {}^{2}H_{3}$ is even lower (ΔG~10 kJ/mol) than that involving the $^{2}T_{3} \rightleftharpoons {}^{3}T_{2}$ interconversion (ΔG~20 kJ/mol; **FIGURE 5**).

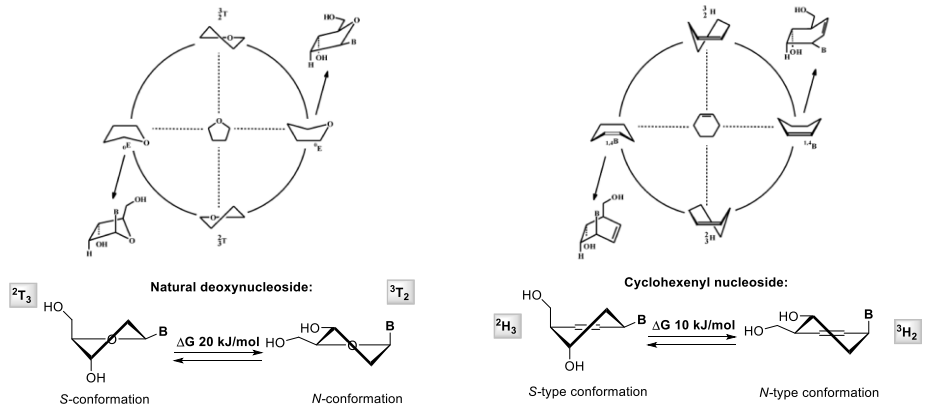

FIGURE 5 (*adapted by ref. 22*). Conformational relationships between natural deoxynucleosides and cyclohexenyl nucleosides.

Because of these considerations, Herdewijn *et al.*[23] synthetized and investigated the properties of both enantiomeric forms of the cyclohexene guanine nucleosides **1** and *ent*-**1** (**FIGURE 6**). They were evaluated against a broad range of human infections and exhibited potent and selective antiviral activity against HSV-1 and 2, VZV and CMV comparable to that of the well-known antiviral drugs acyclovir and ganciclovir (**FIGURE 6**). The above results highlighted how NAs bearing a six-membered moiety drew great attention, as they demonstrated to enable precise positioning of functional groups in the recognition events dealing with the metabolism of nucleosides and their incorporation into viral genomes. This justifies the longstanding efforts in the field, as well as the still ongoing studies aimed to explore other six-membered NAs endowed with even higher therapeutic activity.

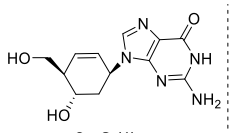

D-Ce-G (1)

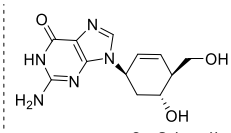

L-Ce-G (*ent*-1)

	Activity (IC_{50}, μg/mL)			
Virus	**D-Ce-G**	**L-Ce-G**	Acyclovir	Ganciclovir
HSV-1	0.002 - 0.004	0.003 - 0.004	0.003 - 0.07	0.001 - 0.01
HSV-2	0.05 - 0.07	0.007 - 0.1	0.02	0.002 - 0.001
VZV	0.41 - 2.8	1.2 - 6.8	0.8 - 28	ND
CMV	0.8 - 0.6	1.7 - 1.5	ND	0.8 - 0.6

FIGURE 6. D- and L-cyclohexenyl guanine as anti-HHV agents.

2.3.2 Results and Discussion

2.3.2.1 Asymmetric Synthesis of D- and L-Cyclohexenyl Nucleosides

On the basis of the promising biological potential exhibited by carbanucleosides (i.e. D- and L-cylohexenyl nucleosides)[23] and discussed in the previous section, this project has been focused on the development of a synthetic approach aimed to the preparation of novel cyclohexenyl nucleosides (CeNAs), once again in both enantiomeric forms (**2a,b** and *ent*-**2a,b**; **Scheme 3**). These, due to the inherent flexibility of the cyclohexenyl unit (rapidly interconverting between the $^{3}H_{2}$ and $^{2}H_{3}$ forms), are able to resemble both the *N* and *S* sugar ring puckers of natural nucleosides resulting suitable substrates either for kinases and polymerases. The main structural modification made on **2a,b** and *ent*-**2a,b**, despite the previously reported examples of cyclohexenyl NAs **1** and *ent*-**1**,[23] is the lack of *sec*-OH group at C5' position conceived with the aim to keep the biomimetic properties of cyclohexene moiety while acting as chain terminators. As shown in **Scheme 3**, the synthesis has started from the inexpensive cyclohexanone **3**, enantioselectively hydroxymethylated (organocatalytic reaction catalysed by D- or L-proline) and then manipulated to obtain the carbonate **4** from which, by the Tsuji-Trost rearrangement, the target nucleosides are efficiently prepared.

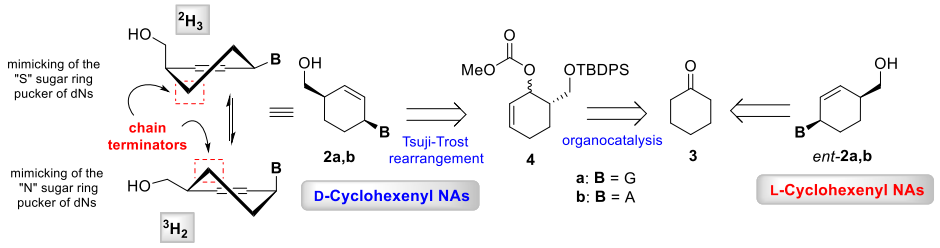

Scheme 3. Retrosynthetic pathway to target CeNAs **2a,b** and *ent*-**2a,b**.

At the moment **2a,b** and *ent*-**2a,b** are involved in a wide antiviral screening (against HHVs, HIV and tropical viruses such as Chikungunya virus, Yellow Fever or Enterovirus71) ongoing at the Rega Institute for Medical Research (KU Leuven, Belgium) under the supervision of Prof. Robert Snoeck, Prof. Graciela Andrei, Prof. Cristophe Pannecouque and Prof. Johan Neytz.

2.3.2.2 Enantioselective Synthesis of the Cyclohexenyl Unit

The enantioselective synthesis of optically active cyclohexenone **6**, involving the organocatalyzed hydroxymethylation of cyclohexanone (**3**) (L-proline/CH_2O), the protection of the resulting alcohol (TBDPSCl/Him) to give **5** and the subsequent Saegusa

dehydrogenation of ketone [LDA/TMSCl, then $Pd(OAc)_2$], has been performed as already described (**SCHEME 4**).[24]

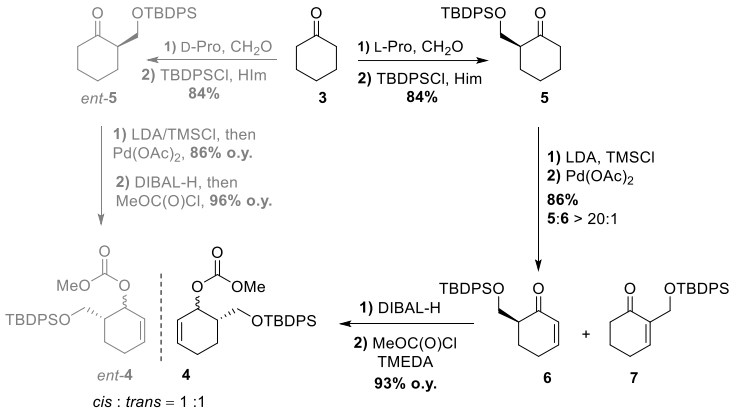

SCHEME 4. Synthetic paths to obtain the carbonates **4** (in black) and *ent*-**4** (in grey).

Ketone **6** was then subjected to reduction with DIBAL-H (to give a 1:1 mixture of *cis* and *trans* stereoisomers) (**SCHEME 4**) followed by the alcohol protection step with MeOC(O)Cl affording the carbonate **4**. The same synthetic path (but using D-proline as chiral catalyst in the first reaction step) described starting by **3** has been applied to finally obtain *ent*-**4** (**SCHEME 4**).

2.3.2.3 CARBANUCLEOSIDES SYNTHESIS

The synthesis of the target carbanucleosides **2a,b** and *ent*-**2a,b** was then approached exploiting the Tsuji-Trost rearrangement.[16] As already described for cyclopentenyl substrates in the introductive section of the chapter, this reaction is typically based on the use of allylic esters or carbonates, which are treated with a bulky Pd(0) catalyst [such as tetrakis-triphenylphosphine palladium, $Pd(PPh_3)_4$] to generate an intermediate allyl palladium complex, then undergoing nucleophilic attack from the less hindered carbon atom, releasing the corresponding cyclopentenyl nucleosides. Since the process involves a double substitution (palladium coordination occurs on the opposite side with respect to substituents and nucleophilic attack on the opposite side with respect to palladium complex), the reaction overall proceeds with net retention of configuration, providing the only *cis*-products.[25] At a glance, the study of the rearrangement of cyclohexene **4** appeared a simple repetition, on a six-membered system, of the work on the synthesis of bioactive cyclopentenyl nucleosides, since the extra-methylene group was not expected to influence the reaction outcome. Accordingly, among the two cyclohexenyl carbonates *cis*- and *trans*-**4**, only the *cis* isomer was at first considered of synthetic utility. Conversely, treatment of the inseparable mixture of *cis* and *trans*-**4** with 6-chloropurine **8**, $Pd_2(dba)_3{\cdot}CHCl_3$ and PPh_3 in a 1:1 THF/DMSO mixture surprisingly led to the

formation of one main nucleoside, identified by ^{1}H NMR as *cis*-**9** [rr(N9:N7) = 6:1, entry 1, **TABLE 1**). The reaction of *cis* and *trans*-**4** with 2-amino-6-chloropurine **10** also furnished nucleoside *cis*-**11** with high stereoselectivity (>20:1), although regioselectivities and reaction times were variable (entry 2) (**TABLE 1**).

TABLE 1. Allylic rearrangement of *cis* and *trans*-**4**.

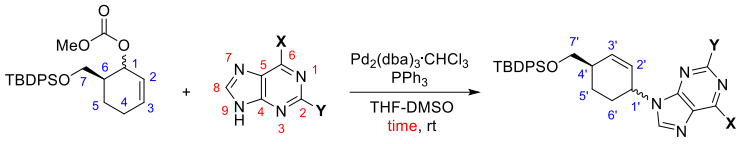

4 **8** (**X** = Cl, **Y** = H); **10** (**X** = Cl, **Y** = NH_2) **9** (**X** = Cl, **Y** = H); **11** (**X** = Cl, **Y** = NH_2)

Entry	Carbonate	Nucleobase	Nucleoside	t (h)	Yield[a] (%)	*cis:trans*	N9: N7
1	*trans*/*cis*-**4**	**8**	**9**	20	76 (65)[b]	>20:1	6:1
2	*trans*/*cis* -**4**	**10**	**11**	18	83 (69)[b]	>20:1	5:1

[a]Sum of regioisomeric N9 and N7 nucleosides.

It is worthy to mention that, to the best of our knowledge, no precedents examples of stereoconvergent Tsuji-Trost rearrangement have ever been reported. Computational studies are indeed ongoing in order to elucidate the reaction mechanism that allow to explain stereochemical outcome of the reaction when performed on cyclohexenyl substrates.

Protected nucleosides **9** and **11** were eventually deprotected (TBAF) to afford **12** and **13** (89-92% yield); treatment of **12** with NH_3 in MeOH afforded the adenine carbanucleoside **2b,** while treatment of **13** with NaOH led to guanine derivative **2a** (**SCHEME 5**).

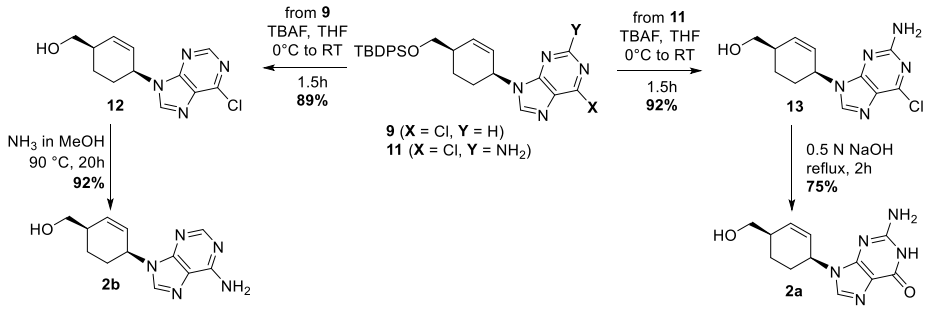

SCHEME 5. Final reaction steps to afford the target nucleosides **2a,b**.

The corresponding L-enantiomers *ent*-**2a,b** were prepared following the same synthetic route.

2.3.3 CONCLUDING REMARKS AND FUTURE PERSPECTIVES

This part of the PhD project has been devoted to the development of a highly regio- and stereoselective route to cyclohexenyl nucleosides **2a,b** and *ent*-**2a,b**. The antiviral potential of these compounds relies on the high conformational flexibility of the pseudosaccharide units, enabling a close mimicry of the bioactive conformations (*N* and *S*) of natural D-nucleosides. In addition, the absence of any secondary hydroxyl function (which would resemble the OH group at the C3' position of natural nucleosides) justifies their employ as chain terminators. From a synthetic standpoint the crucial steps are the hydroxymethylation organocatalytic reaction with D- or L-proline which allowed us to pre-establish the belonging steric series of the final nucleosides and, noteworthy, the allylic Tsuji-Trost rearrangement, an unprecedented example of stereoconvergent case. Because of the evident synthetic applications of this finding, especially if applied to the synthesis of other carbocyclic nucleosides including bioactive cyclopentenyl nucleosides (e.g. the marketed anti-HIV agent Abacavir), further investigation on this topic is currently ongoing. The earliest examples of cyclohexenyl nucleosides obtained are now object of a wide antiviral screening (against HHVs, HIV and tropical viruses such as Chikungunya virus, Yellow Fever or Enterovirus71) ongoing at the Rega Institute for Medical Research (KU Leuven, Belgium) under the supervision of Prof. Robert Snoeck, Prof. Graciela Andrei, Prof. Cristophe Pannecouque and Prof. Johan Neytz. The synthesis and the biological evaluation of the following and other D- and L-cyclohexenyl nucleosides will be object of a paper, that will publish in due course.

2.3.4 EXPERIMENTAL SECTION

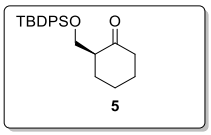

Silyl ether 5. To a stirred solution of 2-(*S*)-hydroxymethyl cyclohexanone[24] (0.15 g, 1.17 mmol) in anhydrous pyridine (3 mL), TBDPSCl (0.36 mL, 1.40 mmol) and imidazole (0.095 g, 1.40 mmol) were added. After stirring for 15' at rt, the reaction mixture was diluted with CH_2Cl_2 and washed with brine until neutrality. The organic layers were dried with Na_2SO_4 and the solvent evaporated under reduced pressure. Chromatography of the crude residue over silica gel (hexane:EtOAc = 96:4) gave the pure (2*S*)-[(silyloxy)methyl]-cyclohexanone (**5**) (0.36 g, 84% reaction yield) as an oil. $[\alpha]^{25}_{D}$ -17.6 (*c* 0.57, $CHCl_3$). ^{1}H NMR (500 MHz, $CDCl_3$), δ: 1.04 (*s*, 9H), 1.42-1.52 (*m*, 1H), 1.61-1.72 (*m*, 2H), 1.85-1.93 (*m*, 1H), 1.99-2.08 (*m*, 1H), 2.23-2.40 (*m*, 3H), 2.49-2.58 (*m*, 1H), 3.67 (*dd*, J = 7.8, 10.5 Hz, 1H), 4.00 (*dd*, J = 4.6, 10.5 Hz, 1H), 7.32-7.45 (*m*, 6H), 7.66 (*d*, J = 7.7 Hz, 4H). ^{13}C NMR (100 MHz, $CDCl_3$), ppm: 24.6, 26.5, 26.8, 27.6, 30.9, 42.1, 52.8, 63.0, 127.7, 129.6, 133.6, 134.8, 135.5, 211.9. Anal. calcd for $C_{23}H_{30}O_2Si$: C 75.36, H 8.25, O 8.73. Found: C 75.27, H 8.28, O 8.76.

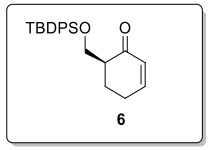

Cyclohexenone 6:. *n*-BuLi (2.5 M in hexane, 0.40 mL, 1.00 mmol) was added to a solution of freshly distilled DIPA (0.16 mL, 1.14 mmol) in anhydrous THF (2 mL), stirred at -78°C under nitrogen atmosphere. After 20', a solution of **5** (0.348 g, 0.95 mmol) in anhydrous THF (1.6 mL) was added dropwise to the mixture. After 1h, TMSCl [2.2 mL, previously distilled and deacidified with a solution of freshly dried triethylamine (TEA) in anhydrous THF] was added and the resulting mixture stirred for 1h at –78°C. After control TLC indicated complete conversion of the starting ketone into the corresponding trimethylsilyl enol ether, the solvent was evaporated under reduced pressure and the mixture filtered on a celite pad washing with pentane (10.5 mL). To a stirring solution of the crude trimethylsilyl enol ether in anhydrous CH_3CN (14 mL), $Pd(OAc)_2$ (0.21 g, 0.95 mmol) was added at rt and the reaction was stirred at the same temperature for 16h. The mixture was then filtered on a celite pad washing with CH_2Cl_2. The filtrate was washed with brine. The organic layer was dried (Na_2SO_4) and evaporated under reduced pressure. Chromatography of the crude residue over silica gel

(hexane:Et_2O = 95:5) gave the pure **6** (0.298 g, 86% o.y.) as an oil. $[\alpha]^{25}_D$ +20.3 (*c* 0.57, $CHCl_3$. ^1H NMR (400 MHz, $CDCl_3$), δ: 1.04 (*s*, 9H), 1.94-2.04 (*m*, 1H), 2.26-2.32 (*m*, 1H) 2.37-2.45 (*m*, 2H), 2.49-2.56 (*m*, 1H), 3.88 (*dd*, J = 7.2, 10.2 Hz, 1H), 3.99 (*dd*, J = 4.2, 10.2 Hz, 1H), 5.99 (*dt*, J = 2.2, 10.1 Hz, 1H), 6.96 (*dddd*, J = 1.2, 3.1, 4.9, 10.1 Hz, 1H), 7.35-7.44 (*m*, 6H), 7.65 (*dd*, J = 1.8, 8.0 Hz, 2H), 7.68 (*dd*, J = 1.5, 7.6 Hz, 2H). ^{13}C NMR (100 MHz, $CDCl_3$), ppm: 19.3, 25.2, 25.6, 26.9, 48.9, 62.8, 127.7, 129.6, 129.9, 133.5, 135.6, 135.7, 150.3, 199.4. Anal. calcd for $C_{23}H_{28}O_2Si$: C 75.78, H 7.74, O 8.78. Found: C 75.70, H 7.76, O 8.81.

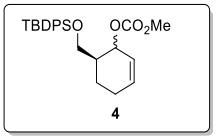

4

Carbonate 4.

Reduction step: to a stirred solution of unsaturated ketone **6** (0.269 g, 0.74 mmol) in anhydrous toluene (8 mL), DIBAL-H (1.5 M in toluene, 0.59 mL, 0.89 mmol) was added at -78°C. After 15', the reaction mixture was warmed to 0°C, methanol and sodium potassium tartrate were added and the resulting mixture was extracted with EtOAc and washed with brine. The organic layer was dried (Na_2SO_4) and the solvent evaporated under reduced pressure.

Protection step: to a solution of the crude allylic alcohol (0.74 mmol) in anhydrous CH_2Cl_2 (14 mL), stirred at 0°C under nitrogen atmosphere, TMEDA (0.11 ml, 0.74 mmol) and $ClCO_2Me$ (0.11 mL, 1.48 mmol) were added. The reaction was stirred for 1 h at the same temperature; afterwards aq. NH_4Cl was added and the resulting mixture extracted with CH_2Cl_2 and washed with brine. The organic layers were dried (Na_2SO_4) and concentrated under reduced pressure. The compound **4** (0.337 g, 93% o.y.) was obtained as inseparable 1:1 mixture of *cis* and *trans* stereoisomers. ^1H NMR (400 MHz, $CDCl_3$), δ: 1.03 (*s*, 4.5H), 1.05 (*s*, 4.5H), 1.65-1.76 (*m*, 1H), 1.85-2.16 (*m*, 4H), 3.56 (*dd*, J = 6.4, 9.9 Hz, 0.5H), 3.64 (*dd*, J = 4.3, 10.2 Hz, 0.5H), 3.67 (*dd*, J = 5.1, 10.2 Hz, 0.5H), 3.72-3.78 (*m*, 3.5H), 5.23 (*dt*, J = 2.0, 7.9 Hz, 0.5H), 5.28 (*bt*, J = 3.8 Hz, 0.5H), 5.69 (*dq*, J = 2.4, 10.1 Hz, 0.5H), 5.88 (*bd*, J = 10.1 Hz, 0.5H), 5.97-6.03 (*m*, 1H), 7.31-7.43 (*m*, 6H), 7.58-7.67 (*m*, 4H). ^{13}C NMR (125 MHz, $CDCl_3$), δ: 19.2, 19.6, 25.2, 26.6, 26.7, 29.6, 40.2, 40.6, 54.4, 54.5, 63.8, 64.0, 70.2, 73.8, 124.0, 125.4, 127.5, 127.6, 129.5, 131.8, 134.2, 135.5, 135.6, 155.4, 155.6. Anal. calcd for $C_{25}H_{32}O_4Si$: C 70.72, H 7.60, O 15.07. Found: C 70.67, H 7.63, O 15.12.

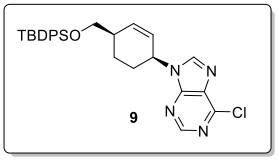

Nucleoside 9. To a solution of 6-chloropurine **8** (35 mg, 0.23 mmol) in anhydrous DMSO (1.6 mL) stirred at rt under nitrogen atmosphere, $Pd_2(dba)_3 \cdot CHCl_3$ (31 mg, 30 μmol) and PPh_3 (60 mg, 0.23 mmol) were sequentially added. A solution of **4** (0.10 g, 0.23 mmol, mixture of *cis*- and *trans*-isomers) in anhydrous THF (1.6 mL) was added dropwise and reaction mixture was further stirred for 20 h. The resulting mixture was then washed with brine and extracted with EtOAc. The organic layers were dried (Na_2SO_4) and concentrated. Chromatography of the crude residue over silica gel (hexane:EtOAc = 70:30) gave nucleoside **9** (0.075 g, 65% reaction yield; dr(cis:trans) > 20:1, rr(N9:N7) = 6:1). ^{1}H NMR (400 MHz, $CDCl_3$), δ: 1.09 (*s*, 9H), 1.39-1.49 (*m*, 1H), 1.75, 1.83 (*m*, 1H), 1.99-2.12 (*m*, 2H), 2.44-2.52 (*m*, 1H), 3.65 (*dd*, J = 6.1, 9.9 Hz, 1H), 3.69 (*dd*, J = 6.4, 9.9 Hz, 1H), 5.28-5.33 (*m*, 1H), 5.89 (*dq*, J = 2.5, 10.1 Hz, 1H), 6.30 (*dt*, J = 1.9, 10.1 Hz, 1H), 7.38-7.46 (*m*, 6H), 7.64-7.69 (*m*, 4H), 8.11 (*s*, 1H), 8.75 (*s*, 1H). ^{13}C NMR (125 MHz, $CDCl_3$), ppm: 19.4, 21.0, 27.1, 28.0, 38.2, 49.9, 66.9, 123.8, 127.9, 130.0, 132.3, 133.4, 135.7, 137.5, 144.6, 151.1, 151.5, 151.8. Anal. calcd for $C_{28}H_{31}ClN_4OSi$: C 66.84, H 6.21, Cl 7.05, N 11.14, O 3.18. Found: C 66.74, H 6.23, Cl 7.07, N 11.17, O 3.17.

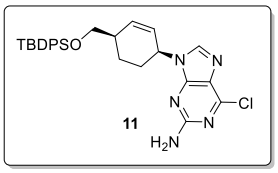

Nucleoside 11. To a solution of 2-amino-6-chloropurine **10** (24 mg, 0.14 mmol) in anhydrous DMSO (2 mL) stirred at rt under nitrogen atmosphere, $Pd_2(dba)_3$ $CHCl_3$ (19 mg, 18 μmol) and PPh_3 (37 mg, 0.14 mmol) were sequentially added. A solution of **4** (60 mg, 0.14 mmol, mixture of *cis*- and *trans*-isomers) in anhydrous THF (2 mL) was added dropwise and reaction mixture was further stirred for 18 h. The resulting mixture was then washed with brine and extracted with EtOAc. The organic layers were dried (Na_2SO_4) and concentrated. Chromatography of the crude residue over silica gel (hexane:EtOAc = 70:30) gave nucleoside **11** (50 mg, 69% reaction yield; d.r (cis:trans) > 10:1, r.r (N9:N7) = 5:1). $[\alpha]^{25}_D$ +66.7 (*c* 0.32, $CHCl_3$). ^{1}H NMR (400 MHz, $CDCl_3$), δ: 1.08 (*s*, 9H), 1.38-1.49 (*m*, 1H), 1.71-1.79 (*m*, 1H), 1.93-2.01 (*m*, 2H), 2.43-2.49 (*m*, 1H), 3.64 (*dd*, J = 6.3, 9.9 Hz, 1H), 3.68 (*dd*, J = 6.6, 9.9 Hz, 1H), 5.02-5.06 (*m*, 1H), 5.82 (*dq*, J = 2.3, 10.1 Hz, 1H), 6.22 (*dt*, J = 1.9, 10.1 Hz, 1H), 7.37-7.46 (*m*, 6H), 7.66-

7.68 (*m*, 4H), 7.75 (*s*, 1H). ^{13}C NMR (100 MHz, $CDCl_3$), ppm: 19.8, 20.9, 26.9, 27.6, 38.0, 49.2, 66.8, 124.2, 125.7, 127.8, 129.8, 133.4, 135.6, 136.6, 141.5, 151.2, 153.2, 158.9. Anal. calcd for $C_{28}H_{32}ClN_5OSi$: C 64.91, H 6.23, Cl 6.84, N 13.52, O 3.09. Found: C 64.80, H 6.25, Cl 6.85, N 13.57, O 3.10, Si 5.53.

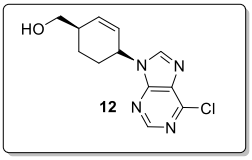

Nucleoside 12. To a solution of **9** (70 mg, 0.14 mmol) in THF (4.4 mL), tetrabutylammonium fluoride (1M solution in THF, 0.14 mL, 0.14 mmol) was added at 0°C. The reaction mixture was stirred at the same temperature for 1.5 h; afterwards the solvent was removed under reduced pressure. Chromatography of the crude residue on silica gel (hexane:EtOAc = 20:80) gave the pure **12** (33 mg, 89% reaction yield). $[\alpha]^{25}_D$ -6.0 (*c* 0.12, CH_3OH). ^{1}H NMR (400 MHz, CD_3OD), δ: 1.48-1.59 (*m*, 1H), 1.78-1.85 (*m*, 1H), 2.07-2.20 (*m*, 2H), 2.37-2.46 (*m*, 1H), 3.62 (*dd*, J = 5.3, 10.7 Hz, 1H), 3.69 (*dd*, J = 6.0, 10.7 Hz, 1H), 5.34-5.40 (*m*, 1H), 6.00 (*ddd*, J = 2.4, 4.0, 10.1 Hz, 1H), 6.28 (*dt*, J = 1.8, 10.1 Hz, 1H), 8.56 (*s*, 1H), 8.74 (*s*, 1H). ^{13}C NMR (100 MHz, CD_3OD), ppm: 21.7, 28.5, 39.4, 51.6, 65.8, 125.3, 132.8, 138.1, 146.9, 147.3, 151.2, 152.8. Anal. calcd for $C_{12}H_{13}ClN_4O$: C 54.45, H 4.95, Cl 13.39, N 21.17. Found: C 54.30, H 4.97, Cl 13.44, N 21.23.

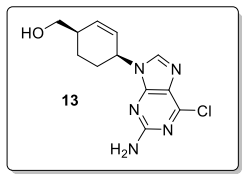

Nucleoside 13. To a solution of **11** (50 mg, 96 μmol) in THF (2.6 mL), tetrabutylammonium fluoride (1 M solution in THF, 96 μL, 96 μmol) was added at 0°C. The reaction mixture was stirred at the same temperature for 1.5 h; afterwards the solvent was removed under reduced pressure. Chromatography of the crude residue on silica gel ($CHCl_3$/MeOH = 95:5) gave the pure **13** (0.025 g, 92% reaction yield). $[\alpha]^{25}_D$ -74.9 (*c* 0.65, CH_3OH). ^{1}H NMR (400 MHz, CD_3OD), δ: 1.51 (*dddd*, J = 3.9, 8.7, 10.8, 15.4 Hz, 1H), 1.73-1.82 (*m*, 1H), 1.97-2.13 (*m*, 2H), 2.33-2.43 (*m*, 1H), 3.60 (*dd*, J = 5.5, 10.8 Hz, 1H), 3.66 (*dd*, J = 6.0, 10.8 Hz, 1H), 5.09-5.14 (*m*, 1H), 5.94 (*dddd*, J = 0.5, 2.4, 3.6, 10.1 Hz, 1H), 6.22 (*dt*, J = 1.9, 10.1 Hz, 1H), 8.06 (*s*, 1H). ^{13}C NMR (100 MHz, CD_3OD), ppm: 21.8, 28.4, 39.4, 50.5, 65.9, 125.3, 125.7, 137.6, 143.4, 151.5.8, 154.8, 161.5. Anal.

calcd for $C_{12}H_{14}ClN_5O$: C 51.53, H 5.04, Cl 12.67, N 25.04. Found: C 51.36, H 5.06, Cl 12.752, N 25.12.

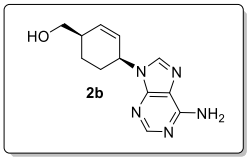

Nucleoside 2b. Nucleoside **12** (20 mg, 0.07 mmol) was treated with a solution of ammonia in MeOH (7 M, 2.4 mL) and heated in a steel bomb for 20 h at 90°C. After cooling, the solvent was removed under reduced pressure. Chromatography of the crude residue over silica gel (CH_2Cl_2:MeOH = 85:15) gave the pure **2b** (17 mg, 92% reaction yield). $[\alpha]^{25}_D$ -3.5 (*c* 0.10, CH_3OH). ^{1}H NMR (400 MHz, CD_3OD), δ: 1.44-1.55 (*m*, 1H), 1.73-1.83 (*m*, 1H), 2.03-2.11 (*m*, 2H), 2.35-2.44 (*m*, 1H), 3.60 (*dd*, J = 5.5, 10.8 Hz, 1H), 3.66 (*dd*, J = 6.0, 10.8 Hz, 1H), 5.16-5.23 (*m*, 1H), 5.95 (*ddd*, J = 2.4, 4.0, 10.0 Hz, 1H), 6.23 (*dt*, J = 1.7, 10.0 Hz, 1H), 8.12 (*s*, 1H), 8.23 (*s*, 1H). ^{13}C NMR (500 MHz, CD_3OD), ppm: 21.7, 28.9, 39.4, 50.6, 65.9, 125.7, 128.05, 134.9, 137.6, 141.8, 153.6, 157.4. Anal. calcd for $C_{12}H_{15}N_5O$: C 58.76, H 6.16, N 28.55. Found C 58.66, H 6.18, N 28.62.

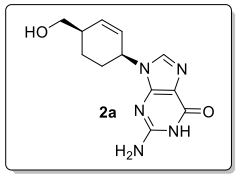

Nucleoside 2a. Nucleoside **13** (45 mg, 0.16 mmol) was refluxed for 2 h in a 0.5 N aq NaOH solution (2.9 mL). Then the reaction mixture was cooled to 0 °C, and 0.5 N HCl was carefully added until neutral. The solvent was removed under reduced pressure and the crude residue was chromatographed over silica gel ($CHCl_3$/MeOH = 80:20) affording the pure **2a** (31 mg, 75% reaction yield). ^{1}H NMR (400 MHz, CD_3OD), δ: 1.46-1.56 (*m*, 1H), 1.72-1.81 (*m*, 1H), 1.95-2.07 (*m*, 2H), 2.34-2.42 (*m*, 1H), 3.60 (*dd*, J = 5.6, 10.8 Hz, 1H), 3.63 (*dd*, J = 6.2, 10.8 Hz, 1H), 4.96-5.03 (*m*, 1H), 5.91 (*ddd*, J = 2.4, 4.0, 10.0 Hz, 1H), 6.18 (*dt*, J = 1.9, 10.0 Hz, 1H), 7.70 (*s*, 1H). ^{13}C NMR (100 MHz, CD_3OD), ppm: 21.8, 28.8, 39.4, 50.1, 66.0, 117.9, 126.0, 137.0, 138.5, 152.6, 155.2, 159.5. Anal. calcd for $C_{12}H_{15}N_5O_2$: C 55.16, H 5.79, N 26.80. Found: C 55.04, H 5.81, N 26.86.

2.3.5 REFERENCES

[1] Schneller, S. W. *Curr. Top. Med. Chem.* **2002**, *2*, 1087.
[2] Mieczkowski, A.; Agrofoglio, L.A. in *Modified Nucleosides: in Biochemistry, Biotechnology and Medicine*; Herdewijn, P., Ed.; Wiley-VCH, **2008**.
[3] Leclerc, E. in *Chemical Synthesis of Nucleoside Analogues*; Merino, P., Ed.; Wiley-VCH, **2013**.
[4] Shealy, Y.F.; Clayton, J.D. *J. Am. Chem. Soc.* **1966**, *88*, 3885.
[5] Boutureira, O.; Matheu, M. I.; Diaz, Y.; Castillòn, S. *Chem. Soc. Rev*. **2013**, *42*, 5056.
[6] Marquez, V. E. in *Advances in Antiviral Drug Design, Volume 2*; De Clercq, E., Ed.; Elsevier Ldt, **1996.**
[7] Schimmel, K.J.M.; Gelderblom, H.; Guchelaar, H.J. *Curr. Cancer Drug Targets* **2007**, *7*, 504.
[8] Vince, R.; Hua, M. *J. Med. Chem.* **1990**, *33*, 17.
[9] "Therapeutic Nucleosides" Daluge, S.M.U.S. Patent **1991**, US5034394.
[10] Matthews, S.J. *Clin. Ther*. **2006**, *28*, 84.
[11] Katagiri, N.; Nomura, M.; Sato, H.; Kaneko, C.; Yusa, K.; Tsuruo, T. *J. Med. Chem.* **1992**, *35*, 1882.
[12] Tino, J. A.; Clark, J. M.; Field, A. K.; Jacobs, G. A.; Lis, K. A.; Michalik, T. L.; McGreever-Rubin, B.; Sulsarchyk, W. A.; Spergel, S. H.; Sundeen, J. E.; Tuomari, A. V.; Weaver, E. R.; Young, M. G.; Zahler, R. *J. Med. Chem*. **1993**, *36*, 1221.
[13] Bisacchi, G.S.; Singh, J.; Godfrey, Jr.; J.D.; Kissick, T.P; Mitt, T.; Malley, M.F.; Di Marco, J.D.; Gougoutu, J.Z.; Mueller, R.H.; Zahler, R. *J. Org. Chem.* **1995**, *60*, 2902.
[14] Jeon, L.S.; Marquez, V.E. *Tetrahedron Lett.* **1996**, *37*, 2353.
[15] Trost, B.M.; Kuo, G.-H.; Benneche, T. *J. Am. Chem. Soc.* **1988**, *110*, 621.
[16] Trost, B. M.; Crawley, M. L. *Chem. Rev.* **2003**, *103*, 2921.
[17] Katagiri, N.; Nomura, M.; Sato, H.; Kaneko, C.; Yusa, IL; Tsuruo, T. *J. Med. Chem.* **1992**, *35*, 1882.
[18] See **Chapter 2.2**-*Novel Piperidinyl Iminosugar-Based Nucleosides as Selective Pharmacological Tools*.
[19] Marquez, V. E.; Hughes S. H.; Sei S.; Agbaria R. *Antiviral Res.* **2006**, *71*, 268.
[20] Gu, P.; Morral, J.; Wang, J.; Rozenski, J.; Busson, R.; Van Aerschot, A.; De Clercq, E.; Herdewijn, P. *Antivir. Chem. Chemother*. **2003**, *14*, 31.
[21] See Chapter 3–Paragraph 1.2: *The Central Role of Sugar Conformation in the Antiviral Activity of Nucleoside Analogues*.
[22] Herdewjin, P.; De Clercq, E. *Bioorg. Med. Chem. Lett*. **2001**, *11*, 1591.
[23] Wang, J.; Froeyen, M.; Hendrix, C.; Andrei, G.; Snoeck, R.; De Clercq, E.; Herdewijn, P. *J. Med. Chem.* **2000**, *43*, 736.
[24] Paolella, C.; D'Alonzo, D.; Schepers, G.; Van Aerschot, A.; Di Fabio, G.; Palumbo, G.; Herdewijn, P.; Guaragna, A. *Org. Biomol. Chem.* **2015**, *13*, 10041.
[25] Crimmins, M. T. *Tetrahedron* **1998**, *54*, 9229.

MODIFIED OLIGONUCLEOTIDES

3

MODIFIED OLIGONUCLEOTIDES

The concept of using synthetic oligonucleotides (ODNs) to control the expression of specific genes dates back to the late 1970s, when from several studies emerged the ''antisense'' approach for targeted gene silencing. AON (antisense oligonucleotides)-based therapeutics have been under clinical investigation for more than 30 years, achieving one approved drug (Fomivirsen, Vitravene). Subsequent to antisense strategy, RNA interference (RNAi) and small interfering RNAs (siRNAs) were introduced as alternative gene silencing strategies. Although siRNAs and AONs are perhaps the most commonly discussed ODN-based agents under development, new systems such as microRNA-targeting ODNs (antimiRNAs), aptamers and DNA/RNAzymes have recently emerged for relevant and ambitious applications. Particularly aptamers are ONs that can specifically bind to a molecular target; by SELEX process, thousands of aptamers have been generated against a wide range of targets, including organic molecules, proteins, peptides, viruses and bacteria. Their medical applications include chemical sensors, imaging molecules, diagnostic assays and therapeutic purposes. However, the most significant obstacles impeding the approvals of ODNs as drugs (aptamers included) are their poor extracellular and intracellular stability, low efficiency of intracellular delivery to targets cells or tissues and onset of side effects. In attempts to overcome their therapeutically limiting features, a wide array of chemical modifications has been developed leading to modified oligonucleotides (MOs). These are rationally designed, allowing specific alterations to many of the inherent properties of ODNs affecting their biological application and potency. The challenge of chemists is the construction of modified oligonucleotides (MOs) endowed with deep structural changes compared to natural ODNs, able to hold the potential for selective cross communication, as well as to enhance nuclease stability, target binding affinity, enzyme interaction, hybridization properties, cellular uptake and pharmacokinetic/pharmacodynamic properties. In this context, replacement of natural (deoxy)ribose moiety with a six-membered ring has led to highly preorganized structures, resulting in potentially excellent candidates for cross pairing with natural/modified complements.

Particularly, the oligonucleotide system composed of (6'→4')-linked 1',5'-anhydro-D-arabino-hexitol nucleotides (HNA) has represented one of the most prominent examples of hexose NAs with capability for cross-communication with natural complements. Thus, on the basis of the above-mentioned considerations, during this PhD research project the attention has been focused on the preparation of MOs containing hNAs (1',5'-anhydro-D-arabino-hexitol nucleosides). The aim was to study

the influence of hNAs in the ability of resulting modified oligonucelotides to bind the thrombin acting as its aptamers and then as anticoagulant agents.

3.1 Synthesis of Modified Thrombin Aptamers as Potential Anticoagulant Agents

3.1.1 INTRODUCTION

3.1.1.1 DNA AND RNA OLIGONUCLEOTIDES AS APTAMERS

Ellington[1] in 1990 coined the term aptamer from the combination of the latin word *aptus* ('to fit') and the greek word *meros* ('part'). Nucleic acids aptamers are indeed, short, single stranded DNA or RNA molecules (20-100 nucleotides) that can specifically bind to a molecular target via three-dimensional structures defined by the perfect shape complementarity between the two parts.[2] Aptamers are usually selected on the basis of their affinities for a target molecule in a selection process called SELEX[3] (Systematic Evolution of Ligands by EXponential enrichment) whose experimental simplified principle is illustrated in **FIGURE 1**. Typically, the libraries used in SELEX process[4] contain about 10^{14}-10^{15} sequences that in the first phase are incubated in presence of the molecular target. The interacting sequences are separated from the others and then amplified (by RT or PCR); this process is repeated several times (8-15 rounds) until the highly specific oligonucleotide with great affinity for the target is identified. The aptamers can fold with various secondary structures (stem, loop, G-quadruplex or kissing hairpins) that finally form a unique three-dimensional structure capable of specific interactions with the target, discriminating against conformational isomers, different functional groups or even amino acid mutations.

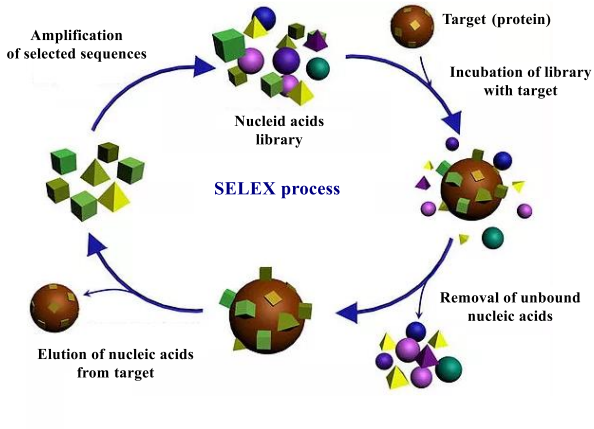

FIGURE 1. Simplifed scheme of the SELEX Process.

By SELEX process, thousands of aptamers have been generated[5] against a wide range of targets, including organic molecules, proteins, peptides, viruses and bacteria. Their medical applications[6] include chemical sensors, imaging molecules, diagnostic assays and therapeutic purposes. However, the pharmaceutical application of aptamers is hampered by the use of therapeutic antibodies which still dominate the global market. The only approved aptamer drug is Pegaptanib (Macugen; Pfizer/Eyetech) targeted

against the VEGF (Vascular Endothelial Growth Factor); many other aptamers are still in clinical trials[7] mainly due to their *in vivo* limitations, such as the metabolic instability (high nuclease degradation susceptibility), rapid renal filtration and rapid distribution into tissues (liver or spleen). Various chemical modifications and conjugations have therefore been developed with the aim to improve their pharmacokinetic properties.[5]

3.1.1.1.1 THROMBIN BINDING APTAMERS

An elective field in which DNA and RNA aptamers are used is represented by thrombotic syndromes, whose disorders lead to significant morbidity and mortality.[8] Hemostatic proteases are obvious enzymatic targets for anticoagulant and antithrombotics agents; thrombin, factor IXa and factor Xa constitute crucial trypsin-like serine proteases involved in the coagulation cascade. Thrombin particularly is the terminal enzyme involved in such cascade; it is directly responsible for the conversion of fibrinogen to fibrin[9] and, on the basis of its multifunctional nature,[10] it has soon been recognized as the major target for the development of inhibitors or modulators. Thrombin-Binding Aptamer (TBA), also named ARC183 (Archemix Corp.) or HD1, a 15-mer DNA structure d(GGTTGGTGTGGTTGG) (**FIGURE 2b**) discovered[11] with SELEX[12] process, represents the best-known example among thrombin inhibitors. TBA is characterized by a chair-like quadruplex structure consisting of two G-tetrads connected by two TT loops (T^3T^4 and $T^{12}T^{13}$) and a single TGT loop ($T^7G^8T^9$). NMR[13] (TBA in solution) and the X-ray[14] (complex of TBA with thrombin) studies, after several ambiguities, have confirmed that the aptamer interacts with the fibrinogen recognition site (exosite I) of a first molecule of thrombin through the two TT loops, while the TGT loop is involved in the interaction with the heparin-binding site (exosite II) of a second distinct thrombin molecule (**FIGURE 2a**).[15] These interactions reflect the strong TBA *in vitro* anticoagulant activity (K_d = 34 nM);[11] its i*n vivo* properties were evaluated on cynomolgus monkeys and sheep first,[16] then it was admnistered by infusion in a short-term canine cardiopulmonary bypass model[17] and the promising results obtained thus led TBA in Phase I of clinical trials. However, because of suboptimal dosing profile, primarily caused by the restricted binding affinity of the aptamer, the trials were halted in 2005. Over the years, many studies have been devoted to the development of more potent derivatives with improved pharmacological activity with the aim to improve the properties of TBA and overcome the drawbacks arising from its use (especially the short *in vivo* half-life, $t_{1/2}$ =1.8 min). Modifications of the original structure[18] have concerned substitutions in the nucleoside residues (i.e. LNA, UNA, RNA, **FIGURE 3**) or in the internucleoside linkages[19] (methylphosphonate or phosphorothioate), inversion of the TBA polarity with 5'-5' internucleoside linkage[20] or the changing of the loops sequence/length.[21]

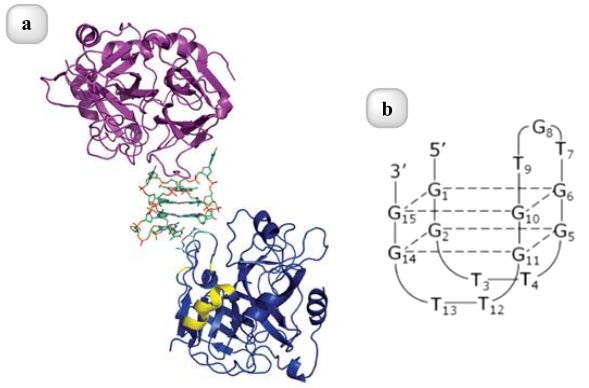

FIGURE 2. a) TBA-thrombin complex; b) schematic representation of the structure of TBA (adapted from ref.8 and ref.25).

LNA (2'-*O*-4'-C-methylene-linked ribonucleotide nucleic acid analogues) substitutions[22] (**FIGURE 3**) at loop region interestingly demonstrated a position dependent effect on the stability of the TBA; indeed, the substitution of G8 with G-LNA increased the stability, whereas, the substitution of T7 decreased it and substitution of T4 disrupted the aptamer. In terms of activity, LNA substitutions did not lead to interesting improvement and only LNA-G2 thrombin aptamer, one of the least stable quadruplexes, demonstrated activity equal to the control aptamer. Modified TBA carrying 2'-deoxyguanine (dG) residues with locked *North* or *South*-bicyclo[3.1.0]hexane pseudosugars (**FIGURE 3**) were prepared[23] by Eritja *et al.;* substitutions at 5, 10 and 14 positions with a locked *South*/syn-dG nucleoside produced aptamers with the same stability of the unmodified one. Replacement at 15 position, on the contrary, induced a strong destabilization of the aptamer, while substitution with the antipodal *North*/anti-dG nucleoside caused a minor destabilization. Remarkably, the insertion of a *North*/anti-dG nucleoside at position 14, where both pseudosugar conformation and glycosyl torsion angle are opposite with respect to the native structure, led to the complete disruption of the G-tetraplex structure supporting the concept that the glycosyl conformation is more restrictive for TBA stability than the sugar puckering.

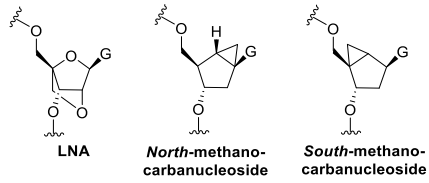

FIGURE 3. Chemical structures of modified carbohydrate moiety in the guanine TBA tetrads.

Second generation DNA aptamers were next synthetized and a great interest was focused on bimodular oligonucleotides[24] encompassing both a duplex and a quadruplex module, adopting a so-called duplex/quadruplex (DQ) conformation. They, because of their

peculiar structure, represent better therapeutic agents compared with those containing a single G-quadruplex domain.[25] RE31, NU172, HD22_27mer and HD22_29mer (see **TABLE 1** for the sequences) belong to the class of anti-thrombin DQ aptamers; on one side RE31[25] and NU172 are both hexosite I inhibitors, while the two HD22 variants are able to bind exosite II of thrombin. RE31 showed a structure (**FIGURE 4**) in which the two domains are strictly interconnected with a continuous stacking of the bases and, particularly, fifteen residues adopt the same antiparallel G-quadruplex structure observed for TBA. Noteworthy, both domains of RE31 interact with the same thrombin molecule but the binding involves only the quadruplex one, as observed, once again, for TBA. The presence of the duplex domain, however, may contribute to make more compact the structure and it is probably involved in the enhancing of the protein affinity which is greater for RE31 with respect to TBA. Altough the high resolution structure of NU172 is not still available, the hypotized structure[26] (**FIGURE 4**) seems to be very similiar to that of RE31; NU172 is able to bind the thrombin at picomolar concentration (K_d= 0.1 nM) and it is in Phase II[27] of clinical trials as anticoagulant agent in patients undergoing coronary artery bypass graft surgery. On the other hand, the HD22 variants present a structure[28] in which the perpedicular orientation of the two domains does not allow a continuous stacking of the bases; however, this peculiar steric combination favours the binding with the exosite II, with which both motifs are able to interact.

Name	***Sequence (5'-3')***
TBA	GGTTGGTGTGGTTGG
RE31	GTGACGTAGGTTGGTGTGGTTGGGGCGTCAC
NU172	CGCCTAGGTTGGGTAGGGTGGTGGCG
HD22_27	GTCCGTGGTAGGGCAGGTTGGGGTGAC
HD22_29	AGTCCGTGGTAGGGCAGGTTGGGGTGACT

TABLE 1. Sequences of thrombin binding aptamers.

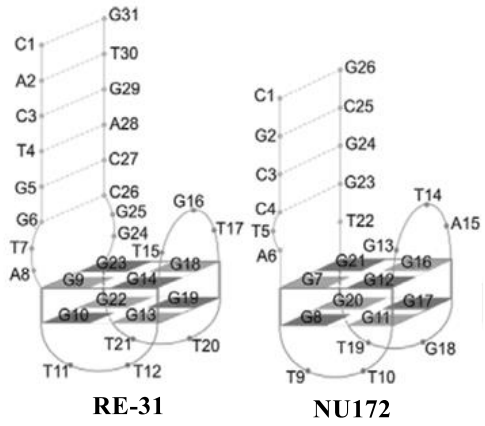

FIGURE 4. DQ aptamers exosite I inhibitors.

3.1.1.2 PREORGANIZED NUCLEIC ACIDS

The desired goals of molecular design (i.e. aptamer design) are the binding affinity and selectivity. High affinity often means slow dissociation from the biological target and therefore a long time for the inhibition of the biological process; the substrate concentration with which it typically occurs is very low. High selectivity means great ability of the substrate in discriminating among different biological targets, thus enhancing the mismatch possibilities. Even if high affinity sometimes does not mean also high selectivity, in several cases, the two goals are simultaneously reached. One of this case occurs when the structural preorganization concept[e] is applied designing modifications which freeze the substrate (i.e. the aptamer) prior to fit, in order to adopt the binding conformation. This event reduces the number of frozen bond rotations during the entropically disfavoured complexation, enhancing thus the affinity. At the same time, the substrate is spatially "organized" with that shape complementary to the desired biological target than the undesired ones, increasing thus the selectivity. One of the strategies used to preorganize helical structures is represented by the design of hexose-DNAs or RNAs. Oligonucleotide analogues bearing a six-membered ring in the backbone hold a central position among conformationally restricted ODNs. Indeed, replacement of a furanose ring with a six-membered unit (e.g. a pyranose ring) involves dramatic differences in flexibility, causing conformational preorganization of the corresponding nucleotide system. This has justified the design of a wide number of

[e] The concept of structural preorganization has been fully introduced in the **Chapter 2.2** (see **2.2.1.3.** *Conformationally Constrained Nucleoside Analogues* in "Novel Piperidinyl Iminosugar-Based Nucleosides as Selective Pharmacological Tools")

hexopyranosyl and other six-membered NAs, whose structures have long been investigated to consider their potential in therapy,[29] diagnostics,[30] synthetic biology[31] and etiology-oriented studies on the structure of natural nucleic acids[32].

3.1.1.2.1 HNA – HEXITOL NUCLEIC ACIDS

In this context, the oligonucleotide system composed of (6'→4')-linked 1',5'-anhydro-D-*arabino*-hexitol nucleotides (hereafter HNA; **FIGURE 5**) has represented one of the most prominent examples of hexose NAs with capability for cross-communication with natural complements (DNA: ΔT_m[f]/mod up to +1.3 °C; RNA: ΔT_m/mod up to +3 °C).[33] The order of duplex stability is HNA:HNA > HNA:RNA > HNA:DNA. Pairing studies of HNA with RNA and DNA showed that the resulting duplexes behave as A-type (RNA) mimics[34] in which the hexitol sugar backbone resembles the conformation of natural D-(deoxy)ribonucleotides frozen in a C3'-*endo* pucker (**FIGURE 5**).

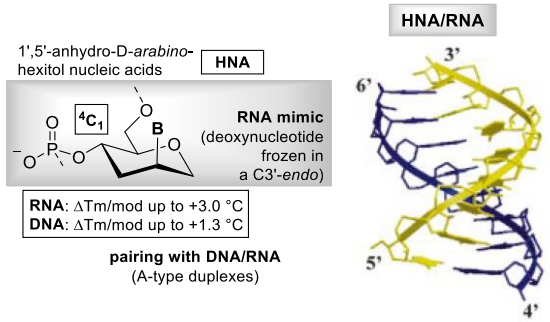

FIGURE 5. Pairing properties of the oligonucleotide system composed of (6'→4')-linked 1',5'-anhydro-D-*arabino*-hexitol nucleotides (HNA).

From a biological point of view, *in vitro* experiments showed that HNA are incorporated by polymerase models[35], by HIV-1 reverse transcriptase[36] and they are not recognized by ligases, methylases and terminal transferases[37]. Moreover, the HNA·RNA hybrid resulted to be a very poor substrate for RNaseH. These results and other[38] highlighted how, among the most relevant examples of conformationally restricted nucleic acids, those bearing a six-membered moiety drew most attention. This justifies the longstanding efforts in the field, as well as the still ongoing studies, aimed to explore their potential therapeutic application (e.g. antisense ODNs, siRNA, aptamers).

[f] The melting temperature (T_m) is defined as the temperature at which two complementary oligonucleotides occur to 50% as single strands and as duplex. Typically these data are extracted from UV–melting curves as the maximum of the first derivative. Although T_m data do not reflect necessarily thermodynamic stability, they are a reliable and widely used measure for thermal stability of duplexes.

3.1.2 Results and Discussion

3.1.2.1 Synthesis of Modified Thrombin Aptamers as Potential Anticoagulant Agents

On the basis of the discussed therapeutic properties exhibited by modifed oligonucletides (MOs) as aptamers and by HNA in terms of target affinity and selectivity, aim of this project was the synthesis and biological evaluation of conformationally preorganized MOs containing *h*NA monomers as new NU172 analogues (**Figure 6**). Guanosine monomer **1** has been synthetized as described in the next paragraph, while thymdine analogue **2** has been furnished by Piet Herdewijn Lab.

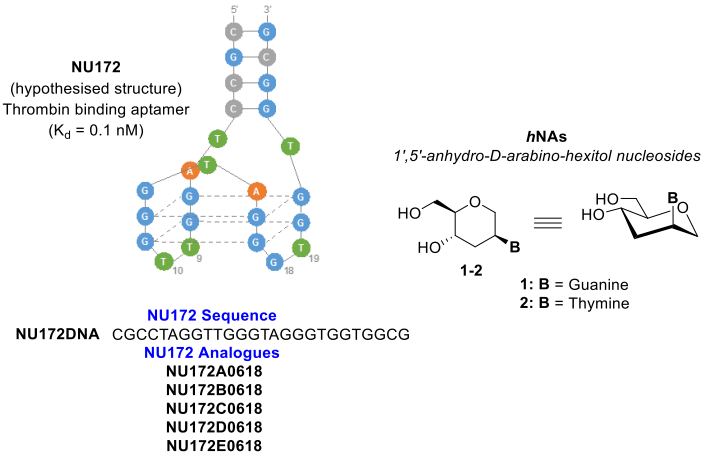

Figure 6. NU172 and its analogues containing *h*NAs.

As discussed in the introductive section, NU172, probably thanks to its peculiar structure, has revealed strong inhibitory activity toward thrombin (K_d = 100 pM)[2] and it is now in Phase II of clinical trials as anticoagulant agent.[39] The project arises from the collaboration with Prof. Piet Herdewijn and his research group (Rega Institute for Medical Reasearch, KU Leuven Belgium) in order to preliminary test the ability of *h*NA modified sequences to bind thrombin and exert anticoagulant properties. The synthesis of monomer **1** has been performed in our laboratories, whereas oligonucleotide synthesis, thrombin binding affinity studies and stability in human serum were carried out at Rega Institute.

3.1.2.2 GUANOSINE MONOMER SYNTHESIS

The building block **1** has been synthetized as described in the *Current Protocols in Nucleic Acid Chemistry* (CPNAC);[40] however, some of the procedures have been tuned up or changed to improve the overall reaction yield. The synthesis started from penta-*O*-acetyl-α-D-glucose **3** which was converted in the corresponding 2,3,4,6-*O*-acetyl-α-D-bromoglucose **4** by treatment with HBr (33% in AcOH); the subsequent dehalogenation reaction was performed by use of Et_3SiH in presence of catalytic amount (10%) of $PdCl_2$ (**SCHEME 1**). Final deprotection step of **5** was then accomplished in typical conditions (MeONa/MeOH) affording 1,5-anhydroglucitol **6**.

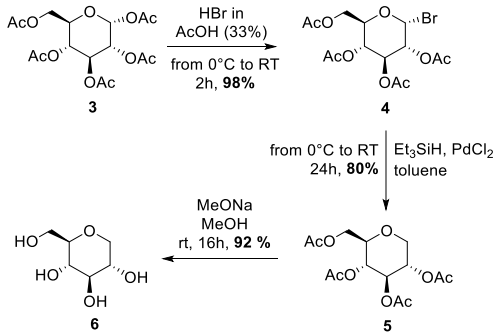

SCHEME 1. Synthetic route to 1,5-anhydroglucitol **6**.

The regioselective benzylidene introduction in O4 and O6 positions was performed with a procedure different to that reported[40] leading to **7** (**SCHEME 2**) with a higher reaction yield (87% - CPNAC 75%). Particularly, **6** was subjected to treatment with benzaldehyde dimethyl acetal in presence of catalytic amount (5%) of CSA in DMF (**SCHEME 2**). At this point, in order to remove the secondary hydroxyl function in C3 position and promote the axial nucleobase insertion in C2 position, a protection of C2-OH position as *p*-toluensulfonyl ester (**8**) was choosen (by stannylene method, 84% reaction yield over two steps) and subsequent OH removal from C3 postion (Barton-McCombie methodology) was carried out. The latter reaction (TBSH/AIBN/toluene) was conducted on xanthate **9,** in turn obtained by treatment of **8** with phenyl chlorothionoformate (**SCHEME 2**).

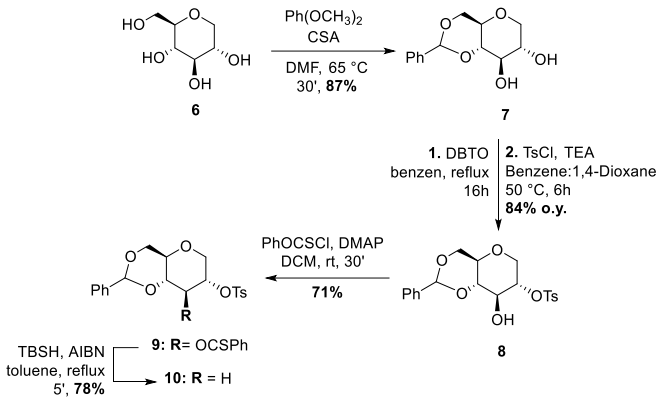

SCHEME 2. Regioselective protections and C3 deoxygenation.

Installation of *p*-toluensulfonyl group at C2 position was planned to stereoselectively introduce the nucleobase by its nucleophilic displacement; this strategy, once again, differs from that reported.[40] 2-Amino-6-chloropurine has been introduced with mild reaction conditions (DBU/DMF/90 °C) affording the desired nucleoside **11** after 48h (**SCHEME 3**). Subsequent acidic treatment contemporary allowed the conversion to the corresponding guanine derivative and the removal of benzylidene group to give **1**. At this point, in order to favour the modified oligomers preparation, it was necessary to promote the conversion of nucleoside **1** into **13**. Therefore, **1** was subjected to a transient *O4* and *O6*-silylation (BSA/pyridine) followed by treatment with isobutyric anhydride to promote the *bis*-protection of the exocyclic nucleobase amino function; subsequent treatment with ammonia and then water, allowed the single removal of isobutyryl group to afford **12** (**SCHEME 3).** Finally, tritylation of primary hydroxyl function *O*6 in typical conditions (MMTrCl/DMF/Py) led to desired **13**, ready to undergo to automatized oligonucleotide assembly.

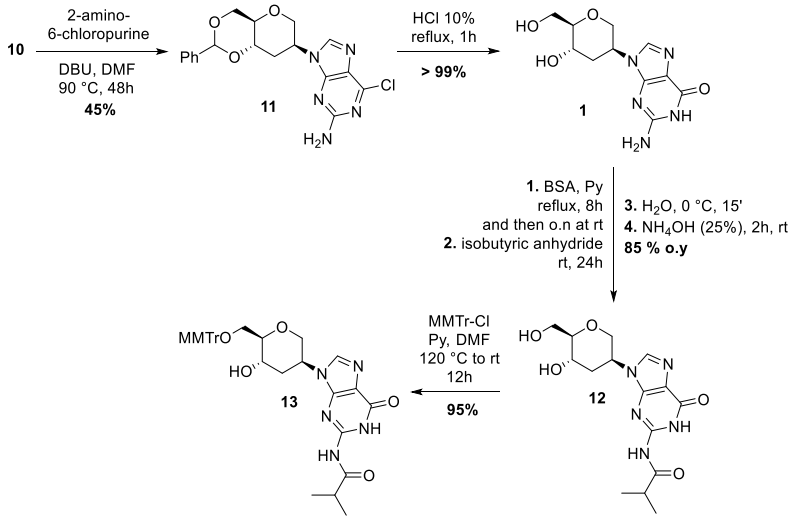

SCHEME 3. Synthetic route to final guanine oligo building block **13**.

3.1.2.3 OLIGONUCLEOTIDES SYNTHESIS

The five anti-thrombin NU172 aptamers analogues containing hexitol nucleotides (*h*NA) have been prepared with a DNA synthesizer by using the phosphoramidite approach (see Experimental Section for details) (**FIGURE 7**).

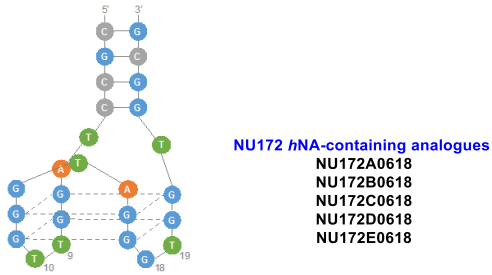

FIGURE 7. NU172DNA sequence and NU172 *h*NA-containing sequences.

Single and multiple substitutions have been considered to evaluate how a preorganized nucleotide is able to influence the aptamer binding affinity with the protein and its susceptibility to nucleases action.

3.1.2.4 BINDING AND STABILITY ASSAYS

We first analyzed the ability of the aptamers to bind to human α-thrombin by electrophoretic gel mobility assay (**FIGURE 8**). Each aptamer was mixed with an equivalent amount of thrombin or incubation buffer (see Experimental Section) and then

analyzed in a native polyacrylamide gel. Compared to unmodified aptamer (NU172DNA), the binding ability of NU172A0618 aptamer resulted interestingly improved of ~ 23%; the affinities of NU172C0618 and NU172D0618 were almost equivalent to the native aptamer while in NU172B0618, the hexitol modification led to a binding reduction of two times. Finally, for the aptamer NU172E0618 the total loss of the aptamer binding ability to thrombin has been observed (**FIGURE 8**).

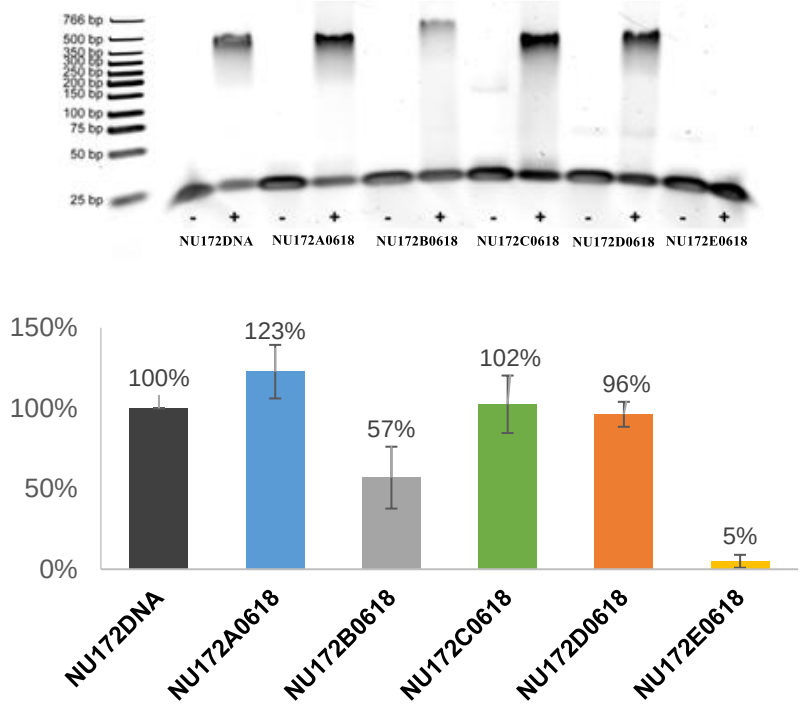

FIGURE 8. Binding analysis by EMSA. Human thrombin (200 nM) was incubated with (+) or without (-) aptamer samples (200 nM) at 37 °C for 2 h. The aptamer-thrombin complexes were separated from the free aptamers on a 6% native PAGE. The relative binding abilities were calculated from their band intensities, normalized by that of unmodified aptamer NU172DNA.

Next, we examined the stability of the variants against nuclease digestion, using 90% human serum at 37 °C (**FIGURE 9**). After 6h, NU172A0618 showed an higher residual activity than NU172DNA (93% and 83 % respectively); after 24h the modified aptamer residual activity resulted once again 1.7 times higher than NU172DNA. On the other hand, NU172C0618, if firstly showed less stability than native aptamer, after 24h and then 48h, exhibited higher residual activity (even more higher of that showed by NU172A0618). In the remaining cases, such as NU172B0618, NU172D0618 and NU172E0618, the aptamer resistance to nuclease degradation was even reduced by incorporation of the modified nucleotides. Finally, we can detect some correlation

between aptamer affinity to thrombin and stability in serum; the tighter binding aptamers (NU172A0618 and NU172C0618) have indeed higher resistance to nuclease hydrolysis.

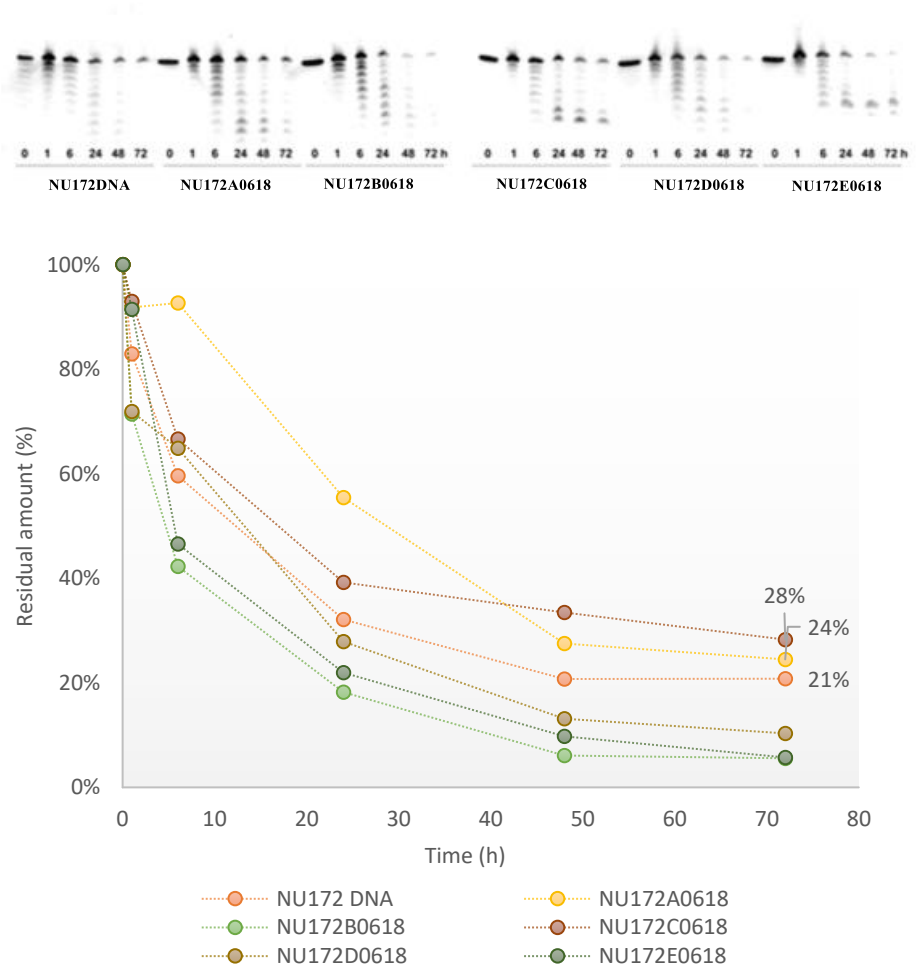

FIGURE 9. Aptamer stability assay in human serum. Unmodified and modified aptamer variants were incubated in 90% human serum at 37 °C for up to 72 h.

3.1.3 CONCLUDING REMARKS AND FUTURE PERSPECTIVES

The research of a biological application for the HNA was the main aim of the above described project. The high affinity and selectivity demonstrated by preorganized systems, such as HNA, led us to conceive the possibility to plan precise modifications of an oligonucleotide sequence that showed interesting biological activity. NU172 is now the most promising thrombin aptamer, now in Phase II of clinical trials, probably adopting a bimodular structure (duplex/quadruplex conformation; DQ aptamer). The most interesting result ragards the aptamer NU172A0618 for which the binding ability resulted improved of ~ 23%; the affinities of NU172C0618 and NU172D0618 were almost equivalent to the native aptamer while for the aptamer NU172E0618 the total loss of the aptamer binding ability to thrombin has been observed. The stability studies in human serum revealed, once again, an extra stabilization for the aptamer NU172A0618 while an equal or reduced stability has been observed in the remaining cases. Taking into account the results obtained, further modifications on the NU172 sequence are currently ongoing aimed to fully establish the role of the key residues involved and absolutely required for the effective binding to the thrombin and furthermore able to improve the stability of aptamers to nucleases degradation.

3.1.4 EXPERIMENTAL SECTION

GUANOSINE MONOMER SYNTHESIS

The 1,5-anhydrohexitol building block **13** for oligonucleotide synthesis (1 mmol, 0.62 g) has been prepared as described in details in the CPNAC[40]; however, some procedures were changed and, noteworthy, the reaction yields sometimes improved. The present experimental section contains thus only the new procedures and the new compounds, fully characterized.

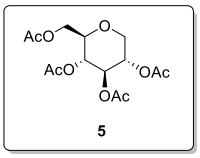

5

Compound 5: 4 (10 g, 0.024 mol) was dissolved in dry toluene (70.0 mL), then Et_3SiH (0.24 mol, 38.0 mL) was added. The mixture was cooled to 0°C and $PdCl_2$ (catalytic amount, 10%) carefully added (0.430 g, 2,44 mmol); after that the mixture was warmed to RT and stirred for 24h. Once filtered on a Celite pad (and washed with EtOAc), the crude was concentrated under reduced pressure and purified by flash cromatography (hexane:EtOAc=80:20) affording **5** as a white solid (6.4 g, 79% reaction yield). The spectroscopic properties of **5** are fully in line with those described in the CPNAC.

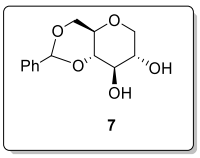

7

Compound 7: 6 (5.8 g, 0.035 mol) was dissolved in dry DMF (60.0 mL) under nitrogen atmosphere; then benzaldehyde dimethyl acetal was dropwise added (6.9 mL, 0.048 mol). The pH was led to 4 by adding CSA (5%) (0.41 g, 1.76 mmol). The mixture was stirred for 30' at RT, quenched with TEA until neutral and then extracted with DCM:MeOH (95:5) and brine; organic layers were dried (Na_2SO_4) and solvent evaporated under reduced pressure. Flash chromatography over silica gel of the crude (chloroform:MeOH=97:3) affords the pure **7** as a white solid (7.1 g, 87% reaction yield). The spectroscopic properties of **7** are fully in line with those described in the CPNAC.

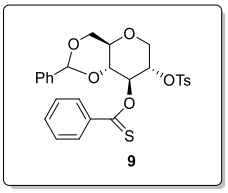

9

Compound 9: once dissolved **8** (10.4 g, 0.026 mol) in dry DCM (150.0 mL), *O*-phenyl chlorothionoformate (4.2 mL, 0.031 mol) and DMAP (6.4 g, 0.051 mol) were added. After 30' the mixture was extracted with DCM and brine, the organic layers dried (Na_2SO_4) and concentrated under reduced pressure. Cromatography over silica gel of the crude (hexane:EtOAc=50:50) afforded the pure **9** as white solid (9.5 g, 71% reaction yield). ^{1}H NMR (400 MHz, $CDCl_3$), δ: 2.41 (*s*, 3H), 3.48-3.54 (*m*, 1H), 3.61 (*t*, J =10.8 Hz, 1H), 3.69-3.75 (*m*, 2H), 4.29 (*dd*, J=6.3, 11.6 Hz, 1H), 4.36 (*dd*, J= 4.6, 10.4 Hz,1H), 4.72-4.79 (*m*, 1H), 5.50 (*s*, 1H), 5.94 (*t*, J=9.5 Hz, 1H), 6.98 (*d*, J =7.6 Hz, 2H), 7.29-7.42 (*m*, 3H), 7.85 (*d*, J=7.7 Hz, 2H). ^{13}C NMR (100 MHz, $CDCl_3$), δ: 21.8, 68.4, 68.6, 71.4, 75.2, 79.0, 81.0, 101.6, 121.8, 126.2, 126.9, 128.1, 128.4, 129.2, 129.6, 130.2, 133.0, 136.7, 145.6, 153.6, 194.3.

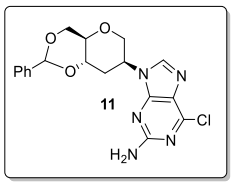

11

Nucleoside 11: once dissolved **10** (4.8 g, 0.012 mol) in dry DMF (190.0 mL), 2-amino-6-chloropurine (4.9 g, 0.028 mol) was added. The mixture was stirred under nitrogen atmosphere for 15'; then DBU (4.3 g, 0.03 mol) was gently added and the mixture was warmed to 90 °C. After 72h at the same temperature, the mixture was extracted with EtOAc and brine, the organic layers dried (Na_2SO_4) and concentrated under reduced pressure. Flash cromatography of the crude (chloroform:MeOH=97:3) afforded the pure **11** as a white solid (2.1 g, 45 % reaction yield). ^{1}H NMR (400 MHz, $CDCl_3$), δ: 2.11-2.20 (m, 1H), 2.59-2.64 (m, 1H), 3.57-3.68 (m, 2H), 3.79 (t, J=9.8 Hz,1H), 4.09-4.15 (m, 1H), 4.37 (dd, J =4.6, 10.7 Hz, 1H), 4.41-4.45 (m, 1H), 4.82 (bs, 1H), 4.98-5.30 (m, 2H), 5.50 (s, 1H), 7.33-7.36 (m, 3H), 7.41-7.44 (m, 2H), 8.31 (s, 1H). ^{13}C NMR (100 MHz, $CDCl_3$), δ: 31.3, 32.9, 51.0, 69.0, 61.5, 73.9, 74.8, 102.2, 126.2, 128.3, 129.3, 137.2, 141.5, 151.7, 153.7, 159.2.

OLIGONUCLEOTIDE SYNTHESIS

Oligonucleotide assembly was performed with an Expedite DNA synthesizer (Applied Biosystems) by phosphoramidite approach. The oligomers were deprotected and cleaved from the solid support by treatment with aqueous ammonia (33%) for 2 h. After gel filtration on a NAP-25 column (Sephadex G25-DNA grade from GE Healthcare) with water as eluent, the crude mixture was analyzed by using a Mono-Q HR 5/5 anion exchange column, after which purification was achieved by using a Mono-Q HR 10/100 GL column (Pharmacia) with the following gradient system: buffer A (10 mM NaOH in 0.1 M NaCl, pH 12.0) and buffer B (10 mM NaOH in 0.9 M NaCl, pH 12.0). After gel filtration on a NAP-25 column with water as eluent, the oligo was re-purified with the following gradient system: buffer A (0.1 M TEAA with 5% CH_3CN, pH 7.5) and buffer B (0.1 M TEAA with 80% CH_3CN, pH 7.5). The low-pressure liquid chromatography system consisted of a HITACHI Primaide organizer with a HITACHI Primaide 1410 UV detector and with a HITACHI Primaide 1110 pump and a Mono-Q HR 10/100 GL column (Pharmacia). The product-containing fraction was desalted on a NAP-25 column and lyophilized. Analysis by mass spectrometry was subsequently performed. Before each analysis, all anti-thrombin aptamers were first folded in the SB buffer (**TABLE 3**) by heating to 95 °C for 5 min followed by slow cooling to 8 °C and equilibration to room temperature.

BINDING AND STABILITY ASSAYS

Electrophoretic mobility shift assay (EMSA). In this assay, 50 µL of the total reaction volume containing 200 nM of renatured anti-thrombin aptamer solution without or with 200 nM of human α-thrombin in SB was incubated for 2 h at room temperature upon shaking at 300 rpm. After incubation, 10 µL of 6× gel loading buffer was added to the samples, and 20 µL of the final solutions was run on a 6% Native PAGE (see **TABLE 3** for details) with 0.5× TBE (running buffer) at 150 V and ~ 18 °C until the bromophenol blue dye was ~ 3 cm below the bottom of the gel wells (~ 1.5 h). The gels were incubated in 1× SYBR Gold Nucleic Acid Gel Stain for 10 min and scanned using the Typhoon 9500 imaging system (Cy2-channel) and quantified with the ImageQuant TL v8.1 software (both from GE Healthcare Life Science). Band intensities of each aptamer variant were measured, normalized by that of unmodified thrombin aptamer and the relative binding abilities were calculated. The EMSA experiment was repeated three times, and the average data are plotted on the graph in **FIGURE 8**.

Stability of unmodified and modified aptamers in human serum. Unmodified and HNA-modified aptamer variants (2 µM each) were incubated in 90% whole human serum at 37 °C in 100 µL total reaction volume. Aliquots (10 µL) of each reaction were taken at

different time intervals (0, 1, 6, 24, 48, and 72 h). Then 10 µL of H_2O was added to each aliquot together with 20 µL of 2× quenching buffer. The samples were denatured at 95 °C for 10 min, then were kept at -20°C until analysis by denaturing 15% PAGE. The gels were incubated in 1× SYBR Gold Nucleic Acid Gel Stain for 10 min followed by visualization using the Typhoon 9500 imaging system (Cy2-channel) and the ImageQuant TL v8.1 software. The analysis was performed two times and average band intensities corresponding to full-size aptamer in each time point (normalized by that at 0 h point) were plotted on the graph in **FIGURE 9**.

TABLE 3. Buffer and solutions used in the studies

Buffer/Solution	Composition	Purpose
SB	40 mM Tris-HCl (pH 7.4), 2 mM $MgCl_2$, 2 mM KCl, 100 mM NaCl, 1 mM $CaCl_2$	Aptamer – Thrombin incubation buffer
1× gel loading buffer	2.5% Ficoll 400, 40 mM Tris-HCl (pH 7.4), 2 mM $MgCl_2$, 2 mM KCl, 100 mM NaCl, 1 mM $CaCl_2$, 0.02% bromophenol blue and xylene cyanol FF	Gel loading buffer for Native PAGE analysis
6% Native PAGE	For 100 mL, 15 mL 40% Acrylamide/Bis-acrylamide (29:1) solution, 5 mL 10× TBE (final 0.5×), 80 mL H_2O	Electrophoretic mobility shift assay of aptamer-thrombin samples
2× quenching buffer	95% formamide, 18 mM EDTA, 0.25% SDS, 0.05% bromophenol blue	Gel loading buffer for 15% denaturing PAGE
15% PAGE	For 100 mL, 37.5 mL 40% Acrylamide/Bis-acrylamide (19:1) solution, 10 mL 10× TBE (final 1×), 52.5 mL H_2O	Analysis of samples after human serum stability assay

3.1.5 REFERENCES

[1] Ellington, A.D. Szostak, J.W. *Nature* **1990**, *346*, 818.
[2] Zhou, J.; Rossi, J. *Nat. Rev. Drug Discov*ery **2017**, *16*, 181.
[3] Tuerk, C.; Gold, L. *Science* **1990**, *249*, 505.
[4] Lancellotti, S.; De Cristofaro, R. *Cardiovas. Hematol. Agents Med. Chem.* **2009**, *7*, 19
[5] Rothlisberger, P.; Hollenstein, M. *Adv. Drug Delivery Rev.* **2018**, http://doi.org/10.1016/j.addr.2018.08.007. *Article in press*.
[6] Zhu. G.; Chen, X. *Adv. Drug Delivery Rev.* **2018**, http://doi.org/10.1016/j.addr.2018.08.005. *Article in press*.
[7] Ismail, S.I.; Alshaer, W. *Adv. Drug Delivery Rev.* **2018**, http://doi.org/10.1016/j.addr.2018.08.006. *Article in press*.
[8] Mann, K.G. *J. Thromb. Haemost.* **1999**, *82*, 165.
[9] Crawley, J.T.; Zanardelli, S.; Chion, C.K.; Lane, D.A. *J. Thromb. Haemost.* **2007**, *5*, 95.
[10] Bode, W. *J. Thromb. Haemost.* **2005**, *3*, 2379.
[11] Bock, L.C.; Griffin, L.C.; Latham, J.A.; Vermaas, E.H.; Toole, J.J. *Nature* **1992**, *355*, 564.
[12] Gold, L.; Brown, D.; He, Y.; Shtatland, T.; Singer, B.S.; Wu, Y. *Proc. Natl. Acad. Sci. USA* **1997**, *94*, 59.
[13] Wang, K.Y.; McCurdy, S.; Shea, R.G.; Swaminathan, S.; Bolton, P.H. *Biochemistry* **1993**, *32*, 1899.
[14] Padmanabhang, K.; Padmanabhang, K.P.; Ferrara, J.D.; Sadled, J.E.; Tulinsky, A. *J. Biol. Chem.* **1993**, *268*, 17651.
[15] Krauss, I.R.; Merlino, A.; Giancola, C.; Randazzo, A.; Mazzarella, L.; Sica, F. *Nucleic Acids Res.* **2011**, *39*, 7858.
[16] Griffin, L.C.; Tidmarsh, G.F.; Bock, L.C.; Toole, J.J.; Leung, L.L. *Blood* **1993**, *81*, 3271.
[17] DeAnda, A.; Coutre, S.E.; Moon, M.R.; Vial, C.M.; Griffin, L.C.; Law, V.S.; Komeda, M.; Leung, L.L.K.; Miller, D.G. *Ann. Torach. Surg.* **1994,** *58*, 344.
[18] Avino, A.; Fabrega, C.; Tintoré. M.; Eritja, R. *Curr. Pharm. Design* **2012**, *18*, 2036.
[19] Zaitseva, M.; Kaluzhny, D., Shchyolkina, A.; Borisova, O.; Smirnov, I.; Pozmogova, G. *Biophys. Chem.* **2010**, *146*, 1.
[20] Russo Krauss, I.; Merlino, A.; Randazzo, A.; Mazzarella, L.; Sica, F. *Acta Crystallogr., Sect. F: Struct. Biol. Commun* **2010**, *66*, 961.
[21] Smirnov, I. Shafer, R.H. *Biochemistry* **2000**, *39*, 1462.
[22] Bonifacio, L.; Church, F.C.; Jarstfer, M.B. *Int. Mol. Sc.* **2008**, *9*, 422.
[23] Saneyoshi, H.; Mazzini, S.; Avino, A.; Portella, G.; Gonzalez, C.; Orozco, M.; Marquez, V.E.; Eritja, R. *Nucleic Acids Res.* **2009**, *37*, 5589.
[24] Lim, K.W.; Phan, A.T. *Angew. Chem., Int Ed.* **2013**, *52*, 8566.
[25] Russo Krauss, I.; Spiridonova, V.; Pica, A.; Napolitano, V.; Sica, F. *Nucleic Acids Res.* **2016**, *44*, 983.
[26] (1) Zavyalova, E.; Golovin, A.; Pavlova, G.; Kopylov, A. *Curr. Med. Chem.*, **2013**, *20*, 4836. (2) Russo Krauss, I.; Napolitano, V.; Petraccone, L.; Troisi, R.; Spiridinova, V.; Mattia, C.A.; Sica, F. *Int. J. Biol. Macromol.* **2018**, *107*, 1697.
[27] https://clinicaltrials.gov/ct2/show/NCT00808964
[28] Russo Krauss, I.; Pica, A.; Merlino, A.; Mazzarella, L.; Sica, F. *Acta Crystallogr., Sect. D: Biol. Crystallogr.* **2013**, *69*, 2403.
[29] Leumann C. J. *Bioorg. Med. Chem.* **2002**, *10*, 841.
[30] Crey-Desbiolles C.; Ahn D.-R.; Leumann C. J. *Nucleic Acids Res.*, **2005**, *33*, e77.

[31] Pinheiro, V.B.; Taylor, A.I.; Cozens, C; Abramov, M.; Renders, M.; Zhang, S.; Chaput, J.C.; Wengel, J.; Peak-Chew, S.Y.; McLaughlin, S.H.; Herdewijn, P.; Holliger, P. *Science*, **2012**, *336*, 341.
[32] Eschenmoser A. *Angew. Chem., Int. Ed.* **2011**, *50*, 12412.
[33] (1) Van Aerschot A.; Verheggen I.; Hendrix C.; Herdewijn P. *Angew. Chem., Int. Ed.* **1995**, *34*, 1338; (2) Hendrix C.; Rosemeyer H.; Verheggen I.; Seela F.; Van Aerschot A.; Herdewijn P. *Chem.–Eur. J.* **1997**, *3*, 110; (3) Hendrix C.; Rosemeyer H.; De Bouvere B.; Van Aerschot A.; Seela F.; Herdewijn P. *Chem.–Eur. J.* **1997**, *3*, 1513.
[34] Lescrinier, E.; Esnouf, R.; Schraml, J.; Busson, R.; Heus, H. A.; Hilbers, C. W.; Herdewijn, P. *Chem. Biol.* **2000**, *7*, 719.
[35] Vastmans, K.; Pochet, S.; Peys, A.; Kerremans, L.; Van Aerschot, A.; Hendrix, C.; Marliere, P.; Herdewijn, P. *Biochemistry* **2000**, *39*, 12757.
[36] Vastmans, K.; Froeyen, M.; Kerremans, L.; Pochet, S.; Herdewijn, P. *Nucleic Acids Res.* **2001**, *29*, 3154.
[37] Vastmans, K.; Rozenski, J.; Van Aerschot, A.; Herdewijn, P.; *Biochim. Biophys. Acta* **2002**, *1597*, 115.
[38] Zhou, J.; Abramov, M.; Liu, F.; Amrane, S.; Bourdoncle, A.; Herdewijn, P.; Mergny, J.L. *Chem.-Eur. J.* **2013**, *19*, 14719.
[39] https://www.clinicaltrials.gov/ct2/show/NCT00808964?term=NU+172&rank=1
[40] Lagoja, I.M.; Marchand, A.; Van Aerschot, A.; Herdewijn, P. *Curr. Protoc. Nucleic Acid Chem.* **2003**, 1.9.1-1.9.22.

GENERAL CONCLUSIONS

The reader will have noticed that every chapter of this PhD thesis already contains its conclusions about the experimental results obtained and the potential future perspectives. However, I would give you more general conclusions trying to explain how the selectivity associated to biomolecular recognition processes is a concept sometimes independent from those "chemical rules" that we have learned over the years. We usually identify the molecules in terms of atoms and of their periodic properties, connectivity and bound strength, R or S stereocenters configuration, conformational behaviour, in terms of contained functional groups and resultant reactivity and thus in terms of nucleophilicity or electrophilicity. The biomolecular recognition processes can be also viewed as chemical reactions between the guests (the enzymes) and the hosts (substrates). However, independently from the nature of the catalysed reaction, the molecular symmetry of the two involved counterparts has a central role into the development of most biological and physiological processes. We know that the "l'Univers est dissymétrique", but the questions about the dissymetrization process at the origin of life, are still unanswered. Proteins made of L-aminoacids and sugars belonging to the D-series are the main result of such a process. The dissymmetry of nature is the reason why until few years ago, the attention was mainly focused only on the use of D-sugars as convenient source of starting material for organic synthesis of complex natural products and for biological investigations. Even, the reason why for a long period it was assumed that nucleoside analogues having only a natural D-configuration, by analogy with the natural ones, could exert biological activity.

Then, the identification of L-sugars as constituents of biologically relevant compounds (i.e. oligosaccharides, antibiotics, glycopeptides and terpene glycosides) has moved the attention toward their synthetic preparation and, on the same line, the discovery of (-)-3TC has challenged the same paradigm in the field of nucleoside analogues discovery as antiviral and anticancer agents.

In other words, these more and more frequent examples of molecules with unconventional chirality but with biological/pharmacological interest, suggested us the idea to view the molecules as chemical entities made of electronic densities which, independently by the above-mentioned classifications, are able to fit the target enzymatic site and furnish biological activity. In this way, as accomplished during this PhD research project, the biological selectivity concept can be revised and in several not accidental cases (as shown), can be useful to reach interesting results in the field of drug discovery.

"If it fits, it sits".

APPENDIX B

PhD Courses

Publications

Training Courses

Congress Schools

Seminaries

Congress participations

Poster and Oral Presentations

Grants and Awards

Abroad Research Periods

PhD Courses

- *Glicoscienza (Prof. Michelangelo Parrilli and Dr Emiliano Bedini), July 5th-12th, 2016.*
- *Corso avanzato di Spettrometria di Massa (Prof. Piero Pucci), July 11th-15th, 2016.*
- *Chimica fisica degli acidi nucleici (Dr Luigi Petraccone), May 17th-19th, 2017.*
- *Synthesis, structure and applications of natural and modified oligonucleotides (Prof. Daniela Montesarchio), July 17th-20th, 2017.*
- *Produzione ricombinante di proteine naturali e mutanti (Prof. Angela Duilio), July 18th-20th, 2017.*

Publications

- *D'Alonzo, D.;***** De Fenza, M.; Palumbo, G.; Romanucci, V.; Zarrelli, A.; Di Fabio, G. Guaragna, A.* ***Synthesis of β-L-2'-Fluoro-3'-Thiacytidine (F-3TC) Stereoisomers: Toward a New Class of Oxathiolanyl Nucleosides?*** *Synthesis* ***2017****, 49, 998-1008.*
- *D'Alonzo, D.;* De Fenza, M.; Porto, C.; Iacono, R.; Huebecker, M.; Cobucci Ponzano, B.; Moracci, M.; Parenti, G.; Priestman, D.; Platt, F.; Palumbo, G.; Guaragna, A.* ***N-Butyl-L-Deoxynojirimycin (L-NBDNJ): Synthesis of an Allosteric Enhancer of a-Glucosidase Activity for the Treatment of Pompe Disease*** *J. Med. Chem.* ***2017****, 60, 9462-6469.*
- *De Fenza, M.; D' Alonzo, D.;* Esposito, A.; Munari, S.; Loberto, N.; Santangelo, A.; Lampronti, I.; Tamanini, A.; Rossi, A.; Ranucci, S.; De Fino, I.; Bragonzi, A.; Aureli, M.; Sonnino, A.; Lippi, G.; Gambari, R.; Cabrini, G.; Palumbo, G.; Dechecchi, M.C.; Guaragna, A.* ***Anti-Inflammatory Treatment of Cystic Fibrosis Lung Disease: Exploring the Effect of Chirality on the Therapeutic Potential of N-Alkyl-Deoxyiminosugars.*** *Manuscript submitted.*

Training Courses

- *NMR Advanced Course, May 3rd-5th, 2017, Bruker Italia S.r.l. Milano.*

Congress Schools

- *43rd Edition of the "A. Corbella" International summer school on organic Synthesis (ISOS 2018), June 10th-14th, 2018, Gargnano (Brescia, Italy)*

.

Seminaries

- *"1,1,2,2-Tetraethoxybutyne - Exciting to Make and Work with" – Prof. Leiv K. Sydnes, January 14th, 2016, Dipartimento di Scienze Chimiche, Università degli Studi di Napoli Federico II.*
- *"Multimodal Approaches for Preclinical Molecular Imaging" – Prof. Luca Menichetti and Prof. Mario Chiariello, February 5th, 2016, Dipartimento di Scienze Chimiche, Università degli Studi di Napoli Federico II.*
- *"The Importance of Catalysis in the Synthesis of Active Pharmaceutical Ingredients" – Dr Michelangelo Scalone, November 25th, 2016, Dipartimento di Scienze Chimiche, Università degli Studi di Napoli Federico II.*
- *"Chemical biology and medicinal chemistry of glycosphingolipid metabolism" – Prof. H. Overkleeft, December 19th, 2016, Dipartimento di Scienze Chimiche, Università degli Studi di Napoli Federico II.*
- *"The future of chemistry written in unconventional reaction media" – Prof. Vito Capriati, February 28th, 2018, Dipartimento di Scienze Chimiche, Università degli Studi di Napoli Federico II.*
- *"Chemical Synthesis and Characterization of Chondroitin Sulfate" – Prof. Tamura, July 23th, 2018, Dipartimento di Scienze Chimiche, Università degli Studi di Napoli Federico II.*
- *"The golden age of Glycoscience – new tools in synthesis and analysis" – Prof. S. Flitch, September 24th, 2018, Dipartimento di Scienze Chimiche, Università degli Studi di Napoli Federico II.*

Congress Participations

- *Challenges in Organic Synthesis: Efficient Processes for Novel Applications, 11th-12th December 2015, Naples (Italy).*
- *XXII International Roundtable on Nucleosides, Nucleotides and Nucleic Acids, 18th-22th July 2016, Paris (France).*
- *XVIIth Symposium on Chemistry of Nucleic Acid Components, 4th-9th June 2017, Český Krumlov (Czech Republic).*
- *Prospettive e sfide della moderna chimica organica. In ricordo di Alessandro Ballio, Gian Paolo Chiusoli e Giorgio Modena, 26th May 2017, Accademia Nazionale dei Lincei, Roma (Italy).*
- *SCI 2017–XXVI Congresso Nazionale della Società Chimica Italiana, 10th-14th September 2017, Paestum (Italy).*
- *XLIII "A. Corbella" International Summer School on Organic Synthesis, 10th-14th June 2018, Gargnano (Italy).*

- *SISOC XII–12th Spanish-Italian Symposium on Organic Chemistry, 2nd-4th July 2018, Ferrara (Italy).*

Oral Presentations

- Maria De Fenza, Anna Esposito, Graciela Andrei, Robert Snoeck, Annalisa Guaragna, Daniele D'Alonzo. "*Novel Piperidinyl Iminosugar-Based Nucleosides as Selective Pharmacological Tools*", XVIIth Symposium on Chemistry of Nucleic Acid Components, Cesky Krumlov, Czech Republic, 4th-9th June 2017.
- Maria De Fenza, Anna Esposito, Daniele D'Alonzo, Annalisa Guaragna. "*Highly stereocontrolled de novo synthesis of N-alkyl L-deoxynojirimycin derivatives and their pharmacological applications in rare diseases",* XLIII "A. Corbella" International Summer School on Organic Synthesis, Gargnano, Italy, 10th-14th June 2018.
- Anna Esposito, Maria De Fenza, Daniele D'Alonzo, Annalisa Guaragna. "*De novo synthesis of L-DNJ and its N-alkylated derivatives*", XVI Convegno-Scuola sulla chimica dei carboidrati, Certosa di Pontignano, Siena, Italy, 17th-20th June 2018.
- D'Alonzo, D.; De Fenza, M.; Esposito, A.; Munari, S.; Loberto, N.; Santangelo, A.; Lampronti, I.; Tamanini, A.; Rossi, A.; Ranucci, S.; De Fino, I.; Bragonzi, A.; Aureli, M.; Sonnino, A.; Lippi, G.; Gambari, R.; Cabrini, G.; Palumbo, G.; Dechecchi, M.C.; Guaragna, A. "*Synthesis of N-Alkylated-L-Iminosugars and their Therapeutic Application in Cystic Fibrosis Lung Disease",* XXXVIII Convegno Nazionale della Divisione di Chimica Organica della Società Chimica Italiana, Milano, Italy, 9th-13th September 2018.

Poster Presentations

- De Fenza, M.; Guaragna, A.; Esposito, A.; Andrei, G.; Snoeck, R.; Di Fabio, G.; Zarrelli, A.; D'Alonzo, D.; "*Novel D- and L-Cyclohexenyl Nucleosides: Asymmetric Synthesis and Antiviral Activity*"-XXII International Roundtable on Nucleosides, Nucleotides and Nucleic Acids, Paris (France), 18th-22th July 2016.
- Esposito, A.; De Fenza, M.; Guaragna, A.; Andrei, G.; Snoeck, R.; Talarico, G.; D'Alonzo, D.; *"Synthesis and Biological Evaluation of D- and L-Cyclohexenyl Nucleosides"* - XVIIth Symposium on Chemistry of Nucleic Acid Components, Cesky Krumlov, Czech Republic, 4th–9th June 2017.
- De Fenza, M.; Esposito, A.; Andrei, G.; Snoeck, R.; Guaragna, G.; D'Alonzo, D.; "*Synthesis and Biological Evaluation of Novel Piperidinyl Iminosugar-*

Based Nucleosides", XXVI SCI – Congresso Societaà Chimica Italiana, Paestum (Italy), 10th-14th September, 2017.

- Esposito, A.; De Fenza, M.; Andrei, G.; Snoeck, R.; Talarico, G.; Guaragna, G.; D'Alonzo, D.; "*Asymmetric Synthesis and Antiviral Activity of Novel Carbocyclic Nucleosides*", XXVI SCI – Congresso Societaà Chimica Italiana, Paestum (Italy), 10th-14th September 2017.
- Maria De Fenza, Anna Esposito, Daniele D'Alonzo, Annalisa Guaragna. "*Highly stereocontrolled de novo synthesis of N-alkyl L-deoxynojirimycin derivatives and their pharmacological applications in rare diseases",* XLIII "A. Corbella" International Summer School on Organic Synthesis, Gargnano, Italy, 10th-14th June 2018.
- Anna Esposito, Maria De Fenza, Giuseppe Punzo, Daniele D'Alonzo, Annalisa Guaragna. "*New O-Glycosidation methods for the synthesis of unnatural oligosaccharides*", XLIII "A. Corbella" International Summer School on Organic Synthesis, Gargnano, Italy, 10th-14th June 2018.
- *Maria De Fenza*, Anna Esposito, Daniele D'Alonzo, Annalisa Guaragna. "*A novel synthetic approach to N-alkyl iminosugars with broad therapeutic potential",* SISOC XII – 12th Spanish-Italian Symposium on Organic Chemistry, Ferrara, Italy, 2nd-4th July 2018.
- Daniele D'Alonzo, Maria De Fenza, Anna Esposito, Silvia Munari, Nicoletta Loberto, Alessandra Santangelo, Ilaria Lampronti, Anna Tamanini, Alice Rossi, Serena Ranucci, Ida De Fino, Alessandra Bragonzi, Massimo Aureli, Alessandro Sonnino, Giuseppe Lippi, Roberto Gambari, Giulio Cabrini, Maria Cristina Dechecchi, Annalisa Guaragna. "*Synthesis of N-Alkylated L-Iminosugars and their Therapeutic Application in Cystic Fibrosis Lung Disease",* SISOC XII – 12th Spanish-Italian Symposium on Organic Chemistry, Ferrara, Italy, 2nd-4th July 2018.

Grants and awards

- *Travel Grant* to attend: "Prospettive e sfide della moderna chimica organica. In ricordo di Alessandro Ballio, Gian Paolo Chiusoli e Giorgio Modena" – Accademia Nazionale dei Lincei, Roma, Italy, 26th May 2017.
- *Fellowship* to attend: XLIII "A. Corbella" International Summer School on Organic Synthesis, Gargnano, Italy, 10th-14th June 2018.
- *Fellowship* to attend: SISOC XII – 12th Spanish-Italian Symposium on Organic Chemistry, Ferrara, Italy, 2nd-4th July 2018.

- *Poster Award* IS3NA Antonin Holy, XXII International Roundtable on Nucleosides, Nucleotides and Nucleic Acids, 18th-22th July 2016, Paris (Francia) – De Fenza, M.; Guaragna, A.; Esposito, A.; Andrei, G.; Snoeck, R.; Di Fabio, G.; Zarrelli, A.; D'Alonzo, D. "*Novel D- and L-Cyclohexenyl Nucleosides: Asymmetric Synthesis and Antiviral Activity*".

Abroad research periods

- 9th April-31st May 2018 – PhD Visiting Scholar at Department of Biochemistry (Supervisor: Prof. Nicole Zitzmann), University of Oxford.
- 1st June-20th July 2018 - PhD Visiting Scholar at Department of Pharmacology (Supervisors: Prof. Frances Platt, Dr David A. Priestman), University of Oxford.